AFFDL-TR-64-181

AD617567

RESEARCH ON ACCELERATED RELIABILITY TESTING METHODS APPLICABLE TO NON-ELECTRONIC COMPONENTS OF FLIGHT CONTROL SYSTEMS

W. F. JOHNSON, et al

Curtiss Division
Curtiss-Wright Corporation

TECHNICAL REPORT No. AFFDL-TR-64-181

MARCH 1965

AF FLIGHT DYNAMICS LABORATORY
RESEARCH AND TECHNOLOGY DIVISION
AIR FORCE SYSTEMS COMMAND
WRIGHT-PATTERSON AIR FORCE BASE, OHIO

FOREWORD

This report was prepared by Curtiss-Wright Corporation, Curtiss Division, Caldwell, N. J., on Air Force Contract No. AF33(657)-11080, "Research On Accelerated Reliability Testing Methods Applicable to Non-Electronic Components of Flight Control Systems", Project No. 8225, Flight Control Equipment Techniques, Task No. 822502, Design Reliability Techniques for Flight Controls. The work was administered under the direction of the Flight Control Division, Air Force Flight Dynamics Laboratory, Wright-Patterson Air Force Base, with Mr. Fred R. Taylor as technical monitor.

The research was administrated and conducted at Curtiss-Wright Corporation, Curtiss Division, Caldwell, N. J., by a task force in Reliability Administration, Value Engineering Section, Engineering Department, with the assistance of the Experimental Engineering Section, Materials Engineering Section, and Technical Section. Individual contributions included: administration, W. F. Johnson, Jr., Reliability Administrator; technical consultant, F. H. Stulen, Chief Scientist; laboratory testing, F. M. McAvoy, Chief Experimental Test Engineer; materials analyses and testing, W. C. Schulte, Engineering Manager-Materials; dynamic studies and data processing, M. Meyer, Engineering Manager-Technical Services.

This is the final report under Contract No. (AF33(657)-11080, and covers the period from May 1, 1963 to May 1, 1964.

This technical report has been reviewed and approved.

W. A. SLOAN, Jr.
Colonel, USAF
Chief, Flight Control Division
Air Force Flight Dynamics Laboratory

ABSTRACT

This study is concerned with the development of techniques for the testing of electromechanical components in time compressed form. The motivating basis for this work is that presently used statistical testing methods require large numbers of samples and long testing periods to compile meaningful MTBF data. The approach employed herein included:

- System failure mode analysis

- Classification and ranking of failure modes in terms of influence and frequency of occurrence

- Physics of failure analysis at part and material levels

"Measured weakening" (pre-cracking) technique was developed and applied to the most predominate failure parts to generate failures in reasonably short test times. In addition, extraneous or unwanted failures were not produced, which is frequently the case when "over load" testing is employed.

An all mechanical position servo unit was selected as a typical energy conversion flight control system component on which tests were conducted to verify the developed techniques for accelerating reliability testing. The tests results indicated that "measured weakening" of mechanical parts can be employed to reduce the number of samples required and the test time involved to perform reliability testing.

TABLE OF CONTENTS

ILLUSTRATIONS

ILLUSTRATIONS (Continued)

ILLUSTRATIONS (Continued)

ILLUSTRATIONS - APPENDIX A

TABLES

INTRODUCTION

The research and study program described in this report was conducted
to advance the state of the art of accelerated testing methods for electro-
mechanical components. It is aimed toward the development of techniques
and standards for economically verifying the reliability predictions made
in the design stage. Utilizing these techniques, the test time and cost
can be reduced below the presently required cost when using conventional
statistical testing methods. The statistical testing techniques are
amenable to electronic parts which cost only a few dollars but is prohi-
itively costly when one speaks in terms of testing hundreds of mechanical
or electromechanical parts. The cost of these parts may vary from one (1)
to ten (10) thousand dollars a piece. Furthermore, in some instances for
aerospace components, the total production lot may not be over a hundred
items so the practice of testing so called representative samples (hundreds)
is completely out of the question. At this point, it is clear that the
need exists for more advanced testing methods to reduce test sample sizes
and times in order to get meaningful MTBF data at economical rates.

Under this program a system failure analysis has been developed that pro-
gresses downward from the system level and thence to the irreducible basic
material level. It has been shown that this analysis can directly relate
the modes of basic material failures in each location to their effects on
the system level functions. A detailed complementing load (stress) analysis,
both theoretical and experimental, can directly relate known system environ-
mental loads of both internal and external origin to material stresses. By
considering the many conceivable material failure points of each of the many
parts, the quantity of failure points thus defined is multiplied. However,
if these failure points are classified by the comparatively few system failure
modes to which they have been related through the failure analysis, their
number can be reduced by eliminating all those points related to non-critical
system failure modes. The decision line separating critical from non-critical
system failure modes (i.e., defining the quantity of material failure points
to be considered) can be located in a ranked hierarchy of these system failure
modes. This can be done by a trade-off between the confidence required and
the resources available for determining the desired type and level of reli-
ability. The number of critical failure points to be considered can be re-
duced further by the load-stress analysis that indicates where very large
margins between maximum loads and minimum strengths obviously exist. The re-
duced number and kinds of basic material failure modes permits the development
of more generally applicable quantitative load-strength-time-failure relations
with more statistical significance at less cost and in a shorter time.

1

The work described above was accomplished under five basic program phases. These phases are illustrated in Figure 1 in the form of a functional diagram. In addition, the phases are listed below with a generalized explanation of the specific work accomplished under each. The phases are discussed in this same order in the body of the report even though some of the efforts were conducted concurrently for technical and economic reasons. The phases are:

The Survey Phase

- Literature Survey
- Environmental Hazards
- Requirements
- Service Reliability Data

The System Analysis Phase

- Task Analysis
- Failure Mode and Consequence Analysis
- Ranked Part Failures
- Load Stress Analysis
- Ranked Causes

The Cost Effectiveness Phase

- Confidence/Resource Criteria
- Effort/Accuracy Criteria
- Reduced List of Critical Causes

Accelerated Testing Phase

- Failure Mechanism Study
- System Test
- Parts Test
- Material Test

The Comparison Phase

- Reduced Life and Failure Mode Check
- Service Life Computation
- Comparison With Service Life
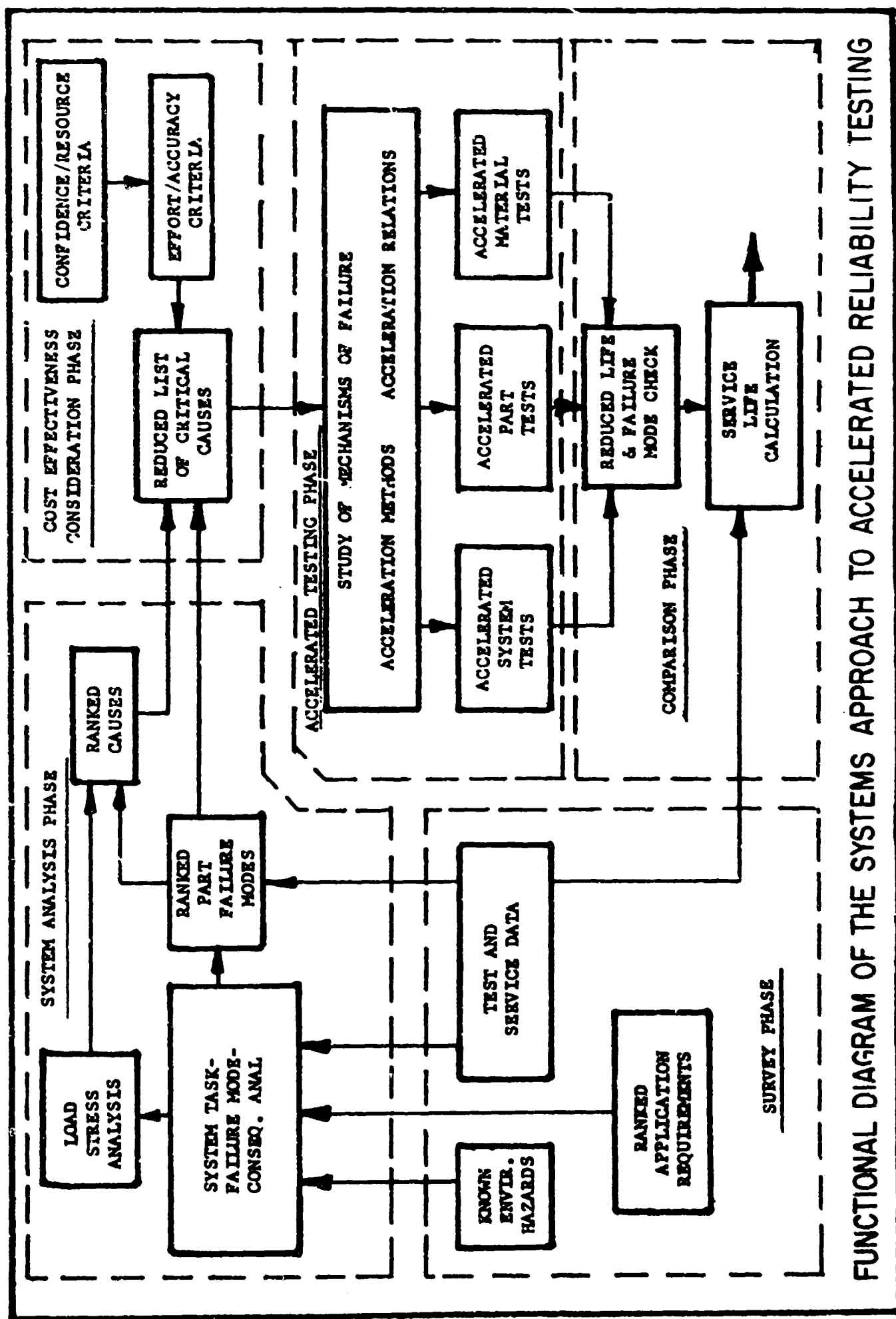
FUNCTIONAL DIAGRAM OF THE SYSTEMS APPROACH TO ACCELERATED RELIABILITY TESTING

FIGURE 1

SYNOPSIS OF PROGRAM EFFORT

The Survey Phase

This was the data gathering phase covering:

- Literature Survey
- Environmental Hazards Survey
- Requirements Survey
- Service Reliability Data Survey

In the Literature Survey technical publications were searched for other approaches to the problem.

In the Environmental Hazards Survey data were collected from the users on:

- Loads and Overloads
- Personnel (Murphy's Law) hazards
- Natural Environmental hazards

In the Requirements Survey the users were questioned to determine the functional requirements as well as the things it should not do with a ranking by preference

In the Service Reliability Data Survey information was collected on individual unit histories, data processing methods were developed and reliability functions were determined for various failure definitions.

The System Analysis Phase

This phase was used to reduce the complexity of the problem by analysis, classification and ranking of failures to permit selection of the relatively few critical items having the predominating influence. The five basic tasks of this phase were:

- Task Analysis
- Failure Mode and Consequence Analysis
- Ranking of Part Failures
- Load/Stress Analysis
- Ranking of Causes

The System Task Analysis related the abstract active and passive tasks of the system to the component tasks and to the materials tasks.

4

The System Failure Mode and Consequence Analysis developed the "ways it can not do it" from the top down - system to part to material - with associated consequence ratings.

The Ranking of Part Failures was done on the basis of consequence ratings.

The Load Stress Analysis considered the external and internal loads and stresses both static and dynamic as well as energy losses between parts.

The Ranking of Causes collected the material failure mode groups and ranked the specific failure points within the groups on the basis of probability of occurrence and consequence rating.

The Cost Effectiveness Phase

This phase was used to develop concepts for relating "costs" of failure at the weapons system level (should such data become available) to the effort that should be expended for accuracy in reliability analysis and testing.

Comparative studies of the effort/accuracy relationship showed significant potential improvement in efficiency using a ranked order sequence in the selection of each successive failure point for testing instead of a purely random one. Criteria for decisions concerning the size of a less than complete consideration were developed.

The Accelerated Testing Phase

This phase was divided into four basic tasks

- Failure Mechanism Study
- System Test
- Parts Test
- Material Test

In the study of failure mechanisms the effort was devoted to exploring in extended depth a limited number of material failure mechanisms. The study of the mechanisms of wear and seizure disclosed many differences in opinion within the state of the art about the fundamentals of these mechanisms. It became evident that the need to resolve these differences prior to developing accelerated test methods would dilute the effort of the program. The major effort was expended in developing accelerated testing methods and relations for the fatigue failure mechanism.

The accelerated system test was used to duplicate external loads, duplicate interactions and to verify and extend the theoretical analysis.

The accelerated parts tests were used to determine production variations of the parts with economical sample sizes, duplicate interactions within the part and to verify the analysis.

The material tests were used to provide data on the material variability which provides the largest source of life variability. Large economical sample sizes are feasible at this level and high acceleration factors are possible with the minimum of complications from interaction.

The scheduling requirements of the program demanded a parallel or concurrent development of the system test, the part tests and the material tests. The conclusions reached at the ends of these tests indicated that data necessary for computation of a specific service life value must come from performance of the three types of tests in sequence; not concurrently.

The sequence required is

1. Materials Tests
2. System Tests
3. Parts Tests

The Comparison Phase

The requirement for failure mode checks in this phase was minimized by the "measured weakening" technique that was developed to force the desired failure modes.

The program scheduling requirements demanded concurrent performance of the three tests phases. This together with the evolved technical requirements for a sequential order for the tests prevented the development of all the data necessary to get specific life values for comparison with the service data. In retrospect it is seen that any subsequent application of these techniques must permit scheduling of the proper sequential order to the tests.

DESCRIPTION OF WORK ACCOMPLISHED

Selected Component

By agreement with the Project Office at the Flight Dynamics Laboratory
the Nozzle Actuation System Power Unit, Part No. 167352-2 (Federal Stock
Number 2995-475-0698), an all-mechanical position servo unit used for
the afterburner exhaust nozzles of the J85-5 engines which power the T-38
supersonic trainers was selected for analysis and testing under this pro-
gram. This unit will be referred to in this report variously as the VEN
Power Unit, Power Unit or VEN Unit.

Literature Survey

The literature survey was conducted in two separate efforts and two separate
lists of the references are presented in this report; one in Appendix A and
one in Appendix B.

In Appendix B is listed the more relevant items of literature found in a
general survey covering the broad fields of accelerated testing concepts in
general, cost effectiveness, systems analysis, statistical concepts, mission
spectra, utility and ranking theory etc. Many of the basic ideas presented
in these references have been incorporated in this program although not
directly enough to be specifically referenced. Instead an abstract of the
contents of each reference is included in a list arranged alphabetically by
authors name.

The specific references employed in the study of the fatigue failure mechanism
are listed at the end of Appendix A in the order in which they were referred
to in the text. These references in the text explain the data used from each
publication and so no abstract is needed in the tabulation of the publications.

Known In-Use Environmental Hazards

This portion of the survey covered the Environmental Hazards for the VEN Power Unit and provided conclusions applicable to defining failures based* on analysis of specified and actual environments.

Definition of Environmental Hazards

For purposes of this portion of the survey phase environmental hazards were defined as those basic and specified installation requirements which the equipment must resist in performing its primary function(s). It therefore has to do with the structural integrity of the equipment, the covering and sealing functions and the interface matching.

List of VEN Power Unit Environmental Functional Requirements

1. **Hold Relative Position**

    1.1   Connect output position to A/C ground

        1.1.1   Connect (3) flex shaft cores to A/C ground
        1.1.2   Connect (3) flex shaft cases to A/C ground

2. **Resist Environmental Hazards**

    2.1   Resist external mechanical hazards

        2.1.1   Resist load
        2.1.2   Absorb overload (protect gearbox but not power unit)
        2.1.3   Resist unwanted signal force
        2.1.4   Absorb excess signal force
        2.1.5   Accommodate input drive misalignment

    2.2   Resist personnel hazards

        2.2.1   Accommodate backward rotation of input power
        2.2.2   Resist improper installation
        2.2.3   Resist interference
        2.2.4   Resist physical damage (handling)
        2.2.5   Resist improper rigging

    2.3   Resist natural hazards

        2.3.1   Resist temperature
        2.3.2   Resist sand, dust etc.
        2.3.3   Resist corrosion
        2.3.4   Resist humidity
        2.3.5   Resist pressure & pressure changes
        2.3.6   Resist vibration
        2.3.7   Resist acceleration
        2.3.8   Resist shock
        2.3.9   Resist explosion

An important part of this survey was to compare the Actual Versus Specified Environmental Requirements.

1. Specified Environmental Requirements

The original design specifications provided by the engine contractor for the design and development of the VEN power unit established specific environmental requirements to be resisted by the device in performing its primary functions in the following areas:

a) Ambient temperature range
b) Attitude (pressure and pressure changes)
c) Humidity (corrosion)
d) Power unit input drive overload protection
e) Excess signal force and rate
f) Input drive misalignment
g) Rigging (external stop adjustments)
h) Reverse input rotation
i) Relubrication periods
j) Minimum useful operating life
k) Hold position against load

2. Inherent structural design characteristics of covers and seals provide resistance to environmental hazards not specified such as:

a) Sand and dust
b) Vibration
c) Acceleration
d) Shock
e) Explosion
f) Physical damage

3. Actual Environment

Results of the survey of the various customers and users of the VEN Power Unit did not indicate a belief on their part that any specification revisions were necessary to cover any new environmental requirements not considered above. From the standpoint of failure and malfunction of the VEN Power Unit to resist environmental hazards affecting operation of the aircraft the survey resulted in establishing a gross ranking of environmental hazard failure modes. These are listed in order of importance (seriousness) of malfunction on operation of the aircraft in Table I.

It was noted that frequent overloads occurred due to deterioration of the nozzle and actuators with time and temperature.

The human factor in the difficult and frequent rigging process has caused a high probability of power unit overload from running against limit stops. No

9

provisions for this were made in the original specifications and it constitutes an actual and unspecified hazard to the power unit. Power unit failures caused by this hazard then became secondary failures and this must be considered when classifying failures as justified or unjustified from the power unit supplier's viewpoint. The system responsibility at the engine manufacturers level is clear.

Table I

SYSTEM/SUBSYSTEM FAILURE RELATIONSHIPS

Rank Order Aircraft Failure Mode	Indication of Failure	VEN Power Unit Failure Mode	Possibility of Occurrence from Experience
0 Safety of Flight	Fire Ignition Explosion Overspeed Explosion	Unknown	Unlikely - no known causes
1 Safety of Flight	No Thrust to Accelerate at wave-off (Nozzle locked or nozzle free)	Not Hold Relative Position	Possible - structural failure, nozzle fixed
2 Mission Abort	a) No MIL Thrust b) No A/B Thrust c) Normal Thrust Too Low	Not Hold Relative Position	Possible Structural Failure Nozzle Full Open

11

Ranked Application Requirements

This portion of the survey phase covered the application requirements for the VEN power unit and provided conclusions applicable to definition of failures based on analysis of specified and actual requirements.

This survey, investigation and analysis established significant modes of failure of the VEN system as it affects functions of the engine and airplane. It was determined that power unit malfunctions could result in aircraft defined failures affecting safety of flight and mission. Two VEN system malfunctions, nozzle fixed open (locked), and nozzle slews full open (runaway) are significant for both safety of flight under very limited but specific flight conditions and for mission abort. It was decided that the VEN power unit detailed part failure mode and consequence analyses would be determined for these two system malfunctions.

The survey also resulted in establishment of a synthesized typical T-38A flight mission permitting estimation of average time of nozzle operation for engine power conditions per flight hour.

VEN Power Unit Functions

In order to establish a means of ranking the requirements of the J85-GE-5 VEN power unit the functions of the unit were listed. The functions were classified as passive and active, the passive being those required to Hold Relative Position of the variable exhaust nozzle and to Resist Environmental Hazards and the active being ones necessary to CHANGE RELATIVE POSITION of the nozzle. The passive function requirements were discussed under Environmental Hazards. The basic characteristics required to CHANGE RELATIVE POSITION are listed as follows:

1. Actuate as needed to close nozzle.

    1.1   Close nozzle to desired position
    1.2   Accelerate close nozzle actuation
    1.3   Close nozzle at desired velocity

2. Not actuate as needed.

    2.1   Decelerate close nozzle actuation
    2.2   Hold nozzle fixed
    2.3   Decelerate open nozzle actuation

3. Actuate as needed to open nozzle.

    3.1   Open nozzle to desired position
    3.2   Accelerate open nozzle actuation
    3.3   Open nozzle at desired velocity

Engine Function Ranking

Based on these passive and active requirements a listing of VEN system and power unit functions's was established as listed in Table II. Each function was listed on an individual card and the cards coded to permit ease in sorting and ranking. Order ranking was done by various engine and aircraft engineering personnel. These included responsible reliability and design people of both the engine and the aircraft manufacturers as well as the test pilot and training command personnel. Results of this ranking are tabulated in Table III in terms of engine functions.

Failure definition, Indication and Cause

From the accumulation of data obtained during the survey trips to the engine and aircraft facilities and operating bases a listing of VEN system caused aircraft malfunctions was established. Table IV provides a listing of the system causes in terms of consequence to the aircraft.

Selection of Significant VEN System Malfunctions

From the listing of Table IV two VEN system malfunctions appear of major significance in the ability of the aircraft to perform its function. These malfunctions are (a) nozzle fixed open and (b) nozzle slews full open. The malfunctions of the nozzle system to close the nozzle too slowly is considered to be similar to a fixed nozzle condition. It was decided on this basis that the detailed part failure mode and consequence analyses would be established on the basis of these two significant VEN system failure modes.

Additional Background Information

The following information established during this investigation was considered to be of value for other phases of the program:

TABLE II

T-38A/J85-GE 5 Variable Exhaust Nozzle System - Power Unit Functional Requirement

Power Unit Characteristics

CODE	FUNCTION
A1	Control A/B EGT (change relative position of nozzle)
A2	Control engine thrust or RPM (change nozzle position per schedule)
A3	Hold position of nozzle fixed
A4	Actuate as needed to close nozzle
A5	Actuate as needed to open nozzle
A6	Resist external mechanical environment hazards
A7	Resist natural environment hazards
A8	Resist personnel hazards
B1	Must not malfunction to cause A/C crash
B2	Must not malfunction to cause A/C mission abort
B3	Must not malfunction to cause A/C mission delay
B4	Must not malfunction to reduce engine performance
B5	Must not allow nozzle to be "free"
B6	Must not allow nozzle to slew to full open position
B7	Must not allow nozzle to slew to full close position
B8	Must not allow nozzle to cock or jam
B9	Must not allow nozzle to oscillate or chatter
B10	Must not allow nozzle to be erratic (jerk or step)
B11	Must not allow nozzle to slew in steps (stepping)
B12	Must not allow nozzle to chatter
202	Hold relative position
201	Change relative position
105	Connect output position to A/C ground
104	Resist environmental hazards
103	Actuate as needed to close nozzle
102	Not actuate as needed
101	Actuate as needed to open nozzle
30	Connect 3 flex shaft cores to ground
29	Connect 3 flex shaft cases to ground
28	Close nozzle to desired position

TABLE II (Cont'd)

CODE	FUNCTION
27	Accelerate close nozzle actuation
26	Close nozzle at desired velocity
25	Decelerate close nozzle actuation
24	Hold nozzle fixed
23	Open nozzle to desired position
22	Accelerate open nozzle actuation
21	Open nozzle at desired velocity
20	Decelerate open nozzle actuation
19	Resist load
18	Absorb overload (protect gearbox)
17	Resist temperature
16	Resist sand & dust
15	Absorb excess signal force
14	Accomodate backward input drive rotation
13	Accomodate input drive misalignment
12	Resist physical damage - (handling)
11	Resist pressure & pressure changes
10	Resist corrosion
9	Resist humidity
8	Resist improper installation
7	Resist vibration
6	Resist acceleration
5	Resist shock
4	Resist improper rigging (of system)
3	Resist interference
2	Resist unwanted signals
1	Resist explosion

TABLE II (Cont'd)

Engine Characteristics

CODE	FUNCTION/MALFUNCTION
E1	Adequate MIL (DRY) thrust
E2	Too low " "
E3	Much too low "
E4	Adequate A/B (wet) thrust
E5	Intermed. " "
E6	No " "
E7	Desired idle speed
E8	Too low " "
E9	Too high " "
E10	No air start
E11	No ground start
E12	Excessive vibration
E13	Accel. too slow
E14	Not accel.
E15	Adequate accel.
E16	Gross overtemperature
E17	Engine fire
E18	Engine explosion
E19	Engine overspeed

TABLE III T-38A ENGINE-VEN MALFUNCTIONS

ENGINE FUNCTION	ENGINE MALFUNCTION	SYMPTOM OR INDICATOR	CONSEQUENCE	POSSIBLE VEN MALFUNCTION
1. Structural integrity	Fire, Ignition explosion, Overspeed explosion	Feel, hear, etc.	Flight safety	None
2. Thrust change (accelerate)	No thrust change (no acceleration)	Feel; noz. pos; RPM	Flight safety (at wave-off) Mission abort	Nozzle fixed slow full open Noz; close. noz. too slowly.
3. Provide MIL thrust	Thrust too low	Below 87% RPM All other measures	Mission abort	Slew full open noz. Nozzle fixed open. Nozzle oscillation
4. Provide A/B thrust	A/B thrust too low	Feel, hear, noz. pos.	Mission abort	Slew full closed noz. Nozzle fixed closed. Nozzle oscillation
5. Control exh. gas temp. ①	Gross over temperature	EGT indicator (abnormal temper.)	Mission abort	Slew full closed noz. Nozzle fixed
6. Control speed ②	Over speed	RPM indicator (abnormal RPM)	Mission abort	Slew full open noz. Nozzle fixed
7. Provide idle speed	Too low idle speed, Too high idle speed	RPM indicator	On ground- mission delay, in flight- nuisance	None
8. Provide ground start	No ground start	RPM ind; fuel flow, EGT	Mission delay	None

TABLE III T-38A ENGINE-VEN MALFUNCTIONS (Cont'd)

	ENGINE FUNCTION	ENGINE MALFUNCTION	SYMPTOM OR INDICATOR	CONSEQUENCE	POSSIBLE VEN MALFUNCTION
9.	Provide air start	No air start	RPM ind; fuel flow	Mission abort	None
10.	Provide low vibration	Excess vibration	Feel; noz. indicator	Mission abort	③ Nozzle oscill-ation

① Gross overtemp. requires dual failure due to overtemp. limiting device in engine

② Gross overspeed requires dual failure due to overspeed governor in engine (limits to 104% RPM) (Pilot used RPM as check on noz. pos. indicators - if noz. pos. ind. shows no chg & engine is at 104% RPM, noz failed at open)

③ No known A/C cases where vibration was noticed.

18

DEFINITION OF FAILURE	INDICATION OF FAILURE	VEN SYSTEM MALFUNCTION
Safety of flight	Aircraft crash Single engine landing Emergency landing	
	Fire Ignition explosion Overspeed explosion No thrust to acceler. at wave-off	No known VEN power unit causes Nozzle fixed open Nozzle slews full open Nozzle closes too slowly
Mission abort (Significant failure)	No thrust to accelerate	Nozzle fixed Nozzle slews full open Nozzle closes too slowly
	Thrust too low (Below 87% RPM)	Nozzle slews full open Nozzle fixed open Nozzle oscillates
	A/B thrust too low	Nozzle slew's full closed Nozzle fixed closed Nozzle oscillates
	Excess engine exhaust Gas temp. (EGT)-incl'd'g engine not start	Nozzle slews full closed (when at shutdown, causes excess EGT on next start.) Nozzle fixed
	Engine overspeed	Nozzle slews full open Nozzle fixed
Mission delay	Unscheduled engine removal	Any of above indications of failure plus power unit oil leak (actual or suspected) Nozzle stepping Unable to adjust Known overload (such as aircraft maneuver)
	Miscell. & nuisance	Engine periodic inspection Minor engine overhaul Major engine overhaul Obvious damage Known contamination Unknown history Cure date expired Convenience removal (with other equipment) Noisy operation Non-repeatability of nozzle position Nozzle fluctuates (at steady state-cruise etc)

TABLE V
SOURCES OF J85-GE-5 VEN POWER UNIT RELIABILITY INFORMATION

LOCATION	TEST METHOD	MEANS OF DETECTION	
CWCD	CPS 6340 Accept. test	Analysis of recorded para- meters	Deadband, signal forces, phase lag attenuation. Output rate, stepping, etc.
GE-SAED	Engine factory test	Engine Stability, EGT, RPM, Accel. Time — Engine response	Engine thrust, Fuel flow, Nozzle area schedule
Norair-Palmdale	Engine test cell	Nozzle area schedule & position (A_8 indicator) EGT RPM Nozzle stepping (A_8 indicator)(specified limit) Visual-nozzle & power unit behavior Engine accel. time-(specified limit)	
"	Aircraft-ground	RPM EGT Nozzle area schedule & position (A_8 ind) Nozzle stepping (A_8 ind.) 2-engine throttle synchronization Engine accel. time-(specified limit)	
"	Aircraft-flight	RPM EGT Nozzle position (A_8 ind.) Nozzle stepping (A_8 ind.) T.O. distance (specified limit) Rate of climb (specified limit) AIC accel. Engine accel.	
ATC base	Flight training	RPM EGT Nozzle position (A_8 ind.) Nozzle stepping (gross)(A_8 ind.) To distance — gross-by feel & observation Rate of climb Loss of thrust	
"	Ground mainten- ance (engine test cell)	RPM EGT Nozzle position Nozzle stepping Fuel flow Visual observation of power unit, flex shafts, nozzle, T-5 motor, A/B fuel control	
Arkansas City (GEO/H)	Engine test cell	Similar means as ATC ground maintenance and factory	

TABLE VI

METHODS OF VEN SYSTEM MALFUNCTION DETECTION

In Flight Conditions

Fire
Ignition explosion   feel-hear-see
Overspeed explosion

No thrust to accel.   feel-noz. position-RPM-fuel flow-T$_2$O. dist.-rate
                        of climb

Nozzle fixed	-	Noz. position - RPM (overspeed) - EGT
Nozzle slews full open-		" " " " - feel lack of thrust
Nozzle closes too slowly	-	Noz. position - RPM roll back-unrecoverable RPM-feel lack of thrust
Nozzle fixed full open	-	Noz. position - RPM - feel lack of thrust when below MIL.
Nozzle oscillation	-	Noz. position - RPM roll back - feel lack of thrust
Nozzle slews full closed	-	Noz. position - EGT
Poor nozzle response	-	Synchronization of throttle position between two engines
Nozzle stepping	-	Noz. position indicator

On Ground (in addition to above)

Nozzle fluctuation	-	Visual observation of unison ring, noz. leaves, T-5 motor, flexible shaft casing (quivers)
Oil leakage	-	Visual observation
Low oil level	-	Flex. shaft quiver

21

TABLE VII

POSSIBLE CAUSES FOR VEN POWER UNIT REMOVALS

Power Unit Condition	Symptom
Inoperative - lock up - jammed - internal failure	Nozzle fixed
Runaway - fails to stop on signal	Nozzle slews open or closed
Single direction operation	Nozzle position indication
Slow output rate	Nozzle slews too slowly
Erratic output - Random output	Nozzle slews too slow or is fixed
Slow response	Nozzle slews too slowly or is erratic
Output stepping	Nozzle moves in steps
Output oscillates - hunts	Nozzle oscillates
Output creep - continues to close at shut-down	Nozzle slews closed
Non-repeatability of output position	Synchronization of throttles
Unable to adjust	Visual
Too high signal force to actuate	Nozzle fixed
Negative signal force to actuate in close direct	Nozzle fixed
Oil leakage	Visual
Oil spurting at vent	Visual
Noisy	Sound
Known overload	Nozzle fixed
Convenience removal with other equipment	
Engine minor O/H	
Engine major O/H	
External damage	
Cure date expired	Specified by
Known contamination	T.O. 00-20 A
Involved in aircraft accident	
Unknown engine history	

TABLE VI-I

T-38A STUDENT FLIGHT TRAINING MISSION AND VEN POWER UNIT ACTIVITY

Estimated T-38A Student Flight Training Mission

Mission	Hrs/ Mission	Cruise %	Hrs.	MIL %	Hrs.	A/B %	Hrs.
Transition	38.75	67%	26.0	25%	9.6	8%	3.15
Instrument	29.00	75%	21.75	22%	6.38	3%	.87
Navigation	21.75	80%	17.4	17%	3.70	3%	.65
Formation	36.50	65%	23.7	20%	7.30	15%	5.50
Optional (extras)	4.00	75%	3.0	15%	.60	10%	.40
Total	130.00 Hrs/ Student		91.85 Hrs.		27.58 Hrs.		10.57 Hrs.
Aver. per flt. Hr per aircraft			.71 hr		.21 hr		.08 hr

Adjusted average time at condition per A/C flight hour.

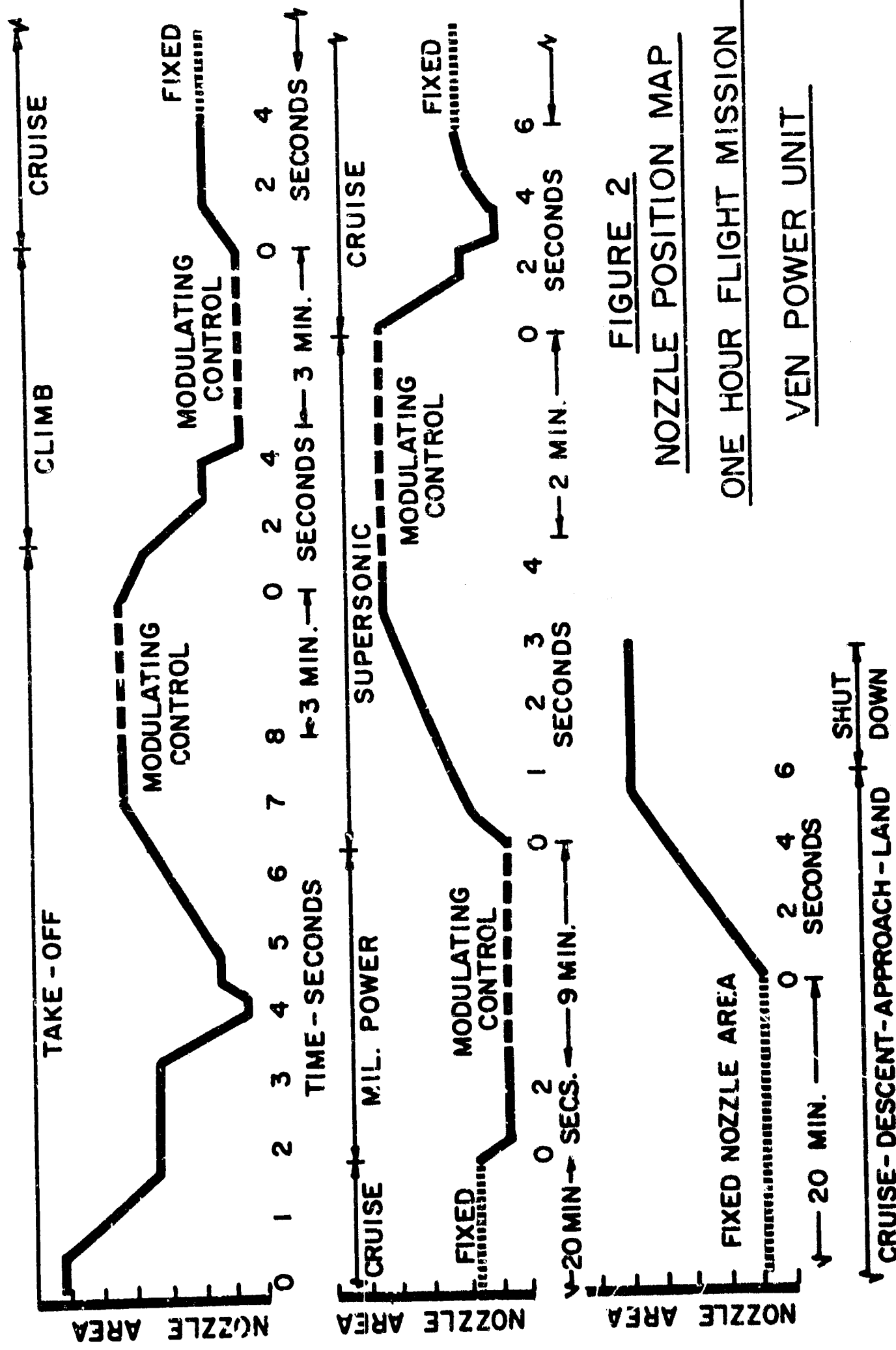| Power Condition	Time	Nozzle Condition	
Idle	3 minutes	Open	⎫ Fixed
Cruise	40 minutes	1/3 open	⎬ Schedule
Military	12 minutes	Closed	⎫ Modulating
After burner	5 minutes	3/4 open	⎬ for EGT control

23

FIGURE 2

NOZZLE POSITION MAP

ONE HOUR FLIGHT MISSION
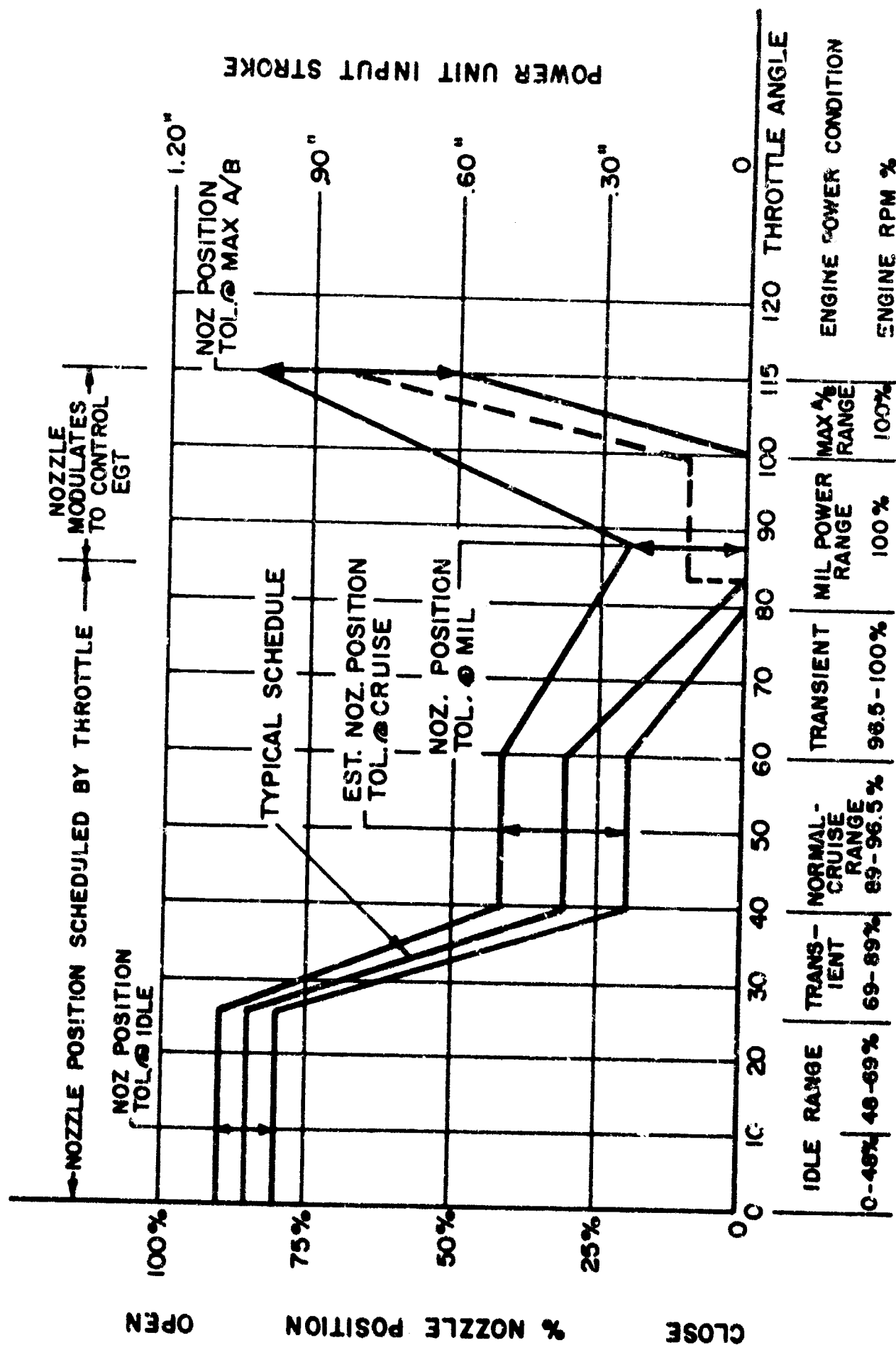
VEN POWER UNIT

24

FIGURE 3 – VEN SYSTEM CHARACTERISTICS

Service Reliability Data

Data Processing

The data processing of the Field Service Data on the J-85 Variable Exhaust Nozzle is divided into six phases:

1) Collection and correlation of data
2) Punching master "Shop" cards
3) Accumulating time since a unit was last in the Service Shop
4) Artificial suspension of incomplete events to measure success time up to a cut-off date
5) Decision making to classify events or periods of operation dichotomously as being successful or as being terminated by a failure
6) Calculation of reliability functions

Flow diagrams of phases one through six are shown in Figs. 5, 6, 7, 8, 9, 10 respectively.

Phase 1 - (Collection and Correlation of Data)

The basic field data is key-punched from the reporting form shown in Figure 4, one card for each line. Each card records the data for either an installation or a removal of a specific power unit and the related engine by serial number. This data is reported randomly from periodic visits to the operating bases. The first machine processing of the data searches the stored list of installations and matches them to form completed event cards. These event cards each describe an engine operating time period and the engine operating hours completed during that period in addition to the installation and removal data.

Phase 2 - (Punching Master "Shop" Cards)

Data on failed and replaced parts from the service shop which handles all inspection, repair and overhaul activity for the power unit is key punched, one part to a card to form a "parts replaced" deck. From this list master shop record control cards are automatically punched defining the form of failure for each power unit that has been in the service shop.

Phase 3 - (Accumulating Operating Time Since a Unit was Last in the Service Shop)

The output of Phase 2 is sorted into the event deck, by 1) power unit serial number 2) installation date. If no "Shop Record Control" card precedes an event this means that the unit was removed then reinstalled without coming into the shop. The "on time", or number of engine hours between installation and removal, may be added to the next event if the Power Unit serial numbers are the same. This accumulated "on time" is called "Time since work order (T.W.O.)".

The events may then be given terminal codes which designate the action taken after a removal, that is:

OV   unit was brought into shop

IN   unit was reinstalled without shop work

LR   removal record that was the last record of the Power Unit

SP   card does not contain a removal ie, Power Unit is recorded as still installed on that engine

The result of this program is the totalling of Power Unit "on times" until terminated by being sent to the CWCD Service Shop. The recording of this total time on the last event card of a Power Unit success history and also recording of that total time on the shop card for transfer of "time to re-placement" on the list of parts replaced under that shop work order on that specific Power Unit.

Phase 4 - (Editing of Incomplete Records)

All the events with no removals on them are made into a deck. The computer places an artificial termination date on the cards, chosen as the latest date that the Shop Records are known to be complete, and computes an arti-ficial "on time" from the mean hrs/day "on time" at each base. This mean hour per day was determined by statistical analysis of the hours/day from all the completed events at each base.

Phase 5 - (Condensing Events to Either Failure or Success)

The accumulated event history* deck is sorted by 1) Power Unit Serial No. 2) Installation date. This puts the history of a particular power unit in chronological order. The computor accumulates the "on time" for each power unit beginning at the event immediately <u>after</u> the <u>last</u> event of that unit <u>defined</u> as terminating in a failure, and ending with the last event in the success history of that power unit. This summation of successful "on time" is punched on a card and defined as a <u>suspended</u> "success item", i.e., suspended before failure.

* Accumulated event history card is defined as the last event <u>before</u> the unit was in the shop with the accumulated on-time since new or since unit was last in the shop.

Phase 6 - (Calculation of Reliability Function)

Phase 6 accepts the output of Phase 5 plus the accumulated event histories defined as terminating in failures. They must be sorted in increasing accumulated time.

If a power unit's period of successful operation is terminated prior to failure it has been termed a suspended item. These suspended items contain information affecting the predicted positions of actual failures within the population. Thus it is not correct to treat only the failed items in com-puting a reliability function.

If only the times to failure are considered, their order members are integral (equi-spaced) counting numbers in the ranked order of increasing times to failure and from these the median ranks can be computed conventionally from the total failed sample size. This assigns too high a population rank to each failed item making the life estimates more conservative than necessary.

When the suspended item success times are included in the population, the times to failure no longer have the same integral order numbers but have fractional order numbers interspersed among the integers 1 through the total population size. This is done at each rank by effectively equi-spacing all the subsequent items in the rank between the last order number and N_f.

The program assigns mean order number to the accumulated histories if they are failures according to the formula

$$M_i = M_{(i-1)} + \triangle M_i$$

where $\triangle M_i = \dfrac{N_f + 1 - M_{(i-1)}}{N_f + 2 - N_i}$ If a test is preceded by a success

or $\triangle M_i = M_{(i-1)}$ If a test is preceded by a failure

M = mean order number
N = sample number
i = subscript for any unit ($f \geq i \geq 1$)
f = subscript for final

With the large number of items available in the data the median rank is derived from the ratio of the mean order number to the total number of items, N_f, plus one.

The survival may be calculated from

$$R = 1 - \dfrac{M_i}{N_f + 1}$$

28

FIGURE 4

DATA COLLECTION FORM

START PHASE 1

FIELD DATA
INSTALLATION
&
REMOVAL
RECORDS

KEY PUNCH
MATERIAL

MATCH INSTALL'S
& REM'S TO
FORM A
COMPLETE EVENT

SORT
1) P.U. S/N
2) I DATE

END

FIGURE 5

FLOW CHART, PHASE 1

START PHASE 2

SHOP RECORDS
OF
PARTS REPLACED

KEY PUNCH

GENERATE ONE
CARD FOR EACH
UNIT IN SHOP

END PHASE 2

FIGURE 6

FLOW CHART, PHASE 2

START PHASE 3

SORT
OUTPUT OF
PHASES 1 & 2
BY
1) P.U. S/N
2) I. DATE

ACCUMULATE
"ON-TIME" AND
TERMINATE AT
A PHASE 2 CARD
OR CHANGE IN S/N

GANG PUNCH
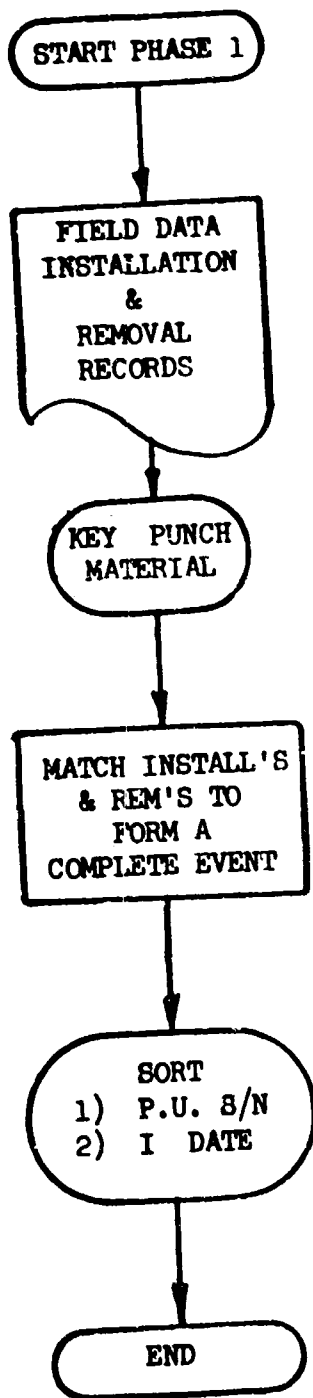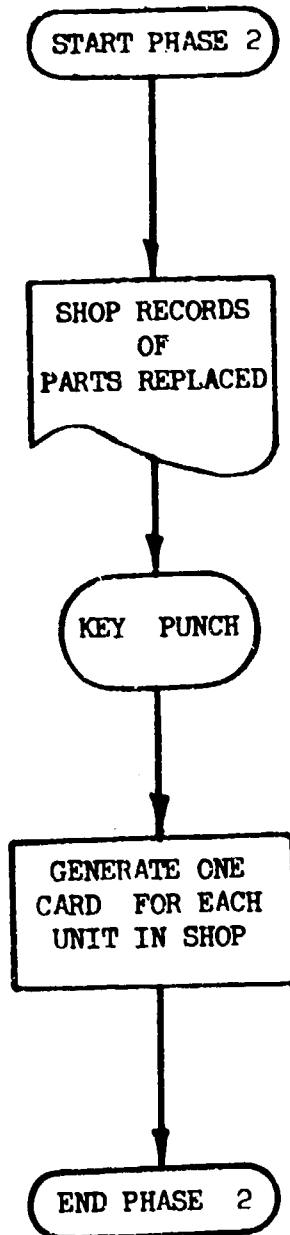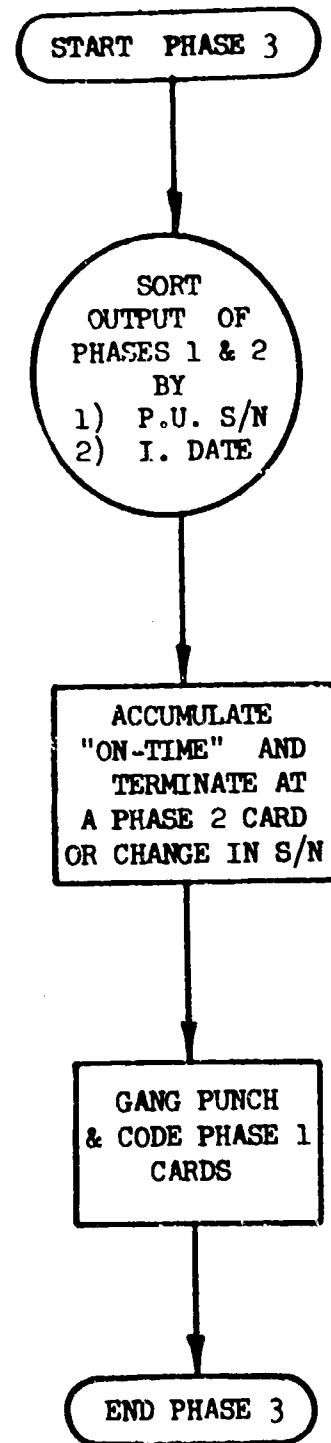& CODE PHASE 1
CARDS

END PHASE 3
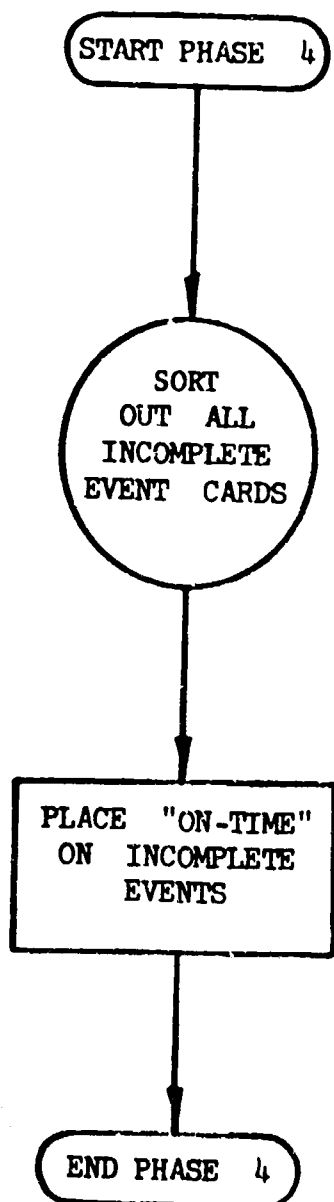
FIGURE 7

FLOW CHART, PHASE 3
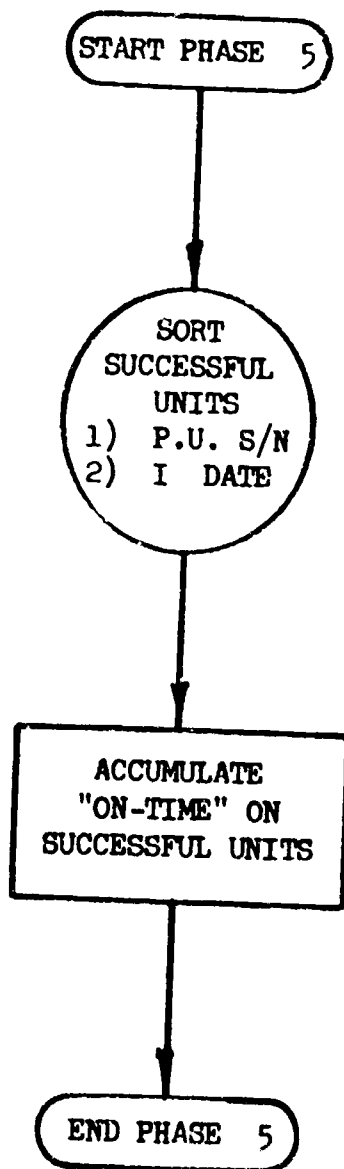
FIGURE 8

FLOW CHART, PHASE 4
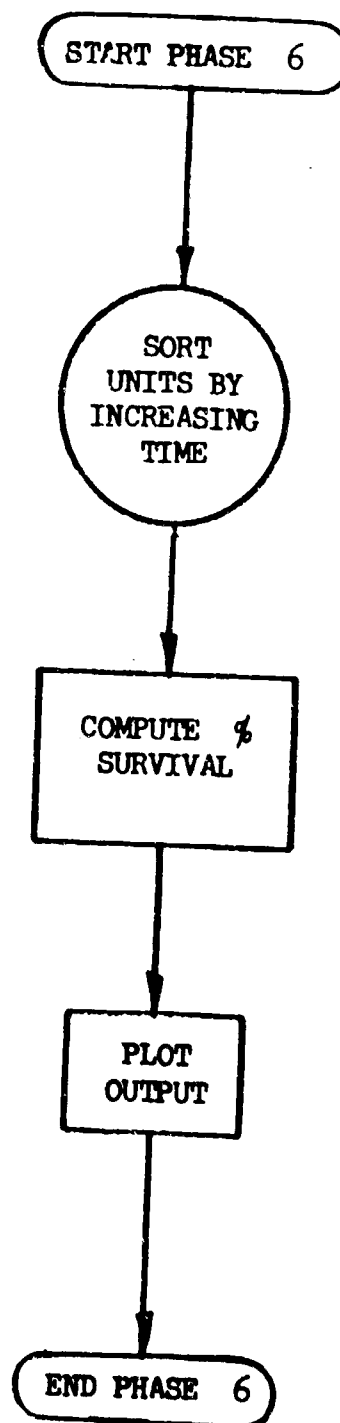
FIGURE 9

FLOW CHART, PHASE 5

FIGURE 10

FLOW CHART, PHASE 6

The Measure of Reliability

The generally accepted definition of Reliability as stated in MIL-STD-721 is

> "the probability that a system, subsystem, component or
> part will perform its intended function for a specified
> period of time under stated conditions".

The determination of the probability requires the definition of the mutually exclusive dichotomous conditions of "success" and "failure" ("will perform" and "will NOT perform"). It becomes apparent rather quickly in a practical consideration that this definition of the line separating "success" from "failure" is a function of the viewpoint of the decision maker, the available "indicators" or symptoms, the system/sub-system/component/part/material interactions, the human motivations, etc.

Since most controls and most humans operate most precisely on error or "difference" signals, it has become an accepted practice to define the character of the failures in reliability analyses and tests rather than the successes. Engineering specifications generally define the successes and only imply the failures in the dichotomy of interest here.

During the survey of Hazards and Requirements, interviews were held with representatives of all levels in the logistics chain including:

> Power Unit manufacturer
> Engine manufacturer
> Aircraft manufacturer
> Air Force Flight Test Operations
> Training Command administrators & technicians
> Instructor pilots
> Materiel Command
> Engine Overhaul facility

It became evident that each had his own viewpoint and decision making symptoms and criteria for determining the line between success and "failure" classifications.

In all cases the "failure"classes have been subsets of the gross population of power units removed from an engine for ANY reason, justified or unjustified and not re-installed on another engine but sent to the repair and overhaul facility (in this case the power unit manufacturer). Of these,many are inspected and returned to service directly. Others have minor cover repairs or seal replacements because of pending cure dates. Still others have internal adjustments made or internal parts replaced as a precautionary measure. Some are overhauled by contract whether necessary or not because as an engine accessory this must be done when the engine is overhauled, etc.

At the other end of the scale are the classes of failures that occur in flight and abort the mission; others that occur in flight but do not affect the mission. Still others are found in preflight and post-flight checks and do not affect the mission. There are even subsets of these classes that are justified. For each of these classifications a time-to-failure distribution exists that is different and likewise a reliability that is different for each specified time.

It became evident that a more specific definition must be provided for the kind of reliability (class of failure) that is of interest before any comparison with the test data may be had.

The collection and analysis of Service Reliability data was quite effective in producing a very comprehensive coverage of the power units in service.

Total No. of Installations recorded	1929
Total No. of power units installed and operating as of 1 November 1963	1100
Total No. of Completed Installation and Removal events recorded	829
Total No. of Units Received at Manufacturers repair and Overhaul facility for which complete replaced parts lists are recorded	453
Range of Installed Unit Serial Numbers	1419

Diagnostic statistical studies of this data promise to reveal the reasons for much of the wide variation between justified and unjustified repair and overhaul action. These studies could also support with high confidence many cost saving revisions in current military maintenance practices.

Use of Weibull type plots such as those in Figure 12 can be most useful for this purpose.

The data plotted in Figure 12 shows a maximum Weibull slope of 1.6 which indicates that the wear-out phase of the power unit has not yet been reached. The maximum time on any power unit is just under 700 hours. The early power unit overhauls dictated by engine overhaul periods have limited the amount of time that could be accumulated on most of the units. A plot of the distribution of the total success time on individual units shows a median time for the power unit design even though a total of 255,000 hours has been accumulated on the number of units in service.

The early failures (infant failures) are evident in the Weibull slopes of about .2 and .4 that occur within the first 80 hours of power unit life. The majority of these have been traced to human failures in misrigging of the actuators and power unit stops. Many others are due to unjustified removals because of the difficulty of determining at the engine assembly level whether the power unit is operating perfectly or not. The diversity and inadequacy of the symptoms and indicators of failure at the line maintenance technicians level are evident from Tables V, VI, and VII.

33

RELIABILITY FUNCTION

LOGISTICS VIEWPOINT OF FAILURE

A : ALL UNITS SENT FOR INSPECTION, REPAIR OR OVERHAUL
B : ALL UNITS WITH ANY PARTS REPLACED
C : ALL UNITS WITH INTERNAL PARTS REPLACED FOR ANY REASON
D : ALL FIELD REMOVALS, JUSTIFIED AND UNJUSTIFIED
E : ALL UNITS REPORTED AS MALFUNCTIONED IN - FLIGHT

NOZZLE ACTUATION SYSTEM

POWER UNIT

TOTAL OPERATING TIME
255,000 HRS.

RELIABILITY

ENGINE OPERATING HOURS - EACH POWER UNIT

FIGURE 11

34

RELIABILITY FUNCTION

NOZZLE ACTUATION SYSTEM
POWER UNIT
LOGISTICS VIEWPOINT

TOTAL OPERATING TIME-255,000 HRS.
TOTAL NO. UNITS - 1419

FIGURE 12

REPLACED
OUTPUT
GEARS

A   B   C   D

WEIBULL SLOPE

LOGISTICS VIEWPOINT OF FAILURE

A: ALL UNITS SENT FOR INSPECTION, REPAIR OR OVERHAUL
B: ALL UNITS WITH ANY PARTS REPLACED
C: ALL UNITS WITH INTERNAL PARTS REPLACED FOR ANY REASON
D: ALL FIELD REMOVALS, JUSTIFIED AND UNJUSTIFIED

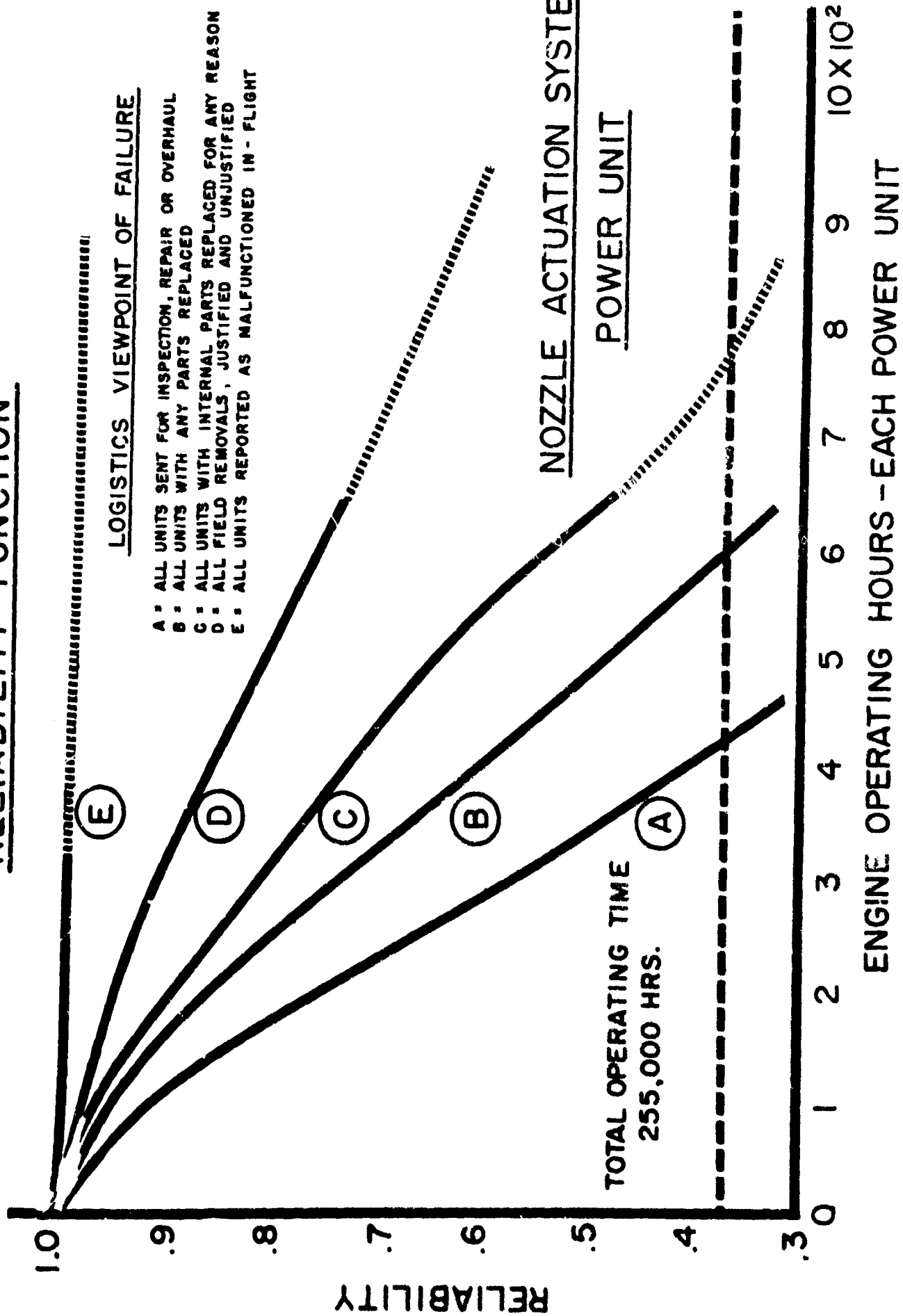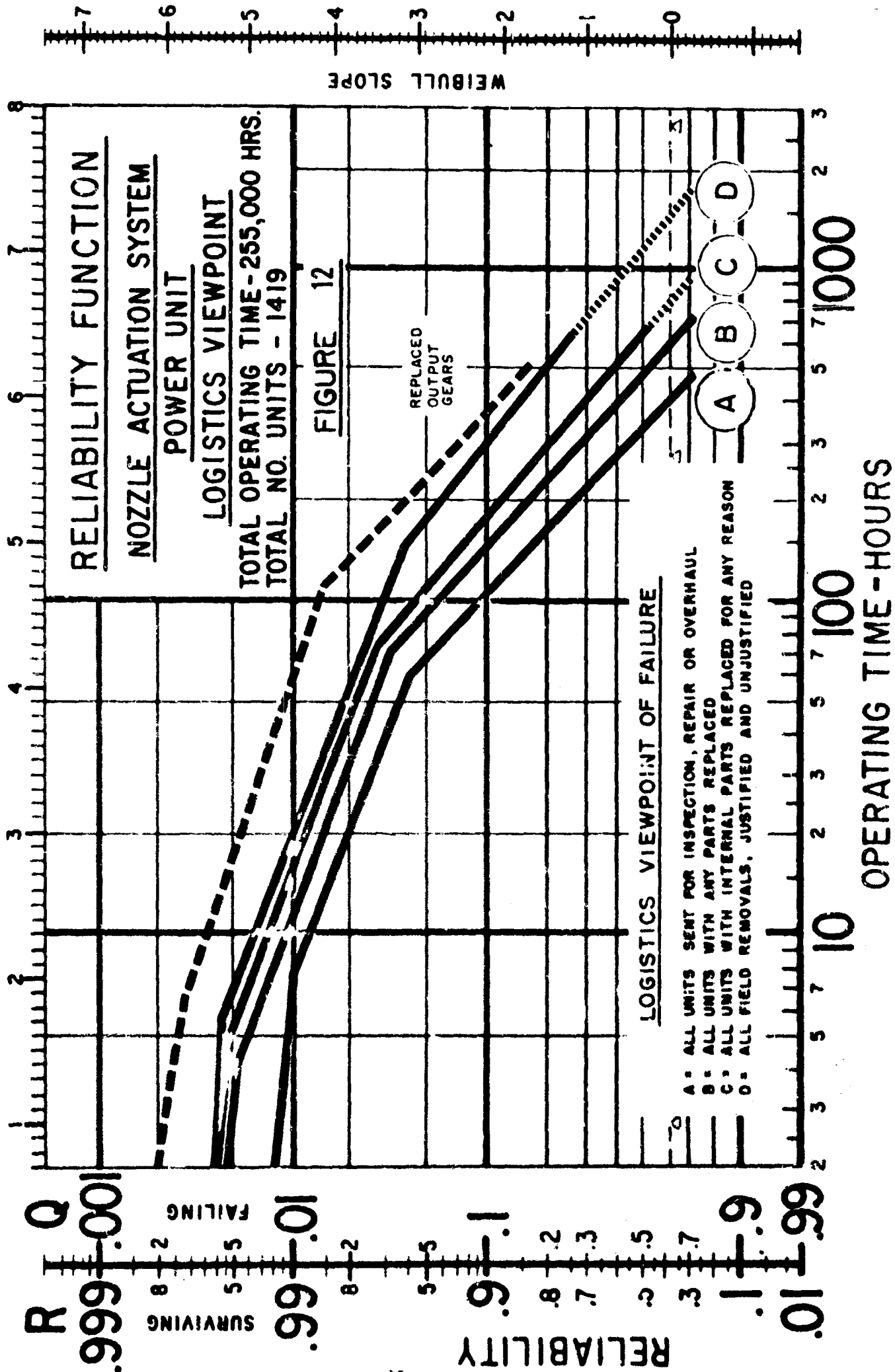OPERATING TIME-HOURS

RELIABILITY

R   Q

FAILING

SURVIVING

35

SYSTEM ANALYSIS PHASE

One of the developments of this program was the extension of a simple reliability analysis method understood and accepted by designers of non-electronic systems. (Reference (B21) in Bibliography)

The Approach

Adequate approximation is used in both logic and mathematics in order to achieve simplicity and ease of understanding. The use of abstraction and two-valued logic are indicated.

Exclusively human is the ability to create a simple mental or physical symbol to represent a complex area of the real world (the invention commonly known as "abstraction"). This powerful approximating tool allows man to sort out a single important idea and to discard temporarily all the less essential complexity. It is the basis of the concept of classifying things into so-called "exclusive" discrete sets; black-white, true-false, positive-negative, and the set of numerical integers.

From it rises the two-valued approximation that assumes two separate classes defined as "success" and "failure" in the broad continuous spectrum of system performance.

Mental conflict arises when the precise boundary between these supposedly "exclusive" classes is sought and the reality of a blended intersection becomes evident.

The conflict is postponed by the creation of an artificially separating decision line located by some measuring parameter. The width of the decision line (a of indecision) is a function of the accuracy of this measuring parameter just like the small but finite tolerances allowed between go and no-go plug gages.

The usefulness of this approximating tool of classification may be exploited in the task and failure analysis with the conflict deferred by sticking near the extremes to avoid the region near the decision line.

This also allows the use of the simple two-valued algebra of logic and classes called "Boolean Algebra" (which also is the algebra of probabalistic mathematics). Everyday simple reasoning (logic) can be recorded by a set of written symbols that represent the words (which are themselves symbols) that are used to describe thoughts;

BLACK is BLACK and not WHITE or:

$$B = B \text{ and } \overline{W}$$

also

WHITE is WHITE and not BLACK or:

$$W = W \text{ and } \overline{B}$$

Here the agreement must be made to ignore GREY which is both:

BLACK and WHITE

which by the simplifying rules of the "invention" requiring exclusiveness, must not exist.

So it is with the mutually exclusive classes of SUCCESS or FAILURE. The generally accepted definition of reliability,

> "The probability that a system will perform its intended function for a specified period of time under specified conditions"

implies the assignment of a FUNCTION or set of TASKS to be performed. Also implied is the definition of a failure state or mode for each TASK so that the probability of the system being in either of the two exclusive states of performance, SUCCESS or FAILURE after some period of time, may be estimated.

The concept that the probability of success plus the probability of failure equals certainty leads to the more tractable probability of failure in the form:

System Reliability = 1 - Probability of
System Failure

Non-electronic reliability is a CONDITIONAL PROBABILITY --- it contains "ifs". This means that the probability of system failure equals the probability of a component part failure occurring and (times) the probability that this failure will cause system failure if it does occur:

$$P(sf) = P(cf) \times P(sf \mid cf)$$

Until recently, in electronics only, this conditional probability nearly always equalled 1.0. In non-electronic systems the conditional $P(sf \mid cf)$ has long been known to vary from 0.000000 to 1.0. This may be called a CONSEQUENCE RATING.

When $P(sf \mid cf)$ approaches 1.0 then $P(cf)$ must approach 0.0 for high reliability. In aircraft this has been called the need for "prime reliability". If by design we can make $P(sf \mid cf)$ approach 0.0 then we need not have high confidence that $P(cf)$ approaches 0.0. This has been done under such names as:

- Fail-safe Analysis
- Failure Effects Analysis
- Failure Mode and Consequence Analysis

The form of the system analysis contains the following:

- What must it do?

    TASKS

- How can it NOT do it?

    FAILURE MODES

- What happens then?

    CONSEQUENCES

37

Failure analyses of the type commonly used in the aircraft industry and the missile industry have had one notable limitation. They are generally performed "from the bottom up". This means that detailed failure modes of individual parts are assumed and these are then extended upward to assess their effect on the system. This generally results in a very random and complex tabulation of cause and effect involving much duplication of thought. Its randomness makes it difficult to organize and rank the conclusions drawn from it.

Another approach has been taken in this program wherein system functions and failure modes are considered first in abstraction and later extended and expanded to the sub-system and then toward the part level. The organization of the conclusions is thus supplied by the system configuration itself. The diversity of the part failure modes to be considered can be reduced at the system level when order of magnitude differences exist between the seriousness of the consequences of the system failure modes. This is a technique for making an analysis of limited scope more efficient by distributing the analytical effort in proportion to these consequence ratings.

Using the simplifying process of abstraction there can evolve two classes of functions that are considered exclusive of each other but together include all of the functions of actuation systems: PASSIVE and ACTIVE.

The PASSIVE function is that assigned to the <u>structural integrity</u> of the system to "<u>HOLD RELATIVE POSITION</u>". This is generally required at the output of the system in all of the six degrees of freedom of relative motion; three translational axes (shears, tensions or compressions) and three rotational axes (couples or moments).

The ACTIVE function to "<u>CHANGE RELATIVE POSITION AS NEEDED</u>" is that requiring an <u>energy</u> source such as that in the prime mover, the <u>interfaces of relative motion</u>, such as bearings, and the "as needed" <u>decision</u> signal for intermittent operation.

The passive function of "HOLD" may be subdivided and re-grouped on the basis of the six degrees of freedom. It may be that five degrees remain fixed continuously and the sixth component of position output (either translation or rotation) is maintained relative to the basic moving elements of the prime mover for continuous output. The output may instead be maintained selectively with reference to either the prime mover or to the fixed reference for intermittent output (such as a servo might produce). The mental boundary of this functional classification must be checked to conform to its assignment exclusively to the <u>structural</u> or <u>volumetric integrity</u> of the system and its mechanical parts as they form a chain of position references resisting externally and internally created loads.

The active function of "change relative position" of "ACTUATE AS NEEDED" may be considered a somewhat more artificial classification but is seen to be most effective in assigning functional responsibility and defining failure mode classifications. Sub-sets of this classification are various ly defined in accordance with the type of actuation required of the system Typical sub-divisions (partitions) of this functional classification are symbolized as follows:

- for a unidirectional continuously operating transmission system;

    ACTUATE = (run with specified speed and torque)

- for a unidirectional intermittently operating actuator requiring a brake (bi-stable):

    ACTUATE AS NEEDED

        ACTUATE (run)

        NOT ACTUATE = (brake with adequately resisting torque or force when output relative position is to be held fixed)

- for a bidirectional continuously reversing servo actuator with no braking function (bi-stable);

    ACTUATE AS NEEDED

        ACTUATE FORWARD

        ACTUATE REVERSE

- for a bidirectional intermittently operating servo actuator with a braking function (tri-stable)

    ACTUATE AS NEEDED

        ACTUATE (run)

            ACTUATE FORWARD

            ACTUATE REVERSE

        NOT ACTUATE (brake)

Further subdivisions of these active functions such as the "STARTING"
and "STOPPING" transients between the "ACTUATE" and "NOT ACTUATE" classes
may be made as more detailed analysis of the system is desired.

An input that the system requires to perform the active functions is the
energy needed at the prime mover or transducer interface to create relative
motion. Where the system active function is to be intermittent an addition-
al input of intelligence or decision signal energy is required to define
the choice between ACTUATE and NOT ACTUATE or between ACTUATE FORWARD,
ACTUATE REVERSE and NOT ACTUATE as the case may be.

In addition, the interfaces (bearing surfaces and running clearances) hav-
ing relative motion must allow the change of relative position.

The binary success/failure concept requiring two mutually exclusive conditions
is most easily employed in the logical inversions:

SUCCESS = NOT FAILURE

FAILURE = NOT SUCCESS

Likewise failure modes of the actuation functions can be defined and symbol-
ized by inversions of the functions themselves as follows:

NOT HOLD POSITION = FREE = failure of the structural or volumetric in-
tegrity of the system as seen at the output where relative position
was to have been held.

NOT ACTUATE = LOCKED (JAMMED, SEIZED) = failure to change relative posi-
tion when desired.

NOT (NOT ACTUATE) = UNINTENTIONAL ACTUATION = changing relative position
when not desired (also called RUNAWAY or HARD-OVER).

Occasionally opposition to the acceptance of assigned word symbols for these
abstractions is encountered because of the semantics involved. This is over-
come by agreement on an adequately detailed definition of the mental concept
for which an abstract geometric symbol like

 or or

is employed. An assigned word symbol may then represent the geometric symbol
and then, without semantic encumbrances, represent the original mental concept.

40

The most complex type of actuation system is the flight control actuation system. All other types may be considered similar to one or two of its three basic sub-systems. These basic sub-systems are:

- the power supply sub-system providing from an energy source a continuously changing relative position with suitable speed and torque capabilities, (or continuously changing volume with suitable flow and pressure capabilities)

- the signal sub-system providing from an intelligence energy source a signal position controlling the connection of the power supply or a fixed position reference to

- the output sub-system which provides the relative position characteristics specified for the entire system.

Each of these sub-systems must be further divided into MOVING and STATIONARY groups with an energy source specified where applicable.

System Task Analysis

The purpose of the Task Analysis was to logically classify the equipment functions as well as the functional contributions required by the related component parts and also the material elements.

The analysis began with an abstraction of the system tasks and hardware. The abstract analysis was followed by a detailed part and material analysis of the power unit.

Abstract System Analysis - The overall VEN Control System hardware is shown by the block diagram of Figure 13. The number with each block is the Hardware Code No. from Table IX. The system hardware of interest for this program is the power unit for the actuation system. This is shown in block diagram form in Figure 14. Here again the block numbers denote Hardware Code No., namely, OUTPUT, POWER and SIGNAL. This level of abstraction is generally sufficient for classifying the hardware.

In the second phase of the abstraction the system functions were classified as being either PASSIVE or ACTIVE. The passive functions are defined as those required to HOLD RELATIVE POSITION of the variable exhaust nozzle while resisting the environmental hazards during various time domains of the flight mission. The active functions are defined as those required to CHANGE RELATIVE POSITION of the nozzle at various times. Lists of each of these functions and the various sub-functions are shown in Tables X and XI.

The third phase of the abstraction was to combine the power unit hardware and the power unit tasks. This was done using "tree" diagrams with Task Nos. and Code Nos.

Another purpose of the abstract analyses has been to reduce the possibilities of omissions in systems of complex functions.

Detailed Part Analysis - From the abstract analysis of the power unit hardware listed in Table IX, it can be seen that each level of abstraction is another adjective needed to properly describe the particular hardware required to perform a particular task. To facilitate the detailed part analysis the power unit hardware was listed in detail. The Ref. No. refers to the Figure and Index No. of Technical Manual, T.O. 6J3-8-4-24, Illustrated Parts Breakdown, Nozzle Actuation System Power Unit, dated 1 July 1963.

42

TABLE IX

HARDWARE CODE NUMBERS

V-000	Vehicle
100.0	VEN control system
20.0	Power unit, actuation system
20.1	Clutch
20.2	Brake
30	Output sub-system
40	Moving parts
50	Open nozzle
51	Close nozzle
52	Fix nozzle
41	Interfaces and/or clearances
50	Open nozzle
51	Close nozzle
52	Fix nozzle
42	Stationary parts
50	Open nozzle
51	Close nozzle
52	Fix nozzle
31	Power sub-system
32	Signal sub-system
21.0	Flexible shafts
22.0	Actuators
23.0	Nozzle
24.0	Engine accessory drive gear box
25.0	Mechanical feed back
26.0	T-5 temperature control
27.0	Main Fuel Control

TABLE X

PASSIVE FUNCTIONS

01	Hold relative position at environment
011	During actuate on desired signal
0111	Through output
01111	Moving
011111	To open nozzle (at environments)
011112	To close nozzle (at environments)
01112	Interfaces
01113	Stationary
011131	To open nozzle (at environments)
011132	To close nozzle " "
0112	Through Power
01121	Moving
011211	To open nozzle (at environments)
011212	To close nozzle " "
01122	Interfaces
01123	Stationary
011231	To open nozzle (at environments)
011232	To close nozzle (at "
0113	Through Signal
01131	Moving
011311	To open nozzle (at environments)
011312	To close nozzle " "
01132	Interfaces
01133	Stationary
011331	To open nozzle (at environments)
011332	To close nozzle (" "
012	During not actuate on desired signal
0121	Through output
01211	Moving
012111	To open nozzle (at environment)
012112	To close nozzle " "
012113	To fix nozzle " "

TABLE X (Cont'd)

01212	Interfaces
01213	Stationary
012131	To open nozzle (at environment)
012132	To close nozzle " "
012133	To fix nozzle " "
0122	Through __Power__
01221	Moving
012211	To open nozzle (at environment)
012212	To close nozzle " "
012213	To fix nozzle " "
01222	Interfaces
01223	Stationary
012231	To open nozzle (at environment)
012232	To close nozzle " "
012233	To fix nozzle (" "
0123	Through __Signal__
01231	Moving
012311	To open nozzle (at environment)
012312	To close nozzle " "
012313	To fix nozzle " "
01232	Interfaces
01233	Stationary
012331	To open nozzle (at environment)
012332	To close nozzle " "
012333	To fix nozzle " "

TABLE XI

ACTIVE FUNCTIONS

02	<u>Change</u> relative position at desired signal
021	<u>Actuate</u> on desired signal (to clutch)
0211	Position <u>output</u> relative to moving power
02111	Provide position relative to moving power
021111	To open nozzle (accelerate & steady)
021112	To close nozzle " "
02112	Allow relative motion
02113	Provide position relative to stationary power
021131	To open nozzle (accelerate & steady)
021132	To close nozzle " "
0212	Position <u>power</u> relative to moving power energy
02121	Provide position relative to moving energy
021211	To open nozzle (accelerate & steady)
021212	To close nozzle " "
02122	Allow relative motion
02123	Provide position relative to stationary energy
021231	To open nozzle (accelerate & steady)
021232	To close nozzle " "
0213	Position <u>signal</u> relative to moving signal energy
02131	Provide position relative to moving energy
021311	To open nozzle (accelerate & steady)
021312	To close nozzle " "
02132	Allow relative motion
02133	Provide position relative to stationary energy
021331	To open nozzle (accelerate & steady)
021332	To close nozzle " "
022	<u>Not actuate</u> on desired signal (to brake)
0221	Position <u>output</u> relative to stationary power
02211	Provide position relative to moving power
022111	To open nozzle (decelerate)
022112	To close nozzle "
022113	To fix nozzle
02212	Allow relative motion

TABLE XI (Cont'd)

|	
02213	Provide position relative to stationary power
022131	To open nozzle (decelerate)
022132	To close nozzle "
022133	To fix nozzle
0222	Position power relative to stationary power
02221	Provide position relative to moving energy
022211	To open nozzle (decelerate)
022212	To close nozzle "
022213	To fix nozzle
02222	Allow relative motion
02223	Provide position relative to stationary energy
022231	To open nozzle (decelerate)
022232	To close nozzle "
022233	To fix nozzle
0223	Position signal relative to stationary energy
02231	Provide position relative to moving energy
022311	To open nozzle (decelerate)
022312	To close nozzle "
022313	To fix nozzle
02232	Allow relative motion
02233	Provide position relative to stationary energy
022331	To open nozzle (decelerate)
022332	To close nozzle "
022333	To fix nozzle
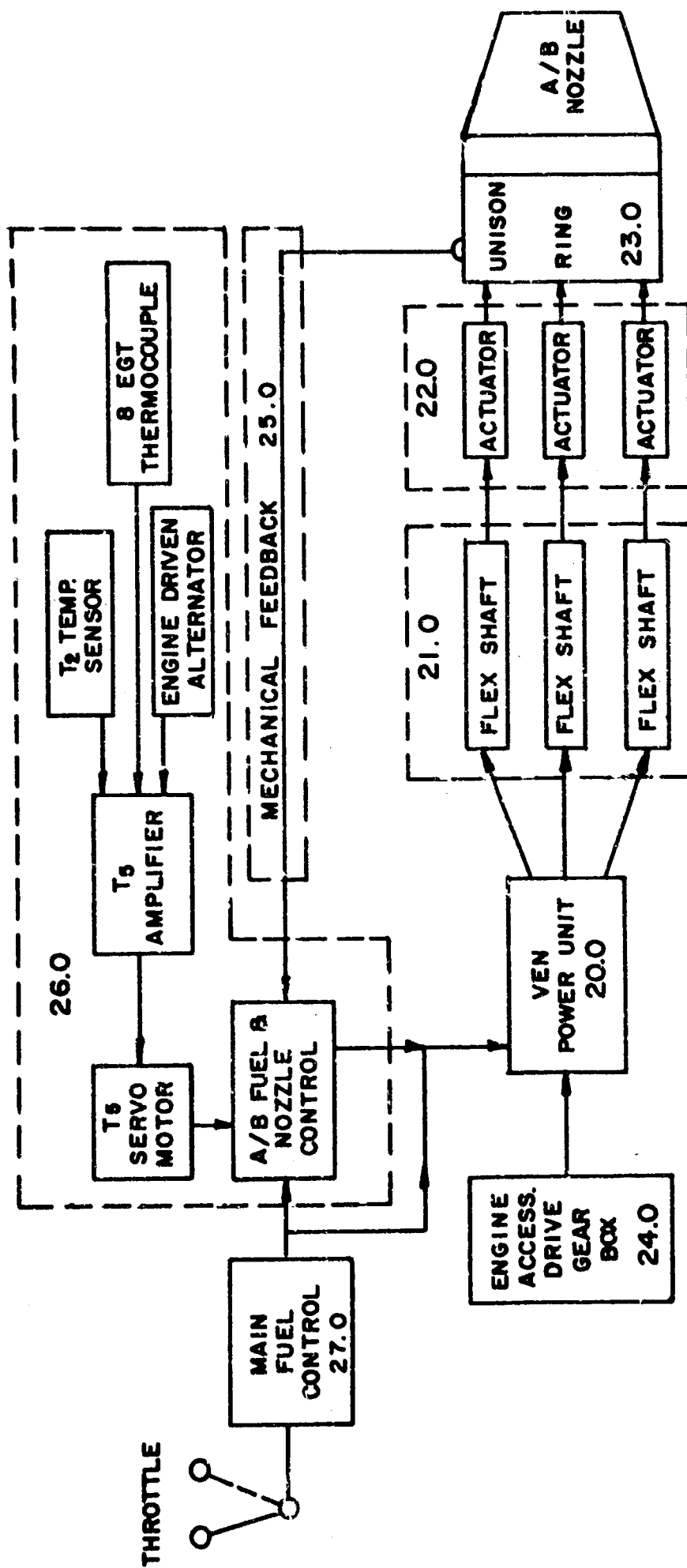
FIGURE 13
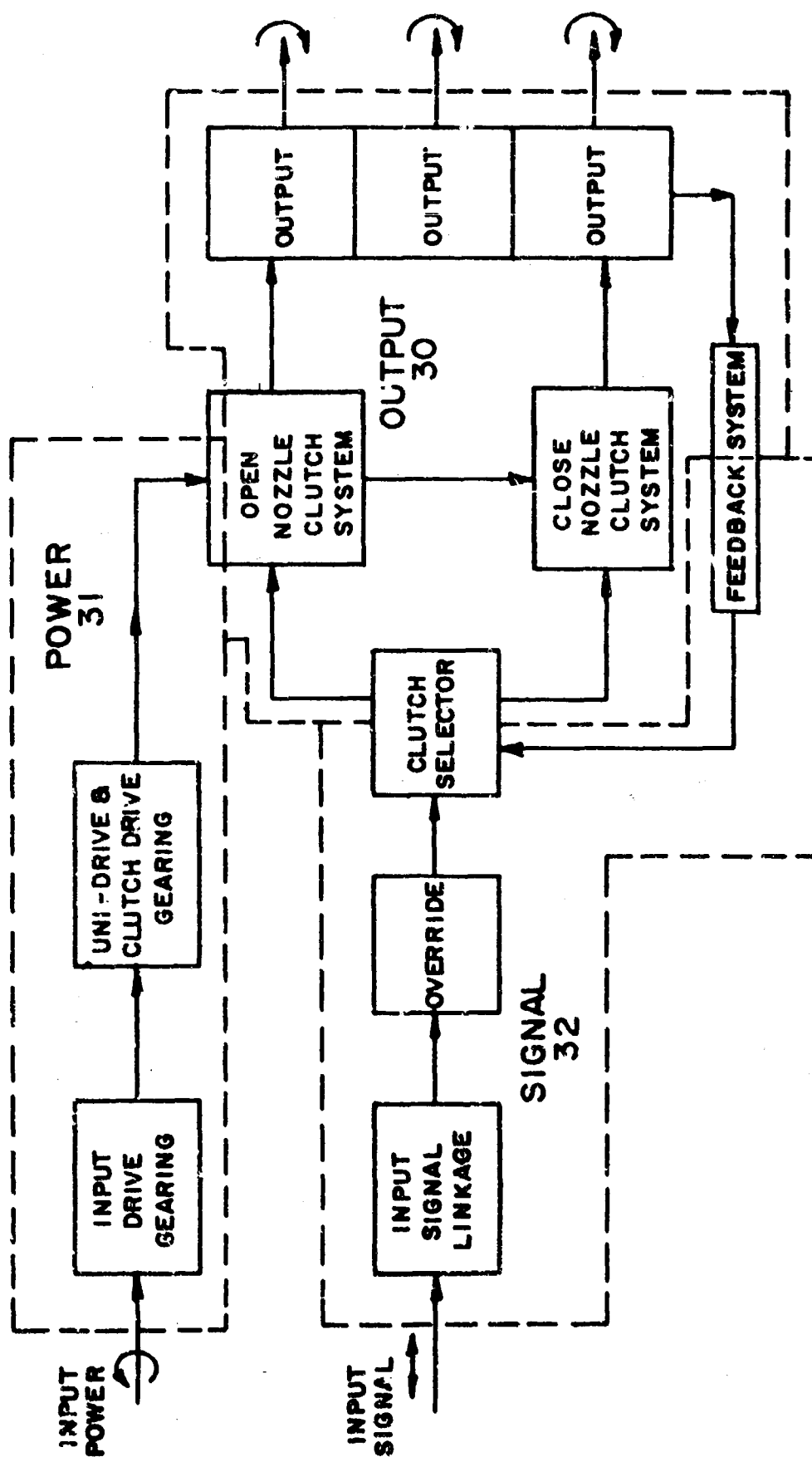
BLOCK DIAGRAM-VEN CONTROL SYSTEM HARDWARE

FIGURE 14

BLOCK DIAGRAM-POWER UNIT HARDWARE

System Failure Mode and Consequence Analysis

The purpose of the failure mode and consequence analysis is to determine in what ways the system cannot perform its functions and what happens if a failure does occur. A form was devised which combined the task analysis and the failure mode analysis. Another phase of this was the construction of failure mode logic diagrams.

The analysis began with an abstraction of the system malfunctions. The abstract analysis was followed by a detailed part and material failure analysis of the power unit. Finally, failure mode logic diagrams were constructed for two system failure modes.

Abstract System Malfunctions

The failures or malfunctions are conveniently listed as the logical inversion of the tasks or functions. For example, the malfunction of the ACTUATE ON SIGNAL task (clutch when asked for) can be listed as NOT ACTUATE ON SIGNAL (doesn't clutch when asked for). Care must be exercised in listing these malfunctions to prevent cumbersome wording. For example consider the task of NOT ACTUATE ON SIGNAL (apply brake when needed). The malfunction could be listed as NOT NOT ACTUATE ON SIGNAL (doesn't brake or stop when supposed to). To some this may appear confusing. Their preference may be NOT ACTUATE ON NOT DESIRED SIGNAL (applys brake when not supposed to). Regardless of how one prefers the wording, if there is agreement on the task or function definitions then NOT performing the function (logical inversion) is considered the failure or malfunction. This is more easily handled by using symbols. In the Task Analysis, tables of the various system and power unit tasks were listed and a numerical symbol assigned for each function. The symbol (0211) signifies the active function of Positioning the Output Relative to the Moving Power During a Desired Clutching Operation, see Table XI. The symbol for not performing this function is here assigned as (90211). For the purposes of this failure analysis the malfunctions or task failure mode numbers are the task numbers preceded by the symbol (9); e.g. (902, 9021, 90111, etc.).

Detailed Failure Mode Analysis by Listing

A sample of the detailed analysis for one branch of the tree diagrams is shown on a representative Task Failure Mode and Consequence Analysis sheet shown in Figure 15.

This highly organized failure mode analysis was made for both the ACTIVE and PASSIVE functions from the system level to the part and material level.

Failure Mode Logic Diagrams (Figures 16 and 17)

From the field surveys of the environmental hazards and the application requirements the decision was made that two VEN system malfunctions are significant for both safety of flight and mission abort. The two system failure modes are:

(1)   LOCKED, OPEN - Nozzle fixed in open position.

(2)   RUNAWAY, OPEN - Nozzle slews full open.

It is these two system failure modes which were analyzed in the construction
of the logic diagrams.

Of the many factors considered, four main ones were recorded and make up
the diagrams. The four main factors are:

(1)   Part contributing to system failure mode

(2)   Qualitative Consequence Rating

(3)   Basic Material Failure Mode

(4)   Redundancy

The part contributing to the system failure mode is shown by a number in a
box such as:

$$\boxed{216}$$
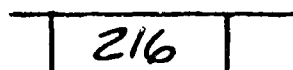
The number is the ITEM NO. assigned to the particular part from the power
unit hardware list.

The qualitative consequence rating is shown by a decimal number such as:

$$\boxed{.32}$$
$$\boxed{. \; 216}$$
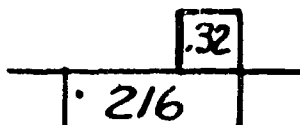
This rating results from the evaluator's estimate of the probability that the
part failure causes system failure. Only four different values were used in
this analysis. A list of the ratings and their definitions are shown on
Table XII.

The basic material failure mode is shown symbolically by another number such
as:

$$\boxed{04,05 \mid .32}$$
$$\boxed{216}$$
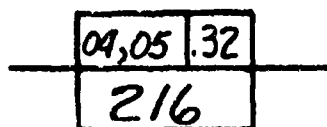
The list of basic material failure modes is shown on Table XIII with the
assigned symbols.

It must be determined if parts are acting in series with other parts (no re-
dundancy) or are in parallel with other parts (redundancy) in the study of
part contribution to system failure. Once this is determined it is shown as:
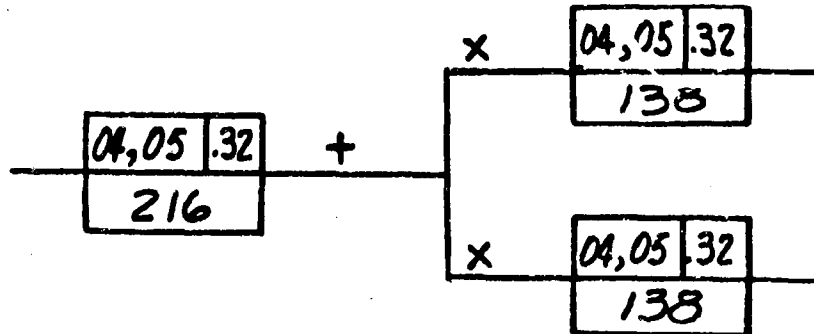
The (+) is a symbolic (OR) and the (X) is a symbol meaning (AND). The
diagram above is read as - "If part 216 fails it is possible that system
failure will occur OR if parts 138 AND 138 both fail it is possible that
system failure will occur". The evaluators estimate of the probability of
system failure as well as the material failures considered can be read from
the diagram.

Logic diagrams for the two VEN system failure modes (1) LOCKED, OPEN and
(2) RUNAWAY, OPEN were constructed and are shown in Figures 16 and 17.

TABLE XII

QUALITATIVE CONSEQUENCE RATING

		R*	Q*
A.	Total failure to complete task	0.00	1.00
B.	More likely not to complete task, but completion is possible	0.17	0.83
C.	More likely to complete task but failure is possible	0.68	0.32
D.	Very unlikely that task is jeopardized	0.98	0.02

* R = Reliability = Probability of Success

Q = Unreliability = Probability of Failure

Table XIII

BASIC MATERIAL FAILURE MODES

MODE	SYMBOL
Fatigue	01
Wear	02
Galling (Surface Seizure)	03
Ultimate (T, C, and S)	04
Yield (T, C, and S)	05
Creep/Rupture	06
Spalling	07
Corrosion	08

PROJECT _____

PREPARED BY_____

INDEX NO.	FUNCTION (TASK)			RANK	MAL-FUNCTION (FAILURE)			
	GROUP OR COMPONENT		MISSION TASK		FAILURE MODE NO.	TASK FAILURE MODE	CODE NO.	ILL ODE
	CODE NO.	TASK NO.						
20.1	021		Actuate on Desired Signal		9021	Not Actuate on Desired Signal	30	0
30	0211		Position Output Relative to Moving Power		90211	Not Position Output Relative to Moving Power	40	0
40	02111		Provide Position Relative to Moving Power		902111	Not Provide Position Relative to Moving Power	50	0
50	021111		To Open Nozzle		9021111	Not In Open Nozzle	20-100	0
							20-103	0
							20-130	0
							20-131	0
							20-136	0
							20-137	0
							20-139	0
							20-140	0
							20-141	0
							20-142	0
							20-150	0
							20-158	0

TASK FAILURE MODE AND CONSEQUENCE ANALYSIS

FAILURE CODE	TASK FAILURE MODE	SOURCE GROUP OR COMPONENT CODE NO.	SOURCE GROUP OR COMPONENT TASK NO.	CAUSATIVE TASK FAILURE OR TASK REQUIREMENTS OF SOURCE GROUP	RECEIVER GROUP OR COMPONENT CODE NO.	RECEIVER GROUP OR COMPONENT TASK NO.	AFFECTED TASK OR TASK REQUIREMENTS OF RECEIVER GROUP
		MAL-FUNCTION (FAILURE)		CAUSE			EFFECT
	Not Actuate on Desired Signal	30	0211	Position Output Relative to Moving Power	100	02	Change Relative Position at Desired Signal
	Not Position Output Relative to Moving Power	40	02111	Provide Position Relative to Moving Power	20.1	021	Actuate on Desired Signal
	Not Provide Position Relative to Moving Power	50	021111	To Open Nozzle	30	0211	Position Output Relative to Moving Power
	Not In Open Nozzle	20-100	0211111	Change Position About Mx Axis (3 Gears)	40	02111	Provide Position Relative to Moving Power
		20-103	0211111	Change Position About Mx Axis			
		20-130	0211111	"			
		20-131	0211111	"			
		20-136	0211111	"			
		20-137	0211111	"			
		20-139	0211111	`			
		20-140	0211111	"			
		20-141	0211111	"			
		20-142	0211111	"			
		20-150	0211111	"			
		20-158	0211111	"			

FIGURE 15

55

CAUSATIVE TASK FAILURE OR TASK REQUIREMENTS OF SOURCE GROUP	CODE NO.	TASK NO.	AFFECTED TASK OR TASK REQUIREMENTS OF RECEIVER GROUP	INDICATION	REDUNDANCY	TIME	QUAL.	QUAN.	REMARKS
sition Output lative to ving Power	100	02	Change Relative Position at Desired Signal						
ovide Position lative to ving Power	20.1	021	Actuate on Desired Signal						
Open Nozzle	30	0211	Position Output Relative to Moving Power						
ange Position out Mx Axis 3 Gears)	40	02111	Provide Position Relative to Moving Power						
Change Position bout Mx Axis									
"									
"									
"									
"									
"									
"									
"									
"									
"									
"									

FIGURE 15

55

FIGURE 16. *FAILURE MODE LOCKED-OPEN NOZZLE*

$+$ = OR
$\times$ = AND
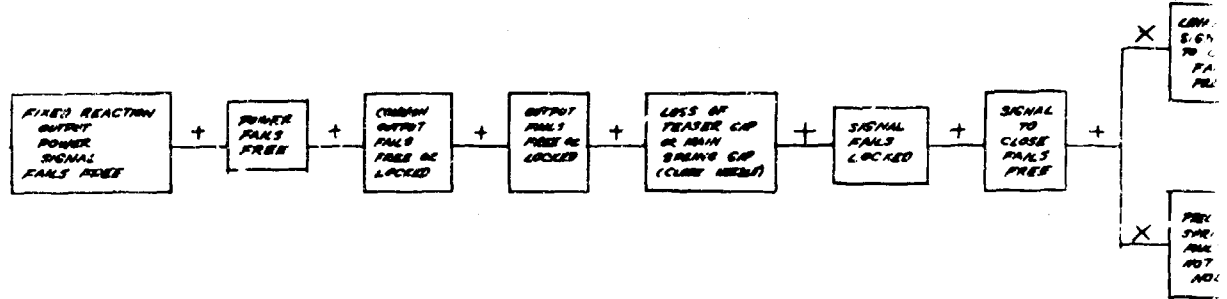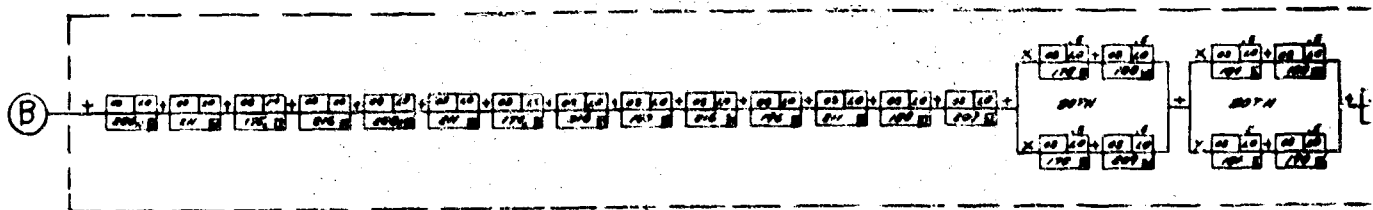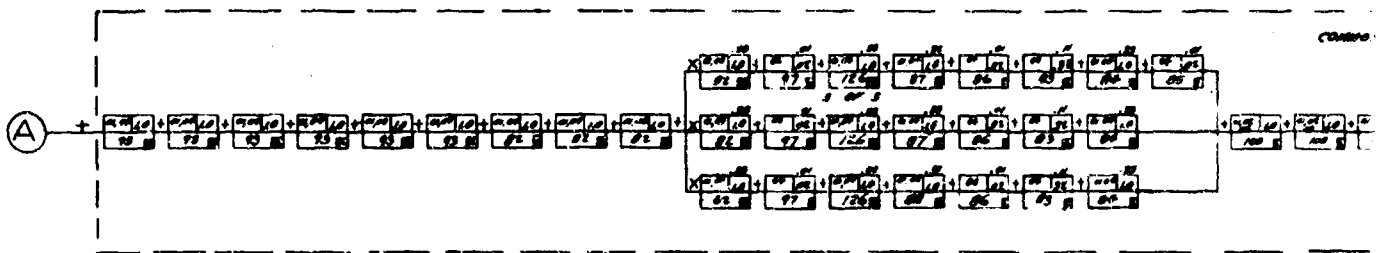
POWER

OUTPUT

SIGNAL

NOZZLE

SIGNAL TO CLOSE FAILS FREE

LINKAGE & SIGNAL TO OPEN FAIL FREE
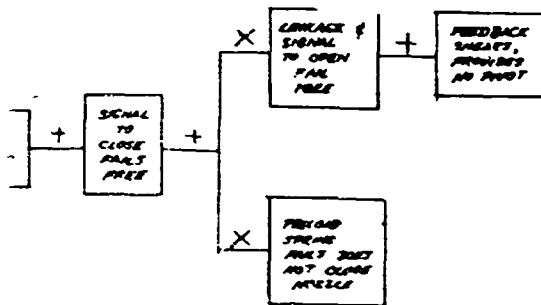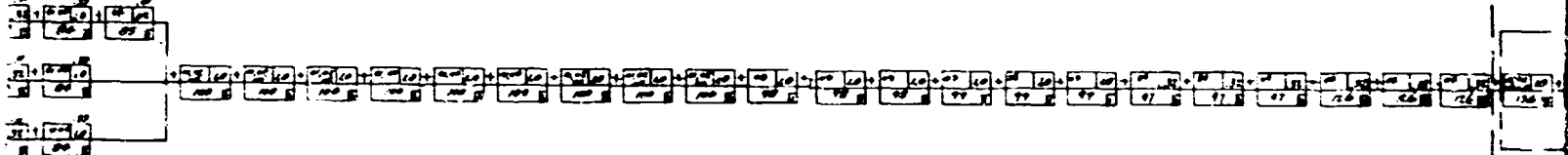
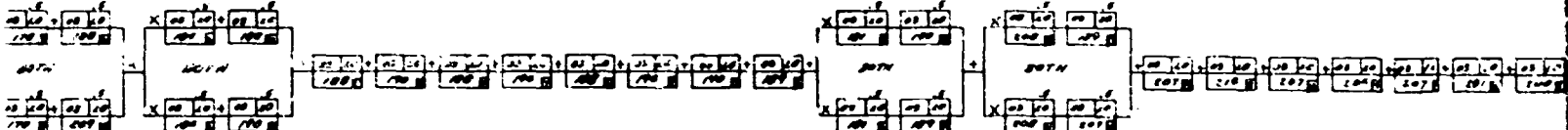FEEDBACK SHEATH, PROVIDES NO PIVOT
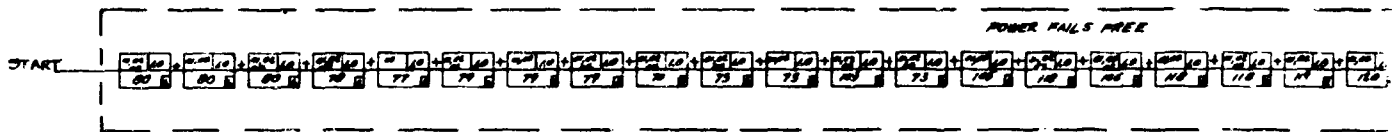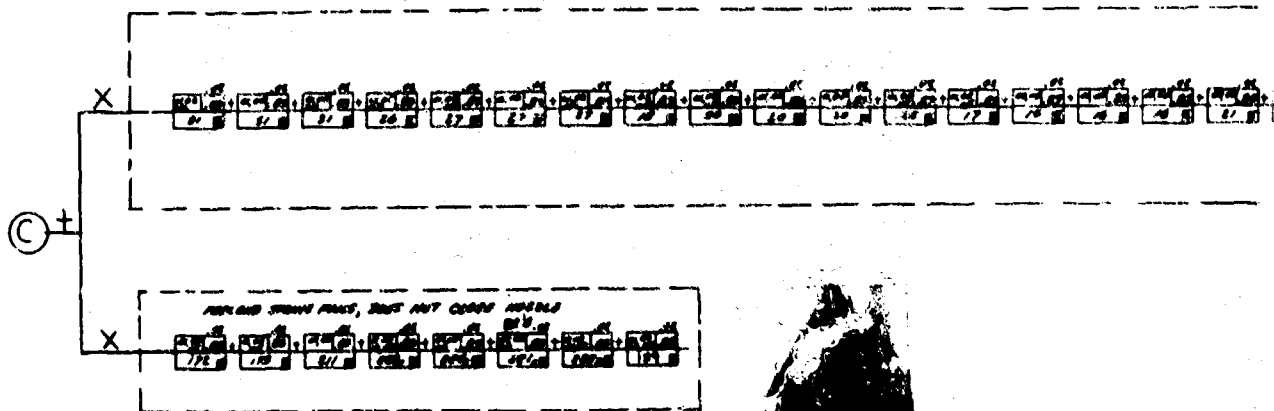
FREE CAP STROKE FAILS DOES NOT CLOSE NOZZLE

LS FREE

COMMON OUTPUT FAILS FREE OR LOCKED

SIGNAL FAILS LOCKED

BOTH

BOTH

BOTH

BOTH

LINKAGE & SIGNAL TO OPEN FAIL FREE

FIXED REACTION, OUTPUT POWER & SIGNAL
HALF PHASE

(CLOSE NOZZLE)

— (B)

SIGNAL TO CLOSE FAILS FREE

— (C)

NOZZLE SHROUD; ASSUMED TO ROOT

FAILURE MODE LOGIC DIAGRAM
(MODE 1A - SUCCESS, OPEN, C.P. = 1.0)

L - 13753

57

FIGURE 17. FAILURE MODE RUNAWAY - OPEN

$+ = OR$
$X = AND$

UNWANTED SIGNAL ENGAGES TO POWER INPUT

LOSS OF DISC GAP (ANALLY)

SEIZURE OF SIGNAL TO INPUT

D

SIGNAL PARTS FAIL FREE

PRELOAD SPRING FAIL, DOES NOT CLOSE NOZZLE

FIXED REACTION FOR OUTPUT AND POWER FAILS FREE

FAILURE MODE LOGIC DIAGRAM

FAILURE MODE LOGIC DIAGRAM
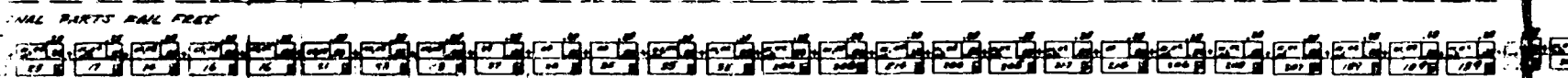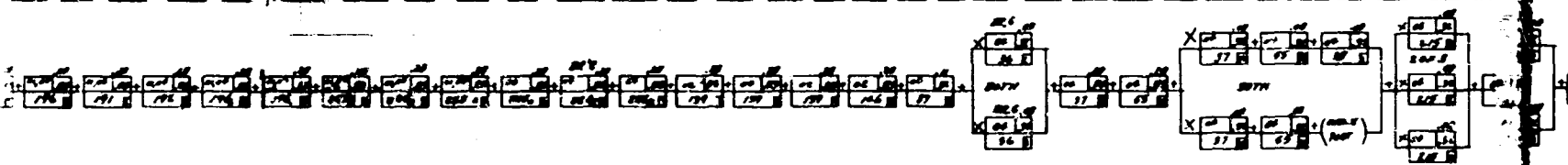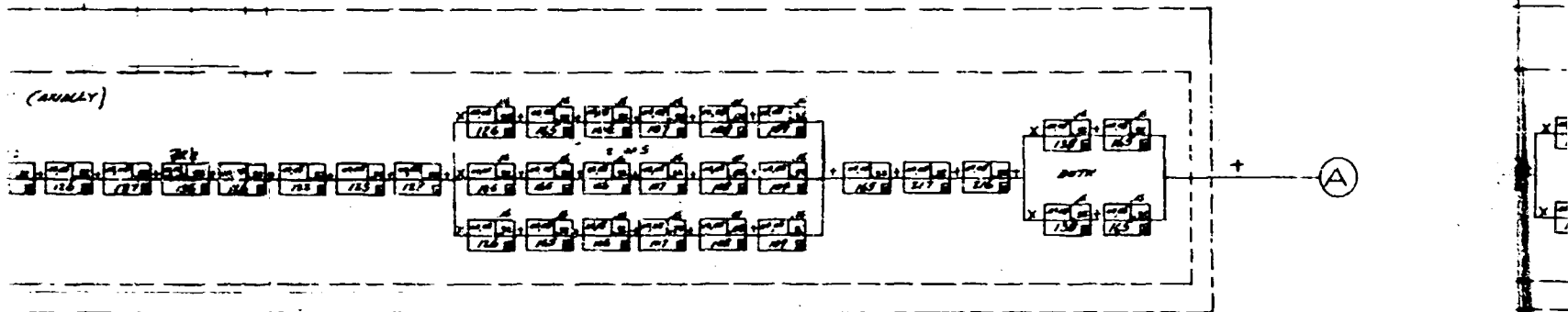
Load Stress Analysis

A conventional static stress analysis was made of most of the parts of
the power unit based on quasi-static loads. A dynamic stress analysis,
based on loads determined by analog studies was also made. Wear-life
parameters were summarized from those outputs from the analog study program
specially designed for this purpose.

These results were employed for ranking purposes to determine the critical
parts as described later in this report.

The entire analysis was initiated with the following simultaneous considera-
tions: a parts discrimination to obtain a nuclei of parts for analytical
purposes, the judicious segregation of significant parameters, and the
selection of appropriate analyses.

A conglomeration of 343 parts in the power unit necessitated a discriminatory
process to obtain a nuclei of parts reserved for analytical purposes. This
was a compromise on the basic plan, made for program scheduling reasons, to
fit a complex program in a short calendar time. The failure mode and con-
sequence analysis should have been first. This was accomplished via a
mental ranking of parts based upon previous experience and general consid-
erations. For instance, the 141 attaching parts and 11 seals were not con-
sidered. However, the 17 gears, 26 bearings and 136 mechanical parts were
considered and mentally ranked.

There are many common parameters which can be employed for an evaluation of
the integrity of parts. An investigation of the available parameters pro-
duced only a few segregated parameters. They are the following: stress,
load levels, bearing lives, cumulative damage and a wear-life parameter.
The evaluation of these parameters form the basis of various ranking criteria
for the nuclei of analyzed parts.

The analysis was subdivided into three phases. (1) a static stress analysis
was accomplished in which two load levels were evaluated for comparative
purposes; (2) a dynamic stress analysis was accomplished in which the data
obtained from the analog study was applied to a few selected parts in order
to establish the cumulative damage during a specified time interval; (3) a
wear-life analysis was accomplished wherein the majority of the wear life
parameters are integrated.

The static stress analysis consisted of three sections. The first was a
gear train torsional analysis, wherein two steady torque levels were applied
independently to obtain the torques for particular gears. The second, the
beam strength of the gear teeth was evaluated and third, the bearing loads
and lives were developed. The static analysis was concluded with a ranking
of gears and a ranking of bearings.

61

The dynamic stress analysis was concerned with the application of dynamic loads to a few selected parts in order to calculate cumulative damages. Due to the limitation of time, a complete dynamic stress analysis of all parts was obviously impossible and therefore another objective was established; namely, to calculate the cumulative damage for a few parts and thereby establish the method of dynamic stress analysis.

The method of analysis used was not complicated but required a number of iterative operations. The time spectrum was defined for a one-hour flight mission and the torque or stress encountered as a function of time. With this information, it was possible, after appropriate calculations, to obtain the torque or stress levels, the corresponding number of cycles, and then the cumulative damage. This method was employed for three parts, the 161718 output reduction gear, the 168622 right hand clutch output gear, and the 166732 right main spring.

The Wear-Life Analysis developed tables of summations of an integrated wear-life parameter for the sample one-hour flight mission. These parameters cannot be, at the present time, directly related to "wear" but are useful for relative ranking within this class of parameters. Recommendation is made that future work consider methods of making this type of data more concrete.

In order to assist in the development of a method for ranking critical parts, the VEN actuation system was simulated on the GEDA analog computer.

A circuit was developed to measure wear parameters of critical parts for wear life determination. Counters were used to record stress spectrum in order to determine fatigue damage.

Records were made of various critical parameters using typical test inputs. These records will be used to determine the dynamic stresses and life of critical parts.

Description of the Analog Simulation

The analog computer simulation was made of the VEN actuation system and included the dynamic elements of the following:

    1.   Power unit drive system.
    2.   Power unit.
    3.   High speed shaft.
    4.   Actuator with friction load.

The power unit drive system consists of a shear link, gears, an over-running spring clutch (drives positive torques, over-runs negative torques) and gearing to the input drive drums. These dynamics have little effect on the operation of the power unit.

The power unit analog simulated the dynamic operation of the elements shown below.
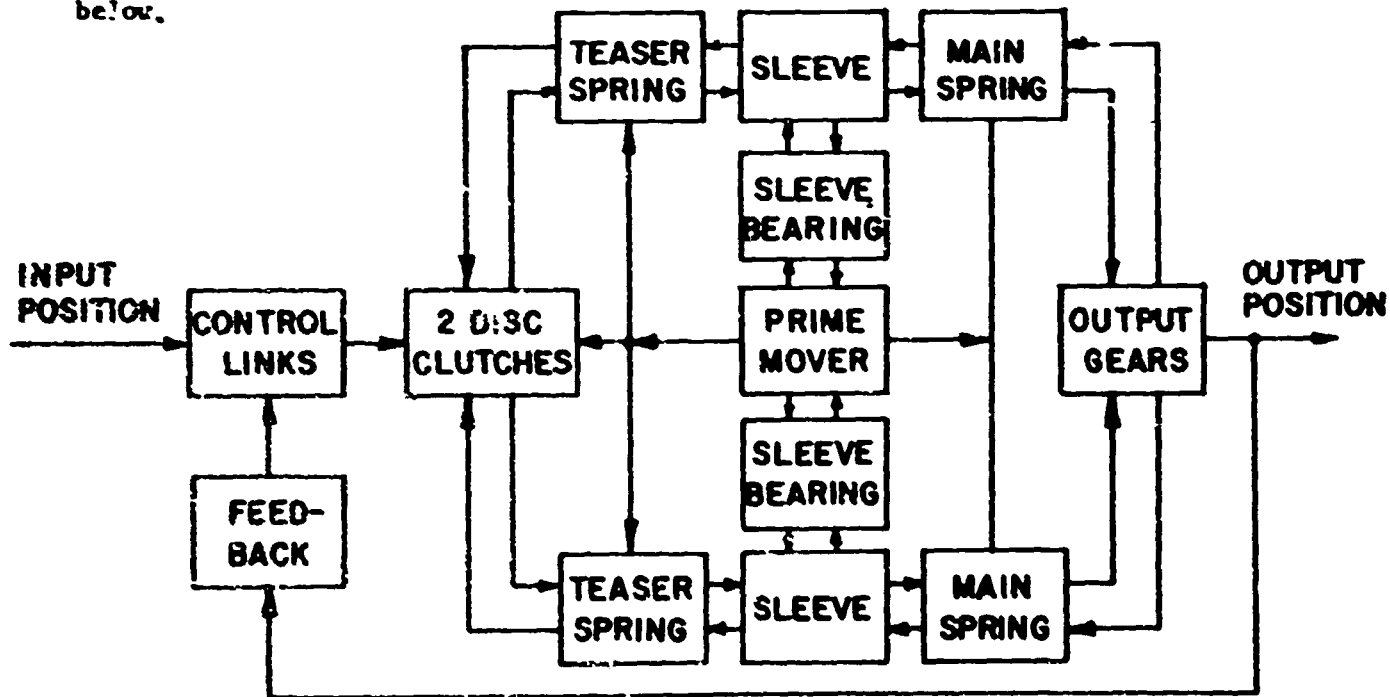
FIGURE 18

The high speed shaft and actuator elements were represented by a spring-mass system with deadzone in the shaft windup angle (backlash in position) and friction type load. One shaft and actuator was made to represent 3 sets by multiplying the reaction torques on the power unit by 3. The arrangement of elements is shown below:

Figure 19 High Speed Shaft and Actuator

Wear can be related to the energy dissipated at a surface or within an element. To provide some insight into this condition, a number of wear parameters were measured. Some of these parameters were in actual units of energy. However, in some cases the force measured was normal to the direction of motion and a coefficient of friction and a radius of action would be required to convert to energy. Actual conversion of the data obtained required additional study or analysis, however, time limitations did not permit this for inclusion in this report.

.4425 LB/$_V$ (REFERRED TO INPUT)

+ Fc

.025 $\frac{IN./SEC}{V.}$ (REFERRED TO INPUT)

$-\dot{\lambda}$ ERR

.0022 IN. LB/$_V$

ℓ_{FB}

5×10^2

I.C.

1.106

$\frac{IN.-LB/SEC}{V.}$
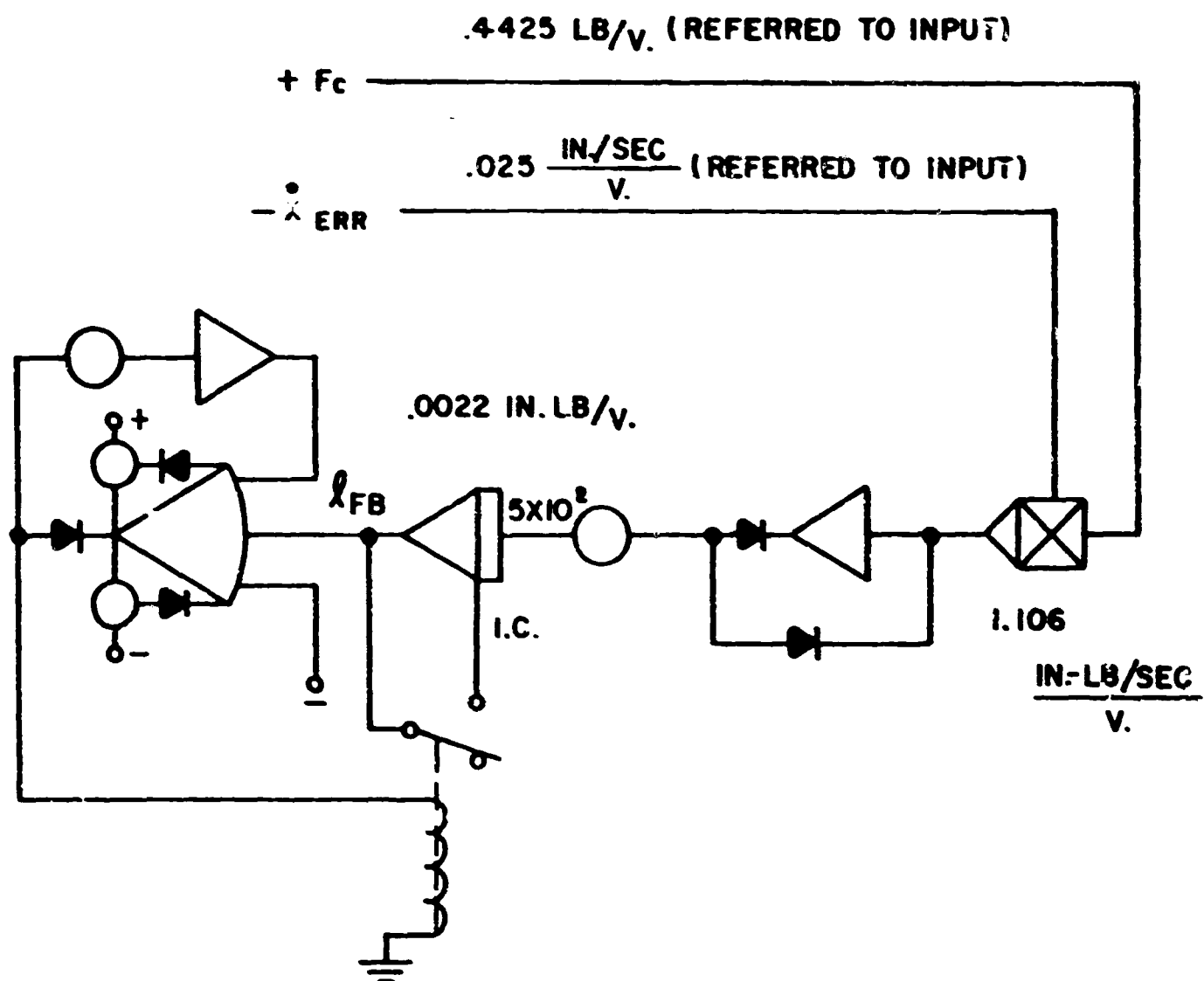
ANALOG CIRCUIT TO DETERMINE

LIFE OF CONTROL LINKAGE

FIGURE 20

65

ω_7 5.31 RAD/SEC/V.

.5 LB/V.

F_c

.53 $\dfrac{LB-RAD}{V.}$

ℓ_0

5×10^2

I.C.

265.5

$\dfrac{LB-RAD/SEC}{V.}$
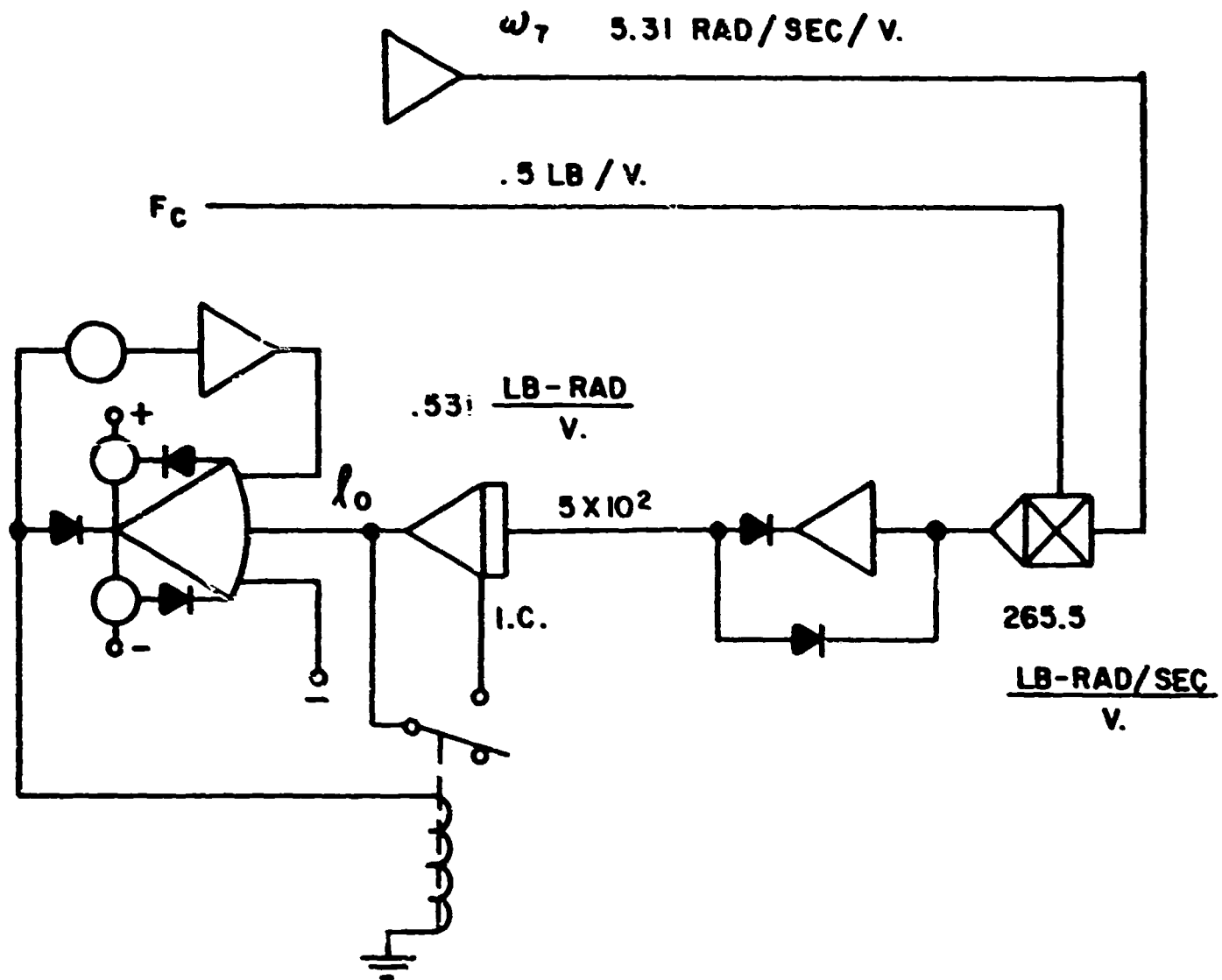
ANALOG CIRCUIT TO DETERMINE

LIFE OF OSCILLATING BEARING

FIGURE 21

$-|F_C| \times R_D$

$-\mu_D$ ----

$+Q_D$ .316 IN. LB/V

SLI

(FROM ACTUATION SYSTEM)

$-2\omega_7$	4 RAD/ SEC /V	1
$-\omega_D$	8 RAD/ SEC /V	1
$+\omega_7$	8 RAD/ SEC /V	1

$(\omega_D - \omega_7)$

8 RAD/SEC/V.

(FROM DRIVE SYSTEM)

.0843 $\frac{\text{IN. LB RAD}}{V.}$

I_D

30×10^2

I.C.

253

IN. LB-RAD/ SEC
V.
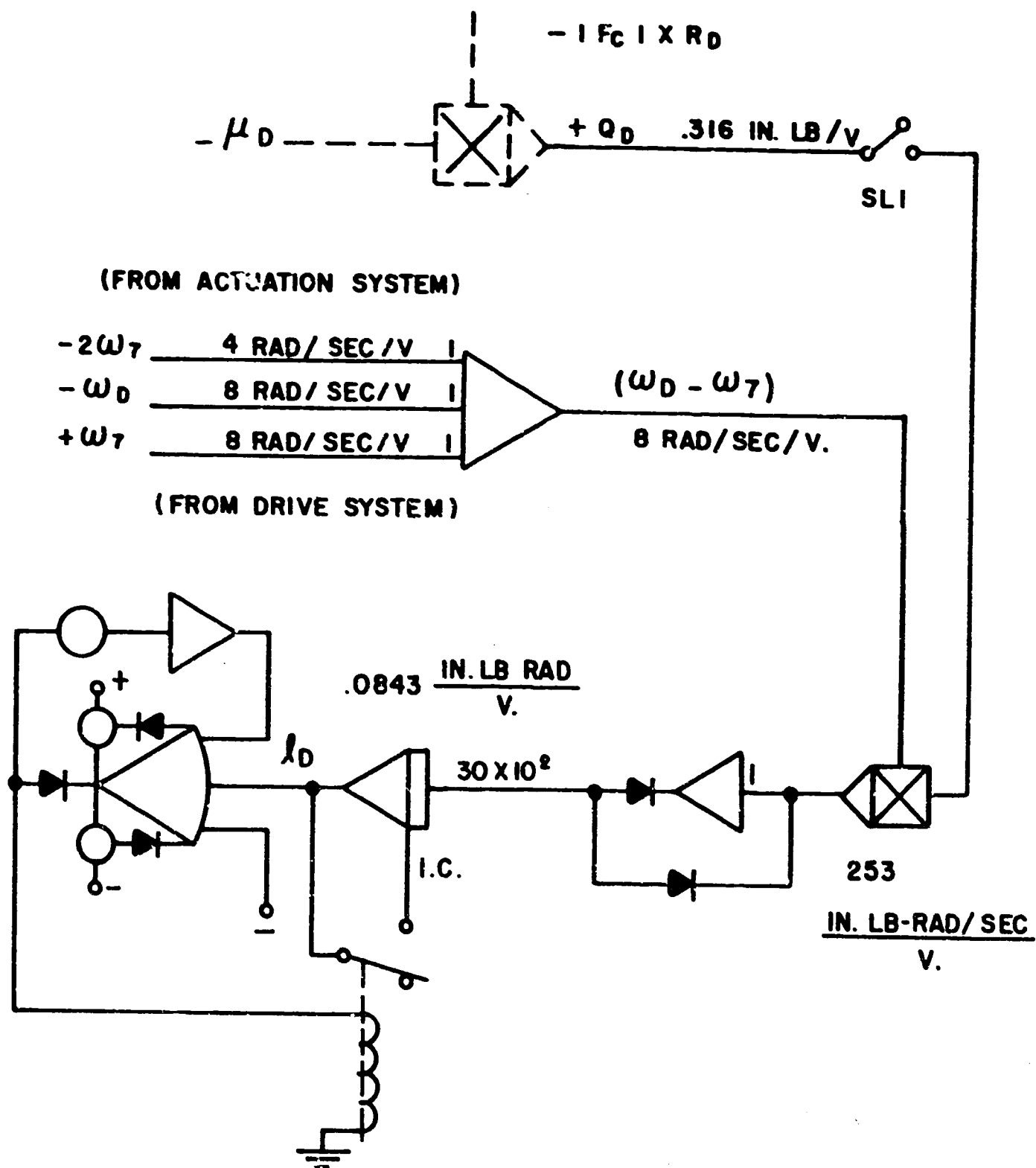
ANALOG CIRCUIT TO DETERMINE

LIFE OF DISC CLUTCH

FIGURE 22
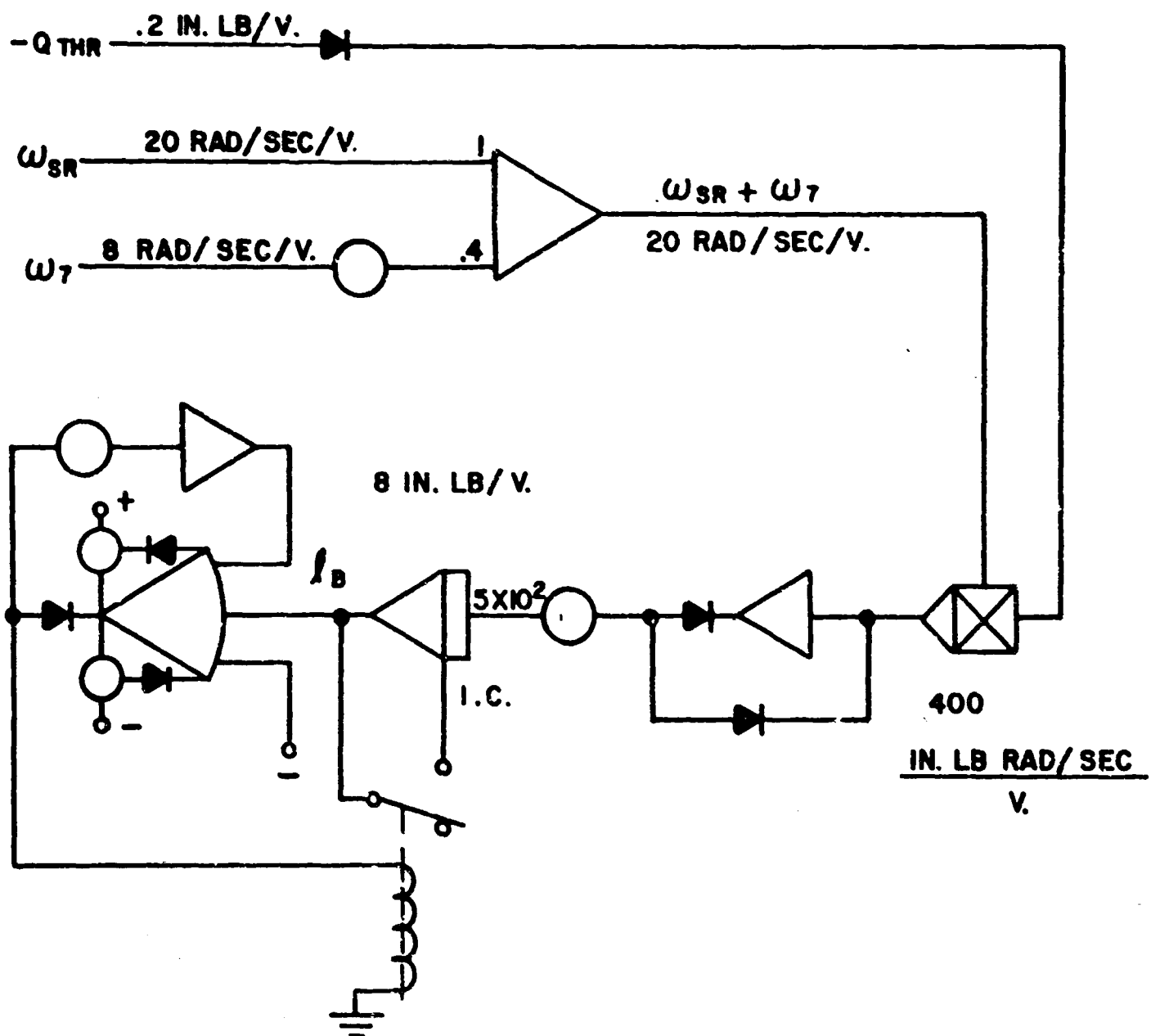
ANALOG CIRCUIT TO DETERMINE

LIFE OF RIGHT SLEEVE BALL BEARING

FIGURE 23
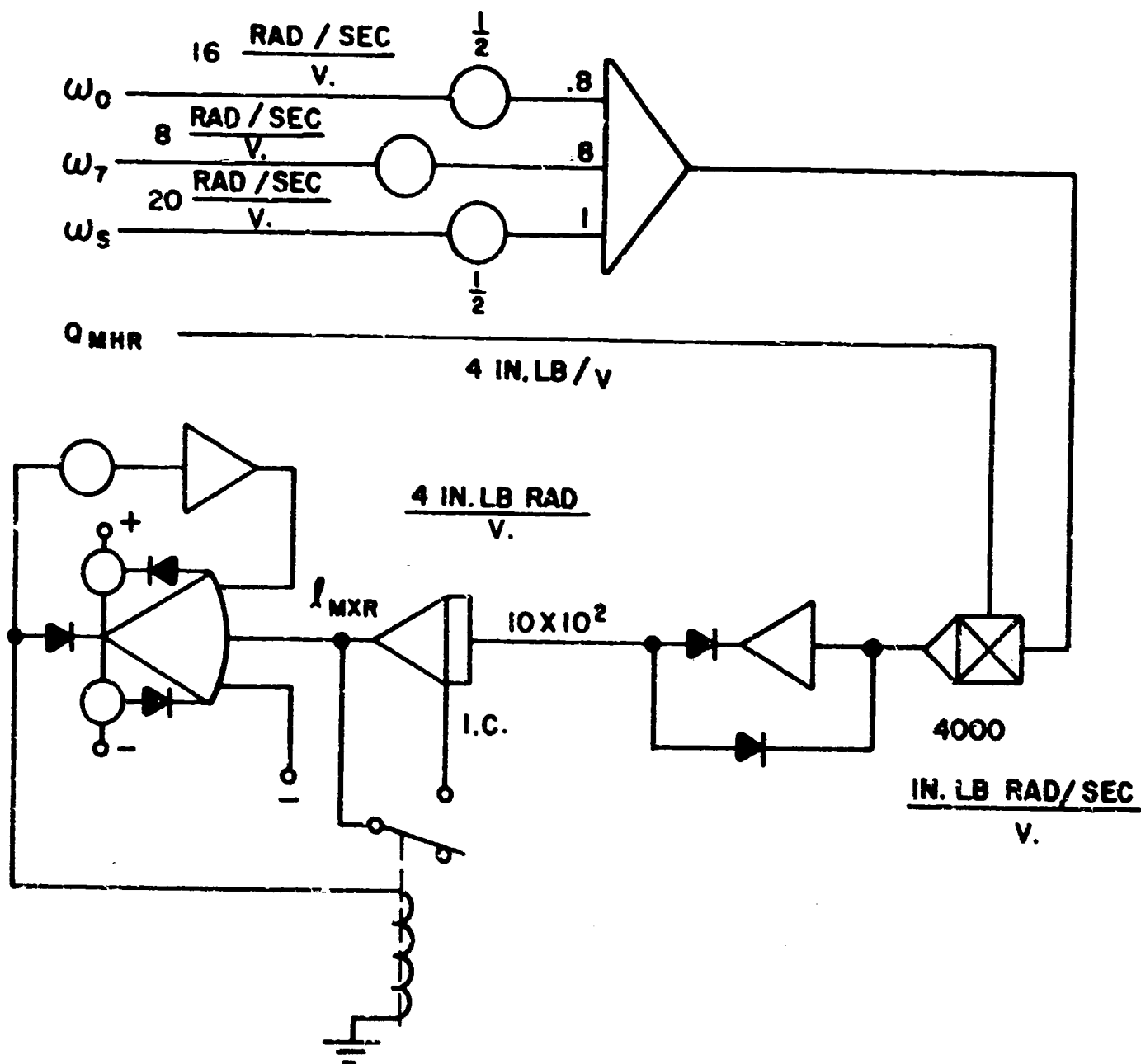
ANALOG CIRCUIT TO DETERMINE

LIFE OF MAIN RIGHT SPRING

FIGURE 24
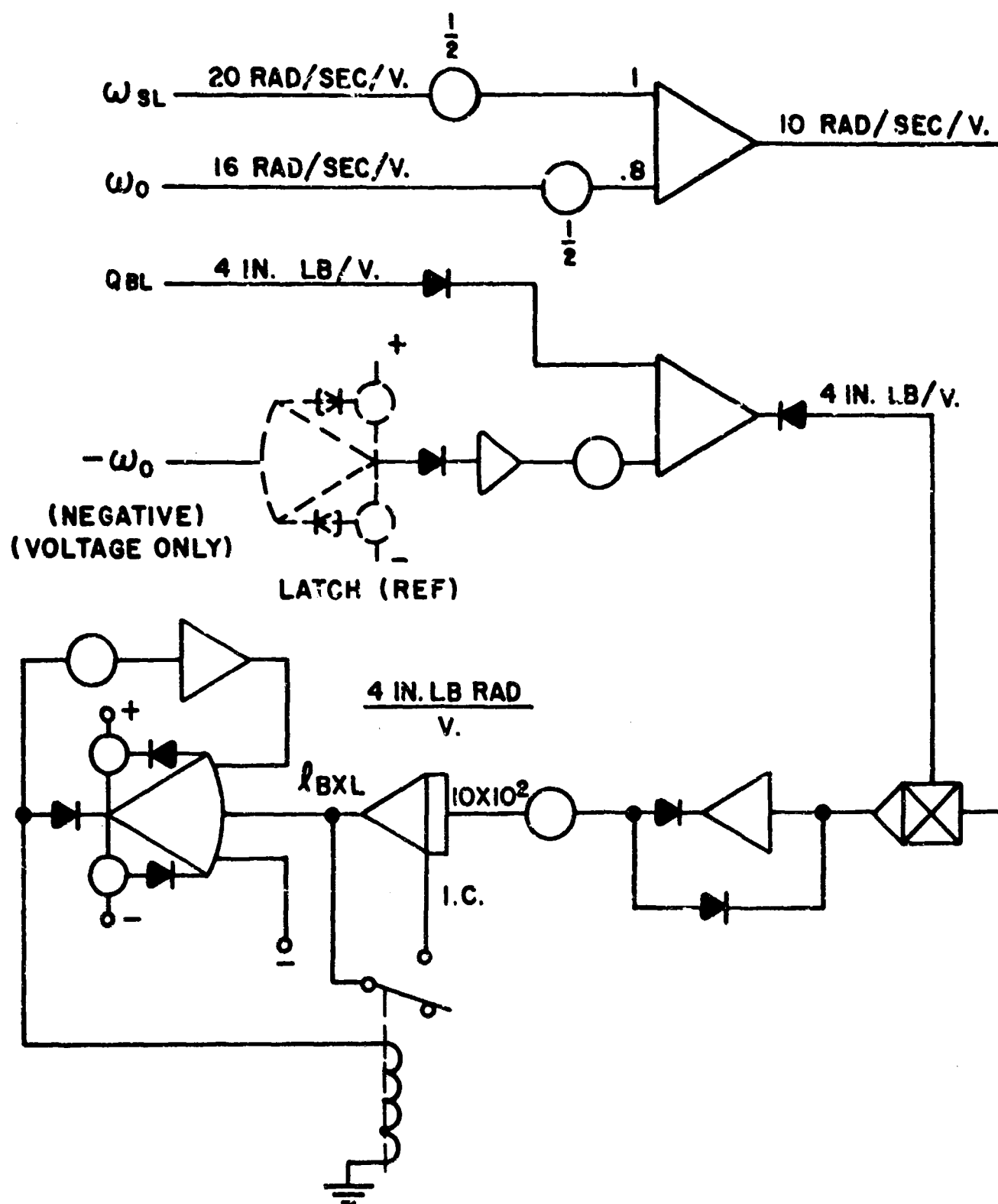
ANALOG CIRCUIT TO DETERMINE

LIFE OF LEFT BRAKE

FIGURE 25

4 RAD / SEC / V.

$-\omega_o$

$+\Delta\theta_{H.S.}$ .I RAD / V.   3Q H.S.

$3G_S K_{HT}$ 5.03 IN.-LB/V.
(REFERRED TO
SPRING SHAFT)

2.0I IN.-LB-RAD/V.

l_{OB} $IOXIO^2$

I.C.

2010

IN. LB RAD/ SEC
—————————
V.
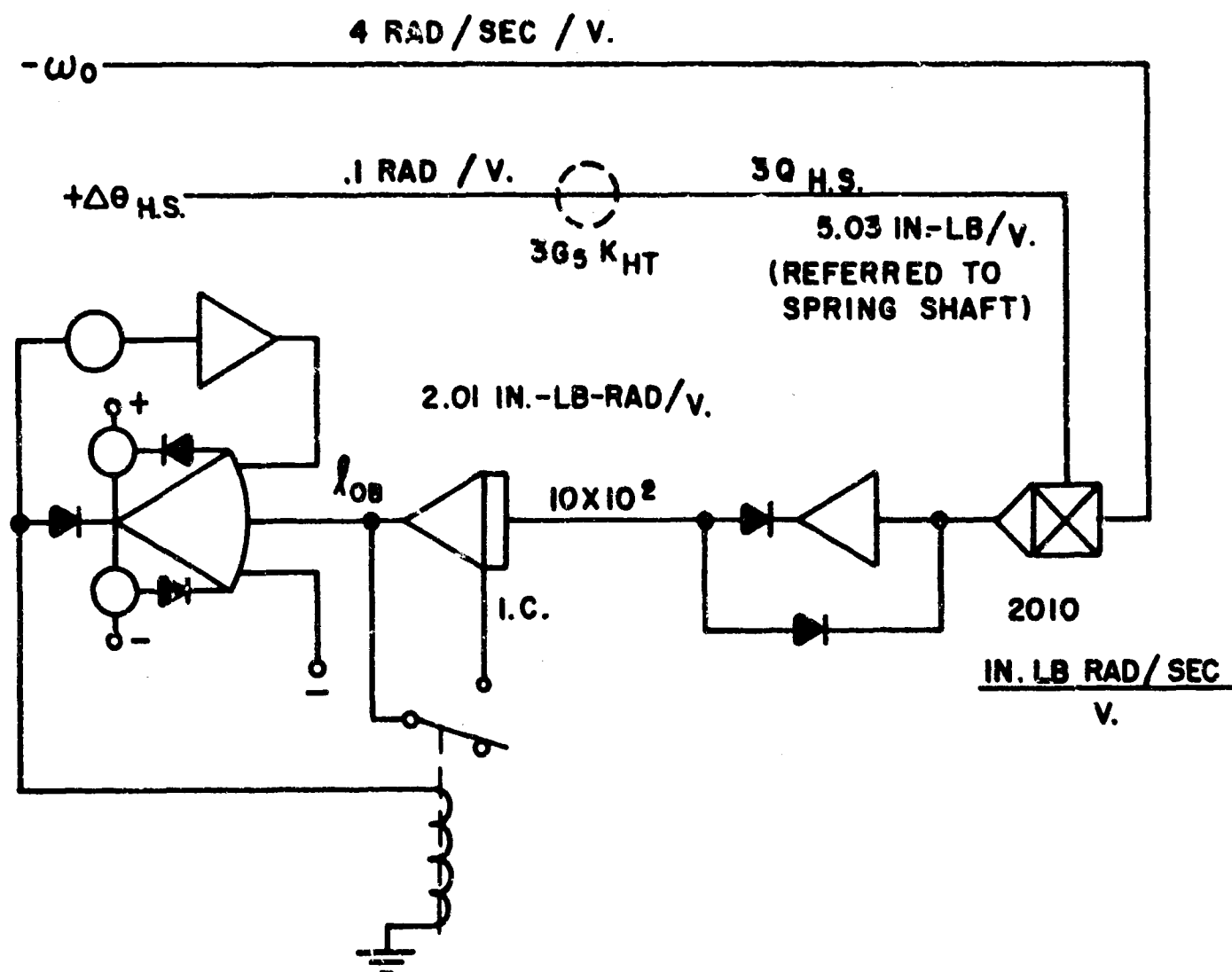
ANALOG CIRCUIT TO DETERMINE

LIFE OF OUTPUT COMPONENTS

FIGURE 26

71
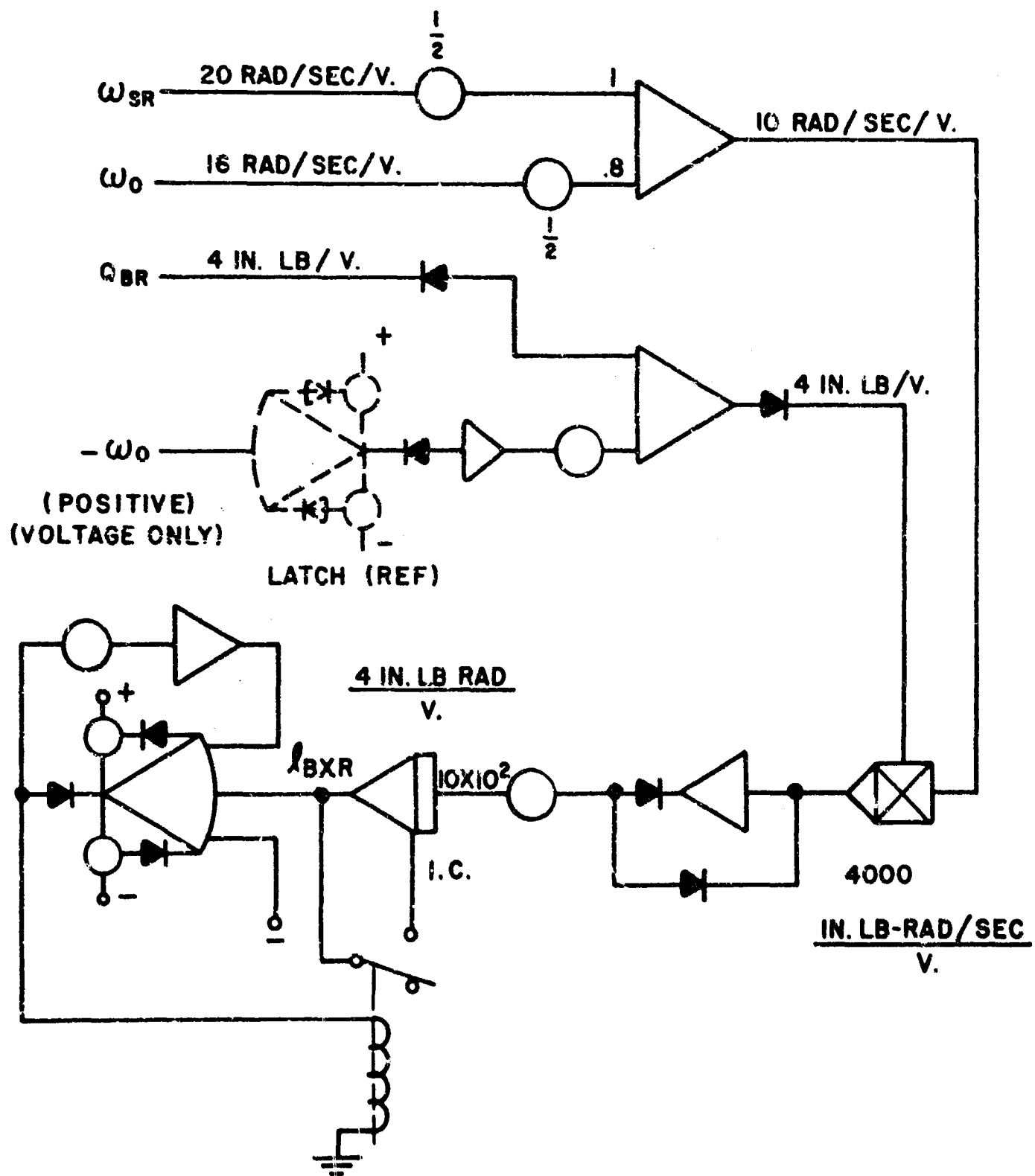
ANALOG CIRCUIT TO DETERMINE

LIFE OF RIGHT BRAKE

FIGURE 27

Ranked Causes

Prior work has looked at the VEN power unit hardware and has considered all the parts that could conceivably cause a system failure of either LOCKED, OPEN NOZZLE or RUNAWAY, OPEN NOZZLE. The main factors considered during the failure mode analyses have been recorded by means of "logic diagrams". The next step, in the effort to assess and accelerate testing for the reliability of a complex mechanical component is the listing of the parts in order of importance. The following describes the methods developed and used in indicating first, the critical parts and second, the most critical parts.

The failure mode logic diagrams of the foregoing step depict the part contributors to the system failure modes, the material failure mechanism associated with the part failure, the probability of part failure causing system failure and the arrangement of redundant or back-up hardware. The decisions for ranking, the mathematical model, the technique for ranking of parts, and the list of ranked VEN parts and material failure modes follow.

Ranking Criteria - The most critical system failure modes were previously defined as a LOCKED, OPEN NOZZLE failure or a RUNAWAY, OPEN NOZZLE. Should either of these system failures be caused to occur, it is considered that the consequences could be loss of flight safety or mission abort. It is logical then to state that the parts contributing to either of these system failure modes will be more critical than the parts not affecting either mode. The logic diagrams are a record of the part contributors. Indicating which of these critical parts is the most critical now becomes the problem. An optimum ranking method would assign each part and material failure mode a numerical value so that they could be listed in order of their importance. It appears that values can be arrived at based on three criteria. The factor for ranking is here expressed as:

$$F(R) = (P_{SF|PF}) \times (P_{PF}) \times (C.I.)$$

where

$F(R)$ = Factor for ranking.

$(P_{SF|PF})$ = Probability that part failure causes system failure.

(P_{PF}) = Probability of part failure.

$(C.I.)$ = Critical influence or number of times each part contributes to a failure mode.

73

In describing the construction of the logic diagrams, one of the terms used was qualitative consequence rating. This was defined as the probability that the part failure causes system failure, as estimated by the evaluator. By definition then:

$$\text{Qualitative Consequence Rating} = (C.R.) = (P_{SF|PF})$$

The logic diagrams serve as useful tools in determining numerical values for two of the three ranking criteria, namely (C.I.) and (C.R.). The (C.I.) value can be gotten for each part by counting the number of times the part appears in all the failure mode logic diagrams. The (C.R.) can be arrived at by the same manner; however, some modification is required where parts are used as redundant or back-up members. The symbol for the modified value has been taken as:

$$(C.R.') = \text{Modified consequence rating}$$

Since it is the average of the (C.R.') and sum of the (C.I.) values that are of interest, the ranking expression now becomes:

$$P(R) = (C.R.') \text{ Avg.} \times (P_{PF}) \times (C.I.)_{TOTAL}$$

Mathematical Model - The logic diagrams form the basis for a mathematical model for ranking the part failures. It was noted in the earlier description of the failure analysis that there were two additional symbols on the blocks of the diagrams which were not discussed. These symbols were used during this ranking phase. The number in the smaller block within the part number block such as:
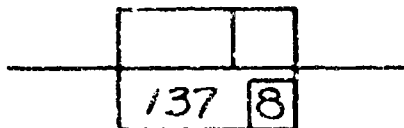
is the (C.I.)$_{TOTAL}$ for that part for all the failure modes analyzed. In the example shown above, part or ITEM NO. 137 could conceivably be a contributor to the two system failure modes a total of eight (8) different times or ways.

The decimal number above the (C.R.) block is the modified value (C.R.') such as:
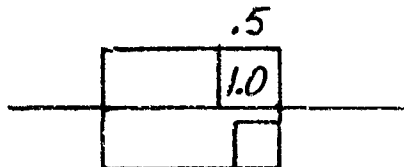
The modified value for each part was arrived at by considering the arrangement of series (no redundancy) or parallel (redundancy) paths of hardware. The rules established and used in this analysis for modifying the (C.R.) are as follows:

If series,	$(C.R.') = (C.R.)$
If double parallel	$(C.R.') = (C.R.)/2$
If triple parallel	$(C.R.') = (C.R.)/3$
If n parallel	$(C.R.') = (C.R.)/n$

74

After the construction of the logic diagrams, the (C.R.') values were
assigned and the mathematical model was evolved. The (C.I.) and (C.R.')
for each part and each system failure mode was counted and recorded. This
was done for the VEN power unit and two failure modes. The individual rank-
ing is based upon the larger $(C.I.)_{TOTAL}$ or larger $(C.R.')_{AVG.}$ as being
the more critical.

To show the results of this ranking method more vividly, plots were made of
$(C.I.)_{TOTAL}$ x $(C.R.')_{AVG.}$ per PART as a function of NUMBER OF PARTS. The
plot for all parts requiring "prime reliability" is shown in Figure 28
and the plot for all the parts not requiring "prime reliability" is shown in
Figure 29 . A "prime reliable" part as used in this analysis is defined as
one with a $(C.R.') = 1.0$. This means that somewhere in the diagrams, a
particular part has appeared in a series arrangement and the qualitative
consequence rating was estimated to be 1.0. If failure of that particular
part did occur, then system failure was certain to occur.

Technique of Ranking Parts - It was stated above that three criteria formed
the basis for a ranking factor. Up to this point values for two of these
criteria were established from the mathematic models evolved from the logic
diagrams. Only the (C.R.') was used for any kind of ranking. The (C.R.')
value for each item determined the first list of critical parts by separat-
ing the "prime reliable" parts from the "non-prime" ones. Of the two hundred
twenty-four (224) items in the parts list, sixty-four (64) were selected as
being more critical from the standpoint of requiring "prime reliability" for
the two system failure modes considered. Of the one hundred sixty items re-
maining (224-64), the analysis designated sixty seven (67) additional items
which were critical by their appearance in the failure mode logic diagrams,
but did not require "prime reliability". Thus the original list of items
was greatly reduced and further efforts to assess and accelerate tests for
the reliability of the power unit needed concentrate only on these critical
parts.

The next step was to rank each list of "more critical" items to determine the
"most critical". Looking at Figures 28 and 29 it first appears that this
could be done using the product of $(C.I.)_{TOTAL}$ and $(C.R.')_{AVG.}$ as the rank-
ing factor. If this reasoning were followed then Housing 126 would be
listed most critical, Arm 188 next, then Gear Assembly 100, Mainshaft 211,
Housing 55, and so on down the curve for the "prime" parts. Looking over
any list of parts ranked by that method, it would be seen that almo.t always,
housing would be at the top of the list marked most critical. However, past
experience in the field of mechanical components has shown that rarely has
a housing or a similar part been the cause of a system failure such as has
been analyzed, mainly because a good mechanical design has recognized in
advance the criticality of such a part due to its complex functions. There-
fore, greater margins of safety are provided by incorporating generous fillet
radii, lower operating stresses, etc.

Allowances for design safety margins are inversely brought into the ranking

75

factor, $F(R)$, by the "probability of part failure" criterion, (P_{PF}). A value for this criterion should be established by the structural analysis for each particular part in question. The analysis is given direction by the material failure modes recorded on the logic diagrams. Once a value has been established for (P_{PF}) the ranking of each list can be accomplished by considering for each part the product of $(C.I.)_{TOTAL}$, $(C.R.')_{AVG.}$ and (P_{PF}). The part with the highest product of these three criteria is the most critical.

The technique for ranking of parts in order of importance is thus summarized as:

(1) Establish relative importance of system tasks.

(2) Construct logic diagrams for the most critical system failure modes.

(3) Establish list of "prime reliable" parts.

(4) Establish values of $(C.I.)_{TOTAL}$ and $(C.R.')_{AVG.}$ for all "prime reliable" parts using logic diagrams.

(5) Establish values of (P_{PF}) for all "prime reliable" parts by means of structural analysis.

(6) Establish ranking factor, $F(R)$, for all "prime reliable" parts by the product of $(C.I.)_{TOTAL}$, $(C.R.')_{AVG.}$ and (P_{PF}).

(7) List parts in order. Part with highest $F(R)$ value is most critical.

List of Ranked Parts of VEN Power Unit - As mentioned above, the recommended procedure for ranking of critical parts is to carry out steps (1) through (3) prior to any structural analysis of the parts. With the data from step (3), the structures analyst could be told on which parts to concentrate his efforts since the total parts list has by then been reduced to only "prime reliable" parts. For the VEN Power Unit, each of the sixty-four (64) "prime" parts designated by step (3) above would be studied and a value for the probability of failure for each part would be established.

However, the structural analysis for this program had been started earlier for program schedule reasons and was essentially completed about the same time as step (3). So instead of the analysis only considering the "prime reliable" parts, the analysis looked at many parts of the power unit. Unfortunately but logically, the stress, life and wear study (structural analysis) did not establish a probability of part failure for each "prime reliable" part. Items such as the input signal linkage system, housings, etc., were not

completely stress analyzed. Therefore, a complete ranked listing was not obtainable within the scope of this program.

Summaries of the results of the Stress-Life-Wear-Analysis present ranked lists of parts based on some value which is representative of (P_{pf}), probability of part failure. From the Static Stress Analysis, came the ranked list of gears based on margin of safety and the ranked list of bearings based on minimum life in hours:

Gears			Bearings	
Item No.	m.s.		Item No.	Life-Hrs.
136	0.11		99	71
137	1.03	*	218	382
100	3.12		135	926
105	4.35		98	955
121	4.71	*	111	1394
118	5.29	*	116	2594
151	5.70			
73	10.6			

From the Dynamic Stress Analysis, cumulative damage for an output reduction gear (Item 100) and the right hand clutch output gear (Item 136) were calculated based on a one-hour flight mission. The following values were obtained:

Gears	
Item No.	Cumulative Damage
136	$D = 5 \times 10^{-2}$
100	$D = 2 \times 10^{-7}$

During the construction of the two failure mode logic diagrams, it was evident that some parts were critical items because of the possibility of failing in the wear failure mode. The analog circuits were adapted to measure various wear parameters for some of the items highlighted by the logic diagrams. From the Wear-Life Analysis, the wear of the items investigated was calculated in terms of relative energy dissipated during a one-hour flight mission. The values are as follows:

---

* Not "prime-reliable" parts.

<u>Wear Parts</u>

Item No.	Energy Dissipated in.-lbs.-rad./flight
Output Bearings Gears, etc.	358,629
130	81,787
131	62,600
166 222	58,205
* 170 ⎱ * 221 ⎰	55,005 (lb.-rad.)
* 138 ⎱ * 139 ⎰	190

Establishing the ranking factor F(R) was the next step to be accomplished. As stated earlier, this factor was expressed as follows:

$$F(R) = (C.I.)_{TOTAL} \times (C.R.')_{AVG.} \times (P_{PF})$$

From Figure 26 , values of $(C.I.)_{TOTAL} \times (C.R.')_{AVG.}$ can be gotten for each "prime-reliable" part. From the above structural analysis summaries some form of a (P_{PF}) value will be used. If the reciprocal of Margin of Safety (1/m.s.) is used as a measure of (P_{PF}) for the parts called gears, then the ranking factor values would be:

Item	$(C.I.)_{TOTAL} \times (C.R.')_{AVG.}$	$\left(\dfrac{1}{m.s.}\right)$	F(R)	RANK
136	4.5	9.10	40.10	1
137	4.3	0.97	4.10	2
100	11.2	0.32	3.20	3
105	4.0	0.23	0.92	4
121	4.0	0.21	0.84	5
118	4.0	0.19	0.76	6
151	3.6	0.175	0.63	7
73	4.0	0.093	0.37	8

If cumulative damage is used as a measure of (P_{PF}) for the two gears studied, it can be readily seen that item 136 will again be ranked higher (more critical) than item 100.

---

* Not "Prime-Reliable" part

78

Item	$(C.I.)_{TOTAL} \times (C.R.')_{AVG.}$	D	F(R)	RANK
136	4.5	$5 (10^{-2})$	$22.5 (10^{-2})$	1
100	11.2	$2 (10^{-7})$	$22.4 (10^{-7})$	2

For the bearings, if the reciprocal of the life ($1/L$) is used as the measure of (P_{PF}) of the three "prime-reliable" parts analyzed, the ranking factor values would be:

Item	$(C.I.)_{TOTAL} \times (C.R.')_{AVG.}$	$\dfrac{1}{L}$	F(R)	RANK
99	3.0	$14.1 (10^{-3})$	$43.3 (10^{-3})$	1
135	4.6	$1.08 (10^{-3})$	$4.96 (10^{-3})$	2
98	3.0	$1.05 (10^{-3})$	$3.15 (10^{-3})$	3

For the items in which wear is the predominate material failure mechanism to cause part failure, the energy dissipated can be used for the (P_{PF}) value. Ignoring the output bearings and gears since they have already been considered in the above examples, the ranking factor values for the remaining items would be:

Item	$(C.I.)_{TOTAL} \times (C.R.')_{AVG.}$	E.D.	F(R)	RANK
130	5.0	$8.18 (10^{4})$	$40.9 (10^{4})$	1
220	3.15	$5.82 (10^{4})$	$10.4 (10^{4})$	2
131	2.5	$6.26 (10^{4})$	$15.7 (10^{4})$	3
166	1.0	$5.82 (10^{4})$	$5.8 (10^{4})$	4

Based on the various lists presented above and a study of Figure 28 , it was decided that the following items would be considered in the design of the experimental program for accelerated testing of material failure modes.

FATIGUE	WEAR	SEIZURE
Item 136	Item 130	Item 188
Item 99	Item 220	Item 211
		Item 201
		Item 189

It should be noted that the items under Fatigue and Wear were decided upon

79

using the technique of ranking parts developed in this report. However, the items listed under Seizure were decided upon after studying Figure 28 choosing the items with a large $(C.I.)_{TOTAL} \times (C.R.')_{AVG.}$ value that were not listed by the ranking technique, and from past experience, mentally assigning a value for probability of part failure. The validity of the choices can only be checked by a study of the field service data reports.

Consequence Rating and Modified Rating

During the construction of the failure mode logic diagrams, qualitative consequence rating values were applied by the evaluator. This value when recorded on the diagram was the evaluator's estimate of the probability that part failure would cause system failure. The evaluator used values from Table XII.

In arriving at the values in Table XII, it was realized that humans have little or no difficulty assessing the two extremes of a decision. For example, at one extreme is the question, "Does part failure cause total system failure?" and at the other extreme, the question, "Is part failure very unlikely to jeopardize the system task?" These are similar to decisions of whether a part is black or white. However, when the part is neither all black nor all white, the decision is more difficult for humans to make. What in between shade is it? Is it more black than white but not all black or is it more white than black but not all white? In a similar manner a failure analyst might ask himself, "If this part fails is system task completion possible but very unlikely?" or, "If this part fails is system task completion possible and more likely? Seeing the need to have values for decisions between the two extremes, it was decided to use a cumulative binomial approximation of a normal distribution $\left[\sum b \ (x, \ n, \ p) \ \text{where} \ n = 10 \ \text{and} \ p = .5 \right]$ to arrive at "in between" values. The curve is shown on Figure 30 where the qualitative probability of consequence being complete failure is plotted as a function of consequence rating. The curve was divided into four consequence ranges, A, B, C & D, and the mean of each range was used to determine a probability value.

These are the ones listed in Table XII. It is felt that the use of this approach closely approximates the non-linearity of human response to decision making. Support for this approach can be found in dissertations on human value and utility systems in References 44 and 45.

The use of these consequence rating values has been a valuable tool in helping to sort out and critically rank parts of a complex mechanical system. Going beyond the scope of this study, even greater use can be made of the consequence rating value. If many modes of system failure are considered, each mode would be assigned a value and eventually be considered in rating of each part in the failure mode. In addition, further refinement of the assigned value near the critical extreme (A = 1.0) can be achieved by experienced evaluators being capable of more closely estimating the probability of consequence being complete failure. In the analysis

of the foregoing report, only one C.R. value was used at the critical extreme. Of the parts considered, more resolution in ranking of "prime parts" would result if instead of using a C.R. value of 1.0, a value of .99 (1 chance out of 100 task would be completed) or .999 (1 chance out of 1000) or .9999 etc., are properly estimated and applied. It can be seen that differences of 10 to 1 and 100 to 1 can be achieved, and differences such as these greatly help in ranking "prime parts".

In the foregoing, it was explained that for the analysis certain rules were established for modifying the C.R. values depending upon the arrangement of the part in relation to redundant or standby hardware. The rules that were established and applied, uniquely down-graded the consequences if part failures occurred but stand-by hardware was available. This approach presented a convenient method for helping to rank the various parts considered in the two failure mode logic diagrams. However, further work should be done to establish more probabilistically rigorous rules in order to make greater use of the mathematic model evolved from each logic diagram.

Probability of Part Failure (P_{PF}) - Failure Rate

One of the criteria for ranking of critical parts is termed "Probability of Part Failure (P_{PF})". This can be measured by failure rate of the part, which is expressed as number of failures per unit of time. Unfortunately, failure rate data for components of complex mechanical hardware of flight control systems is hardly ever available prior to fabrication and extensive testing. Without these data, accurate reliability predictions of new systems is almost impossible. Makers of components such as catalog bearings, fasteners, etc., may have published lists of generic failure rates for their products; however, the number of standard or catalog items used in mechanical flight control systems is a small percentage of the total number of parts. And unless failure rates for each of the components is available, reliability predictions or ranking of critical parts are of limited value.

In an attempt to assess the probability of success (or failure) of the various parts of a mechanical component a structural analysis is carried out. This is performed with a prescribed set of operating conditions, and generally the result is a value which is labeled design safety margin, or factor of safety, or hours life, or cumulative damage for each part considered. Herein lies the problem. With the present state-of-the-art, a variety of terms or values are used, depending upon the type of part or mechanism of failure, to describe the estimated part success or inversely the part failure. What is greatly needed is a common factor for all types of parts and all types of material failure modes, so that all parts of a system can be properly ranked. Further work must be carried out to develop means by which a gear subjected to bending fatigue, a housing subjected to ultimate loading, a bearing under radial and thrust loads and a push rod or clutch discs subjected to material wear can be assessed for probability of part failure by a common factor. Until this is done, the best attempts to rank critical parts are subject to the variability of the experience and skill of the human evaluators.

RANKING OF 64 "PRIME" PARTS

OF POWER UNIT

FIGURE 28
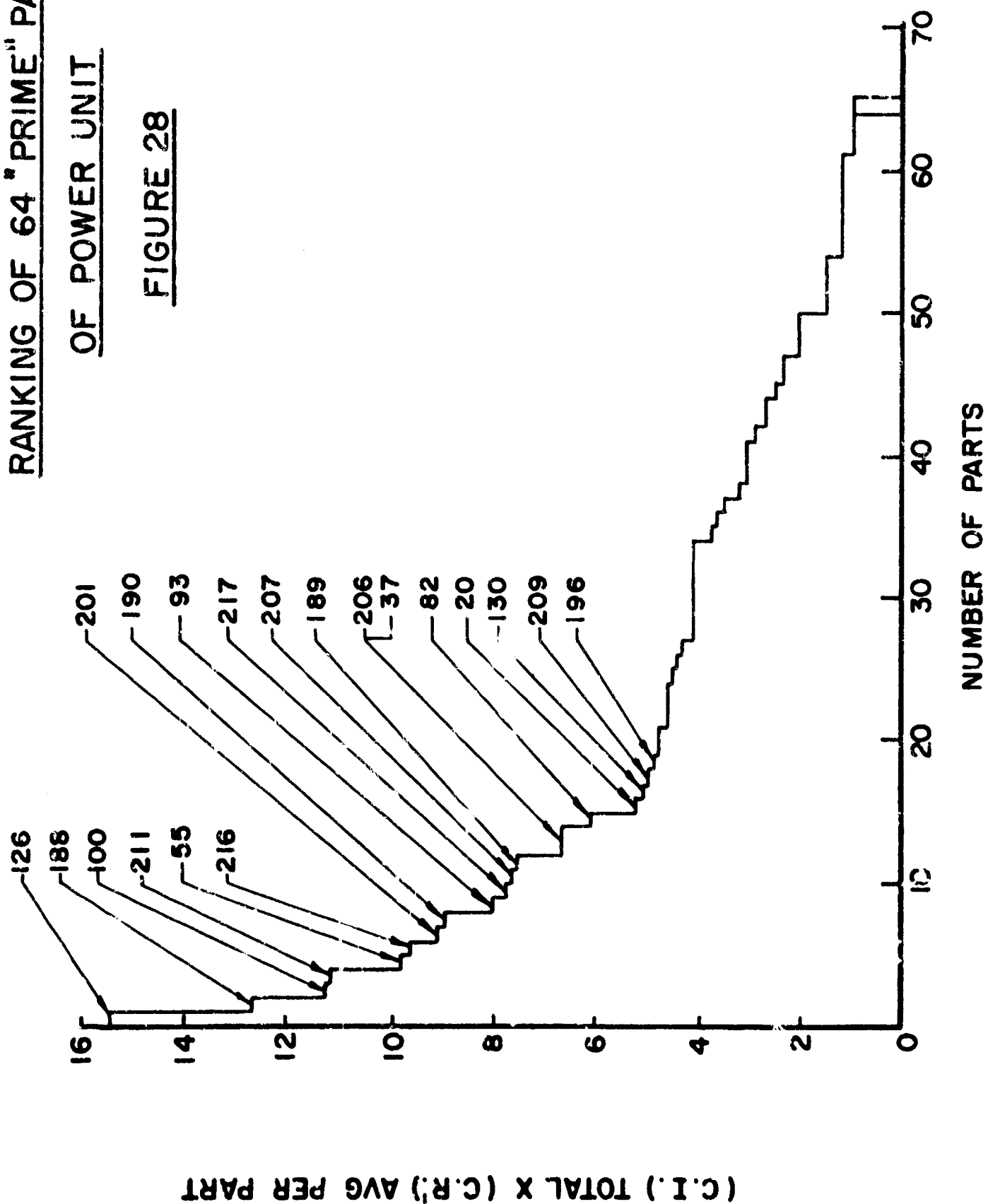
RANKING OF 67 "NON-PRIME" PARTS

OF POWER UNIT

FIGURE 29

FIGURE 30
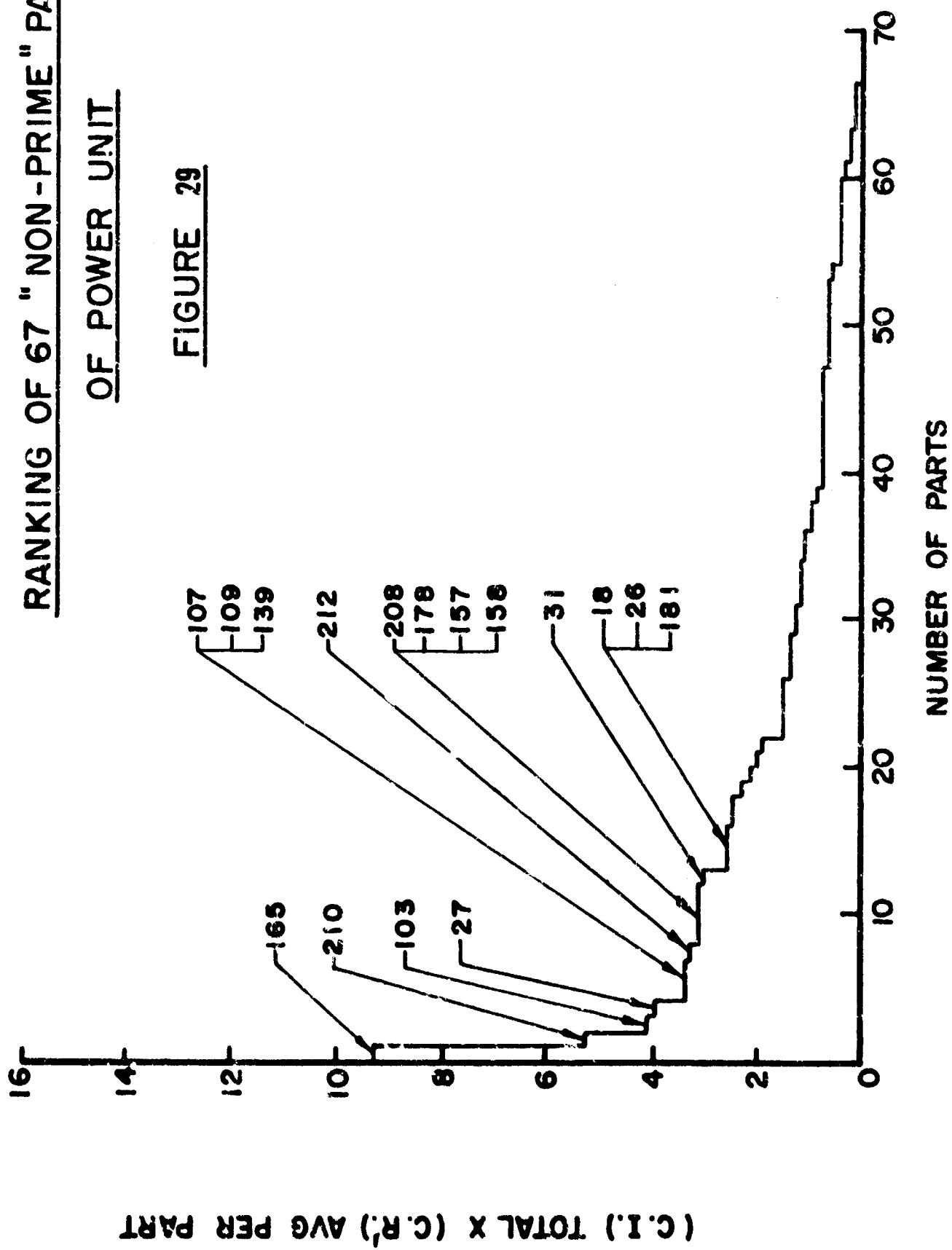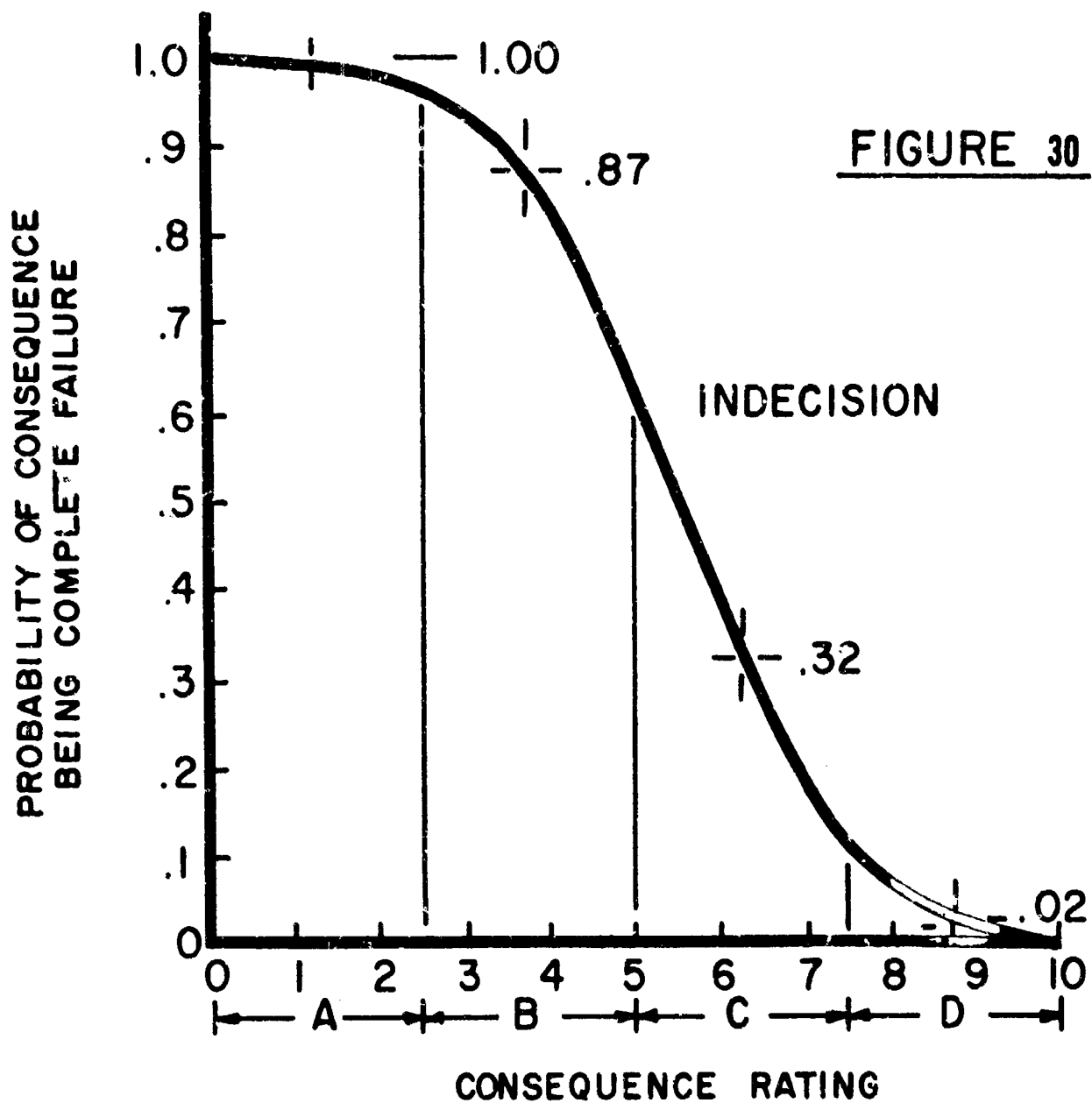
RANK	RATING	PROBABILITY
1	A	1.00
2	AB	.98
3	B	.87
4	ABC	.73
5	AC	.66
6	ABD	.63
7	BC	.59
8	ABCD	.55
9	AD	.51
10	ACD	.45
11	BD	.43
12	BCD	.40
13	C	.32
14	CD	.17
15	D	.02

84

COST EFFECTIVENESS CONSIDERATIONS

A complete cost-effectiveness consideration consists of three basic parts:

- Confidence/Resource Criteria
- Effort/Accuracy Criteria
- Reduced List of Critical Causes

This phase was conceived as a method for providing information relating
the expected time and dollar costs of failure at the aircraft and engine
levels of the system to the time and funds that should be expended in
analysis and testing. This relationship might theoretically at least, be
developed to apply to future programs in supporting the development of
higher inherent design reliability in equipments and in supporting more
extensive reliability testing.

The required data for establishing the customer's confidence/resource
criteria (the measure of customer willingness to make resources of time
and funds available for obtaining a given confidence in attained reliability)
must come from some future long range analysis of total costs.

Likewise the actual cost in time and funds of obtaining a given confidence
in a test program is a function of the complexity, performance capability,
calendar time and contractor. Data for a specific relationship in terms of
time and money may possibly be obtained from other government studies like
those reported in ASD-TDR-62-751.

However, comparative studies of methods of organization of a reliability test
program show significant improvements in efficiency. This efficiency is a
function of the randomness or orderliness in the selection of each successive
failure point for testing.

Effort/Accuracy Criteria

The cumulative "cost" of failure for the total of all the possible failure
points in a system may be normalized to a value of 1. The risk function,
F (n), of being ignorant of some portion of this total cost is reduced as a
function of the amount of effort expended to gain knowledge in the form of the
cumulative probability of occurrence of the failure costs. The effort ex-
pended may be measured in terms of the number of failure points, n, considered
for test out of the almost infinite number of possibilities.

The efficiency of some less than complete consideration (limited by availability
of finite time and funds) is influenced by the relative marginal decrease, G,
in risk obtained by the consideration of each successive failure point.

$$G = \frac{1}{F} \frac{dF}{dn}$$

Integrating this marginal decrease in risk over some partial number of considerations, n, we obtain the value for the remaining risk:

$$\int_0^n G\,dn = -\int_0^{F(n)} \frac{dF}{F} = -\ln F(n)$$

$$F(n) = \exp\left[-\int_0^n G\,dn \right]$$

$$= e^{-\int_0^n G\,dn}$$

For comparative purposes, we may consider some characteristic number of failure points, N, which leave a risk, F, of e^{-1} or 37% such that

$$\int_0^N G\,dn = 1$$

Where F(n) has a distribution of the form

$$F(n) = e^{-\left(\frac{n}{N}\right)^k}$$

It may be plotted as a series of straight lines on ln ln by ln coordinates with slopes a function of k as shown in Figure 31.

Then the function G is of the form

$$G(n) = \frac{k}{N}\left(\frac{n}{N}\right)^{k-1}$$

For the case where the sequential order of consideration of the n failure points is purely random (typified by k = 1), the relative marginal decrease in risk for each successive consideration, averaged over a large n , is a constant. When the sequence of consideration of the n failure points is obtained from a ranking in an order progressing from most important to least important, G may be called a ranking function. When the resolution between successive steps in this ranking function becomes higher (represented by smaller values of k) the ranking function assumes shapes approaching those shown in Figure 32 much as do Figures 28 and 29 .

86
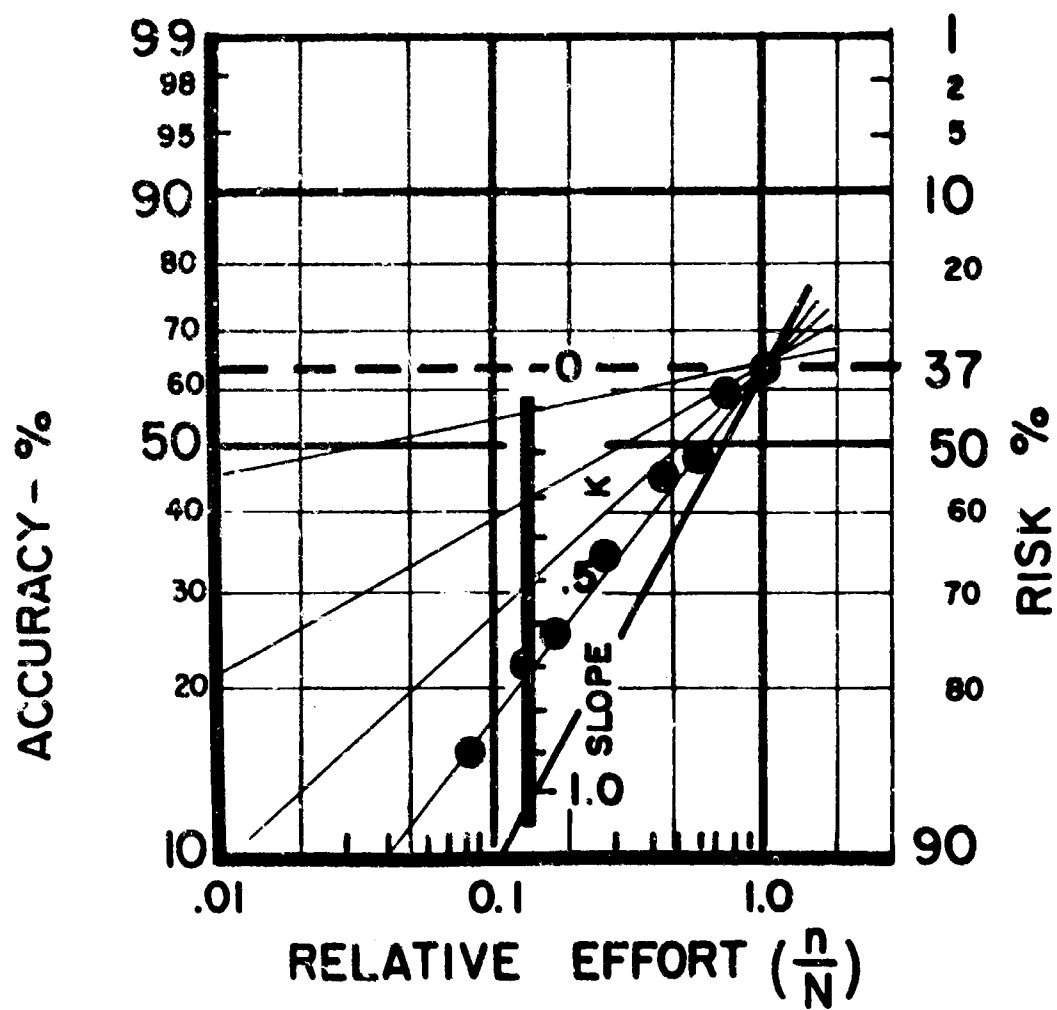
FIGURE 31

EFFORT / ACCURACY CRITERIA

When the accuracy for a less than complete consideration having a high ranking resolution (k < 1) is compared with that of a purely random consideration, (k = 1) the difference in accuracy is shown in Figure 33.

It can be seen from Figure 33 that an optimum efficiency is obtained for less relative effort when the ranking function has the greatest resolution (k is smallest)

Greatest resolution in the importance ranking function is obtained when the costs of certain failures far exceed the value of the equipment or cost to repair (as in flight safety applications) and when a greater depth of analysis is used (more system failure modes considered).

The ranking function of Figure 28 when plotted on Figure 31 after normalizing shows a slope approaching .7 and suggests an optimum relative effort at about .3 . If actual costs of failure at the aircraft level were obtainable and applied this resolution would be drastically improved.

Reduced List of Critical Causes

The comparison between the shape of the theoretical ranking function for k = .7 and the ranking of the "prime " parts of the power unit is shown in Figure 34. Figure 33 then suggests the location of the critical/non-critical decision line at about n/N = .3 (8 parts). Many other factors would influence this choice in a practical case where true costs are known.

For the purposes of this program the clutch output gear on the gear-drum assembly was selected as the most critical part for which to develop the accelerated testing methods.

$$G = \frac{k}{N} \left(\frac{n}{N}\right)^{k-1}$$
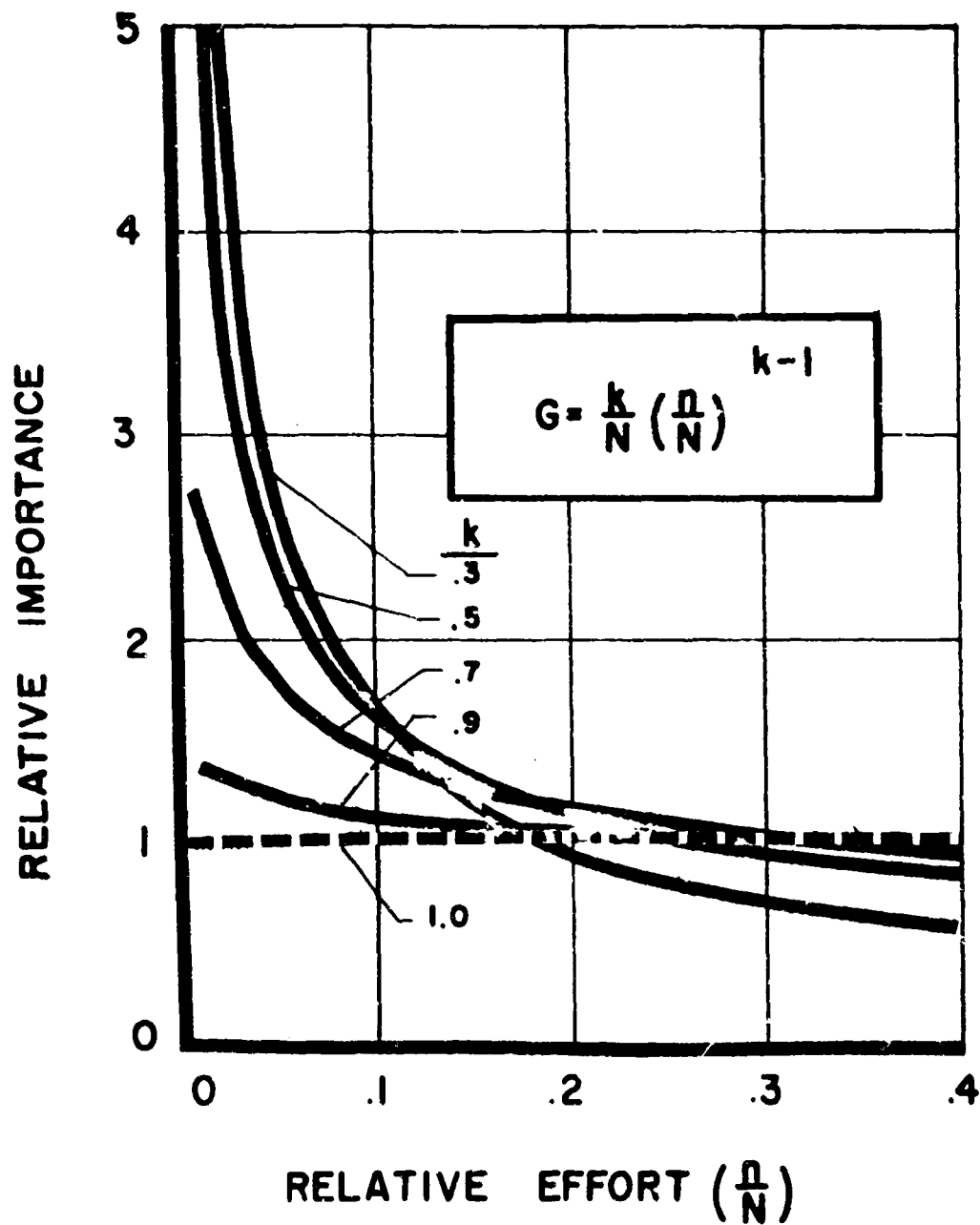
FIGURE 32

RANKING FUNCTION SHAPES
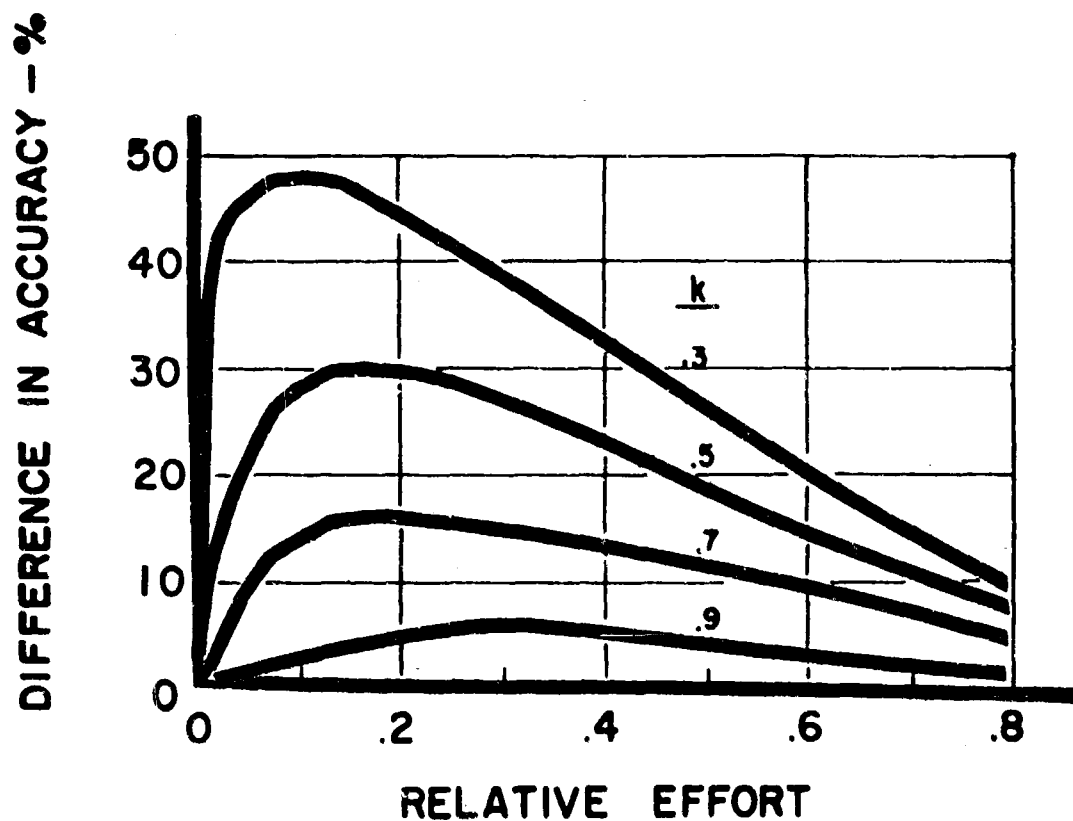
FIGURE   33

IMPROVEMENT IN ACCURACY
OF
RANKED ORDER CONSIDERATION
OVER
RANDOM ORDER CONSIDERATION
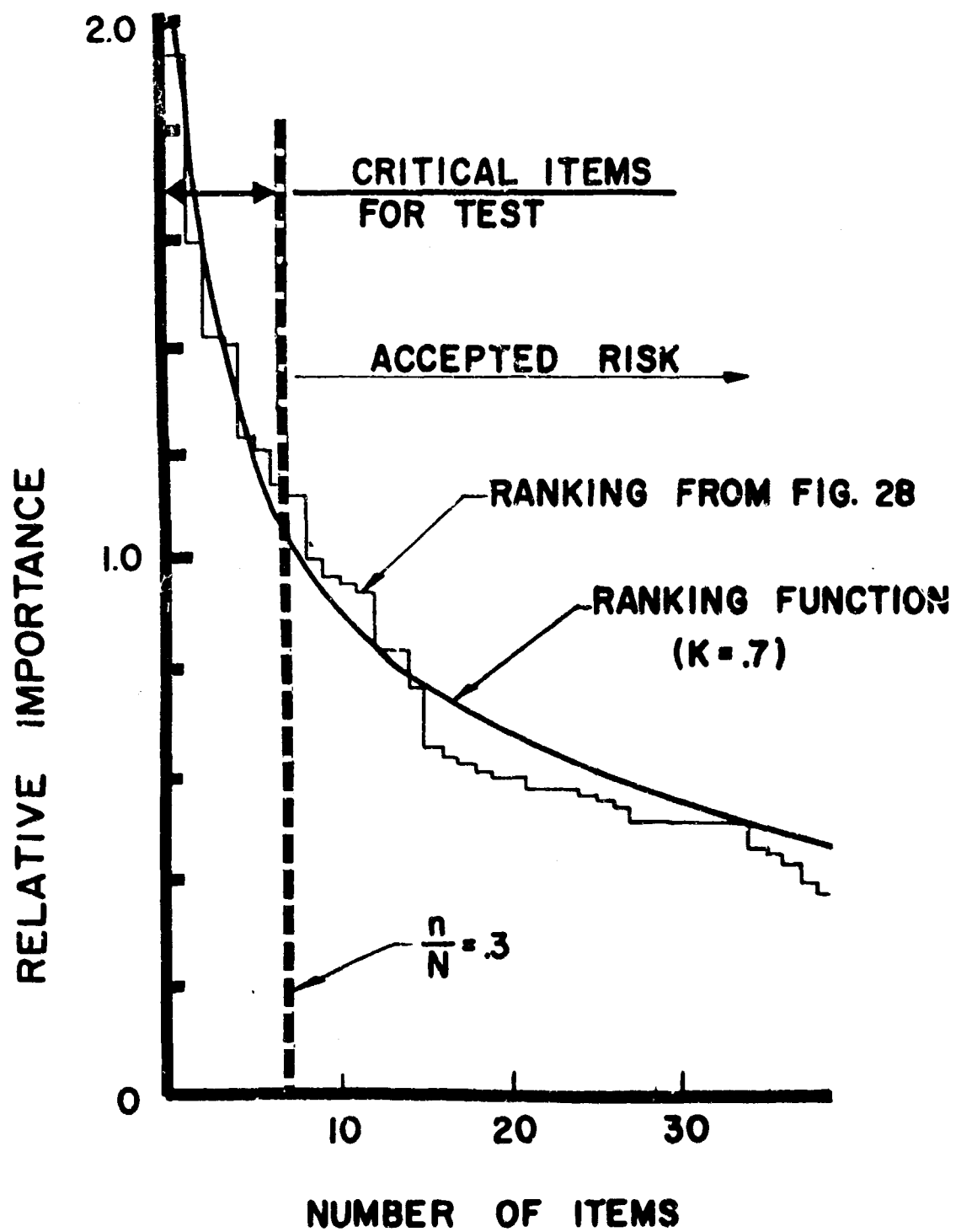
FIGURE 34

REDUCED LIST OF CRITICAL ITEMS

ACCELERATED TESTING PHASE

Study of the Mechanisms of Failure

The only reasonable commonality in the infinite variety of non-separable parts in non-electronic components is found at the material level. It is at the material level that the real foundation of non-electronic reliability has been built whether it be in aircraft structures and equipment, bridge structure, or automotive mechanical equipment.

When reliability testing methods are developed for the system level of equipment the tests must necessarily all be separately designed and any data resulting therefrom is seldom applicable with any great confidence to a different kind of system. However, any techniques developed for testing at the material level are more generally applicable to the uses of the same materials in many other kinds of systems. This reasoning has supported the heavy emphasis on material failure mechanisms in this program. It also is believed the hypothesis that any real step forward in accelerating testing of flight control components would be taken through more comprehensive understanding of material failure mechanisms.

One material failure mechanism, fatigue, was selected for study in this program. The theory supporting the method of accelerating fatigue testing is described in Appendix A.

STUDY OF THE FATIGUE FAILURE MECHANISM

A detailed discussion is presented in Appendix A of the various factors involved in estimating a fatigue acceleration relationship for a structural or machine element. The conventional S-N curve has been interpreted as consisting of an initiation stage and a crack propagation stage; these two regions being separated by the "damage line".

The crack propagation formula introduced by Cummings, Stulen and Schulte was used to derive a fatigue acceleration law. For the special case of zero mean stress, this formula is very similar to the Corten-Dolan formula except that "damage" is interpreted in terms of certain characteristic crack lengths. It has been shown that, by a simple modification, this same formula can be used for the locally notched material.

The critical dynamic crack length and its associated stress were used in computing the acceleration relationship in fatigue. This permitted the evaluation of the contribution of the lower stresses in the spectrum to the fatigue damage in accordance with the concept of Henry.

The criterion of failure has been based on a certain allowable reduction in the static strength of the member or the attainment of the critical <u>static</u> crack length.

The formula of Coffin for low cycle fatigue is recommended, and this formula probably represents a crack propagation S-N curve since the initiation period at high stresses is very small. However, this formula is not yet directly comparable to the high-cycle formula because of the added complication of crack joining at low cycles and high stresses. Techniques have still to be developed to adequately account for the effective length of joining cracks.

The essential parameters that phenomenologically described the fatigue process are listed below:

(1)   The constants ℓ_o or ℓ_o'.

(2)   The crack propagation parameters; α, k, b.

(3)   The parameters of the critical dynamic crack length.

(4)   The parameters of the critical static crack length.

(5)   The value of ℓ_{f_r}, s_r, and N_r.

A fatigue acceleration relation which takes into account the effect of the steady or mean stress has been hypothesized.

Accelerated Systems Test

The purpose of the system test program was to duplicate the aircraft and engine mission profile as it applied to the VEN Power Unit. The engine exhaust nozzle area schedule determines the input position signal to the VEN Power Unit and its signal activity. The exhaust nozzle actuator loads determine the loading on the output of the power unit.

By testing the power unit through the full range of normal operating loads and signals distributed as they occur in the aircraft mission, a fully representative sample of the expected life history was obtained. Special attention is brought to the fact that the loads and stresses were not increased beyond the normal range to create abnormal failure modes. Instead, the selected critical areas, namely the roots of the teeth of the output gear, were "measurably weakened" to fail in an abnormally short time in exactly the failure mode selected at the normal loads.

The mission profile was determined during the survey phase with considerable attention given to the distribution of the loads and the signal profile.

The first attempt at accelerating the test program was a thorough analysis of this profile to find out what areas could be condensed or eliminated in accordance with their effect on the selected critical failure mode.

The output activity was recognized as being zero during certain portions of the one-hour training flight mission when the engine nozzle area remained constant. These were eliminated and the modulating or pulsing periods (four in number in the aircraft mission profile) were seen to permit condensing to two periods of different load intensity.

This first condension reduced the test activity needed to duplicate the dynamic activity of the critical area in a one-hour mission to five minutes (an immediate acceleration factor, F_1, of 12/1).

The next attempt at acceleration was the pre-cracking or "measured weakening" of the critical areas of the gear teeth. This was intended to initiate the crack propagation stage discussed in the theoretical analysis. A procedure was developed for periodic inspection of the gear teeth for crack measurement. In this procedure special provisions were made to inspect the teeth without introducing the chance for human error in disassembly and re-assembly of the unit that might have caused failure of the parts unrelated to service use after normal production acceptance testing. Rigid routines and instructions were prepared and followed to insure that no foreign matter that would be excluded by the cover and seals was introduced into the mechanism during handling inspection.

Instrumentation was provided for monitoring and controlling all the important environmental parameters of the test as well as measuring of gear-tooth life cycles as they related to the number of missions run. Three power units were selected at random from the production line (although later numbered serially) prepared for testing and modified for instrumentation with special care given to seeing that the modifications would in no way influence the test data.

The power units were tested for a total of 539 missions simulating 539 hours of flight.

The test rig was designed to duplicate the engine system installation of the VEN Power Unit. The rig consisted of a mounting table mounting a 15 horsepower variable speed drive connected to a pillow-block supported power unit drive shaft by a positive drive toothed belt. The speed could be varied as required and measured by an electronic counter pulsed by a magnetic pickup on the drive shaft. The power unit mounting pad and drive shaft corresponded to the mounting pad on the engine accessory gearbox. The power unit input arm was connected by a linkage to a roller chain drive controlled by the cycling mechanism. (See Fig. 35 .

The cycling mechanism controlled both power unit input position and output load in accordance with the modified mission profile.

The loading system used three ball screw actuators and three flexible shafts of the type actually used on the engine to duplicate the dynamic output impedance. The actuators were connected through a strain-gage instrumented Morehouse ring to a cast iron slider. This slider was clamped between two constrained leather pads by an air cylinder to duplicate the friction loading of the engine nozzle leaves. The cast iron-leather combination was specially selected because of the negligible difference between the static and kinetic coefficients of friction and because of the relative invariance of this coefficient of friction with use.

Three air-pressure regulators, solenoid-valve controlled, were connected to each air cylinder to provide a statistically selected range of loads derived from actual engine test data. (See Figures 36, 37 and 38).

The input signal profile was produced through the action of a hydraulic servo piston operating a spring loaded roller chain. This roller chain rotated a sprocket to which was attached a lever arm and linkage connected to the power unit input.

The hydraulic servo system was programmed by a radial cam cut to duplicate the dynamic portions of the nozzle area profile of a typical aircraft mission. The cam follower operated by this cam positioned an induction potentiometer. The signal from this potentiometer was compared with that from a similar feed-back potentiometer attached to the servo piston rod. The two potentiometer signals were compared in a demodulator and the error signal amplified to control the hydraulic servo valve to correct the servo piston position. (See Fig. 39).

In the jet engine control loop of which the VEN Power Unit is a component, area modulating pulses originating in the T_5 amplifier are fed into the VEN Power Unit during portions of the engine operating spectrum. These pulses were simulated by a solenoid controlled sprocket idler which shortened the roller chain when energized by deflecting it sideways. During this pulsing the cam was caused to dwell at the proper steady nozzle area so that the servo piston remained motionless.

TABLE XIV

DETAILS SHOWN IN PHOTOGRAPHS

1. Power Unit
2. Ball Screw Actuators
3. Flex Shafting
4. Load Air Cylinders
5. Servo Piston
6. Cycler
7. E-Put Meters
8. Load Monitor (Oscilloscope)
9. Pulse Solenoid
10. Load Calibration Switches
11. Cam
12. Cam Position Transducer
13. Dwell & Load Control Cam
14. Demodulator
15. Dwell Timer
16. Pulse Timer
17. Load Sequence and Load Calibration Switch
18. Power Switch
19. Mission Timer
20. Oscillator
21. Amplifier
22. Cam Drive Motor
23. Servo Position Transducer
24. Morehouse Rings
25. Air Regulators
26. Chain Drive

FIGURE 35

1. Power Unit
2. Ball Screw Actuators
3. Flex Shafting
4. Load Air Cylinders
5. Servo Piston
6. Cycler
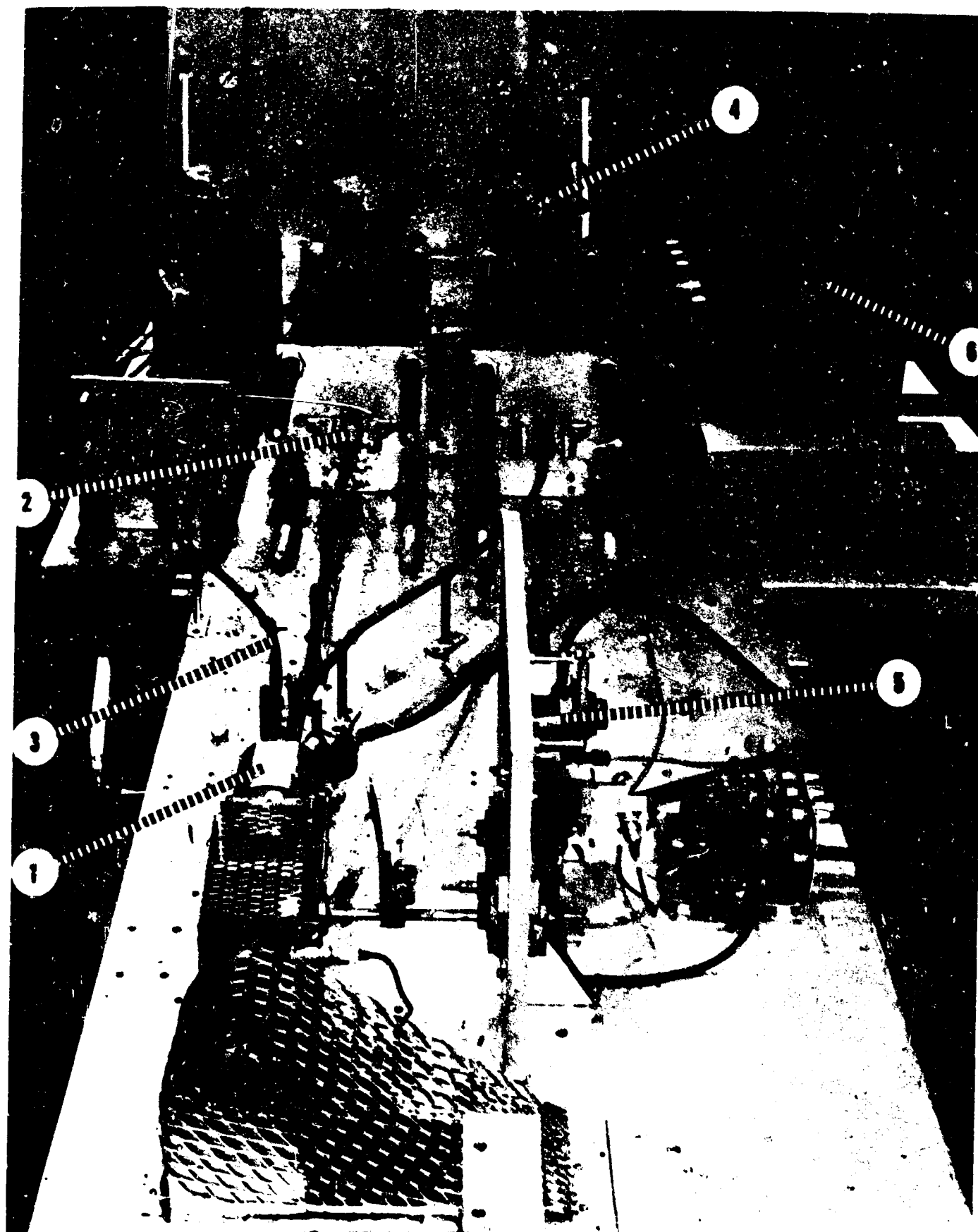
SYSTEM TEST EQUIPMENT

FIGURE 35
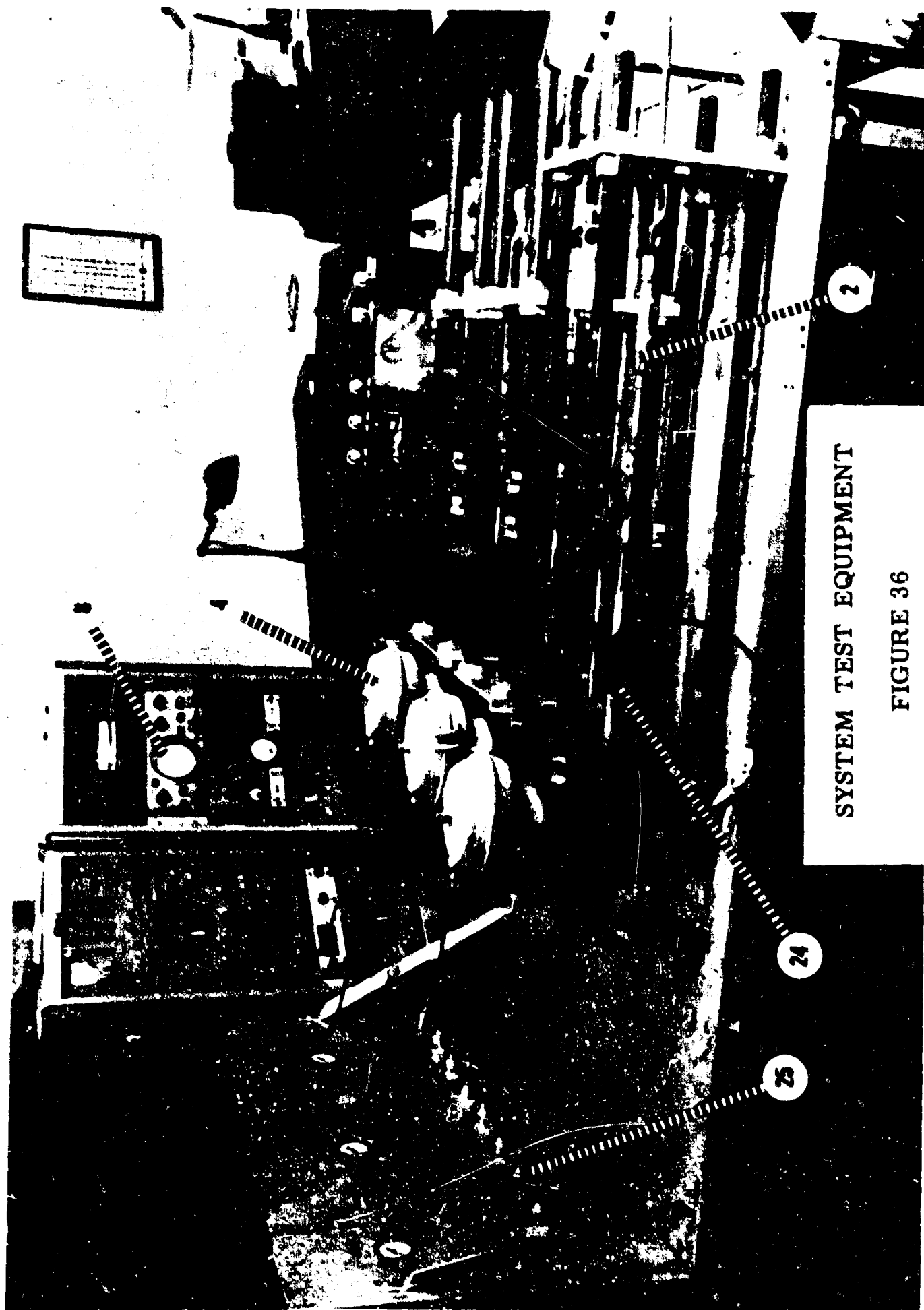
SYSTEM TEST EQUIPMENT

FIGURE 36

FIGURE 36

2. Ball Screw Actuators
4. Load Air Cylinders
8. Load Monitor (Oscilloscope)
24. Morehouse Rings
25. Air Regulators

TYPICAL ENGINE TEST RECORD
PROVIDING LOAD DATA FOR
VEN SYSTEM TEST
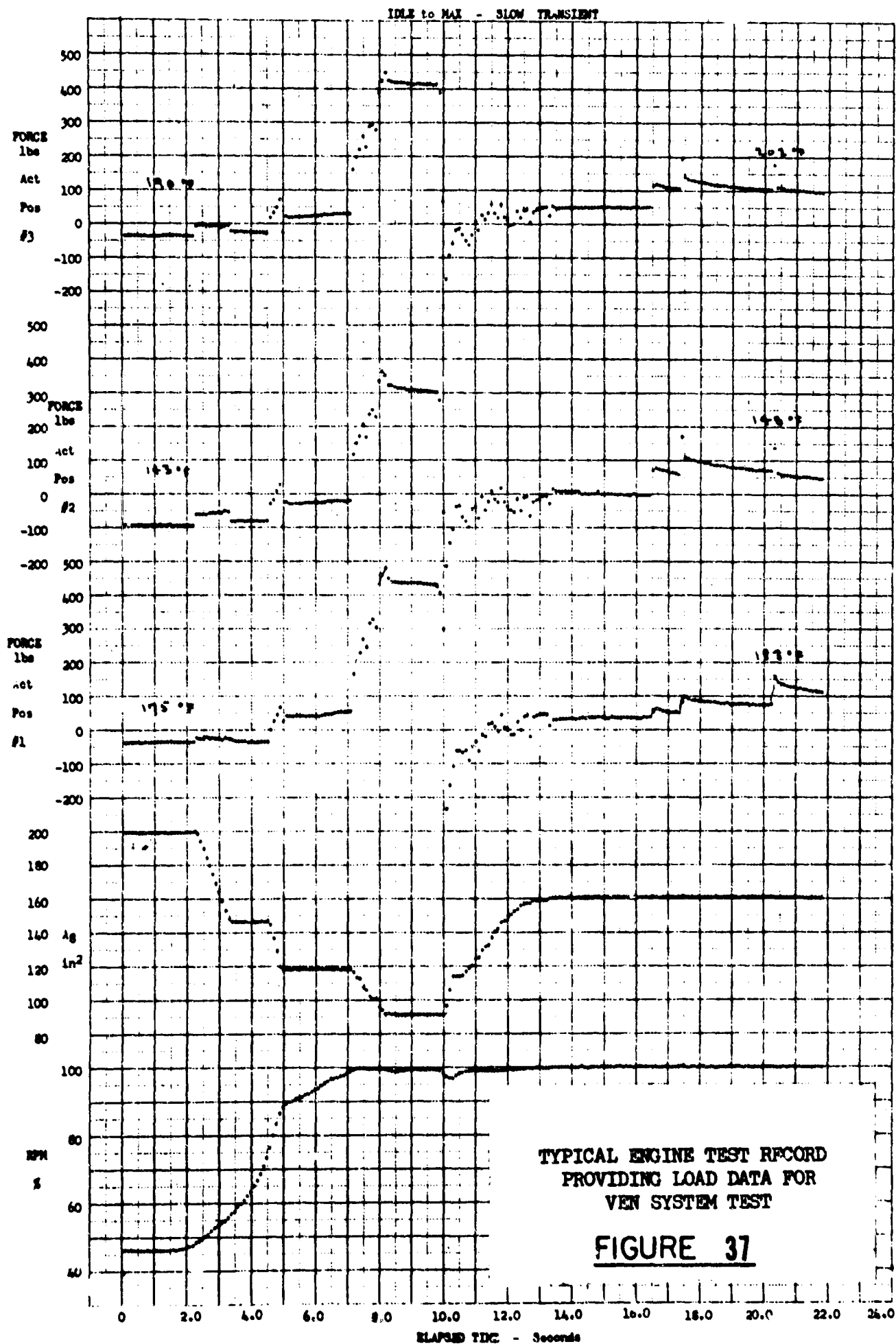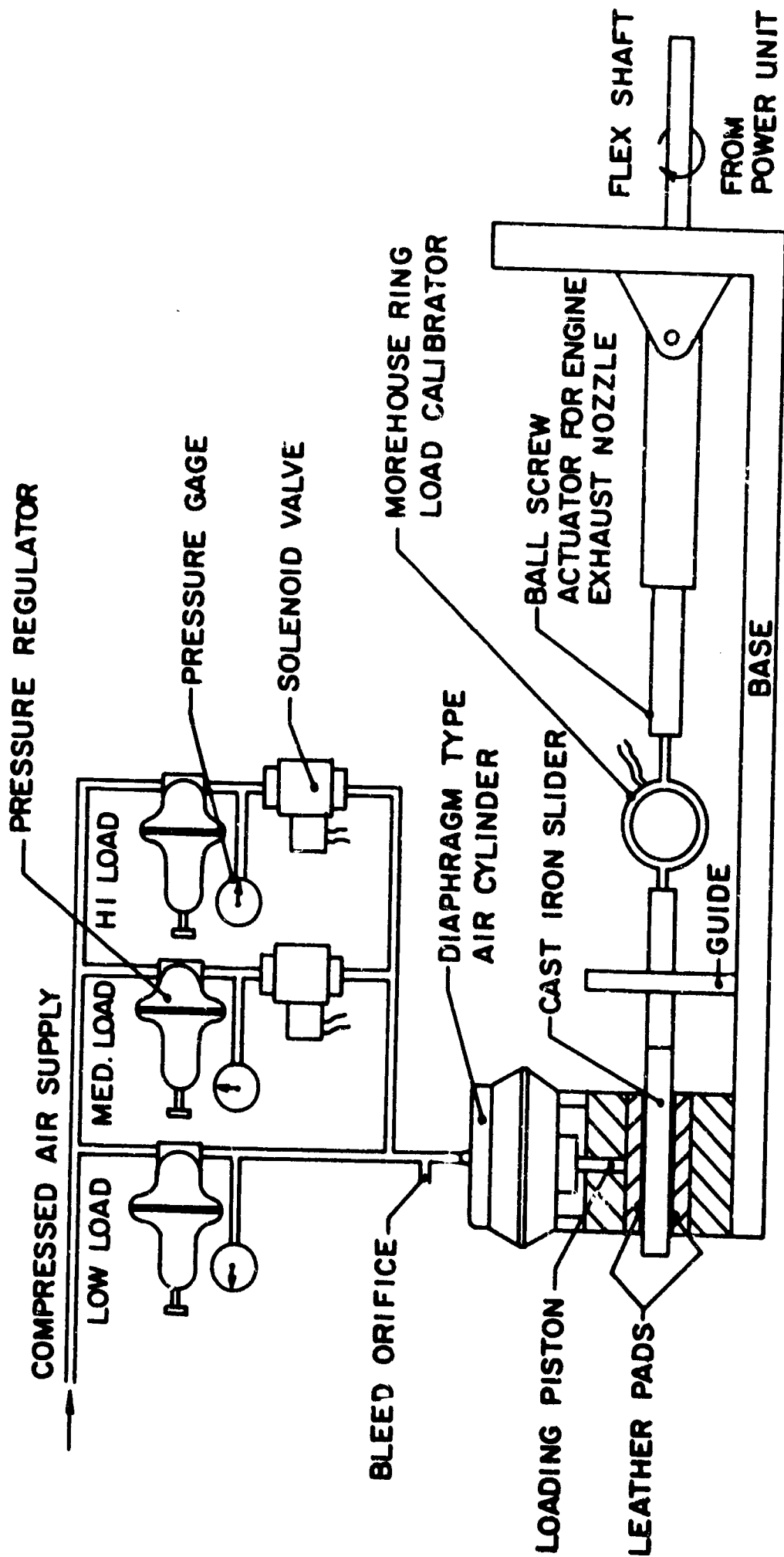
FIGURE 37

LOAD SIMULATOR FOR EACH OF THREE ACTUATORS

VEN POWER UNIT SYSTEM TEST

FIGURE 38

FIGURE 39

5. Servo Piston
9. Pulse Solenoid
23. Servo Piston Transducer
26. Chain Drive
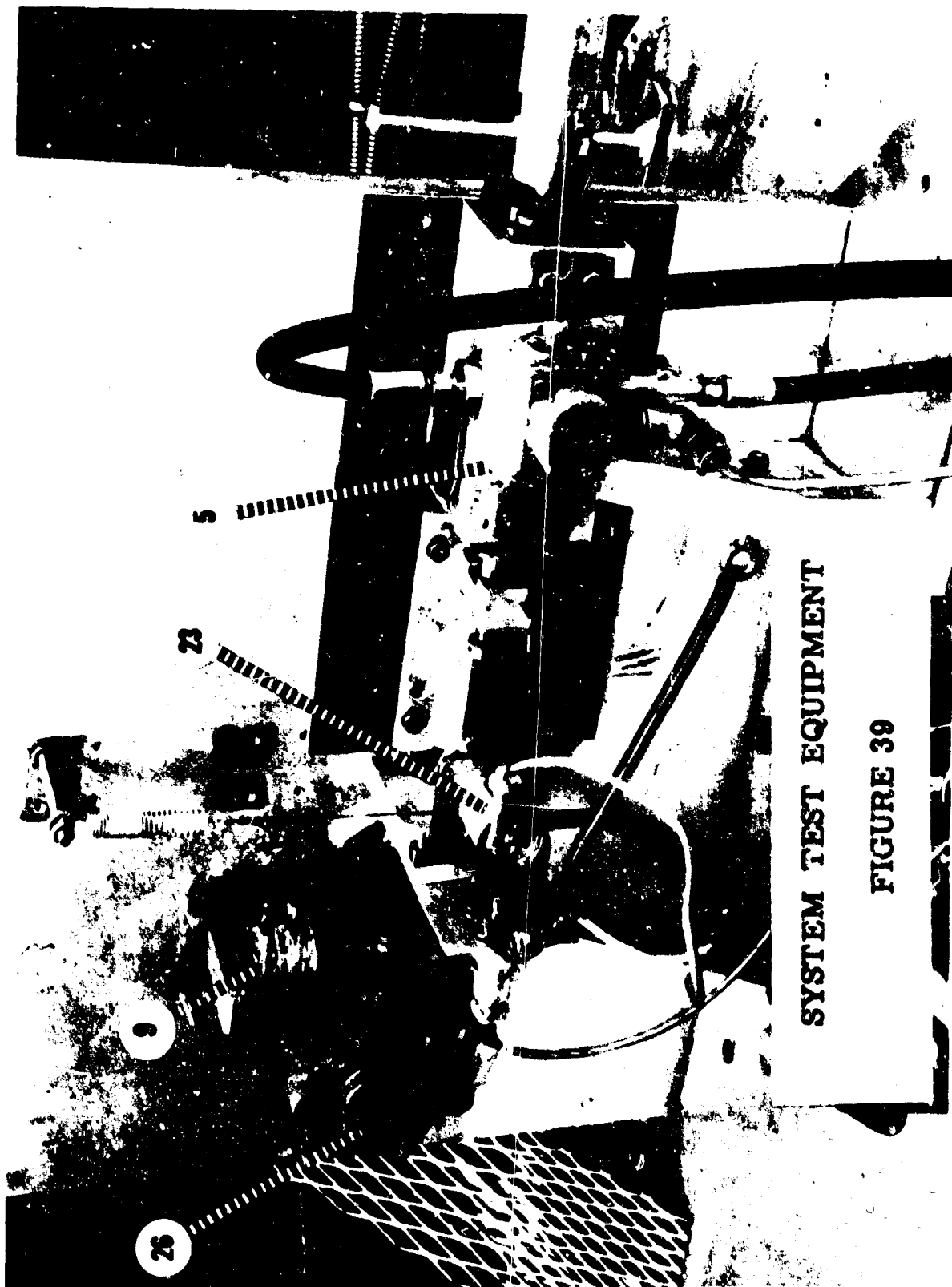
SYSTEM TEST EQUIPMENT

FIGURE 39

103

The cycling mechanism contained the cam drive motor, the cam dwell timer, the pulsing solenoid timing sequence and the load solenoid timing and sequencing shown schematically in Figures 40, 41, 42 and 43.

The instrumentation was of two general categories: that to monitor and control the environmental parameters, and that to make measurements of the dependent variables of interest. (See Figure 44).

In the environmental control area an electronic counter was used to monitor input drive speed accurately according to the mission profile.

Strain-gage bridges on the three Morehouse rings in the loading mechanism monitored the dynamic load on the output actuators. A recording oscillograph kept a permanent record of these loads for analysis and comparison with the mission load spectrum.

A recording thermocouple monitored power unit temperature to warn of any irregularities in the normal energy dissipation of the power unit that might alter the validity of the test.

To relate gear tooth stress cycles to the number of aircraft missions a pick-up was designed and constructed which counted the number of times an indexed gear tooth on the output gear in question passed any of six equally spaced fixed angular positions. This information could then be converted to the number of tooth engagements experienced by each tooth on the gear and all the mating gears. Since this gear makes many revolutions in going between output position limits, and oscillates in uneven fractions of turns while modulating, a simple revolution counter would not show the uneven distribution of cycles between the teeth on the same gear.

The gear position pick-up consisted of an extension quill shaft connected to the output gear being tested, a seal and bushing assembly where the shaft extended through the power unit cover, a slotted disc attached to the shaft and an array of six exciter lamps and six photocells positioned equi-angularly about the quill shaft. (See Figure 45).

The slotted disc was aligned with an indexed tooth on the gear. The slot in the disc provided an aperture through which a lamp beam could pulse the photocell aligned with it as the disc rotated with the gear. Six electronic event counters, each one attached to a photocell, recorded the number of times the indexed tooth passed a given angular position. Successive readings showed the rate of accumulation of tooth cycles as a function of missions completed and the variation of this from tooth to tooth.

The instrumentation used in this systems test is listed in Table XVI.

INDUCTION POTENTIOMETER

SERVO VALVE

AMPLIFIER

DEMODULATOR

OSCILLATOR

INDUCTION POTENTIOMETER

SERVO PISTON

SIGNAL PULSE SOLENOID

CAM FOLLOWER

HYD OIL PUMP

IDLERS

ENGINE NOZZLE AREA SCHEDULE CAM FOR I HOUR MISSION

POWER UNIT INPUT LEVER

CHAIN
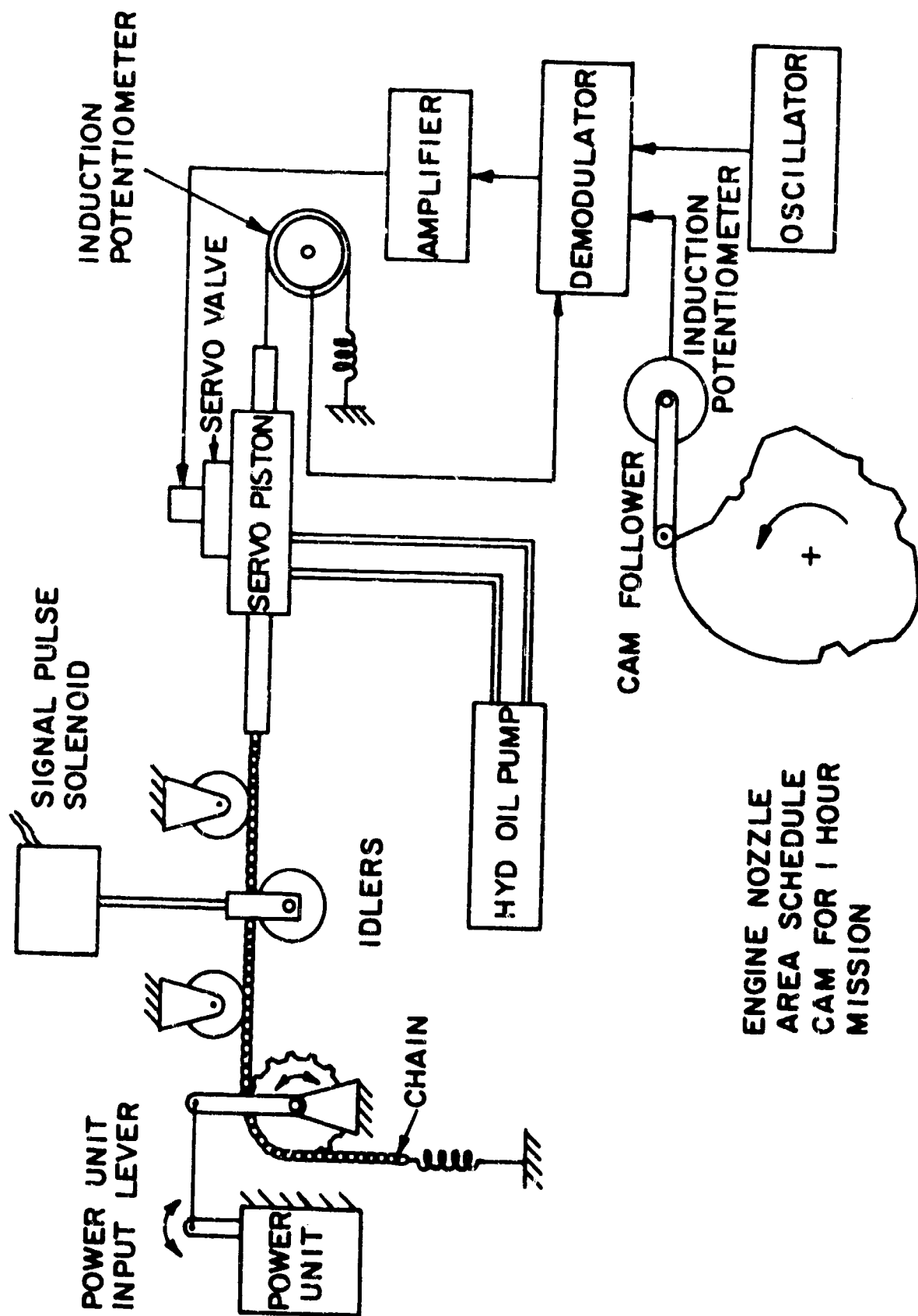
POWER UNIT

MISSION PROFILE SIMULATOR FOR INPUT SIGNAL

VEN POWER UNIT SYSTEM TEST

FIGURE 40

MISSION PROFILE CYCLER FOR SYSTEM TEST
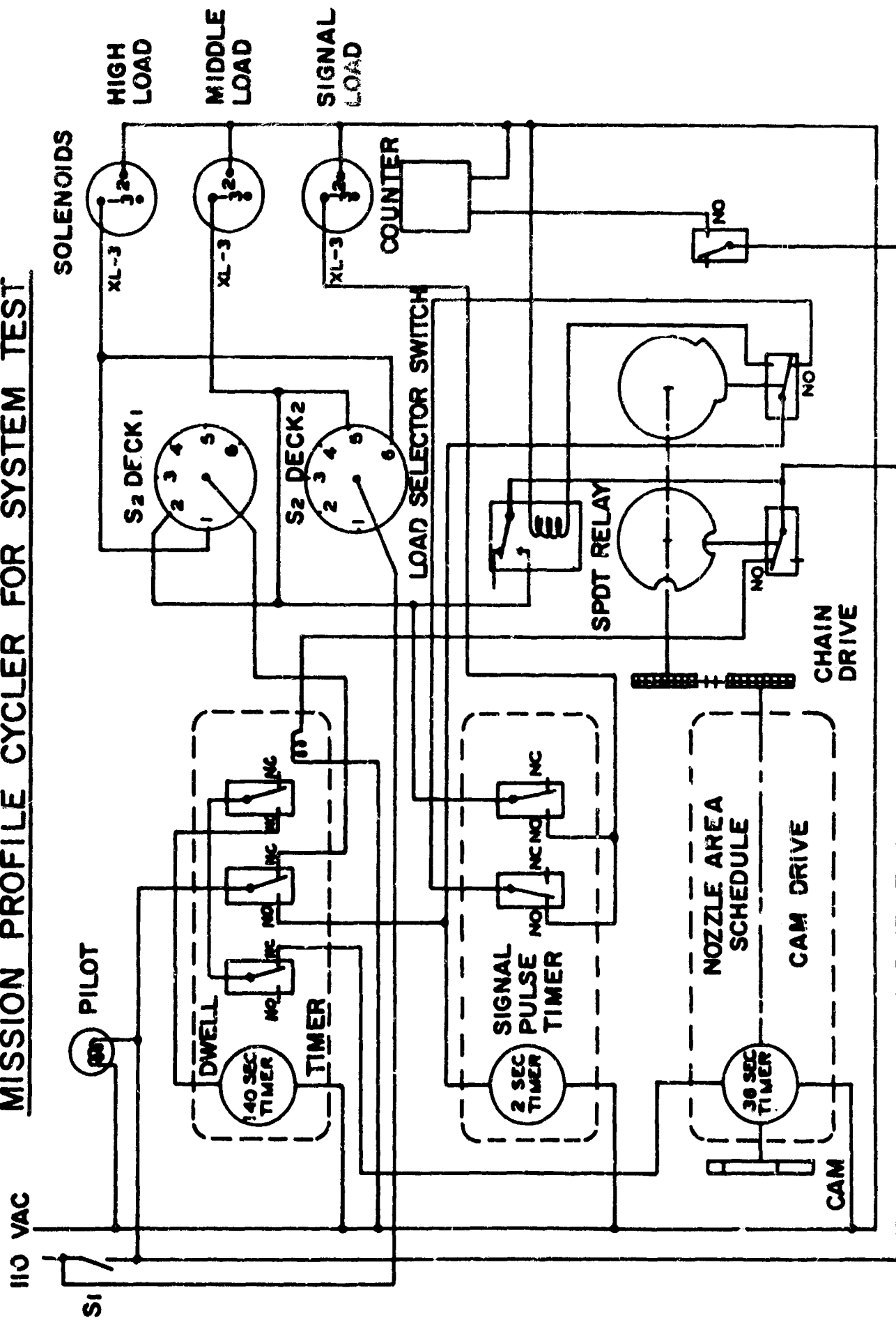
FIGURE 41

FIGURE 42

17. Load Sequence and Load Calibration Switch
18. Power Switch
19. Mission Timer
20. Oscillator
21. Amplifier
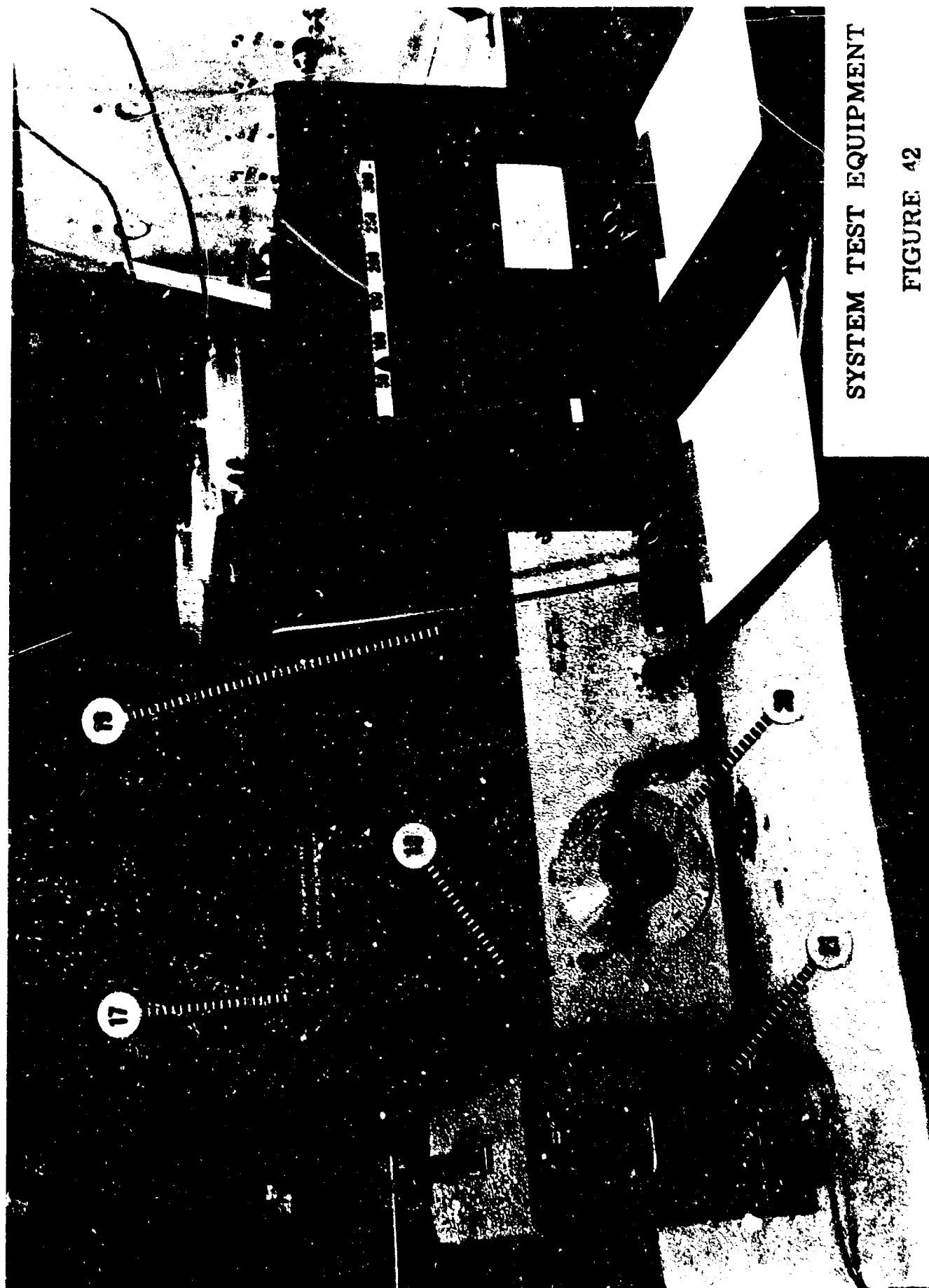
SYSTEM TEST EQUIPMENT

FIGURE 42

FIGURE 43

11. Cam
12. Cam Position Transducer
13. Dwell & Load Control Cam
14. Demodulator
15. Dwell Timer
16. Pulse Timer
17. Load Sequence and Load Calibration Switch
22. Cam Drive Motor

110
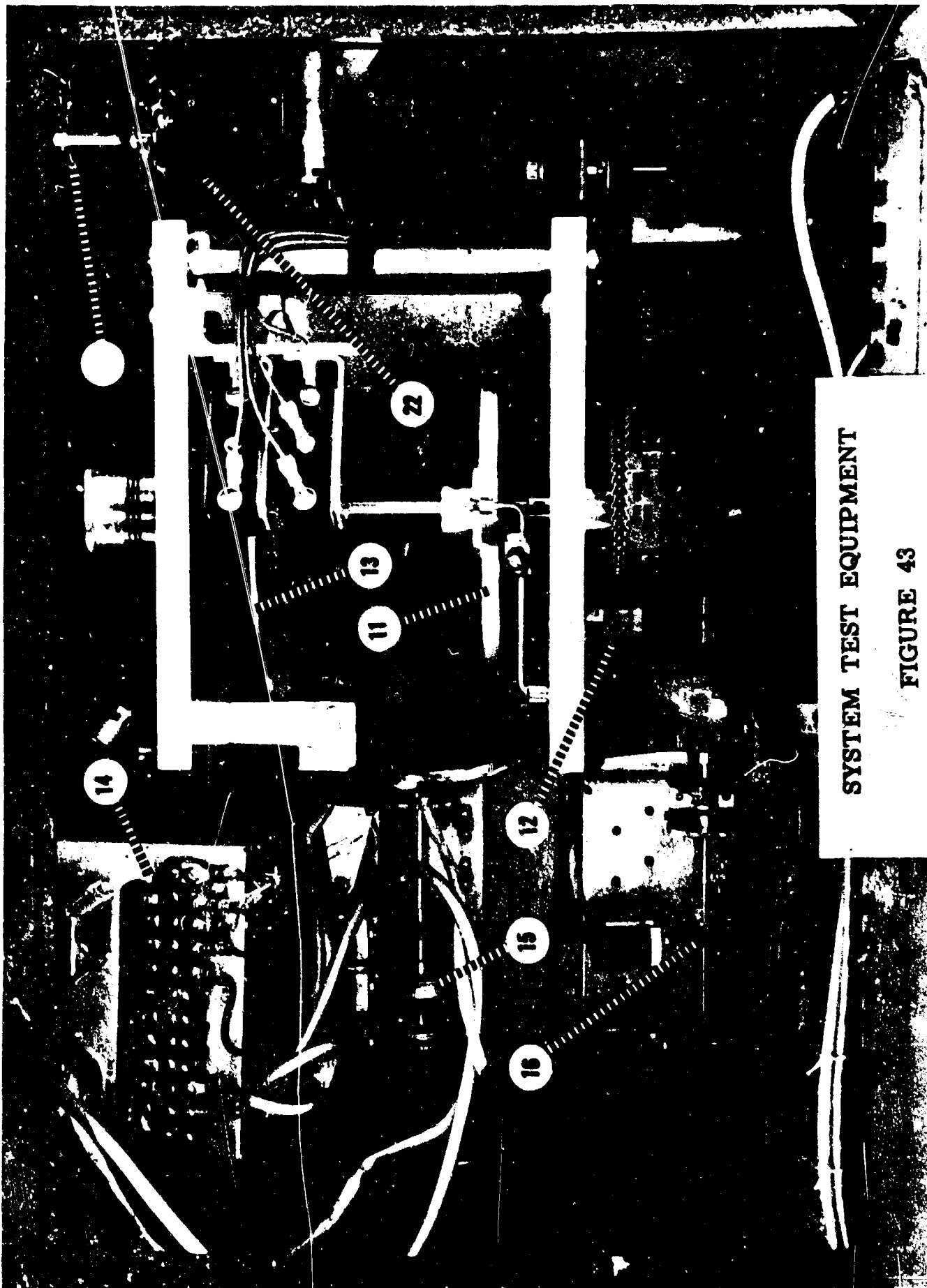
SYSTEM TEST EQUIPMENT

FIGURE 43

111

FIGURE 44

7. E-Put Meters
8. Load Monitor (Oscilloscope)
10. Load Calibration Switches

SYSTEM TEST EQUIPMENT

FIGURE 44

ARRAY OF 6 EXCITER LAMPS

SLOTTED DISC

ARRAY OF 6 PHOTOCELLS

OUTPUT TO EVENT COUNTER(S)

OUTPUT GEAR BEING TESTED

INDEX MARK

EXTENSION SHAFT

1 2 3 4 5 6
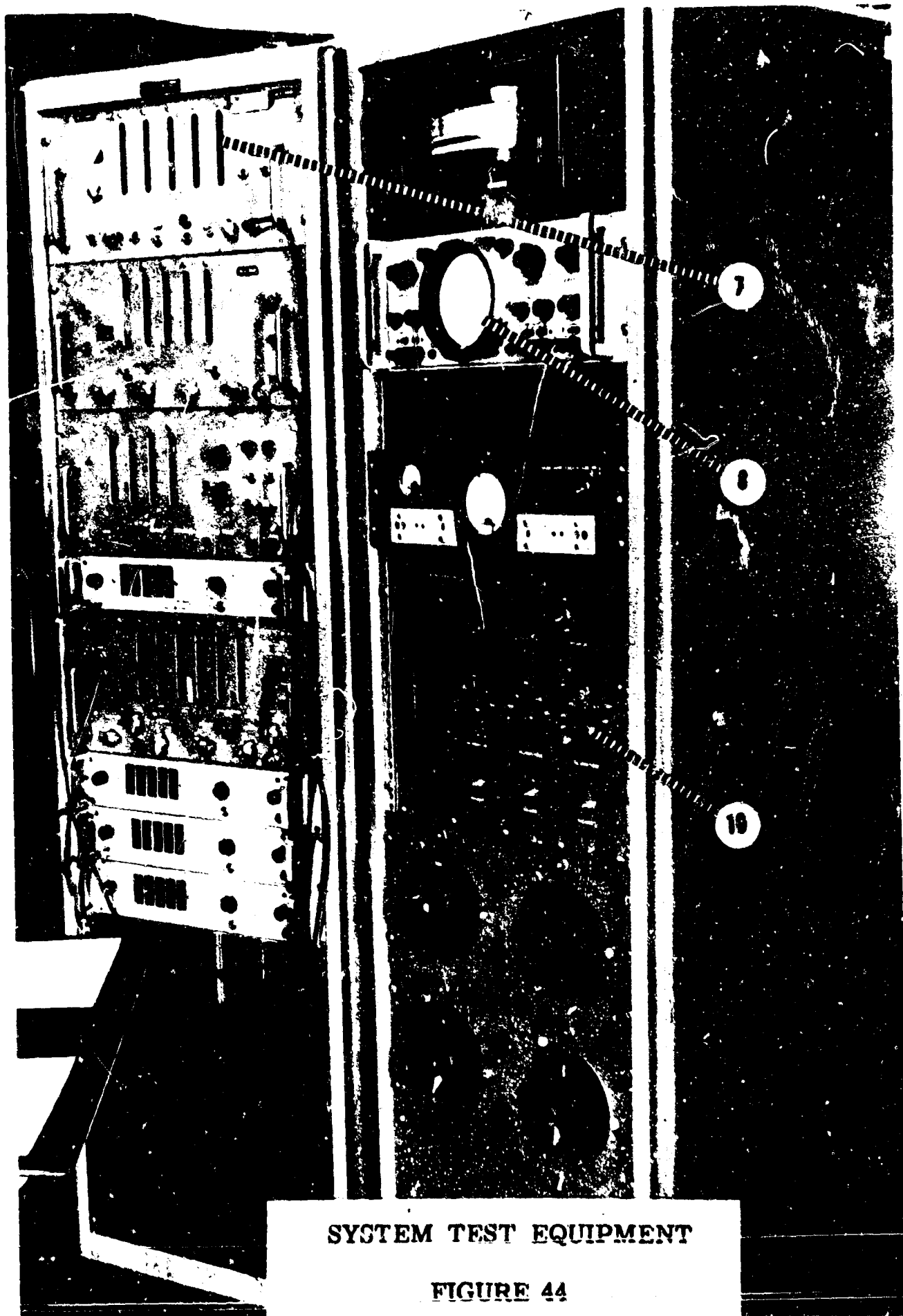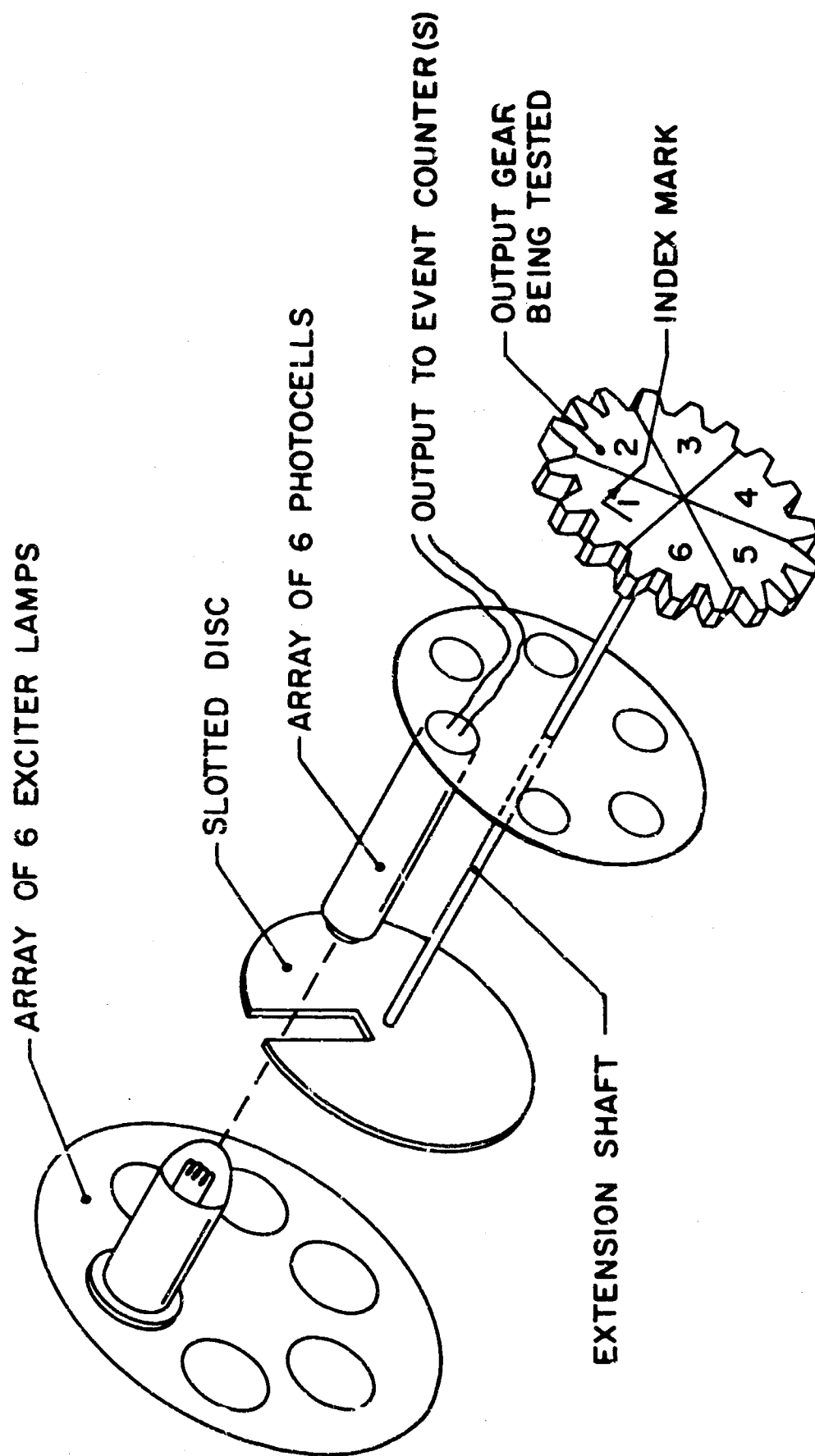
INSTRUMENTATION FOR COUNTING TOOTH LOADING CYCLES

VEN POWER UNIT SYSTEM TEST

FIGURE 45

TABLE XV

INSTRUMENTS USED IN SYSTEM TEST

Description	Test Parameter or Use
Temperature Recorder	Power Unit Temperature
Audio Oscillator Model 200 ABR	Excitation for the Induction Potentiometer
D.C. Amplifier	Amplify Error Signal of Potentiometers
Oscilloscope Model 130C	To Monitor Loads
E-PUT Meter Model 554B E-PUT Meter Model 554B E-PUT Meter Model 7150-38 E-PUT Meter Model 7360C	Drive RPM Tooth cycle counter #1 Tooth cycle counter #2 Tooth cycle counter #3
Event Counter 5212A Event Counter 5212A Event Counter 5212A	Tooth cycle counter #4 Tooth cycle counter #5 Tooth cycle counter #6
3 Morehouse Rings	Actuator Load Monitor

115

Systems Test Plan

The test plan was devised to employ the theory of crack propagation rates and stress to significantly reduce the time necessary to perform a system test to failure in the material fatigue mode on the part(s) selected as the most critical. The plan was based on the following approach:

If
   - the critical parts could be measurably weakened or pre-cracked by artifically creating a crack in the critical area

and if
   - this pre-crack were greater in length than the critical dynamic crack length of the material

but
   - some amount smaller than the critical static crack length under the normal operating loads

then
   - crack propagation should be rapid, continuous, and relatively invariant for a given load spectrum

so that
   - the system operating time to failure will be considerably shorter than that for conventional test methods

and
   - the failure mode desired will be deliberately forced with relatively little probability of another occurring other than secondarily (as an effect).

The acceleration factor for relating the number of missions to failure in this accelerated test to normal service life is developed in the following manner:

   - Periodic inspections of the pre-cracked critical parts are made during the test to measure the changing crack length as a function of the number of missions completed and correlated with the number of stress cycles or tooth engagements

   - The logarithm of the crack length is plotted (using the logarithm ordnate of semi log graph paper) as a function of stress cycles (on the linear scale)

   - Using regression analysis the median slope of the linear portion of the crack propagation function (below the critical static crack length) is obtained and extrapolated down to the critical dynamic crack length of the material. This extrapolation is considered justifiable on the basis of the low variability of the crack propagation stage.

- The median slope of the crack propagation function is used to compute an "equivalent constant vibratory stress level", S_{eq}, from the relationship shown in Equation (1) and from the material constants k and α previously derived.

- The intercept of the linear extrapolation of the propagation function with the critical dynamic crack length defines the lower limit, N_o, of the interval $(N_{fr} - N_o)$ while the number of cycles at complete failure, N_{fr}, defines the upper limit. This completes the minimum system test phase. More confidence in the accuracy of the experimental data may be had by running three system tests (each on a different unit since secondary failures generally destroy the unit). The system load spectrum on one should center around the median of the load range, and the other two units should be tested at load spectra centered at the extremes of the load range (perhaps 2 or 3 σ from the median).

Each of these units will demonstrate a different crack propagation rate and number of cycles from pre-crack to final failure. However, when the log of the crack length is again plotted against a linear scale of cycles a check can be had on the three values providing a range of "equivalent constant vibratory stress" and their relationship to the three load levels imposed as well as three simultaneous comparisons of the material constants k and α.

The determination of the early and more variable portion of the life is left to testing at the part level at the "equivalent constant vibratory stress" where stress cycling rates may be accelerated and where the sample sizes and test costs are more economically adjusted to give adequate confidence in the more variable area.

In the development of methods of "measured weakening" or pre-cracking of the gear teeth several unsuccessful attempts were made to develop adequate repeatable methods. Making a "stress-raising notch" was attempted by grinding with thin discs but the disc edges broke down on the carburized material which had a Rockwell C-60 hardness. Files were not obtainable with fine enough edges for these 32 pitch teeth. Electric etching was found to be uncontrollable in the current level.

The successful repeatable method was finally developed that used a tungsten wire electrode with a chisel edge in a capacitor discharge resistance spot welder. The energy discharge could be controlled by selecting a fixed capacity and a precise charging voltage. Experiments with various capacities and changing voltages were checked by microscopic examination of etched metallurgical sections of the fused area. Proper selection of energy level left a brittle martensitic spot of metal when the fuzed area cooled. This brittle spot was surrounded by a sharp, definable and repeatable shrinkage crack of a length equal to the width of the chisel edge on the tungsten electrode.

The selection of the size crack to be produced was made at the early stage of the test program and quite some time before the material test specimens

(R. R. Moore specimens) were received.

Based on past experience, the stress analysis of the gear teeth and the data in Figure A5 a pre-crack length of .030 inches was selected. Each end of each fillet on each side of each tooth on each output gear (144 places on each power unit) was pre-cracked by the controlled spot welding method. The presence and size of the pre-crack was verified by magnaflux methods and examination under a microscope with a measuring relicle. The location of these pre-crack marks is shown in Figure 46.

The gears were reinstalled in the power units with special care taken to see that no human-introduced errors in assembly would invalidate the test.

The power units were run a total of 539 missions with periodic inspections for crack growth and computation of the number of tooth stress cycles accumulated per mission.

When crack propagation did not proceed as fast as was assumed, it became evident that the acceleration factor for this particular test would not be as high as believed possible. The system test was halted after the 539 missions so that the material tests could be brought further along to substantiate or invalidate the theoretical assumptions.

Program scheduling decisions made for the most effective use of the contract calendar time had specified that the materials testing phase be run concurrently with the system and parts testing instead of prior to these other two phases. A calculated risk was recognized in delaying the outcome of the materials test so that the actual materials data would serve chiefly as post-facto verification of the assumptions made earlier in the system and parts testing.

Subsequent analysis of data from the materials testing described elsewhere in this report showed that the residual compressive stress in the carburized case of the gear tooth material was considerably higher than had been estimated. This made the "non-propagating" crack length for the normal operating stresses in excess of the .030-inch size of pre-crack used on the gears in the assembly test. This high residual compresses stress accounted for the fact that the crack propagation during the system test did not proceed as fast as it could have.

It is recommended that any subsequent test programs not compromise the proper order of testing so that test acceleration may be optimized with the proper materials parameters available before the more complex and costly system testing is begun.

The system test provided the comprehensive data necessary for relating tooth stress cycles to missions with the high statistical confidence. This cycles/mission ratio forms a part of the second acceleration factor, F_2, developed in the parts test phase.

113

.030 IN.

INDEX MARK FOR
TOOTH IDENTIFICATION
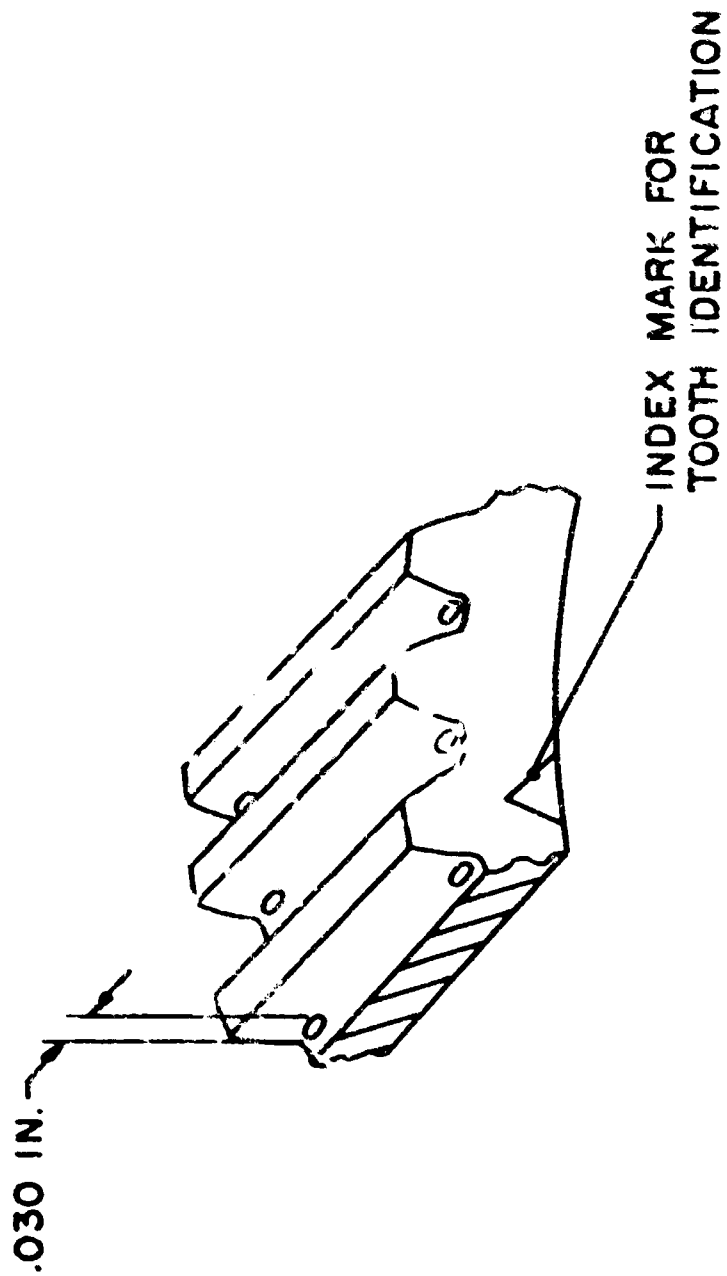
SECTION OF OUTPUT GEAR SHOWING PRE-CRACK

SPOT-WELD MARKS AT MAX. STRESS POINTS

FIGURE 46

Accelerated Parts Test

The first step in the parts testing program was to design and develop a system capable of fatigue testing a gear from a production VEN power unit. The main criteria for the test system were adjustability of applied load and frequency during operation for maximum compression of test time plus precision fixturing for accurate, repeatable tooth loading from gear to gear.

The method chosen was a combination of an electrodynamic shaker system for the vibratory load and a relatively soft spring shock cord for the steady load. The sinusoidal vibratory load was superimposed on a somewhat higher steady load so that the gear tooth was never unloaded during the period of a cycle, thus avoiding an impact condition. A typical cycle would be adjusted to have a minimum tooth load of 20 pounds force with a maximum of 380 pounds force and noted as 200 pounds steady, ± 180 pounds vibratory. The dual test rigs are shown in Figure 47.

The gear holding fixture was precisely machined and finally assembled using precision gauge blocks to obtain the desired line of load application on the gear tooth. The design allowed the gear holding plug to be simply but repeatedly inserted in the fixture and rotated until the test tooth contacted the loading rack insert. The plug was clamped in position at this point and a precision gauge block measurement check made to confirm the proper load application line. The vertical position of the rack holding block was maintained by flexure plates attached at either end and fastened to the fixed base plate thus allowing horizontal motion at the loading member while restricting vertical and lateral motion. (See Figs. 48, 49, 50, 51, and 52).

Installation of the test gear specimen in the fixture was followed by application of the steady load, the magnitude of which was set by the output from the precalibrated Morehouse ring and monitored on the SR-4 strain indicator. The dynamic load was applied by increasing the oscillator output voltage to the amplifier-vibration exciter system until the output voltage from the force gauge-amplifier system reached the required level. The force gauge signal was also monitored by oscilloscope for detecting tooth chatter (indicating vibratory load larger than steady load) and wave shape distortion (indicating possible start of a tooth crack). Frequency of applying fatigue cycles was manually adjustable at the oscillator and could be increased or decreased even while running with careful simultaneous compensation for system gain to maintain oscillator output voltage. During the course of testing operation over a range of from 50 to 500 cps was found to be satisfactory although the system is not limited by these extremes.

Cycle counting was accomplished by triggering an electronic digital readout counter as the vibratory load was applied.

The test gears (obtained from the production line) originally contained eighteen teeth, but were prepared for test by removing two teeth between each test tooth resulting in a test specimen with six teeth. This procedure was adopted to provide clearance for the driving rack and to insure isolation of each test tooth from the preceding fracture. (See Figure 49).

121

TABLE XVI

DETAILS SHOWN IN PHOTOGRAPHS

1.   Shaker Control Panel
2.   Shaker
3.   Impedance Head (Force Gage)
4.   SR-4 Steady Load Indicator
5.   Morehouse Ring
6.   Shock Cord
7.   Force Monitoring Oscilloscope
8.   Gear Test Fixture
9.   Test Gear
10. Gear Mounting Plug
11. Fatigue Cycle Counter

FIGURE 47

1.   Shaker Control Panel
2.   Shaker
4.   SR-4 Steady Load Indicator
7.   Force Monitoring Oscilloscope
11. Fatigue Cycle Counter

122
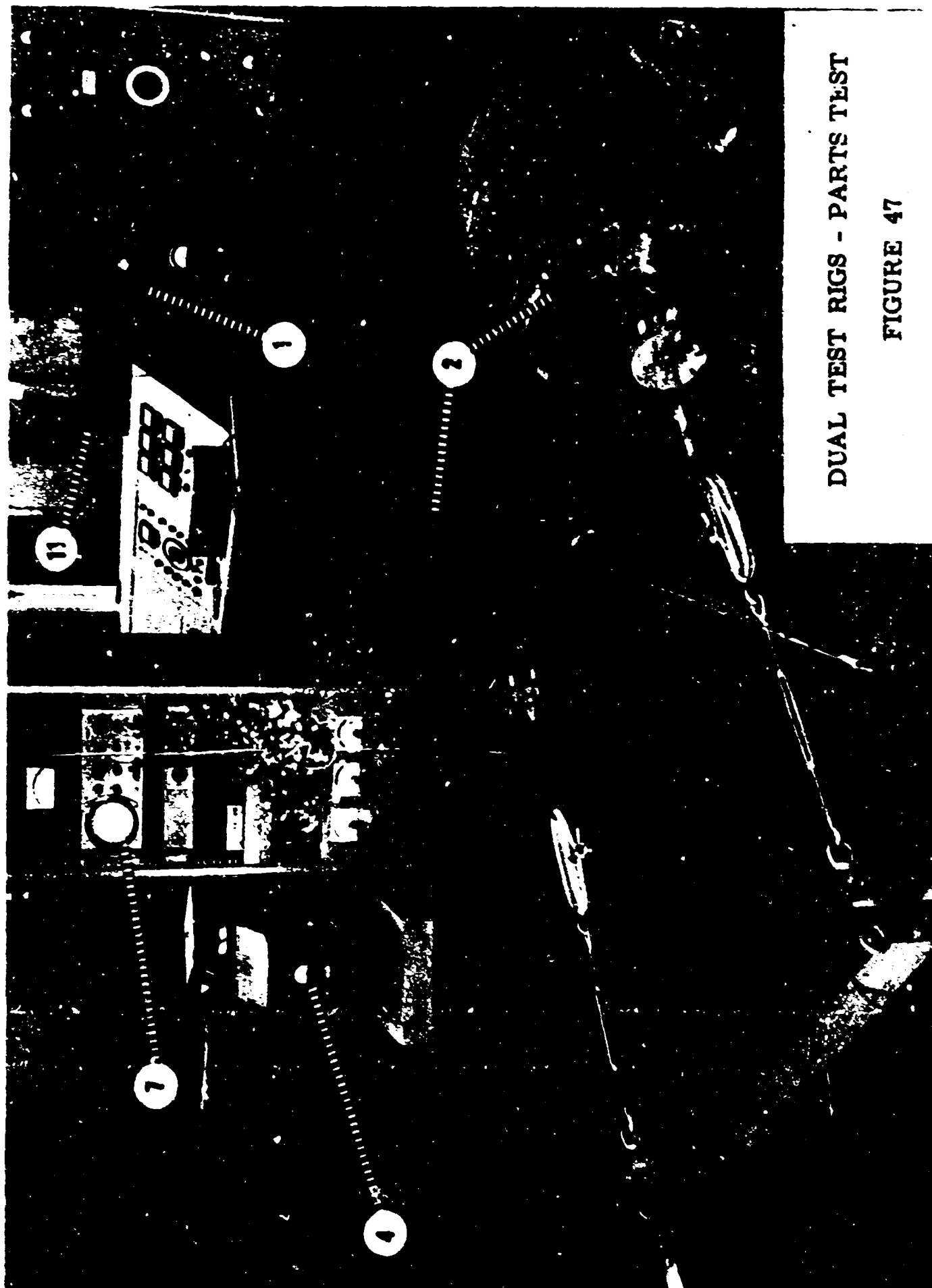
DUAL TEST RIGS - PARTS TEST

FIGURE 47

123

PRECISION GAGE WIRE

SIMULATED RACK TOOTH

TOOTH CONTACT POINT

CONNECTION TO STEADY LOAD

₵ OF PLUG

ENLARGED VIEW B

GEAR ADAPTER PLUG ASSY

CONNECTION TO FORCE (IMPEDANCE) GAGE AND ELECTRODYNAMIC VIBRATOR

SEE ENLARGED VIEW B

TEST GEAR

LOADING BLOCK

STEADY LOAD

FLEXURE SPRINGS

BASE

CLAMPING BLOCK

RACK TOOTH
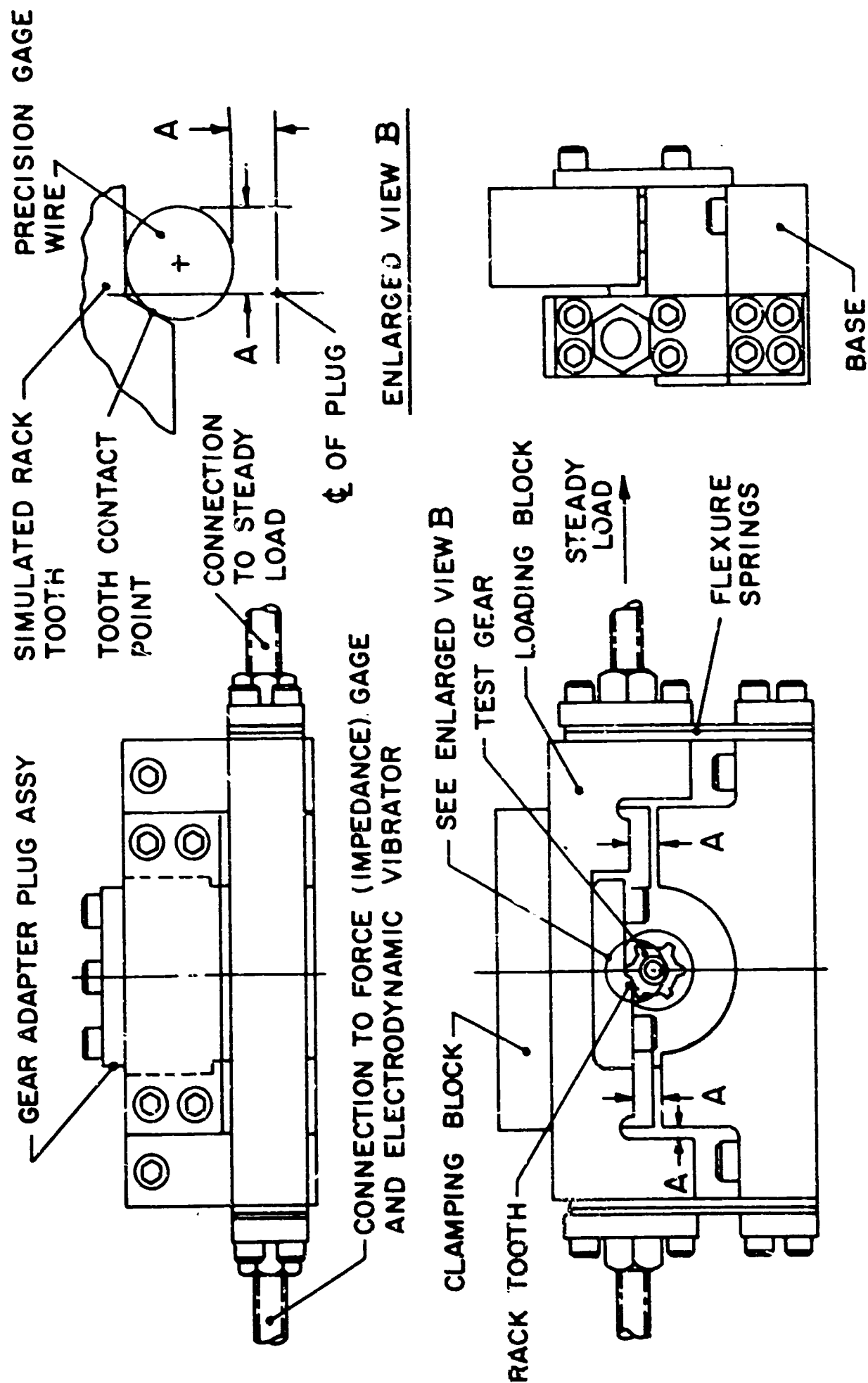
PRECISION GAGING SURFACES AT A.

GEAR TOOTH FATIGUE TEST FIXTURE

FIGURE 48

124

GEAR LOCATING PLUG

SAMPLE OUTPUT GEAR (S) FROM PRODUCTION LINE

SET SCREW AND KEY

CLAMPING PLATE

A

A

A

TWICE SIZE

TEETH REMOVED TO CLEAR "RACK TOOTH" IN TEST RIG

A = PRECISION LOCATING SURFACES ON NORMAL PRODUCTION GEAR
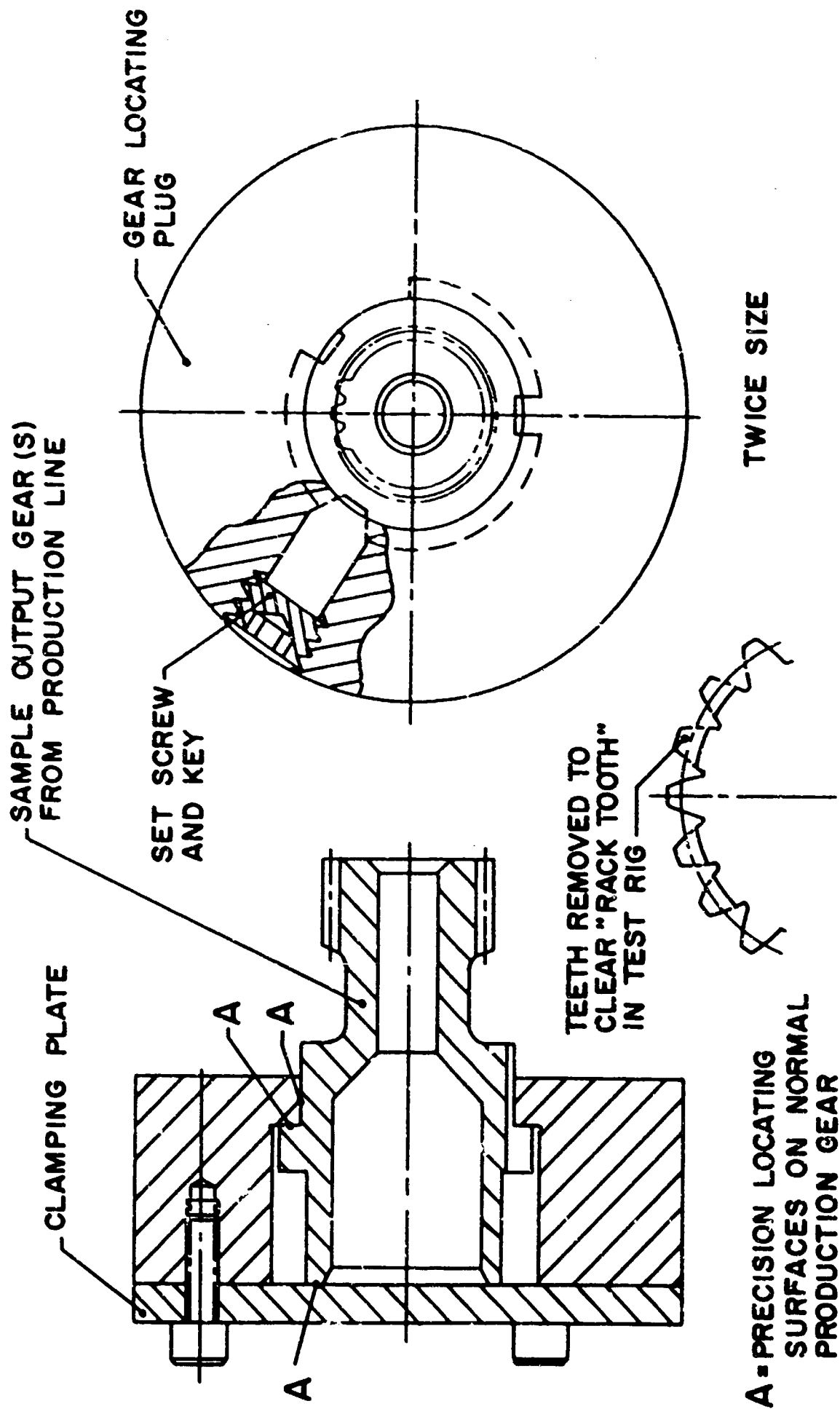
PRODUCTION GEAR SAMPLE MOUNTED FOR POSITIONING IN FATIGUE TEST RIG

FIGURE 49

125

FIGURE 50

2. Shaker
3. Impedance Head (Force Gage)
4. SR-4 Steady Load Indicator
5. Morehouse Ring
6. Shock Cord
8. Gear Test Fixture
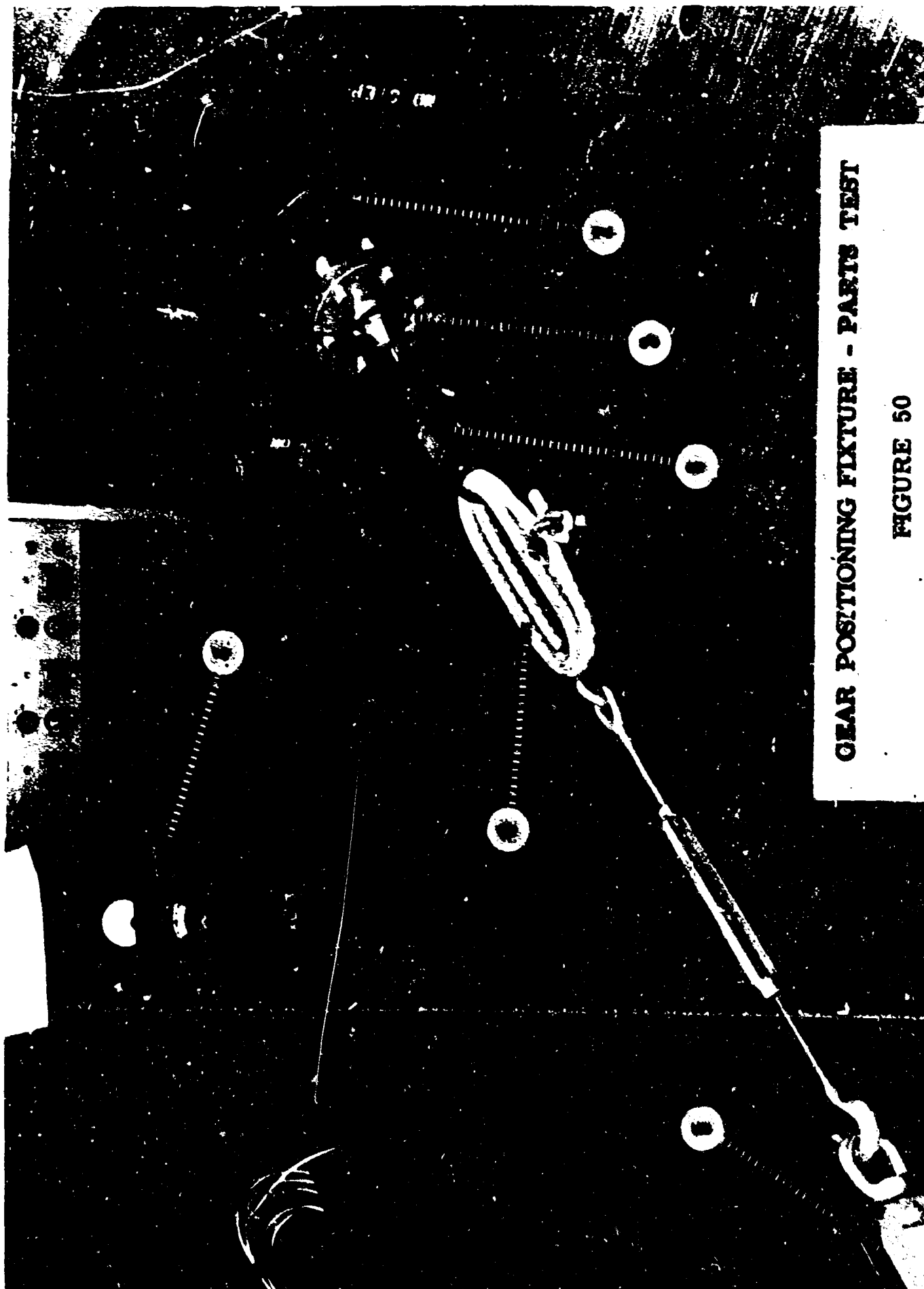
GEAR POSITIONING FIXTURE - PARTS TEST

FIGURE 50

FIGURE 51

2. Shaker
3. Impedance Head (Force Gage)
6. Shock Cord
8. Gear Test Fixture
9. Test Gear
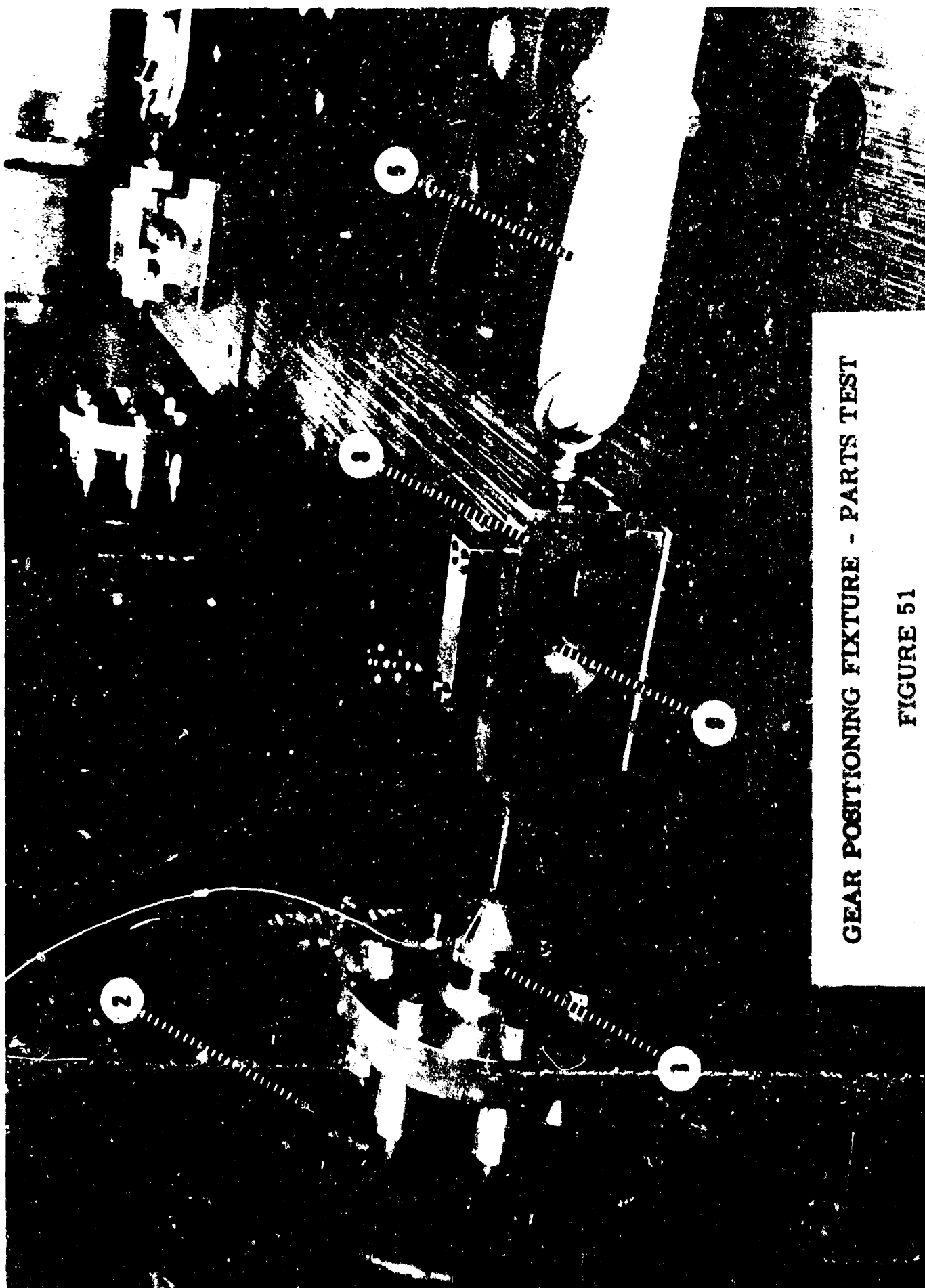
GEAR POSITIONING FIXTURE - PARTS TEST

FIGURE 51

FIGURE 52

3. Impedance Head (Force Gage)
6. Shock Cord
8. Gear Test Fixtures
9. Test Gear
10. Gear Mounting Plug
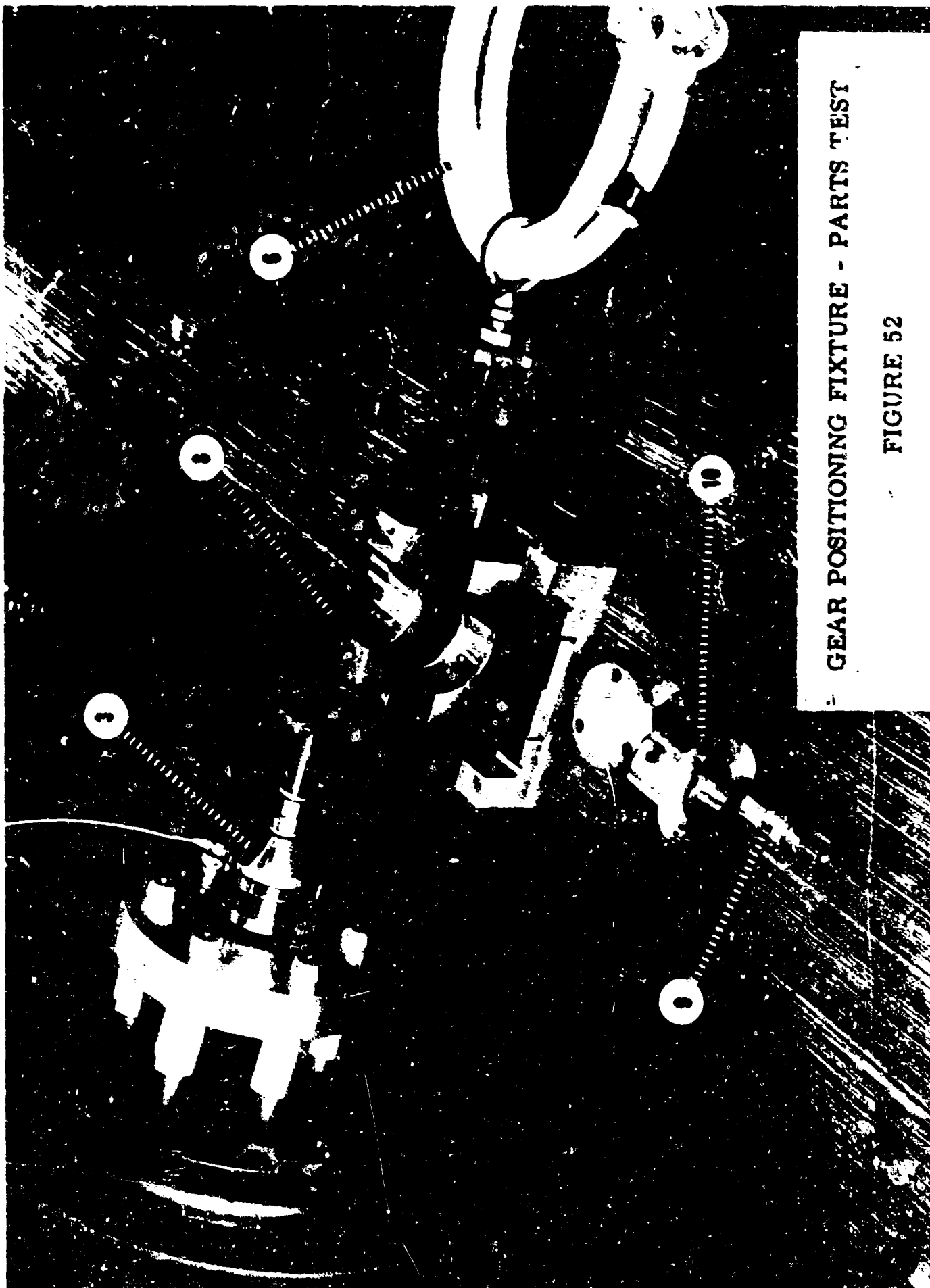
GEAR POSITIONING FIXTURE - PARTS TEST

FIGURE 52

Parts Test Plan

In the parts testing, the ultimate plan was to test a reasonable sample of production gears at an "equivalent vibratory stress" determined from the crack propagation rates measured under normal loads with pre-cracked gears in the system test.

Each of the sample gears was to be tested until cracked to the critical dynamic crack length. The study of the fatigue failure mechanism described earlier, indicated that the greatest variability but shortest duration in fatigue life would occur in this crack development phase. The speed and economy of testing many relatively cheap gears at high cycling frequencies to obtain a measure of this variability was evident.

The distribution of cycles to "failure" (in this case achieving the critical dynamic crack length) thus obtained quickly and at minimum test cost must be added to the cycles to propagate the crack from critical dynamic crack length to final fracture obtained from the systems test. This systems test is run with only a few samples because of the low variability encountered in the propagation stage and the relatively high cost of system testing.

The preliminary portions of the test plan contained provisions for check-out of stability, repeatability and effectiveness of the test rig.

They also provided for developing an S-N diagram to correlate loads and stresses. Additional steps included experimentation for developing techniques for measuring crack lengths and propagation rates, verifying the precision of the pre-cracking technique and its acceleration of failure, and in determining how high an acceleration factor could be obtained in testing.

Establishment of Test Load-Stress Relationship

To relate the test loads on the gear tooth in the parts testing to material stresses it was necessary to calculate the bending stress at the critical section of the tooth root fillet.

The fillet contour of a thin section of a production 167262 Output Gear was determined by tracing from a 31.25 x optical projection, considering several tooth spaces. This was done to account for production tooth profile variations from the theoretical drawing specifications.

The Worst Load Radius of the 167262 Gear as meshed with its mating 167263 gear was calculated as the maximum radius of single tooth loading. This was calculated from the minimum O.D. of the 167263 gear. (See Figure 53).

The projected height of the worst load radius was calculated as well as the offset distance and operating pressure angle at that radius.

132

These values were used to position the loading rack tooth profile with respect to the centerline of the tested gear in the gear tooth test rig using gauge wires and gauge blocks. This set of conditions produced the maximum stress at the same critical section created by the meshing of the 167263 Gear with the 167262 Gear in the actual assembly. The gaging method is shown in Figure 43.

The location of the critical section was determined graphically under these conditions of loading to locate the anticipated origin.

A stress load ratio of 418 psi/lb. of tooth load was used to set loads in the testing. A check of this was made by plotting the S-N data from the tested teeth together with that of the R.R. Moore specimens testing in the materials test program.
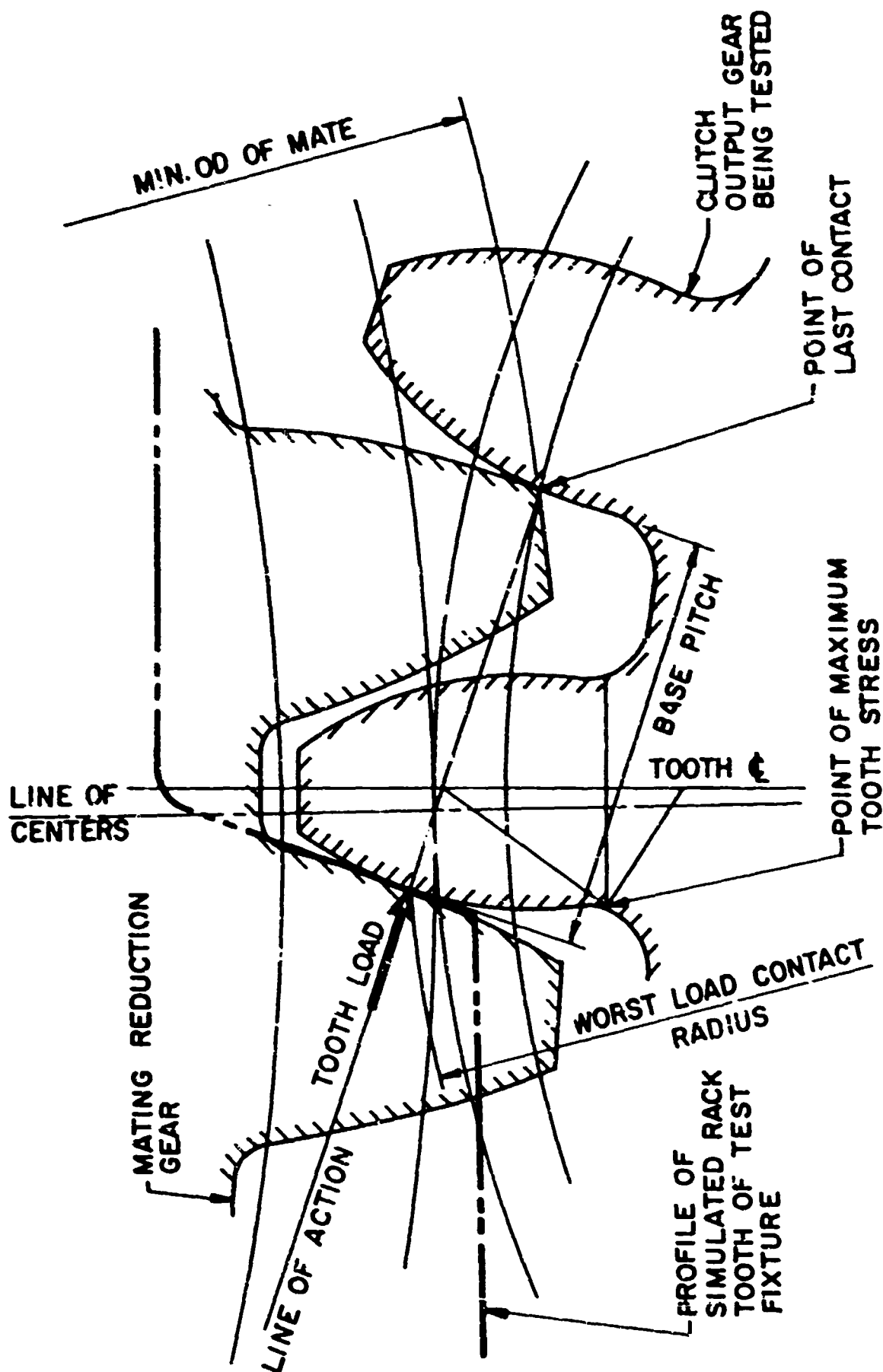
LAYOUT OF TOOTH ENGAGEMENT SHOWING MAXIMUM

LOAD AND STRESS POINTS

FIGURE 53

134

Testing

The first gear to be installed in the test fixture was intended for checking
rig operation, tooth loading pattern and testing techniques. The first few
runs also served to establish workable steady vibratory load ratios and con-
firm expected fatigue life at various loads. However, as rig operation appear-
ed completely satisfactory from the first tooth tested, all preliminary data
could be included in the results.

An impedance head, which produces an acceleration signal as well as a force
signal at the driving point, was used in one of the two rigs. As this data
for analyzing the mechanical impedance of the gear fixture system was avail-
able observations of force, acceleration and their phase relationship were
made over a range of 20 to 1000 cps. Analysis of the data showed no unwanted
resonances or anti-resonances over the required range of 50 to 500 cps.

After breaking several teeth completely and stopping several teeth with vis-
ible fatigue cracks started it became apparent that the change in magnitude
of the signal from the force transducer was a good indicator for the start
of propagation of a fatigue crack. A portion of the test was devoted to an
attempt to quantitatively relate the change in force signal to crack origina-
tion and crack propagation. Several gears were run in an attempt to establish
"beach" marks in the fatigue pattern by first establishing a small crack in
the tooth, then by running at a reduced vibratory load level for a period and
then by running again for a period at the original high level. This alternate
high and low level running was continued until the tooth broke. However, this
method was set aside when beach marks were not readily detected. Subsequent
analysis of the data gave evidence that a descrepancy in the test procedure
had precluded the desired results. This renewed the belief that further in-
vestigation at some later date might find this technique a useful method of
measuring crack propagation.

An investigation of a gear weakened by pre-cracking in the corners of the
tooth root by a small spot weld mark produced a propagating crack in a very
short time. An inspection at 32,000 cycles revealed a .030" crack developing
from this pre-crack. Subsequent inspections at regular intervals provided
data for a curve of crack propagation vs. cycles with the final crack length
measured at 0.227" just prior to complete failure. Several gears were used
to establish S-N curve data by testing over a wide range at loads. Another
attempt at determining crack progression consisted of running the six teeth
of one gear specimen until a change in force response was noted and then
stopping the test. However, each tooth was stopped after a progressively
larger change in force response (indicating development of a larger crack).
The gear was then heat treated for a period of time in order to oxidize the
metal inside the crack so that later after the tooth had been broken off
quickly and completely with a high load, oxidized areas might be discernable.
The results of this test showed promise.

The first tooth (having the smallest change in force response) with no externally visible crack produced very slight indications of the typical blue oxide discoloration. The second and third teeth with still no externally discernable cracks produced small discolored areas in the order of a few thousandths of an inch in length. The fourth tooth with an easily visible crack showed the blue discoloration over roughly one half of the final fractured area. The fifth tooth with a large visible crack was oxidized over approximately two-thirds of the final fractured area. The last tooth broke completely off before the heat treatment showing that the full range of response change had been covered.

Observations made during the period of testing indicated that the system was extremely stable prior to the development of a crack in a tooth. Variations in response during steady state appeared less than 0.5%. Consequently changes of 1% or more could readily be detected and the system shut down for inspection for locating a crack.

This testing proved that detection of the start of a crack in a gear tooth by its impedance change could be made earlier than by any other known method. Further exploration of this technique and more comprehensive correlation of crack size with impedance change is recommended.

Accelerated Materials Test

The materials test phase of this program was initiated to establish the material constants necessary to develop the acceleration factors to relate fatigue life to crack propagation in accordance with the theory previously discussed.

Fifteen material test specimens were procured in accordance with detailed specifications shown in Table VIII and Figure 60 . Five of the specimens were selected at random and run at constant stress levels to complete failure at 10,000 cycles per minute with the results as follows:

Specimen No.	Stress ksi	Cycles to Failure
C-8	± 150	32,000
C-4	± 135	129,000
C-6	± 120	896,000
C-10	± 110	19,912,000
C-15	± 100	81,278,000

It was decided on the basis of this data to generate cracks deliberately in some specimens to develop methods of making them to a prescribed size.

To develop methods of making cracks of a prescribed size it was decided on the basis of the foregoing data to run specimens at a stress level of ± 140,000 psi to form cracks deliberately. This stress level was selected because it promised to develop cracks in a short time (under 129,000 cycles or 13 minutes at 10,000 RPM) but not so short a time that crack propagation was too rapid to stop or to measure.

These tests were stopped periodically and the specimens inspected with a 30 x binocular microscope with a measuring reticle in the lens system. Typical crack development histories are shown in Figure 54 The ability to generate a crack .030 to .033 in. long at this stress level was demonstrated. Certain of these specimens cracked at ± 140,000 psi were then run at lower stress levels 80,000, 95,000 and 100,000 psi to failure with the crack propagation rates determined during periodic stops for inspection and measurement with the microscope. The data is plotted in Figure 55.

One specimen (C-9) was run for 140,000 cycles at ± 140,000 psi and no crack was seen. After 150,000 cycles a crack .0304 inches long appeared. Such rapid appearance of a crack indicated that the crack had started and grown below the surface (probably at some large inclusion) before opening to the surface. The stress was lowered to ± 80,000 psi and crack progress was monitored until failure after 47,000 more cycles. Examination of the fractured surface after failure confirmed that the origin of failure was sub-surface. The inclusion which initiated failure was .0022 inches long by .0012 inches wide and .024 inches below the surface. The appearance of the fractured surface is shown in Fig. 56 .

137
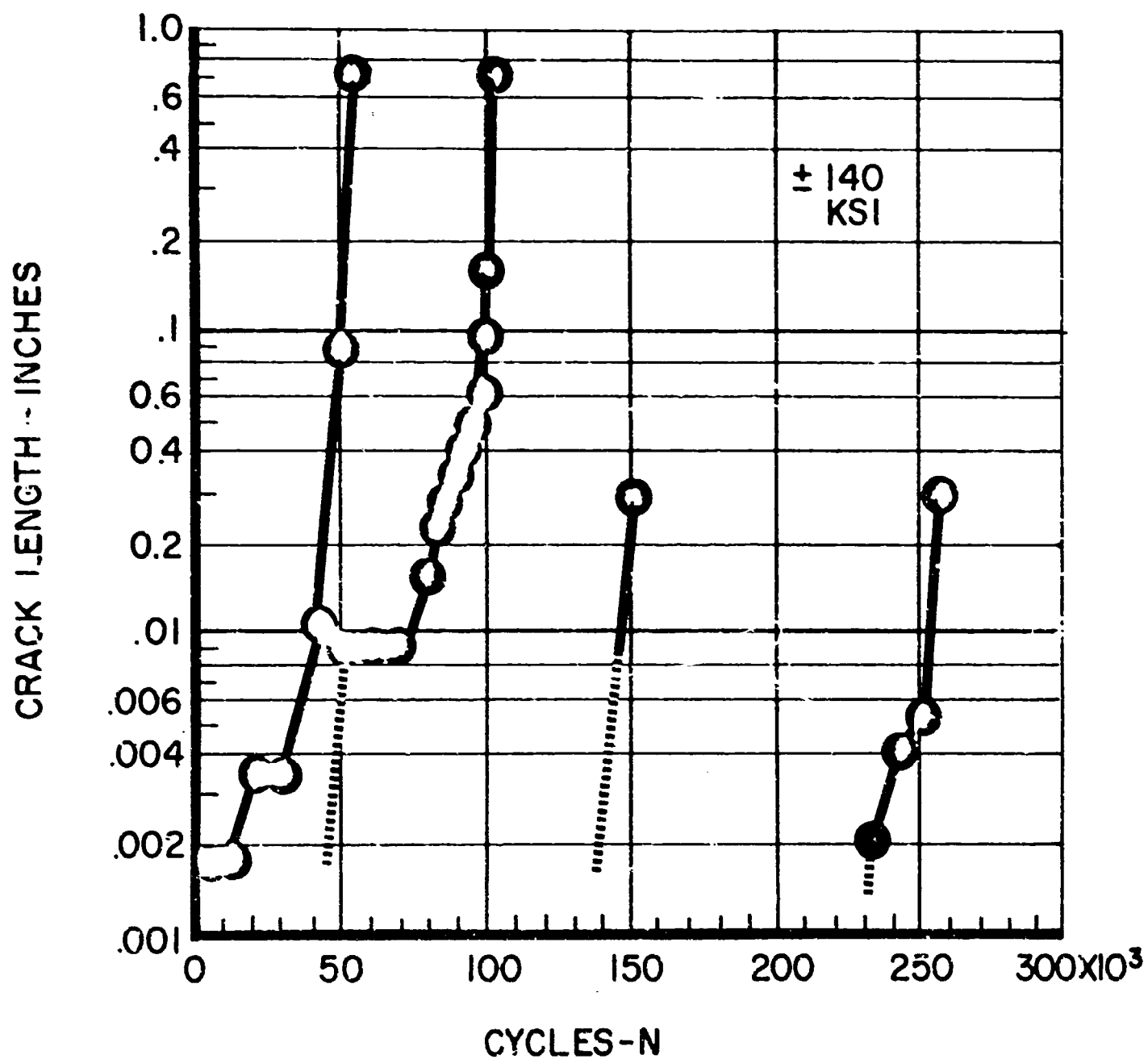
CRACK DEVELOPMENT & PROPAGATION HISTORIES

FIGURE 54

138
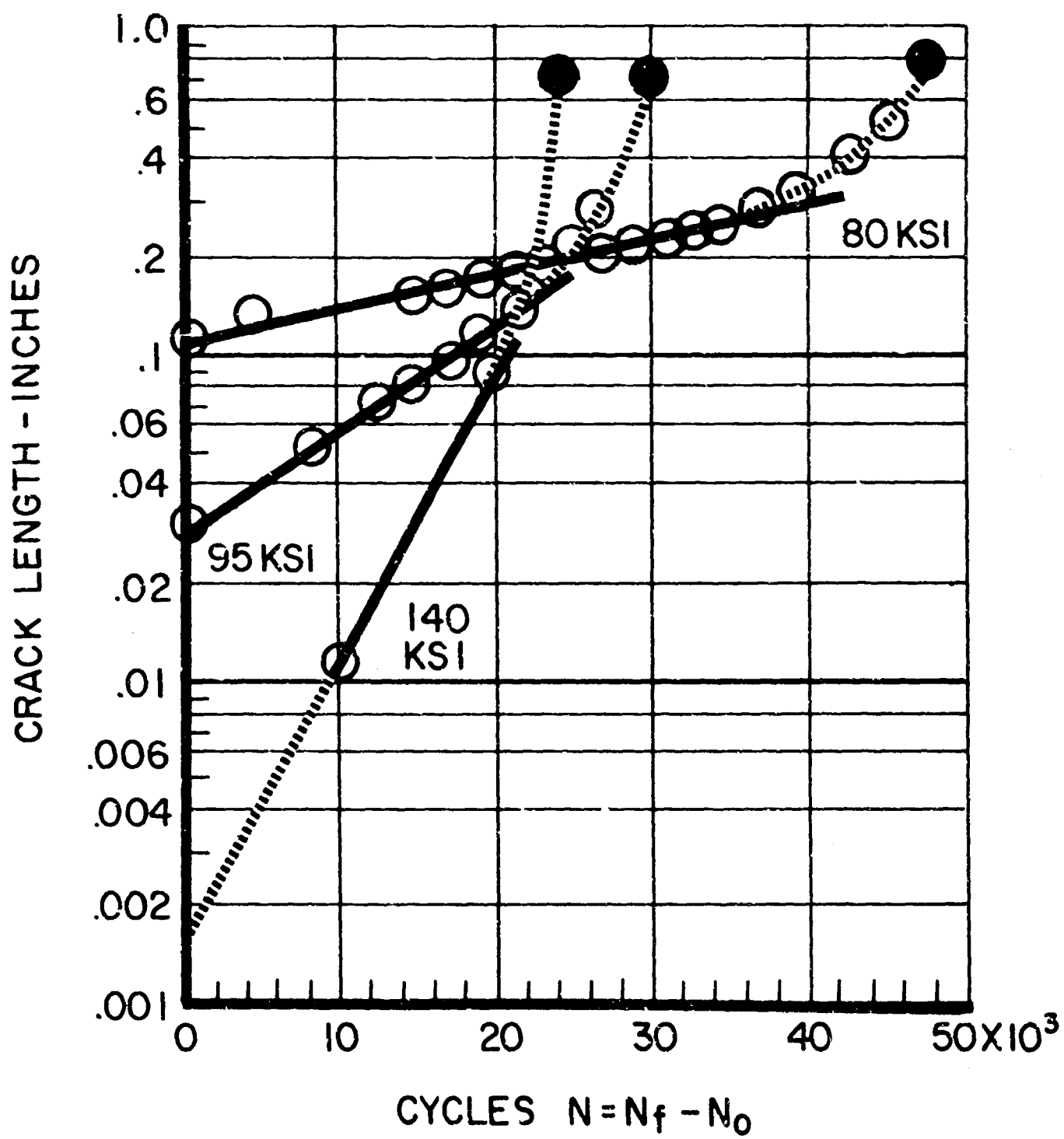
CRACK PROPAGATION STAGE

CARBURIZED GEAR MATERIAL

FIGURE 55

Sample C-9	Sample C-13	Sample C-11
80 KSI	100 KSI	140 KSI

MAGNIFICATION 4.2 X

FIGURE 56

The effective length of the crack was determined from the fractured surface after failure to be .104 inches at the time it appeared on the surface at .0304 inches and the 80,000 psi testing was started.

A verification of the efficacy of the capacitor discharge welder method of pre-cracking was made by making a .03 inch mark (identical to those made in the gear tooth fillet radius) at the midpoint of specimen (C-12). A 100,000 psi stress level was selected to minimize the length of the test and still make propagation slow enough to monitor. The crack propagation rate was identical to that for the specimen pre-cracked by first running at ± 140,000 psi to develop a crack .0297 inches long and then continuing at ± 100,000 psi to failure.

The next step of the material test program was planned to determine the critical dynamic crack length in the normal operating range of stresses experienced in the fillet at the root of the critical power unit output gear. At these stresses cracks are very minute and slow in developing in the early stages of the fatigue life, visual observation, even with the highest power microscopes becomes subject to the vagories of human vision and boredom. A photographic method previously developed was used to record the appearance of the specimen periodically throughout the test. When a crack became readily visible with the naked eye it could be located on the photographic record and readily traced backward and measured in the pictorial history of the crack. The equipment used in this photographic method is shown in Fig. 57.

The photographic method as developed, used 35 mm fine grain film and a magnification of approximately 4 x. Although a higher magnification might appear to be preferred, it was necessary to be sure that the cracks developed would be in the field of view and this entire field in focus. The 4 x magnification was the practical compromise. With the use of a fine grain film and a fine grain developer, the image on the film was easily projected on a screen to give a clear picture at magnification of 100 x. This enabled measurements of crack length with accuracies in the order of .0005 inches.

Oblique lighting of the polished specimen produced light reflections from the edges of the crack against a dark background. The negative shows a dark crack against a light background in the projected image. A positive print appears as shown in Figure 58.

To obtain a complete picture of the surface of a specimen, 18 pictures were taken around the circumference. The shaft of the fatigue testing machine was indexed for this purpose.

The individual fields overlap enough to insure complete recording of all possible cracks. Initial photographs of the surface before any running is started were taken to facilitate locating cracks since small imperfections and inclusions on the surface make a sort of map of the specimen surface. One specimen photograph was made to include a ruler divided into hundredths of an inch to adjust the projected image of the film to 100 x magnification and facilitate accurate measurement of the crack length.

141

FATIGUE CRACK PHOTOGRAPHIC RECORDING EQUIPMENT

FIGURE 57
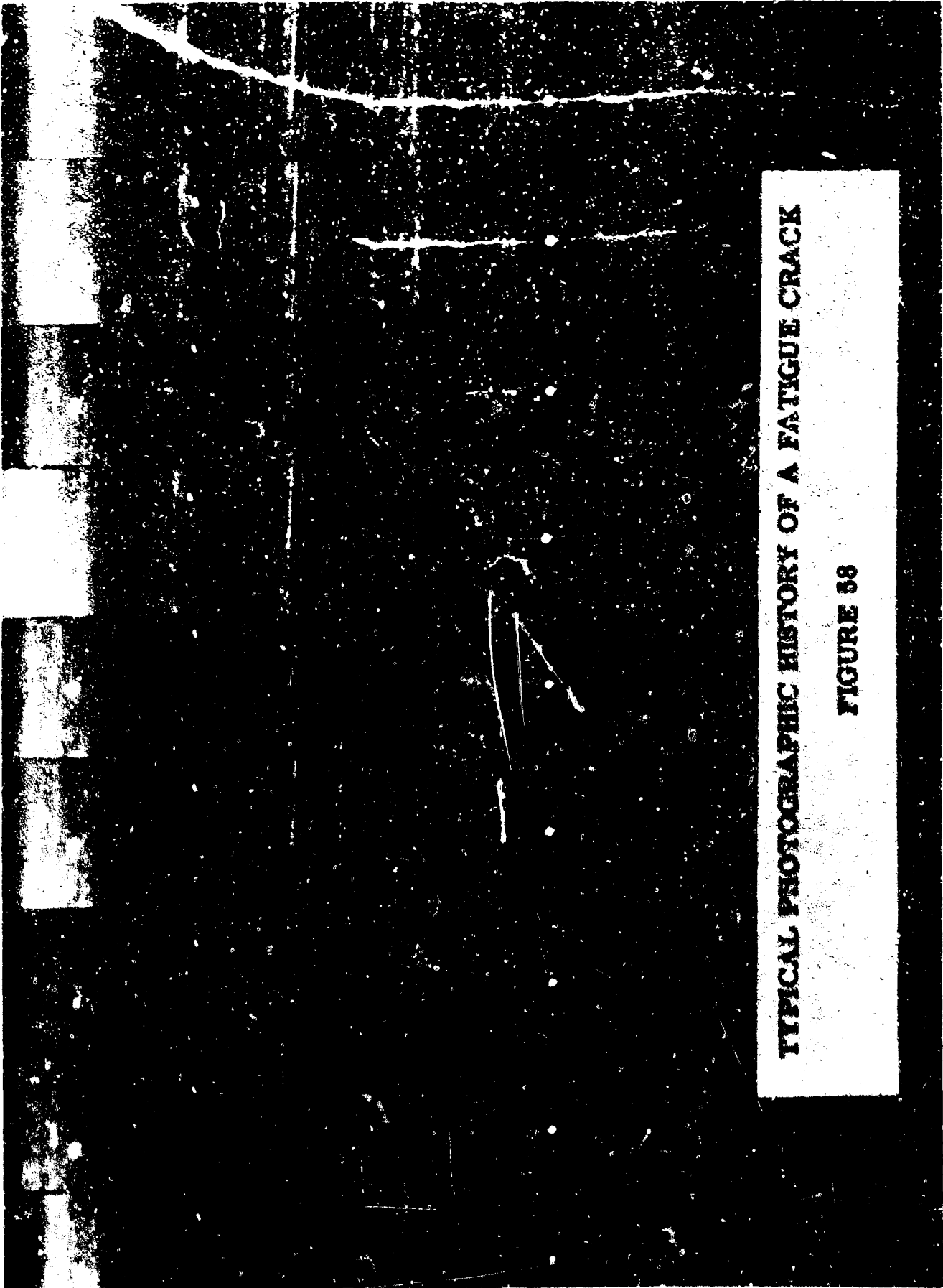
TYPICAL PHOTOGRAPHIC HISTORY OF A FATIGUE CRACK

FIGURE 58

143

Specimen C-3 was tested as a control for comparison with previous
data at ± 140,000 psi, but failed after 54,000 cycles somewhat sooner
than expected since photographs were spaced at 10,000 cycle intervals.
A second specimen, C-2, developed the first visual crack .030 long at
260,000 cycles. Subsequent inspection of the film shows the crack first
appeared after 230,000 cycles when it was .002 inches long. At 240,000
cycles it was .004 in. long and grew to .005 in. at 250,000 cycles. At
this point it was decided to obtain the crack propagation rate at the
normal operating stresses. So this specimen, C-2, already cracked
(.033 inches long) was run for 1,000,000 cycles each at the following
stress levels with no measurable increase in crack size:

$$\pm\ 60,000\ psi$$
$$\pm\ 65,000\ psi$$
$$\pm\ 70,000\ psi$$
$$\pm\ 75,000\ psi$$
$$\pm\ 80,000\ psi$$
$$\pm\ 85,000\ psi$$
$$\pm\ 90,000\ psi$$

When the stress level was increased to ±95,000 psi crack growth
proceeded steadily to failure.

It was this data that finally gave a measure of the residual com-
pressive stress in the hardened carburized case of this material and
brought to light the reason for the poor acceleration factor obtained
in the systems test.

A residual compressive stress has long been known to be created in
the case of carburized steels in heat treatment. It is a major
reason for use of this material for gear teeth requiring high relia-
bility. It serves to raise the "non-propagating" crack size for
each given stress level. ("Non-propagating" here means no signifi-
cant propagation under 10^6 cycles although slow and intermittent
crack development does proceed with an accumulation of cycles in
excess of 1,000,000).

Subsequent analysis of certain portions of the data from the various
material specimen tests provided the correlation between "non-propa-
gating" crack length and stress level for this material as shown in
Figure 59 . Plotted with this same data is that from Figure A5
for 4340 through-hardened steel. The normal operating stresses of
the critical gear teeth being tested in the system test lie within
the range of 60,000 to 85,000 psi. The .030 inch pre-crack size
selected for the gear tooth fillets early in the system test program
was well above the non-propagating crack length curve for the 4340
steel but unfortunately below that found later as shown in Figure 59
for the carburized MS 5260 (AISI 9310) steel.

144

MATERIALS TEST DATA
"NON-PROPAGATING" CRACK SIZE
FOR
CARBURIZED GEAR MATERIAL
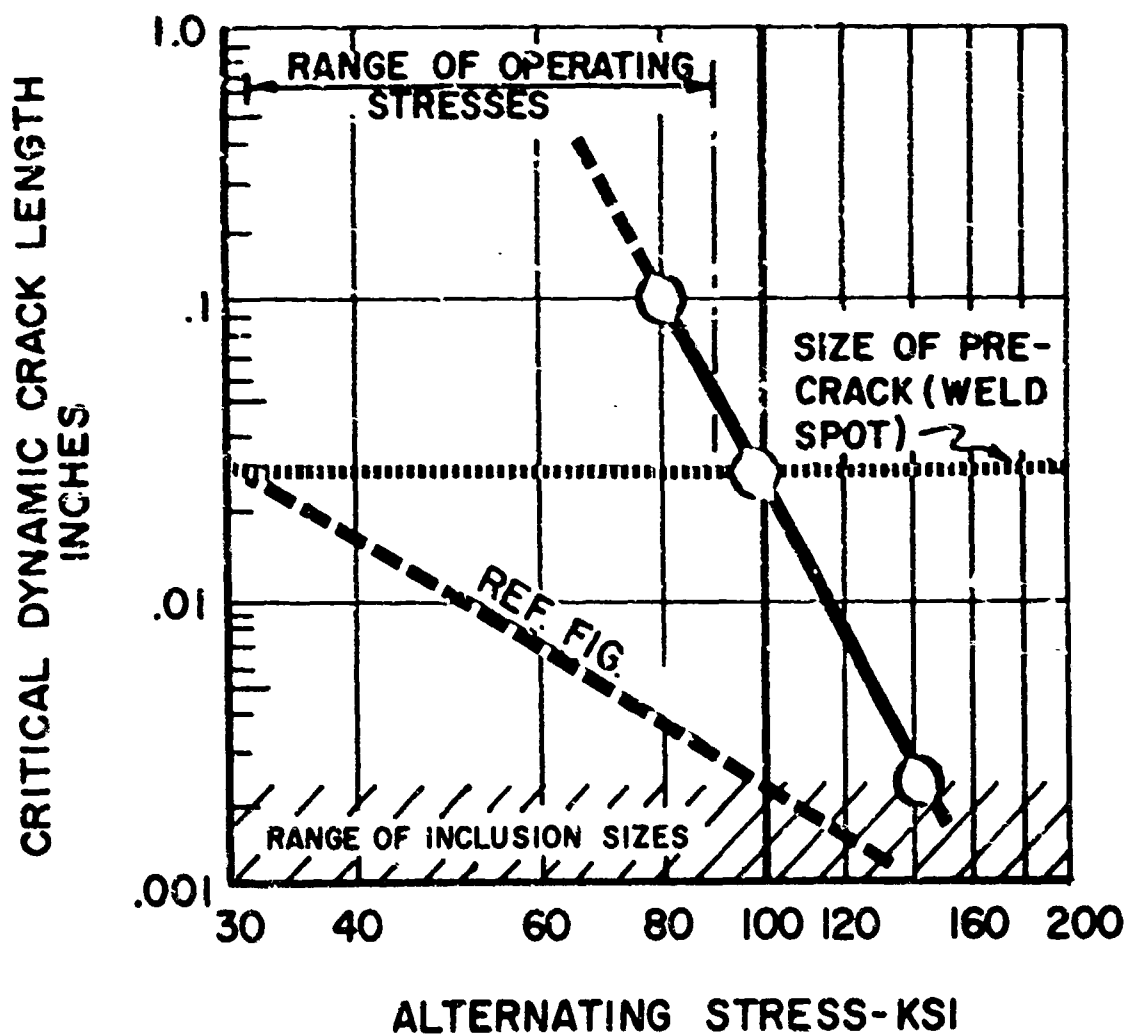
FIGURE 59

Had this material data been obtained prior to the system testing, a pre-crack in the order of .200 inches long might better have been used on the gear teeth. It is estimated that had this been known earlier, the system test could have been shortened to something in the order of 20 missions to failure or approximately 100 minutes of actual running time.

Analysis of the data shown in Figure 55 using Equation (1) established the material constants for this material as:

$$\alpha = 4$$
$$k = 2.3 \times 10^{-24}$$

The materials test program served to verify the theoretical approach to accelerated fatigue testing through crack propagation studies. The required constants for the gear tooth material were established as planned.

Scheduling of the three phase test program in any further application of these techniques should place the three phases in the **sequential** order:

1. Materials tests

2. System tests

3. Parts tests

to have the information required for the start of each phase available in the proper form from the preceding phases.

TABLE XVII

Material Fatigue Test Specimen Specification
(R. R. Moore Rotating Beam Type)

All R. R. Moore fatigue specimens are to be machined and ground in accordance with the following basic procedure, maintaining identity of each specimen throughout the cycle (identify specimens on recess of tapered area).

1. Rough machine using coolant - leave center section approximately .020 oversize using AMS 6260 steel (AISI 9310) supplied by production stores and identified by heat number.

2. Finish machine using coolant - leave center section approximately 0.008 oversize.

3. Grind center section to approximately 0.002 oversize using coolant and freshly dressed wheel which follows template having same contour as specimen.

4. Heat treat as follows:

   Carburize in salt at 1550°F for one hour.

   Transfer to neutral salt at 1480°F and hold 20 minutes.

   Oil quench.

   Temper 275°F for 3 hours.

   Case hardness to be Rockwell 15N 90 - 90.5 and case depth to be .012 - .013 inches deep.

   Core hardness to be Rockwell C38.

5. Polish specimen to size in a longitudinal direction only (no cross polishing) using three or four successively finer mesh abrasive cloths and a lapping lubricant so as to obtain a finish of 2 micro-inches RMS max. Care must be taken to make sure that polishing is done without any burnishing or localized heating.

6. Stress relieve at 275°F for 3 hours.

7. Dip specimen in a fingerprint neutralizing, water displacing rust preventive oil and wrap carefully prior to shipment. Vendor to be approved by Metallurgical Department.

SMOOTH CONTINUOUS CURVE
POLISH LONGITUDINALLY
ROUGHNESS NOT TO EXCEED
2 MU IN RMS

.23 DIA.

5.00R

1.00R

TAPER .625 PER FOOT
INCLUDED ANGLE TO
FIT GAUGE
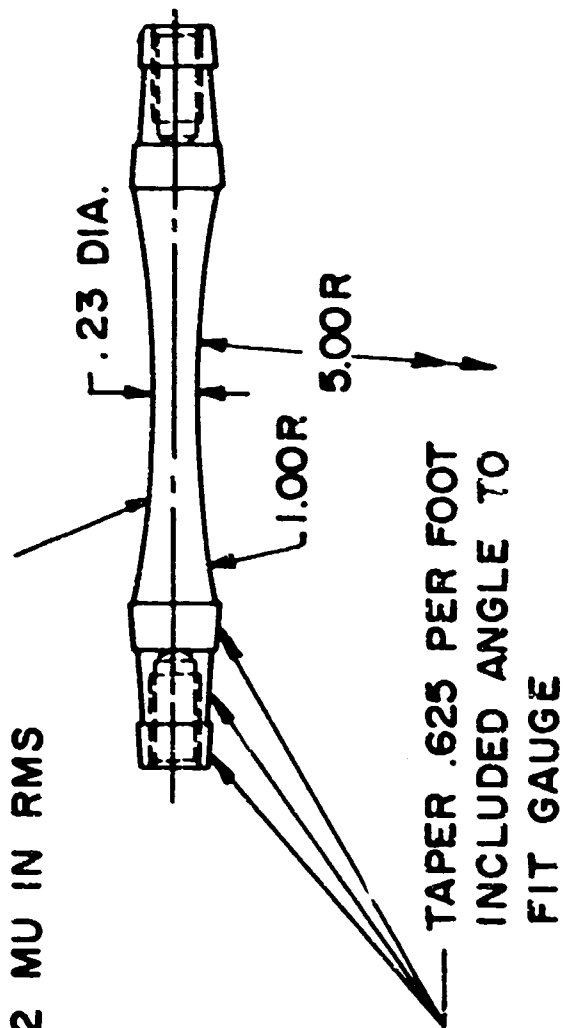
ROTATING BEAM FATIGUE TEST SPECIMEN

FIGURE 60

148

Reduced Life and Failure Mode Check

The requirements for effort on this task were reduced to a minimum by the earlier developments of the program. Use of the "measured weakening" approach forces a specific failure mode to occur. The originally anticipated need to check the failure mode produced with that being investigated was eliminated.

The use of overstress methods, excessively accelerated, generally produce a "try-it-and-see" approach to development of failure modes not inherent in the methods developed for use in this program.

The parallel or concurrent scheduling of certain phases of this program required for efficient program planning within the contract time period prevented the complete sequential development of all the test data necessary to obtain a specific reduced life value. Previous sections of this report have discussed the evolved necessity of a specific sequential order to the development of the test data to permit the determination of such a specific reduced life value.

The system test phase showed that consideration of the active/inactive portions of the mission profile enabled test duration compression (or acceleration) of 5 times.

A permissible tooth stress cycling rate in the parts test (200-500 cps) was found to be approximately 100 times that occurring in the compressed system test (approx. 10,000 cycles per hour of mission time).

A permissible fatigue cycling rate in the materials test (10,000 rpm on the R. R. Moore test sample) was found to be approximately 60 times that occurring in the compressed system test.

A possible shortening of the system test using the proper pre-crack size ("measured weakening") to between 5% and 40% of the normal time to failure was verified in tests to failure of precracked gears in the parts tests program.

Service Life Prediction

Each of the test phases required to develop the acceleration relations required for this portion has been validated theoretically and proven feasible separately but not repeated sequentially to obtain specific combined values because of program limitations. Development of specific life predictions is dependent upon this sequential development of combined values.

Comparison with Service Use

The necessity for further understanding of what "kind" of reliability was of most concern became evident. A wide deversity of the classification of failures was encountered in the Survey Phase and in the analysis of the Service Data. Study beyond the intent of this program must be devoted to this problem so that an approach of practical use to the Air Force may be taken instead of the many more idealistic concepts of failure classification.

Until specific success/failure criteria are defined for each specific set of hardware there will be as many different reliability functions to compare with as there are failure classifications. To evaluate all of these is presently impractical. Future work may provide a sound basis for selection of a few pertinent failure classes not presently justifiable.

150

Conclusions and Recommendations

This effort resulted in the development of techniques whereby testing time required for electromechanical components can be reduced below that normally required with statistical testing methods. Techniques were developed for applying "measured weakening" (pre-cracking) to a small output gearing mechanism to accelerate fatigue failure in a fraction of the previously required time.

To accomplish this, the approach followed and the resulting conclusions were as follows:

- Determined that state of the art reliability testing generally follows the statistical testing procedures that require large numbers (hundreds) of parts and last for long periods of time.

- Selected an all mechanical spring clutch position servo (J-85 variable engine nozzle unit) as a typical control component on which to verify the testing techniques developed.

- Performed a system failure analysis to isolate and reduce the predominant material failure modes for this unit to a select few. The failure modes selected were -- fatigue, wear and seizure.

- Developed techniques for accelerating failure modes by "measured weakening" of individual part areas.

- Applied the "measured weakening" to the output gear of the servo to accelerate fatigue failure. The required test time was less than 20% of normal test time using conventional methods.

The concept of "measured weakening" permitted:

- system testing at normal variations in operating loads, environments and conditions to

  a. avoid development of extraneous failure modes usually associated with "overstress" testing

  b. accumulate mission/cycle data for component tests

  c. account naturally for interaction between modes

  d. duplicate normal energy losses and their effect on the integrity of the overall system

151

- reasonably short testing times to failure in the full system configuration where testing is most costly

- evaluation of the highly variable portions of the fatigue life at the part and material level where the testing and the required increase in sample sizes are most reasonable in cost

- extreme time compression of the longer and more variable portions of the fatigue life by using the high cycling rates permissible at the part and material level using adjustable frequency loading devices

- duplication of the type of failure that has its origin in a non-predictable circumstance (an overload that produces a given crack) and then proceeds by the "wear-out" mechanism of crack propagation to complete failure.

Other serendipitous conclusions were drawn from the research conducted under this program. These conclusions follow.

There are as many values of the reliability function as there are definitions of failure. These definitions and the criteria that determine the success/failure dichotomy vary at each stage of the long chain from original supplier to ultimate user. Requests for reliability numbers must be more explicit than has generally heretofore been recognized.

Many design analyses in the past have been based on worst-case analyses and requirements. Normal case probabilities are not easily determined directly from this kind of analysis.

Considerable work still needs to be done on the other modes of material failure to develop enough understanding to suggest approaches to accelerating tests to failure in these modes. This is not a simple undertaking.

Specific developments recommended to improve and augment the work done under this program are:

- further investigation of the promising use of dynamic response changes as an early measure of fatigue crack development

- improvement in the accuracy of measurement of cracks near the inclusion size level

- development of pre-cracking methods for other types and hardnesses of material than those considered under this program

- evolution of techniques applicable to other mechanical failure modes such as wear, corrosion etc.

The following general recommendations are made:

A study should be made of ways to include in component specifications the things they should not do together with a ranking of items from most desirable to least desirable (most undesirable). This departure from today's all-or-nothing-at-all specifications would aid considerably in optimization of not only the design effort but also the approach to reliability testing.

A study should be made to develop a standard for the most useful definitions of failure for flight control systems. Cost effectiveness studies should supplement these to establish the relative costs of these failures to the Air Force. These are necessary for more efficient apportionment of effort in the reliability area.

APPENDIX A

Study of the Fatigue Failure Mechanism

The approach to accelerating the testing of the fatigue failure mode has been through the study of the concept of cumulative fatigue damage. Much work has been done in this area to define the milestones in the fatigue life of materials. When these milestones are related to life fractions we have the tools to relate some small portion of this life reproduced in testing to the full normal life span to failure.

Considerable work has been expended during the last 30 years to develop a satisfactory cumulative fatigue damage relation. Recently, Grover (1) has made a comprehensive survey of the existing cumulative damage theories and has concluded "Most relations so far advanced have one or more of the following limitations: (1) no physical mechanism is clearly defined so the relation contains factors identifiable with concepts useful in design (or life prediction), (2) too many experimental data are required for engineering calculations, (3) mathematical calculations are cumbersome". He goes on to say "It is suggested that . . . a better theory should be based on a realistic account of the physical mechanism or mechanisms involved". An extensive bibliography in this field is to be found in references (1) and (2). In most of the theories, no account is taken of the fact that a crack formed at a high stress level may lower the "fatigue limit" of the component and thus allow the crack to propagate at stresses below the original fatigue limit. One exception to this general situation is the method proposed by D. L. Henry (3). A further criticism of most proposed theories is that they do not take into account the manner in which a crack is formed and propagates until complete failure. Still another objection is the loose, ill-defined term, "damage", that generally exists in the literature.

In recent years a more realistic contribution to the fatigue "damage" of metals and structures has been the study of the initiation and rate of propagation of fatigue cracks. These observations are often not compatible with assumptions that previous investigators have used in developing their fatigue damage laws, and consequently the validity of previously proposed laws is open to question. In 1955, Demer (2) made a comprehensive summary of fatigue crack propagation. Schijve (4), in 1956, presented an excellent survey and discussion of crack propagation and some additional data on crack propagation. He says "Fatigue crack propagation studies are considered to be a more refined phenomenological evaluation of fatigue test results. They may therefore allow a more rational approach to establishing relations for several general fatigue problems".

During the last few years, an increasing amount of experimental data has become available on the nature of the initiation and propagation of fatigue cracks. Also a limited amount of data has been observed on the existence and nature of non-propagating cracks. Although there still exist some contradictory statements on the nature of crack propagation in the literature, a large portion of the recent literature appears to be consistent. A brief review of the existing knowledge of crack initiation and propagation, serves as a basis for the approach to accelerating the fatigue failure mode taken in this program.

The Nature of Crack Initiation and Propagation

It is generally concluded by most investigators that the number of cycles involved in propagating a fatigue crack between the time it is very small and the time complete failure occurs is a major portion of the total number of cycles to failure. Conversely, the number of cycles that is involved in initiating a very small crack is a somewhat minor part of the total number of cycles except, perhaps, for stress levels near the so-called fatigue limit. It is this observation that first suggested an approach to accelerating the fatigue failure mode in a test program. The actual division of the fatigue process into these two stages has been somewhat dependant on the resolving power of the techniques used to detect the first micro-crack. For example, the authors of references (5, 6) in testing small rotating-beam specimens of high-strength steels observed micro-crack lengths of the order of 0.0005 inches at about 5 to 10% of the total number of cycles to failure. Hunter and Fricke (7-9) in testing aluminum alloys found that this "precrack" stage depended on the type of alloy that they tested. In the high-strength aluminum alloys they found that the precrack stage was about 20 to 40% of the total number of cycles except near the so-called fatigue limit where this ratio became higher (equal to 100% at the fatigue limit).

Statements have appeared in the literature (7) that contradict the above. These suggest that visible cracks, especially in small laboratory specimens, occur near the final fracture. This can be true since a visible crack might be 1/16 or 1/8 of an inch long and most of the cycles had already been consumed in propagating a micro-crack of 0.001" length to this value, and the rate of propagation at this visible size may be very high so that only a few additional cycles are required for complete fracture.

There seems to be no disagreement in the literature that once a micro-crack becomes sufficiently large it will propagate in a relatively continuous fashion until complete fracture occurs. However, there is some discussion in the literature as to what constitutes an initial crack, since a technique that adequately identifies the initiation of a microscopic crack has not been difficult to develop. Some authors (10, 11) indicate that strain-hardening, or in some cases strain softening, occurs during slip within the crystals during the first applications of stress. This is followed by cracking along the slip bands (Hempel, Thompson, etc., References 12, 13) and some of these adjacent cracks eventually join to form a single micro-crack which then propagates by itself.

In order to simplify this picture of crack initiation and propagation into one that can be used for engineering purposes, Schijve (4) (and earlier Langer (14)) suggested that the total number of cycles to failure be divided into two stages; (1) a precrack or initiation stage and (2) a crack propagation stage, admitting that they found the division between these two stages arbitrary since it depended on the limiting size of the crack that could be observed.

Recently, careful tests (6, 8, 15) have shown that when the microcrack is small, of the order of the grain size in a polycrystalline material, there are extended periods during this early propagation when the instantaneous

rate of crack propagation becomes essentially zero; that is, the crack stops propagating. As the crack becomes longer these so-called "hesitation periods" apparently become so small that they are not apparent to the experimenter except by continuous observation of the crack growth (15). However, for all practical purposes, the crack growth may be considered continuous except during the early stages when the hesitation periods are sufficiently pronounced to be readily observed.

It has been established from crack propagation studies (4) that the final or crack propagation stage is a relatively larger part of the total life at high stresses than at the lower stresses near the fatigue limit.

Another point that has been observed in crack studies (4, 6) on plain specimens is that the variability in the fatigue life to complete failure is largely caused by the high variability in the initiation stage. A relatively small part of the variability of the total fatigue life can be attributed to the crack propagation stage. This situation can be readily rationalized on the following basis. During the crack propagation stage, the front of the crack tip is sufficiently large to plastically affect many hundreds, or thousands, of grains, so that its growth on the average is dependent on some average gross property of the metal. On the other hand, the number of cycles to initiate a crack is dependent on the strength of the weakest microscopic spot and these individual strengths are considerably more variable than the average strengths.

The variability in the total number of cycles to failure has been found to be greater at stresses near the fatigue limit than at the higher stresses. This is to be expected on the basis that the crack initiation stage is more significant near the fatigue limit.

In parts whose geometry alone does not cause a high stress gradient and a single high stress point the number of cracks that initiate at or near the high stress area increases when the stress level is increased. A detailed discussion of this fact and the relation to inclusion size in high-strength steels is given in reference (16). In that study it was found that, at low stresses, cracks started only at the largest inclusions, while at the high stresses cracks initiated at small as well as at large inclusions. Furthermore, at the higher stresses, the number of small cracks per unit area is so great that these cracks often join to form one single crack that dictates the final fracture area. Mann (17), Peterson (18), and Marco and Starkey (19), have also reported this effect from multiple nuclei at high stresses.

Description of the S-N Curve and the "Damage" Line

Nearly all S-N curves obtained from laboratory tests represent complete fracture of the specimens. Such information is not realistic since the failure criterion of a critical full-scale machine or structural part is usually based on observations at periodic inspections of a certain maximum allowable crack length which is often only a very small fraction of the periphery of the critical section of the part.

Figure A_1 shows a log-log plot of a typical median S-N curve representing complete fracture. The upper branch of this curve is roughly a straight line provided the alternating stress does not extend to a value that is too high. The lower branch of the S-N curve is either horizontal, or has a slightly downward slope.

Between this S-N curve for complete fracture and the ordinate corresponding to one cycle lies a line that many years ago was called the damage line. The use of this former concept of a "damage" line will be retained in this report. However, a more precise and mathematical definition will be given for this line.

In the period of 1930 to 1940, a number of investigators attempted to determine the position of a "damage" line in respect to the fracture S-N curve for various materials. (A review of this early work is to be found in Battelle's book "Prevention of the Fatigue of Metals".) In this type of test, specimens were prestressed for a number of cycles at stresses above the fatigue limit and were then retested at the fatigue limit. If the specimen failed at the fatigue limit, then the damage line was considered to be located below the point corresponding to its prestress conditions. If it survived for the required number of cycles, the damage line was considered to be located above the point corresponding to its prestress conditions. By testing a sufficient number of specimens in this manner, it was possible to locate, at least roughly, the position of the damage line. Usually, it was found that this damage line was somewhat parallel to the fracture S-N curve, but in some materials investigators concluded that no damage line existed above the fatigue limit since damage started very early at low overstress.

This type of test seems to have been discarded after about 1940, since no significant papers appear to have been published on this method after that time. This is probably because the concept is misleading; it certainly does not mean that damage does not occur before the damage line is reached. However, the damage line can be interpreted in terms of the critical dynamic crack length associated with the fatigue limit. As explained later, there is a critical dynamic crack length associated with each stress level. Therefore, at the fatigue limit, there is a maximum crack length that will not propagate regardless of the number of imposed cycles. It will be seen later that deliberately created cracks (weakening) were designed with this in mind. The damage line represents the number of cycles at each stress level to initiate a micro-crack of a length equal to this critical crack length (ℓ_o)
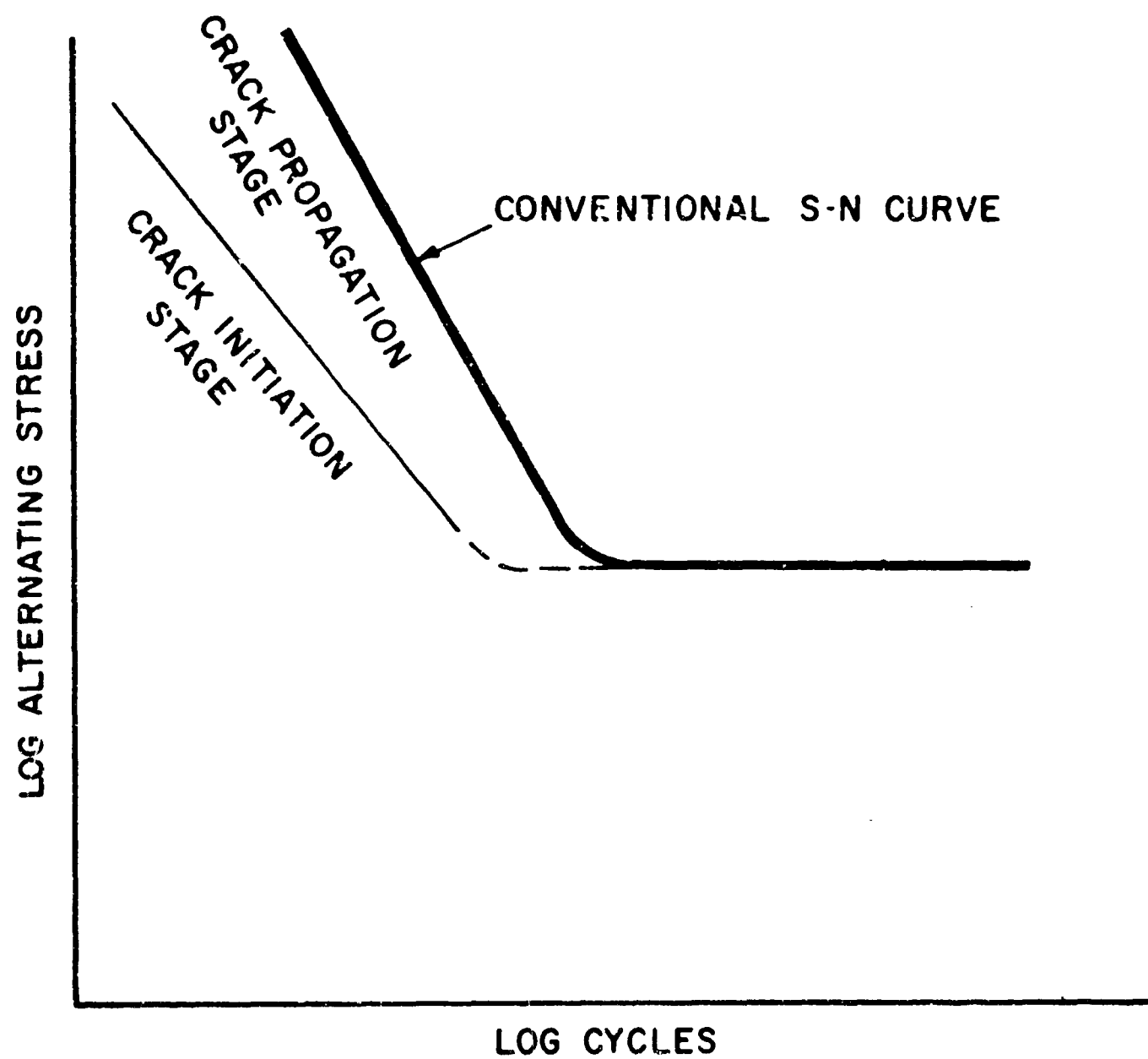
THE S-N CURVE

FIGURE A1a

The S-N curve diagram. Axes labeled LOG ALTERNATING STRESS (vertical) and LOG CYCLES (horizontal). Shows a bold MEDIAN FRACTURE LINE (CONVENTIONAL S-N CURVE) and a thin MEDIAN DAMAGE LINE, with intervals labeled N_0 and $N - N_0$.
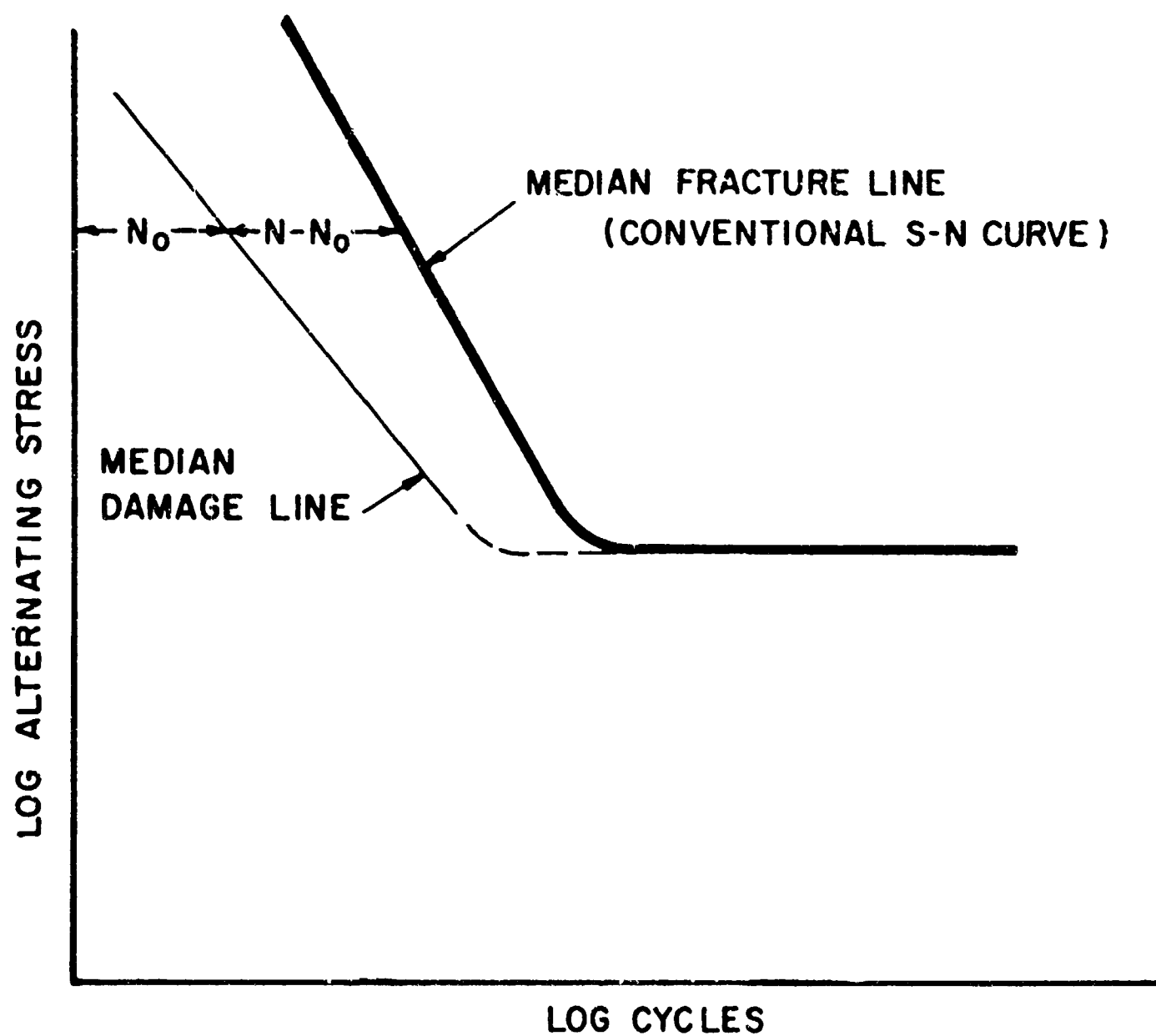
THE S-N CURVE

FIGURE A1b

at the fatigue limit. That is, if the specimen is prestressed at a condition corresponding to a point just below the damage line, its fatigue limit will not be affected.

It is postulated that the damage line is therefore a convenient and definite boundary separating the initiation or precrack stage and the crack propagation stage, provided it can be defined in the specific manner proposed above (see Figure A1).

Between the "damage line" and the final S-N curve for complete fracture lies the crack propagation stage. This stage is subjected to little or no scatter since the rate of crack propagation is dependent, among other factors, on certain bulk characteristics of the metal.

As noted above, most, if not all, of the scatter in the final S-N curve for complete fracture is caused by the large scatter in the initiation stage. Since there is practically no scatter in the crack propagation stage, the distribution of the fatigue lives for complete fracture has a definite minimum value which corresponds to the number of cycles of the crack propagation stage (provided we define the start of the propagation stage by a constant ℓ_0). Therefore, any proposed distribution function for fatigue life must allow for this definite minimum number of cycles. Crudely speaking, the lower boundary of a "scatter band" of failures is the true lower limit of life and may be used as the estimate for the S-N curve of the propagation stage.

Because of the indefiniteness of the length of the initiation stage, its high variability and the unpredictable nature of its relatively long hesitation periods, no completely satisfactory mathematical model has been developed to relate the length (in cycles) of this stage as a function of the stress level and nature of the initial stress raisers. Testing of actual parts and materials is required to develop the empirical relationships. This testing is of relatively short duration however because it requires only testing for the length of the initiation stage, some 5 to 10% of the total life for ferrous materials.

The lower branch of the conventional S-N curve is believed to be caused by a peculiarity in the initiation stage. At stresses near the median fatigue limit or near the average long-life (say 100×10^6 cycles) strength, the tips of the embryonic micro-cracks run into "road blocks" in the form of stronger grains which either prohibit entirely further growth or reduce the rate significantly during the progress when the tips of the cracks are finding more circuitous paths around the road blocks. Some investigators are of the opinion that, in metals exhibiting strain-aging, the work hardening during the fatigue process is sufficient to prevent the formation of submicroscopic cracks, or at least is sufficient to prevent their further growth.

Up to this point, the S-N curve and its corresponding damage line have been

discussed for smooth specimens or parts. In considering the S-N curves of notched parts or specimens, notches may be described in the following manner. One type occurs when the region of the notch is a relatively small fraction of the material at the maximum stress; in other words, this notch is a localized notch or stress raiser. An example of this is a hole in a uniformly loaded plate. Another example is a small nick in a part, or (in the techniques developed in this program) a shrinkage crack caused by a deliberately placed electric weld spot. The inclusions in materials are this type. Another type notch extends throughout the region of maximum stress. One example is the fillet between two adjacent diameters of a rotating shaft. Round fatigue specimens having a circumferential notch are this type. Another example is the fillet at the root of a gear tooth.

Relatively simple relations exist between the S-N curve for fracture of notched specimens and the corresponding curve for the smooth specimen.

The upper branch of the S-N curve for complete fracture of a localized notched specimen lies to the left of that of the corresponding branch of the smooth specimens, and in the range of stress corresponding to the upper branch of the smooth S-N curve is closely related to this latter branch in the following way. In this range of stresses, the initiation stage for the notched specimens is only a small fraction of that for the smooth specimens, that is, micro-cracks are formed at a much lower cycle-ratio. After this crack which initiates at the notch extends a small distance from the notch, the crack then behaves in the same way as the length of crack in the smooth specimens that is equal to the notched crack length including the length of the original notch. After this point is reached, the crack in the notched specimen progresses at the same rate as that in the smooth specimen. In other words, in this range of stresses the total cycles to failure of the notched specimen is equal to a considerable portion of the number of cycles of the propagation stage of the smooth specimen provided the original notch is very small.

The above reasoning leads to an interesting and practical result. If, on the surface of a smooth specimen, a very small discontinuity such as a very small hole (0.005" D), a small electric arc mark, or a rough machined surface is introduced, the initiation period will be practically eliminated, and the total cycles to complete failure represent only a portion of the propagation stage. By making a correction for the size of the initial notch, the propagation stage may be accurately computed. In this way, the highly variable nature of the initiation stage can be eliminated and a laboratory procedure is provided to determine an S-N curve for the propagation stage only. This stage, having relatively little variability required fewer test specimens to establish a minimum life with reasonable confidence.

The lower branch of the S-N curve of locally notched specimens may be conservatively located by dividing the ordinates of the lower branch of the smooth specimens by the theoretical or geometric stress concentration factor. The actual position of this lower branch, however, may be somewhat above

this estimate. This is caused by the following factors. First, there is a statistical size effect in that the amount of material at the base of a notch of some part configurations can be less than that at, or near, the maximum stress of a smooth specimen so that on the average the material at the base of the notch may not have as large an inhomogeneity as in the smooth specimen. The second reason is that, at the lower stresses, a notched specimen can develop non-propagating cracks that do not lead to failure, so that the actual failure curve lies above the theoretical position. The importance of this source of error declines with increasing cleanliness and homogeneity of the material.

The S-N curve for the second type of notched specimen is related to the smooth S-N curve in a different way than that for the first type notch. One can still expect this second type notch S-N curve to be closely approximated by dividing the ordinates of the smooth S-N curve by the geometric stress concentration factor. However, there are three reasons why the upper branch of the notched specimen may lie somewhat to the right of this constructed curve. The first reason is that the crack will propagate somewhat slower than the crack in the smooth specimen (which is at the higher stress level) once this crack has extended into the lower stress region below the notch resulting from the stress gradient. The second reason is that there is less probability of the larger inclusions existing at the base of the notch than in the surface of the smooth specimens. Another reason (mostly of academic interest because of the small error involved) is that compressive stresses develop at the base of the notch in a ratchetting effect, reducing the rate of crack propagation.

A Relation for Crack Propagation

Several relations have been proposed for the rate of crack propagation (6, 20, 21, 22, 23). Cummings, Stulen and Schulte (6) proposed an analytic expression for crack propagation in the propagation stage as follows:

$$\log \frac{\ell}{\ell_a} = k\, s^{\alpha}\ (N - N_a) \ - - - - - - - - - - - - (1)\ast$$

The lengths of the propagating cracks in plates of 2024-T3 and 7075-T6 alloys reported in the work of McEvily and Illg (25) have been plotted from the original data using semi-log plots. Typical graphs are shown in Fig. $A2$. From such graphs, it can be shown that the above formula fits the experimental data very well, at least up to the crack lengths that do not exceed 20% of the plate width. Analysis of these rates of crack propagation for 2024S-T3 indicated that the exponent, α, of stress in formula (1) is equal to 3.53.

Crack propagation studies (6) on 4340 steel heat-treated to high hardness have indicated stress exponents of the order of 3 to 5. Liu and Corten (26) have found the exponent for 7075-T6 to be 5.8 and obtained the same value for a hard-drawn wire.

Equation (1) is not necessarily limited to those stresses that are at or above the fatigue limit, since it has been shown that cracks will propagate at lower stresses provided they are sufficiently large initially. The lower stress levels at which the crack or cracks will continue to propagate depends on the size of the crack. A larger crack will propagate at lower stresses.

One important invariant property exists for equation (1). Equation (1) can be shown to be exactly the same form if the "starting length", ℓ_a is changed to any other value, say, ℓ'_a. In this case, we simply change N_a to N'_a, the number of cycles associated with the new starting length, ℓ'_a. From this property, as well as from the fact that the rate of propagation after the crack tip encloses a sufficient number of grains is related to some bulk property of the metal, it is postulated that the constants α and k are material constants.

Another important property exists for equation (1) as follows. Equation (1) is independent of the stress concentration factor and is valid for specimens with small local notches as well as smooth specimens provided (1) the stress is calculated as a nominal stress and (2) the propagation is computed after the crack tip has progressed beyond the influence of the original notch.

Suppose that two specimens are identical except for the sharpness of the original stress raisers. In one specimen we might have a circular hole while in the other a slender elliptical hole (see Fig. A3). Let both be subjected to

---

* Frost and Dugdale (24) proposed the same formula at about the same time.
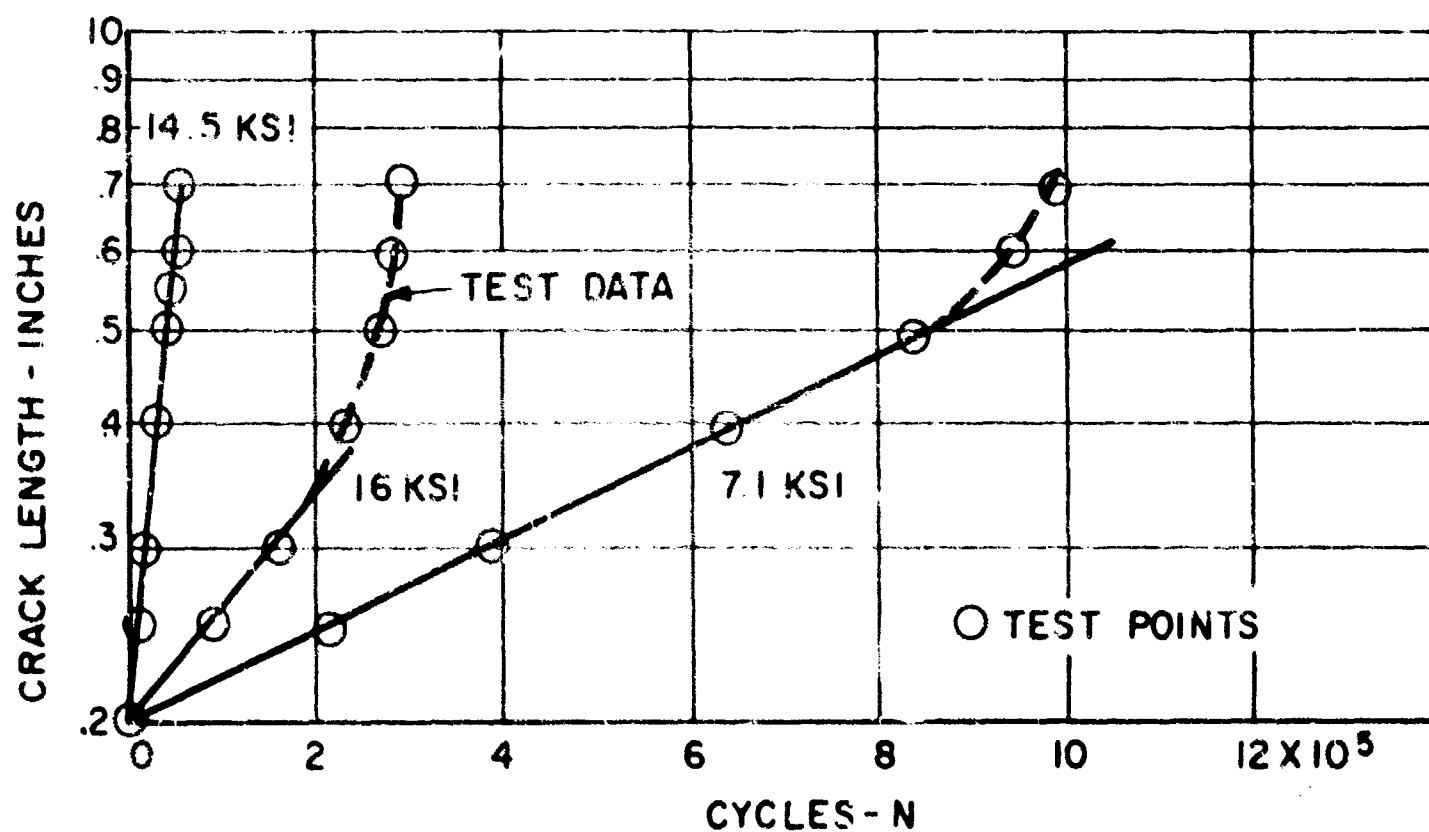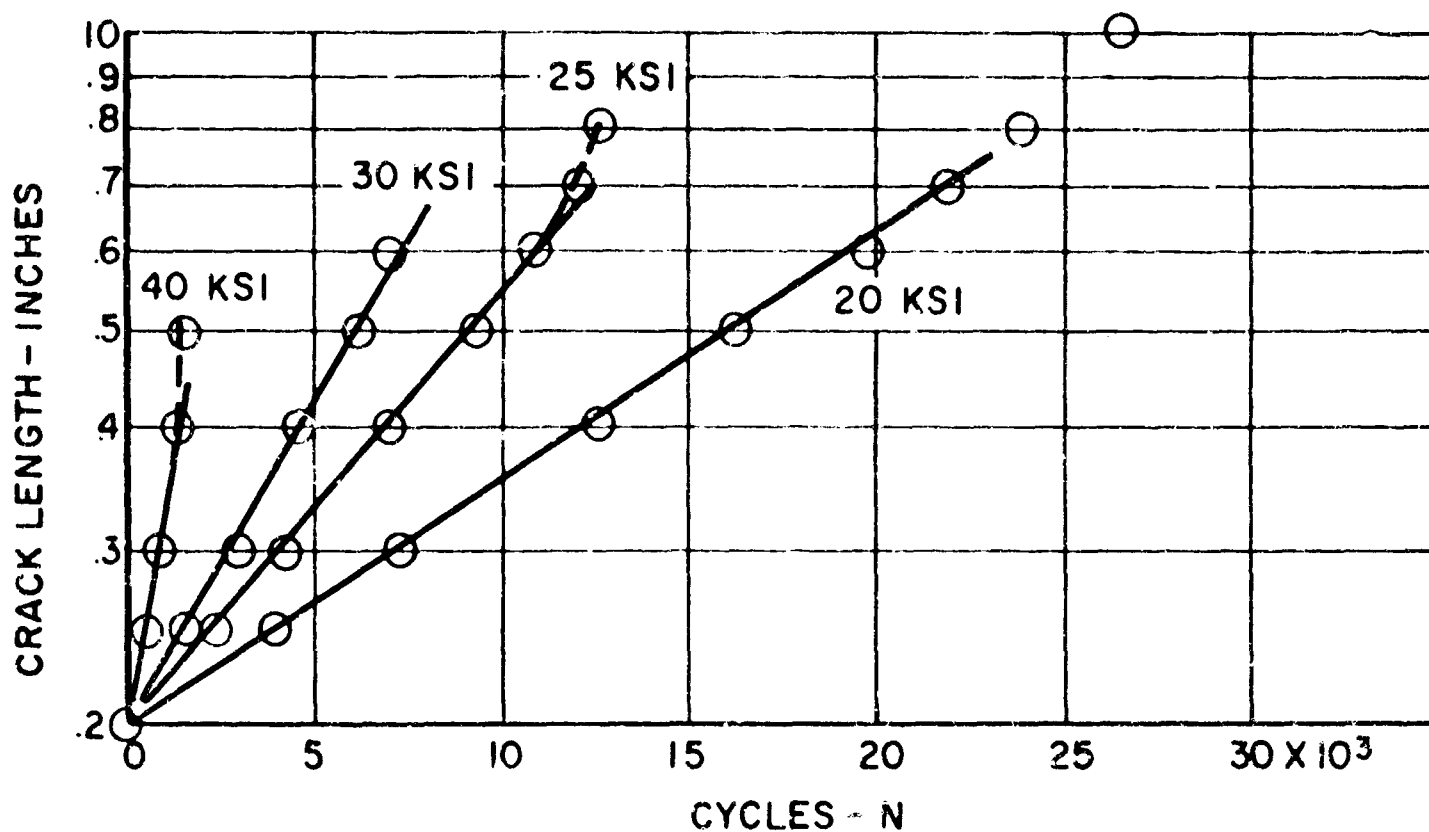
FIGURE A2

FATIGUE CRACK PROPAGATION
OF 2" WIDE SHEET OF 2024S-T3

DATA TAKEN FROM NACA TN 4394

A-11
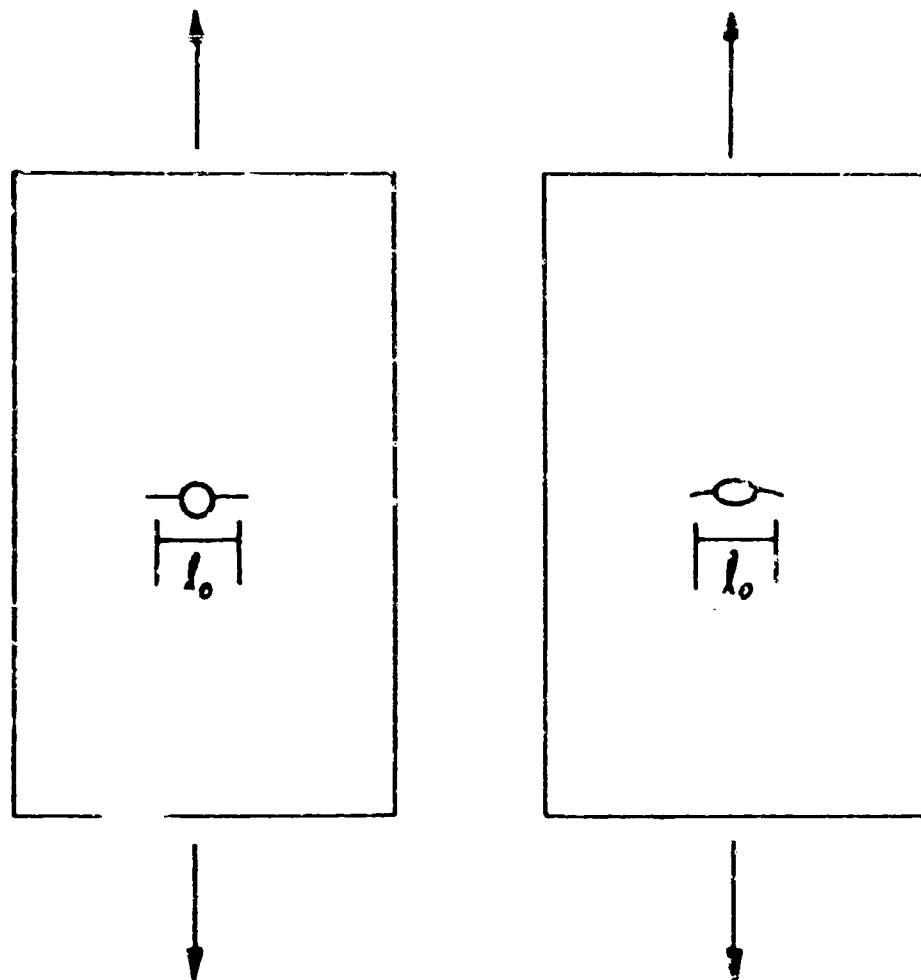
FIGURE A3

DIFFERENT STRESS RAISERS

the same nominal vibratory stress. The crack in that specimen having the sharper (elliptical hole) will be initiated first. However, if the cracks are grown to the same length, which is sufficiently large in respect to the lengths of original stress raisers, the rates or propagation are no longer influenced by the original notches and will then be equal. In order that the original notch have no influence on the rate, the crack must progress a distance equal to something less than one notch radius from the base of the notch. This situation explains why the variability in the crack propagation stage is low in specimens while the variability in the precrack stage is high and accounts for most of the variability in the total number of cycles to failure.

The exponent, α, which is also needed in cumulative fatigue damage computations, depends on the material, its heat-treatment, the amount of steady stress, and the stress gradient.

There is no known logical reason at present to believe that α (and k) are affected by size (other than the change in the stress gradient). Larger parts of the same geometry subjected to the same type of loading will have a lesser stress gradient in the maximum stressed region so that the rate of crack propagation will be higher when compared on the basis of the maximum stress at the concentration. There should be no corresponding "size effect" in uniformly stressed parts.

On the basis of the information at present available, it is postulated that ℓ_a may be taken to be equal to ℓ_o, the crack associated with the damage line as discussed earlier. In other words, it is postulated that the "damage line" indicates the start of propagation.

Formula (1) can be used for the crack propagation S-N curve for which there is no initiation period and the crack starts with an initial length, ℓ_o; that is, N_o is equal to zero. The final crack length, ℓ_f, is the length of crack where static failure occurs. The formula for the fracture S-N curve under these special conditions is:-

$$ k \, s^{\alpha} \, N_f = \log \frac{\ell_f}{\ell_o} \quad - - - - - - - - - - - - - - (2) $$

In the case of the locally notched specimen, the initiation period is very small at nominal stresses comparable to those of the upper branch of the smooth S-N curve. In this case the above formula closely represents the S-N fracture curve (upper branch) of the locally notched specimen with the exception that ℓ_o is replaced by ℓ_o' (the size of the localized notch).

Relation of the Propagation Formula to Damage

As discussed in the foregoing, an accurate relation for the growth of a single crack in the propagation stage is given by:-

$$\log \frac{\ell}{\ell_0} = k \ s^{\alpha} \ N_p \quad - - - - - - - - - - - (3)$$

where N_p is the number of cycles measured from the start of the propagation stage, and ℓ_0 is the crack length defining the damage line or the start of the propagation stage.* In this expression, the quantities ℓ_0, k and α are probably material constants for a fixed linear distribution of stress.

In the following development it has been assumed that a given material is subjected to a prescribed stress spectrum which might be described by a series of alternating stresses, s_i, and corresponding number of imposed cycles, n_i. The problem is to determine the "fatigue damage" after the material has been subjected to this spectrum or the number of times this spectrum may be repeated before failure occurs.

The order of the imposed stresses, s_i, is taken to be random with time, the probability of stress s_j occurring for the next cycle being in proportion to N_j/N_T, where N_T is the total number of cycles in the stress spectrum. Under this condition, there is a chance that some of the first cycles will occur at high stresses where the initiation stage is relatively small so that most of the fatigue is taking place in the propagation stage. This is a conservative approach to the estimate of fatigue life.

Another assumption that will be made is that the overall effect of stress-interaction may be neglected, since it appears reasonable that this will not cause a bias on the cumulative damage provided the sequence of imposed stresses is random and does not form a pattern. (There seems to be some confusion in the literature concerning the definition of stress interaction. This is discussed later).

Now, if the process is considered to start at the propagation stage with an initial crack length of ℓ_0, and a series of stresses (s_1, s_2, s_3, . . ., s_z) are imposed, the crack propagation formula may be used to estimate the final crack length, ℓ, in the following manner:

$$\log \frac{\ell_1}{\ell_0} = k \ s_1^{\alpha} \ n_1$$

$$\log \frac{\ell_2}{\ell_1} = k \ s_2^{\alpha} \ n_2$$

$$\log \frac{\ell_3}{\ell_2} = k \ s_3^{\alpha} \ n_3$$

---

* In the subsequent development, it is assumed that high stresses, resulting from overloads originating from random and non-predictable human errors, occur early in service, so that the initiation stage is exceeded early in the process and N_0 is equal to zero for all practical purposes.

$$\vdots \qquad \vdots$$

$$\log \frac{\ell_z}{\ell_{z-1}} = k\, s_z^{\alpha}\, n_z$$

These equations are added and the rule of logarithms is used so that:

$$\log \frac{\ell}{\ell_o} = k \sum_{i=1}^{i=z} s_i^{\alpha}\, n_i \qquad \text{where } \ell = \ell_z$$

Suppose, for a reference test, the highest stress in the spectrum, s_r, is selected as well as the corresponding number of cycles, N_r, in the propagation stage, then:-

$$\log \frac{\ell_{fr}}{\ell_o} = K\, s_r^{\alpha}\, N_r$$

Here, ℓ_{fr} is the length of the fatigue crack at failure at the reference (highest) stress, s_r. This length may correspond to the <u>critical static crack length</u> for the material at the maximum imposed alternating stress, or it may correspond to that length where the static strength of the part is seriously reduced.

When the former relation is divided by the latter relation:

$$\frac{1}{N_r} \sum_{i=1}^{i=z} \left(\frac{s_i}{s_r}\right)^{\alpha} n_i = \left[\frac{\log \frac{\ell}{\ell_o}}{\log \frac{\ell_{fr}}{\ell_o}}\right]$$

Since the quantity $\left[\dfrac{\log \frac{\ell}{\ell_o}}{\log \frac{\ell_{fr}}{\ell_o}}\right]$ increases from zero to unity as the crack

length ℓ grows from ℓ_o to ℓ_{fr}, the bracketed quantity will be defined as the <u>fatigue damage parameter</u>, D.

Then we have:

$$\frac{1}{N_r} \sum_{i=1}^{i=z} \left(\frac{s_i}{s_r}\right)^{\alpha} n_i = \left[\frac{\log \frac{\ell}{\ell_o}}{\log \frac{\ell_{fr}}{\ell_o}}\right] = D \quad - - - - - (4)*$$

---

* Equation (4) resembles the Corten-Dolan cumulative fatigue damage law (27) but differs in that the exponent, α, is that occurring in the crack propagation formula, and the cycle-life of the reference stress is determined from the "crack propagation" S-N curve.

It is noted that the crack can be relatively quite small resulting in high damage. The following numerical example illustrates this point.

$$\ell_{fr} = 0.200 \text{ in.}$$

$$\ell_o = 0.002 \text{ in.}$$

$$\ell = 1/10^{th} \text{ of } \ell_{fr} = 0.020 \text{ in.}$$

$$D = \frac{\log 10}{\log 100} = \frac{1}{2}$$

In this case, a crack that is only $1/10^{th}$ of the fracture length causes 1/2 of the fatigue damage.

This illustrates the important rule that fatigue cracks do not have to be large to be dangerous. It also illustrates the reason why some investigators have failed to note the presence of cracks until the fracture cycles have almost been reached, thus giving an erroneous impression of the location of the damage line.

It is important to note that the above cumulative damage law may be modified slightly for use with localized notches. In this case, the crack, after it has propagated a short distance beyond the notch or imperfection, acts in the same fashion as a crack of equal length in a smooth specimen. Here the crack length of the notched specimen includes the length of the initial notch.

Primes will be used for the locally notched specimens. Then the damage formula becomes:

$$\frac{1}{N'_r} \sum_{i=1}^{i=z} \left|\frac{s_i}{s_r}\right|^{\alpha} n_i = \frac{\log \frac{\ell}{\ell_o}}{\log \frac{\ell_{fr}}{\ell_o'}} = D' \;\; - - - - - (4a)$$

The quantity ℓ'_o may be approximated by the length of the localized notch in a direction perpendicular to the stress direction. More precisely, it may be taken equal to this latter length multiplied by a number greater than unity (say 1.25) because the initial crack quickly propagates through the localized high-stress field around the notch.

The values of N_r', the reference number of cycles of the propagation stage of the notched specimen is calculated from:

$$\log \frac{\ell_{fr}}{\ell'_o} = k \, s_r^{\alpha} \, N_r' \;\; - - - - - - - - - - - - - (5)$$

Dividing this by the corresponding relation for the smooth specimens leads to:

$$N_r' = N_r \left[\frac{\log \frac{\ell_{fr}}{\ell_o'}}{\log \frac{\ell_{fr}}{\ell_o}} \right] \text{- - - - - - - - - - - - -(6)}$$

The above expression may be also used to estimate the fracture S-N curve (without the initiation period) of smooth specimens from the data of locally notched specimens. Here, the values of ℓ_o, ℓ_f, ℓ_o' and N_r' are known and the solution for N_r is obtained from the above expression.

There is no valid rational reason to believe that the propagation formula is dependent on size, at least when the crack is small. It would appear that the quantities, ℓ_o, k and α are material constants, independent of size. The only quantity that may be dependent on size is the length (ℓ_f) of the crack and the number of cycles, N_f, for complete fracture.

The use of the locally notched specimen results in a simple method of obtaining the material constants, k and α. The use of locally notched specimens reduces the initiation period at sufficiently high stresses to a small value that can be neglected. If the specimens are tested at two stress levels, (1) and (2), the division of their crack propagation formulas leads to:-

$$\frac{\log \frac{\ell_{f_1}}{\ell_o'}}{\log \frac{\ell_{f_2}}{\ell_o'}} = \frac{k \, s_1^{\alpha} \, N_1'}{k \, s_2^{\alpha} \, N_2'} = C$$

or

$$\left(\frac{s_1}{s_2} \right)^{\alpha} = \frac{N_2'}{N_1'} \, C \text{- - - - - - - - - - - - - - - (7)}$$

From this, the value of α can be obtained after the ℓ_f's have been measured. The value of k can be obtained from equation (5).

Stress Interaction Effects

Up to this point, the effect of "fatigue damage" that was incurred at one stress level on the rate of "damage" at another stress level was not considered. It has been assumed up to this point that the crack propagation (equation 1) is dependent only on the existing stress level, the instantaneous crack length and the number of cycles accumulated to this point. No allowance was made for the case where the crack up to this point had been propagated at stresses other than that under consideration. It is apparent that the condition of the metal especially near the front of the crack tip will depend on the previous stress history in addition to the instantaneous crack length and the instantaneous stress level.

The same comments apply to the critical dynamic crack length. For example, we may have cracks of the same length in different specimens of the same material, but these may have been formed initially at different stress levels. Under these different conditions of crack formation, the amount and degree of work-hardening (or softening) as well as the amount of "damage" and plastic deformation in that region immediately in front of the crack tips will differ among the specimens. For this reason, it would be expected that the critical stress may vary between cracks of the same length. This effect will be defined herein as stress interaction.

If the crack has been formed at a relatively high stress, the degree and amount of work-hardening, plastic deformation, damage, etc., in the tip region is relatively large compared to the case where the crack (same length) has been formed at relatively low stress.

The effect of stress-interaction has been recently investigated by Hudson and Hardrath ("Effects of Changing Stress Amplitude on the Rate of Fatigue-Crack Propagation in Two Aluminum Alloys", NASA TN D-960, Sept. 1961). They show no effect if the high-stress cycles follow the low-stress cycles in crack propagation. On the other hand, when the crack is formed at high stress and is followed by a low stress, there is a measurable period of cycles when the crack is not propagating. This delay in cycles increases for increases in the difference of the two stress levels. In fact, if this difference is sufficiently large, the crack may never continue to propagate regardless of the number of cycles.

For more precise analyses of acceleration factors for metal subjected to a spectrum of stresses, it is suggested that further work should introduce a "stress-interaction factor, $\emptyset$". This factor, $\emptyset$, would be zero when there is a "cycle delay" in the propagation of the crack at a stress level that is lower than the preceding stress level. This nullifying condition extends for a number of cycles, that is, in itself, a cumulative effect. The factor, $\emptyset$, would be unity when the stress levels are increasing with time.

Further effort is required to establish the quantitative cumulative relations for the "delay-cycles". What is needed is a quantitative relation for the delay-cycles when various stress levels follow a specific high stress level.

It is proposed that the stress-interaction factor, $\emptyset$, be introduced under the summation sign in the cumulative fatigue damage formulas. This factor may be taken equal to unity for simplicity and in development of acceleration factors.

Non-Propagating Cracks and the Critical Dynamic Crack Length

In the foregoing, a relation for crack propagation was proposed and discussed. The question that now arises is whether a crack, small or large, will reduce the original fatigue limit or long-life fatigue strength of the material. In this section, this question will be discussed and data will be presented showing the effect of fatigue cracks in lowering the original fatigue limit.

It has been reported in the literature that fatigue cracks can be formed in highly notched specimens, at a given stress level, that after attaining a small length permanently stop in their propagation. These are called "non-propagating cracks". Furthermore, fatigue cracks that have been initiated at notches at relatively high stresses have failed to propagate when the stresses have been reduced at sufficiently low values. Data obtained in the testing phase of this program does illustrate this point. However, the amount of data in the literature on non-propagating cracks is very limited.

Some information on non-propagating cracks is summarized in reference (28). To quote: "Not only hesitation periods but also non-propagating cracks, in notched specimens of an aluminum alloy, were found by Hunter and Fricke (9). These non-propagating cracks, which were found at stresses below the 'endurance limit', have been determined by Frost and Phillips (29) to occur, at least in the case of an aluminum alloy, in cases where the notch K_t is at or above a 'critcal value'. This critical value is high, which means that the notch must be very sharp. Under such conditions a crack can originate under nominal fatigue stresses well below the fatigue limit of a specimen. Coffin (30) proposed an interesting and plausible explanation for non-propagating cracks. He postulates that when a crack is initiating under fully reversed applied loading, the local stress at a notch (stress concentration) is fully reversed, but, after a crack initiates and propagates beyond the stress concentration effect of the notch, the crack can close during the compression part of the cycle thereby lessening the damaging effect (slip) for part of the complete cycle. He believes that this reduction in reversed slip caused by the closing of the crack will be enough to slow down the propagation, and unless the load is severe it may stop further growth of the crack. He considers this to explain also the fact that externally superimposed compressive steady loads increase (in many cases) the fatigue life of materials. (A different explanation of the effect of superimposed compression might be the biasing effect on shear of the normal component, on the shear (slip) planes, of the compression, as suggested earlier in this paragraph. It may be, of course, that each explanation is partly correct"). (This, of course, is the explanation of the effectiveness of carburized case hardened gearing wherein the case has residual compressive stresses resulting from the carburizing process).

In reference (31), some non-propagating cracks were observed in smooth specimens of high-strength steels that were tested at a stress equal to the average fatigue limit. These grew to lengths not greater than about 0.003 inches in 10^6 cycles, and failed to grow larger after 10^7 cycles. These data are listed in the following table:

Non-Propagating Cracks (Reference 31) in SAE 4340

Steel, 190 ksi UTS, Stresses at ±85 ksi, at 10,000 RPM

Kilocycles	Crack Length, Inches			
0	0.0004	0.0000	0.0000	0.0012
25	.0013	.0011	.0010	.0020
50	.0016	.0015	.0013	"
75	"	"	"	"
100	"	"	.0015	"
150	"	.0016	"	.0021
200	"	.0020	.0016	.0023
250	"	"	"	.0024
300	"	"	"	"
350	"	"	"	"
400	"	"	"	.0026
500	"	"	"	"
600	"	"	"	.0031
700	"	"	"	"
800	.0018	"	"	"
900	.0019	"	.0019	"
1000	.0020	"	.0021	"
2000	"	"	"	"
10,188	"	"	"	.0032 (10,000 kc)
10,208[a]	.0037[a]	.0110[a]	.0055[a]	Failed[a](10,062 kc)
10,255[a]		Failed[a]		

a. Stress raised to ±110 ksi.

It is suspected that micro-cracks also form at stresses below the fatigue limits of polycrystalline metals but do not propagate because of effective crack-stoppers (in the form of stronger grains) in their paths.

In eference (25), McEvily and Illg studied the rates of crack propagation in two high-strength aluminum alloys. In this study, they produced fatigue cracks in notched specimens of a predetermined length by subjecting them to a stress of ±10 ksi. In this study, they determined the limiting stress level below which these cracks would not propagate. These data follow:

Non-Propagating Cracks
(From NACA TN 4394, Reference 25).

2" Wide Specimens

Material	Stress - ksi	Length of Initial Crack-in.	Remarks
2024-T3	4.0	0.50	Did not propagate after 10^8 cycles
"	5.3	0.50	Failed
"	5.1	0.16	Did not propagate
"	6.0	0.13	" " "
"	6.5	0.13	" " "
"	7.1	0.14	Failed
7075-T6	3.2	0.91	Did not propagate
"	3.5	0.50	" " "
"	4.7	0.50	Failed
"	5.1	0.16	Did not propagate
"	5.5	0.17	" " "
"	5.6	0.16	Failed

12" Wide Specimens

Material	Stress - ksi	Length of Initial Crack-in.	Remarks
2024-T3	5.1	0.16	Crack did not propagate
7075-T6	5.1	0.15	Crack did not propagate

From this table, it is seen that a critical crack length of 0.50 inch corresponds to a stress of about 5,000 psi in 2024-T3, whereas a length of 0.13 inch corresponds to about 7,000 psi. The critical crack length is therefore very sensitive to the stress level, being inversely proportional to approximately the fourth power of the stress.

As noted before, non-propagating cracks have been found to be present at the base of notches in specimens that have been subjected to stresses below the nominal fatigue limit. Lessells and Jacques (32) found them to be formed at stresses that were only 45% of the fatigue limit. Frost and Phillips found non-propagating cracks in notched specimens if the radius of the notch was sufficiently small. Hunter and Fricke (9) found that "Cracking occurred at stresses considerably below the notch endurance limit". (These would, of course, be non-propagating cracks.)

In references (16, 33), the authors show that the size of the critical nucleating inclusion in a high-strength steel specimen determines, to a very large extent, the fatigue limit of that specimen; the larger the size, the smaller the fatigue limit becomes. One might speculate that these small inclusions are in effect crack generators, the size of an initial crack being

about the same as the size of the spheroidal inclusion. If this is assumed
to be true, it is found that the critical size of the "crack" varies in-
versely as about the third or fourth power of the stress. Also, in Prot
tests on several heats of 52100 (33), a distinct correlation between inclu-
sion sizes and fatigue strength was found. These data are plotted in Fig. A4
on log-log paper. If the initial crack length is approximated by the inclusion
size, the value of the exponent of the inverse stress is found to be 5.1. In
Fig. A4, it is seen that this inverse power law seems to fit the data reason-
ably well.

Henry (3) proposed a theory of fatigue damage in which he assumed that the
fatigue limit continuously decreased as the number of cycles increased. His
theory agreed reasonably well with some experimental data of Bennett, and is
in agreement with this present hypothesis that the "critical" stress (or
fatigue limit) decreases with increase in the crack length.

Okubo and Minamiozi (34) found that the notch reduction factor of a cylindri-
cal hole in a fatigue specimen decreased towards unity when the size of the
hole was decreased to very small values. This is in agreement with the fore-
going idea that the stress for continuous crack propagation is inversely re-
lated to the size of the initial discontinuity generating the initial crack.

Cracks can propagate even at very low stresses provided their initial lengths
are sufficiently large. There appears, therefore, to be some limiting length
of crack associated with each stress level such that propagation does not
occur.

Tests were made to determine whether this concept of a critical dynamic crack
length was valid or not. For this purpose, a number of rotating beam specimens
of AISI 4340 steel, heat-treated to an ultimate tensile strength of 190 ksi,
were tested. The specimens were first run at a stress level above the fatigue
limit for various cycle-ratios so that various lengths of fatigue cracks would
be generated. The largest crack on each specimen was accurately measured, and
each specimen was then tested for 10^7 cycles at a sufficiently low stress level
so that the crack did not grow to any significant extent. The stress level was
then raised by a small amount and the test rerun for 10^7 cycles. This process
was repeated until fracture occurred. (The critical stress for each crack
length is between the last and next to last stress level.) The results of these
tests have been plotted in Fig. A5 Here the critical dynamic crack length may
be reasonably represented by a straight line on a log-log plot.

On the basis of the foregoing data, the following hypothesis has been developed.
For each stress level, there is a critical "dynamic" crack length such that
propagation will not occur even in a very large number of cycles if the initial
crack is smaller than this critical value. This dynamic critical crack length
(not to be confused with the critical static (self-propagating) crack length)
appears to be related to the stress by the following suggested formula:

$$s^\beta \, \ell_d = c$$

One point concerning the above equation is that crack propagation can occur even at very low stresses provided the crack is sufficiently large. This situation indicates that cumulative damage laws or acceleration relations for spectrum loading that are based on the _original_ S-N curve cannot be correct since those stresses below the original fatigue limit will contribute eventually to the propagation of the crack.

This has been found to be of specific importance in this program wherein failure has been seen to progress by the fatigue "wear out" mechanism after originating in non-predictable human error circumstances of mis-rigging and overloading.

RESULTS OF PROT TESTS ON
HEATS OF 52100 STEEL

FIGURE A4

EXPONENT = 5.12

GEOMETRIC MEAN DIAM. OF INCLUSION X 1000, INCHES

STRESS - KSI

A-25
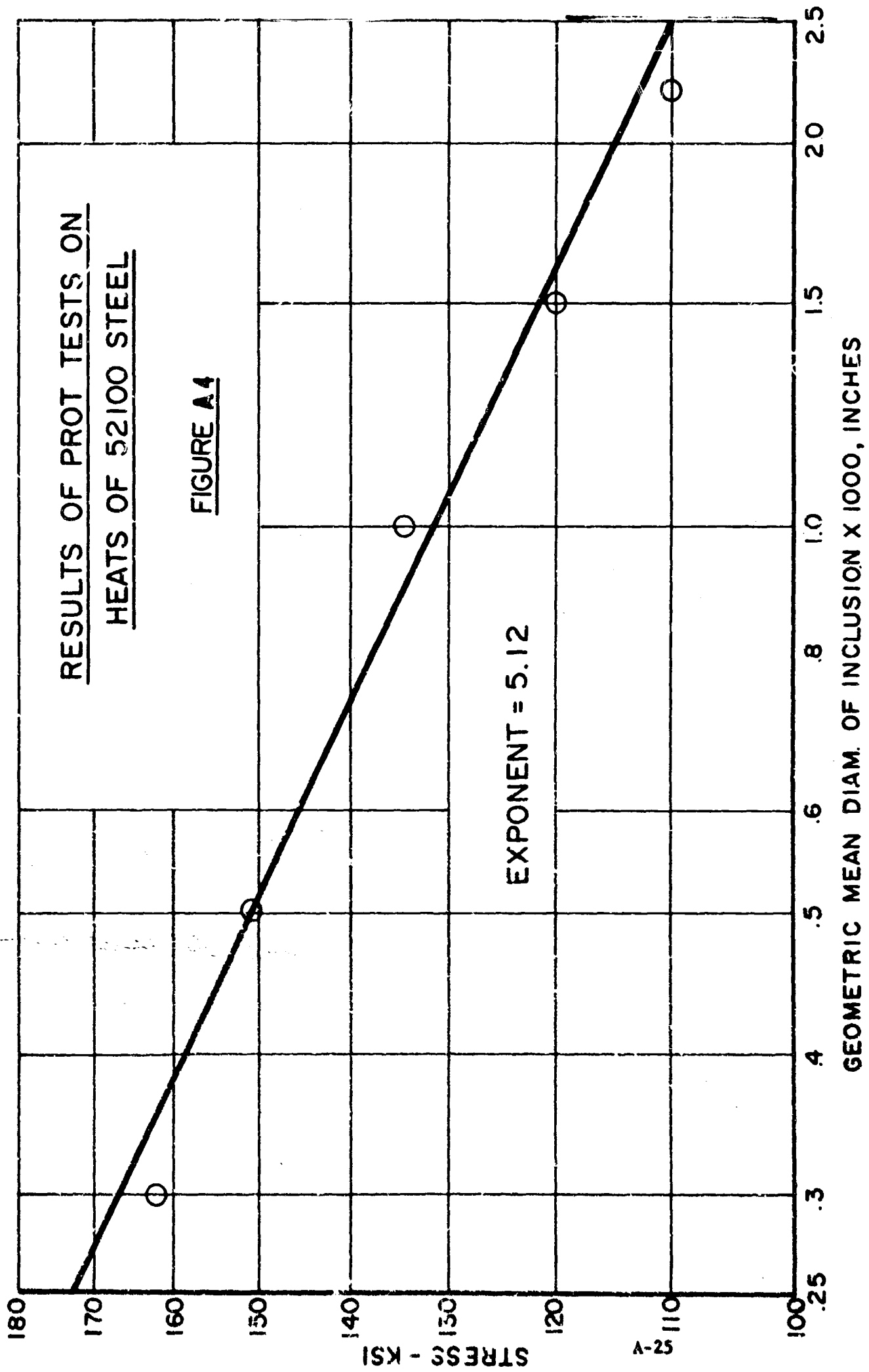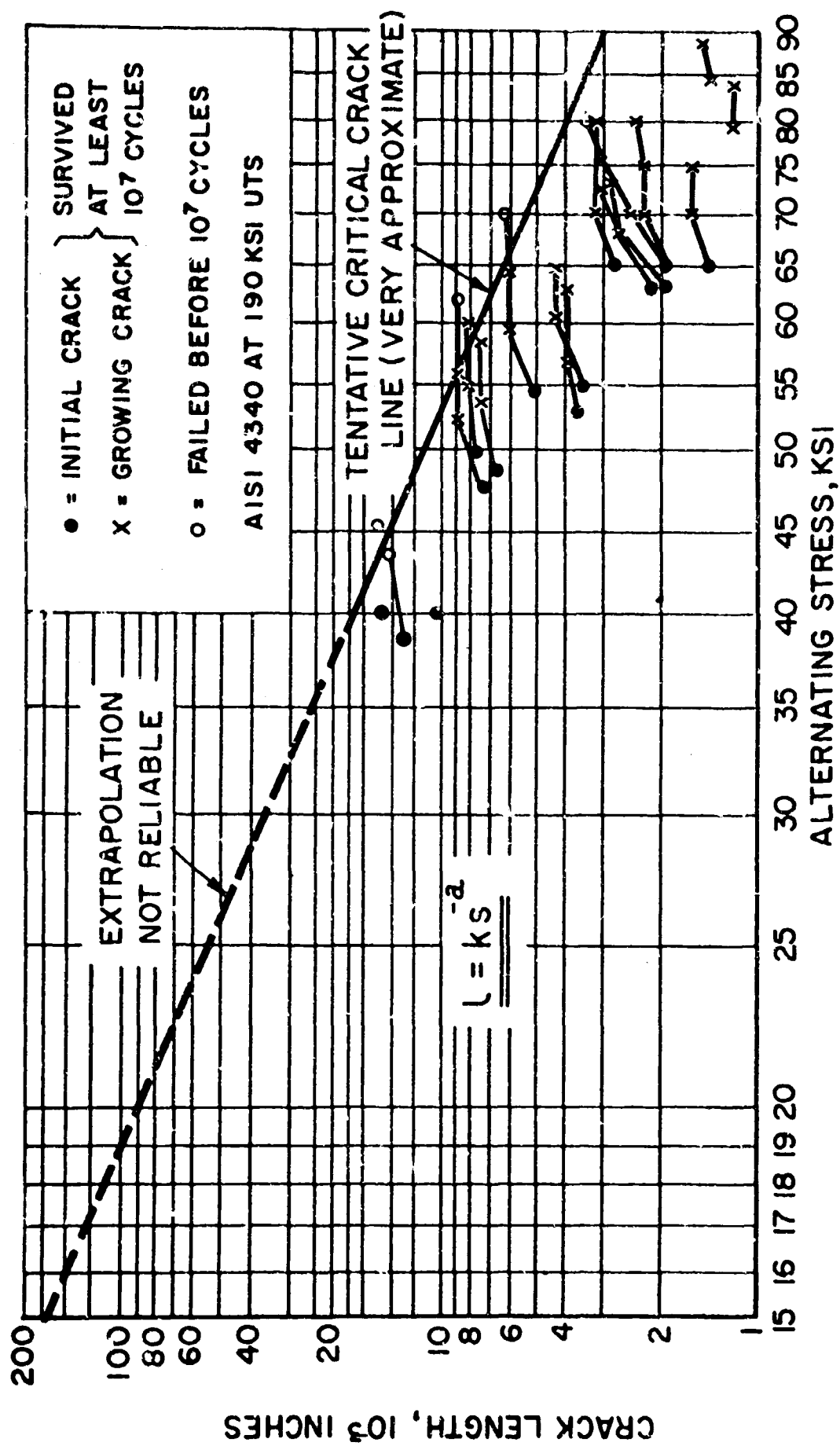
CRITICAL DYNAMIC CRACK LENGTH

FIGURE A5

A-26

The Critical Static Crack Length

In parts that have failed in service by fatigue, the final fracture sometimes happens at a very rapid rate. Prior to this final rupture, the fatigue crack progresses at a finite, but increasing rate until it reaches some critical size such that the next cycle of stress causes complete fracture. Partly responsible for this critical condition is the fact that, for a fixed load, the decreasing area increases the nominal stress. However, even had the nominal stress been uniform (by decreasing the cyclic load) a critical crack size which will result in sudden fracture might be encountered. Although this sudden fracture might occur either under a cyclic or a steady load, it is essentially "static" in nature. (This critical static crack length is not to be confused with the critical dynamic crack length previously discussed.)

The practical importance of having this critical static crack size sufficiently large is obvious. In aircraft structures, if this critical crack length is much greater than that which can be easily detected at overhaul and its attainment requires a number of service overhaul periods, the condition may be acceptable. If, on the other hand, the critical crack size for the maximum stresses imposed is so small as to be readily missed during inspection, a potentially dangerous situation may exist. Since only one load application (or perhaps a few) is necessary for complete fracture after the critical size is reached and since this critical size decreases rapidly with increase in stress, the maximum static load that a crack of a given size can withstand is a measure of safety of the structure.

Another practical example is the limiting of the size of defects in high-strength steel missile cases. Using existing data on high-strength steels, the critical sizes of defects in a high-strength steel are estimated to be very small if the design stress is over about 200,000 psi.

Irwin revised the Griffith static-failure theory of brittle materials for more-or-less ductile engineering materials. His relation (which is similar to Griffith's original relation) states that the product of the square of the net-section stress and the critical crack length is proportional to a certain material constant. This constant is dependent on the degree of constraint of the metal at the tip of the crack, that is, plane strain causes a greater restraint than plane stress, hence, a lower value of the constant. McClintock (35, 36) has also treated this problem theoretically in some detail.

Most laboratory fatigue specimens tested at constant load finally fail from excessive stress and display a more-or-less slow static type of failure, not the sudden rupture described above. The size of small laboratory specimens is usually less than the critical static crack length for many materials. For this reason, this catastrophic type of failure is not observed in laboratory tests of many materials. For example, using the relation discussed by Irwin (37) for the critical crack size and his factor for 4340 steel at moderate hardnesses, the critical crack length is estimated to be larger than the periphery of a small rotating beam specimen at fatigue stresses near the

fatigue limit. However, some recent fatigue tests on very hard steels conducted at relatively high stresses showed evidence that the critical crack length was only 0.03 to 0.10 inches and was followed by rapid failure. In these tests, the fractured surface displayed two distinct types of areas, one representing the original fatigue crack and the other a rapid fracture. Fig. A6 is a drawing of a typical fracture surface of one of these specimens. Fig. A7 is a plot of the critical crack length measured on the outside surface of rotating beam specimens as a function of the test stress for several high-strength steels.

The critical crack size has several important relations in considering the fatigue life of a part of structure. If fatigue cracks do develop in a part in service, the above relation determines the crack size at which the maximum expected static or alternating load in service will cause complete collapse of the structure. In the estimate of the acceleration relations of a part in service, the analysis should be based on the growth of the fatigue crack compared to the critical static value for the maximum expected load.

FRACTURED SURFACE OF A
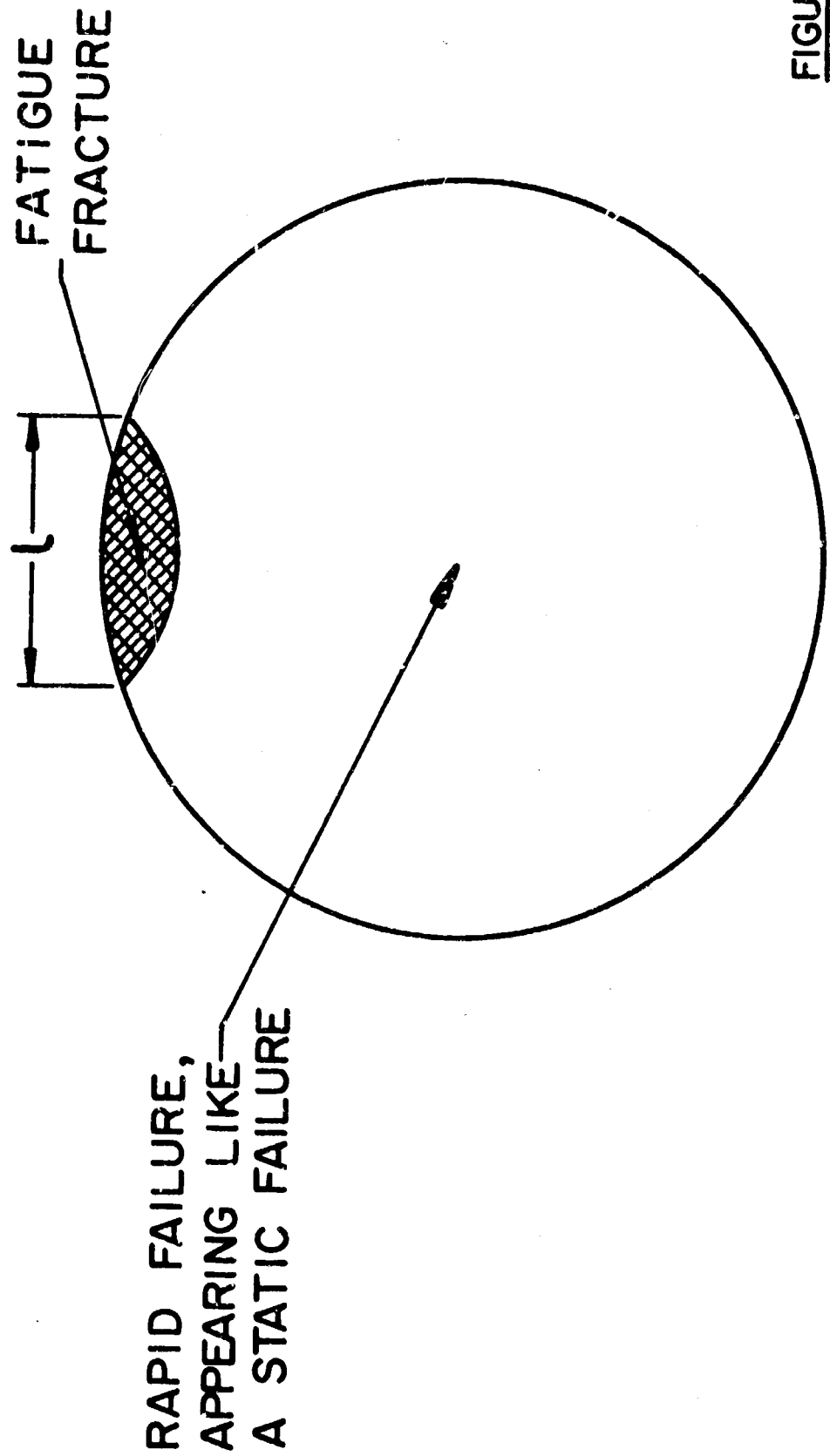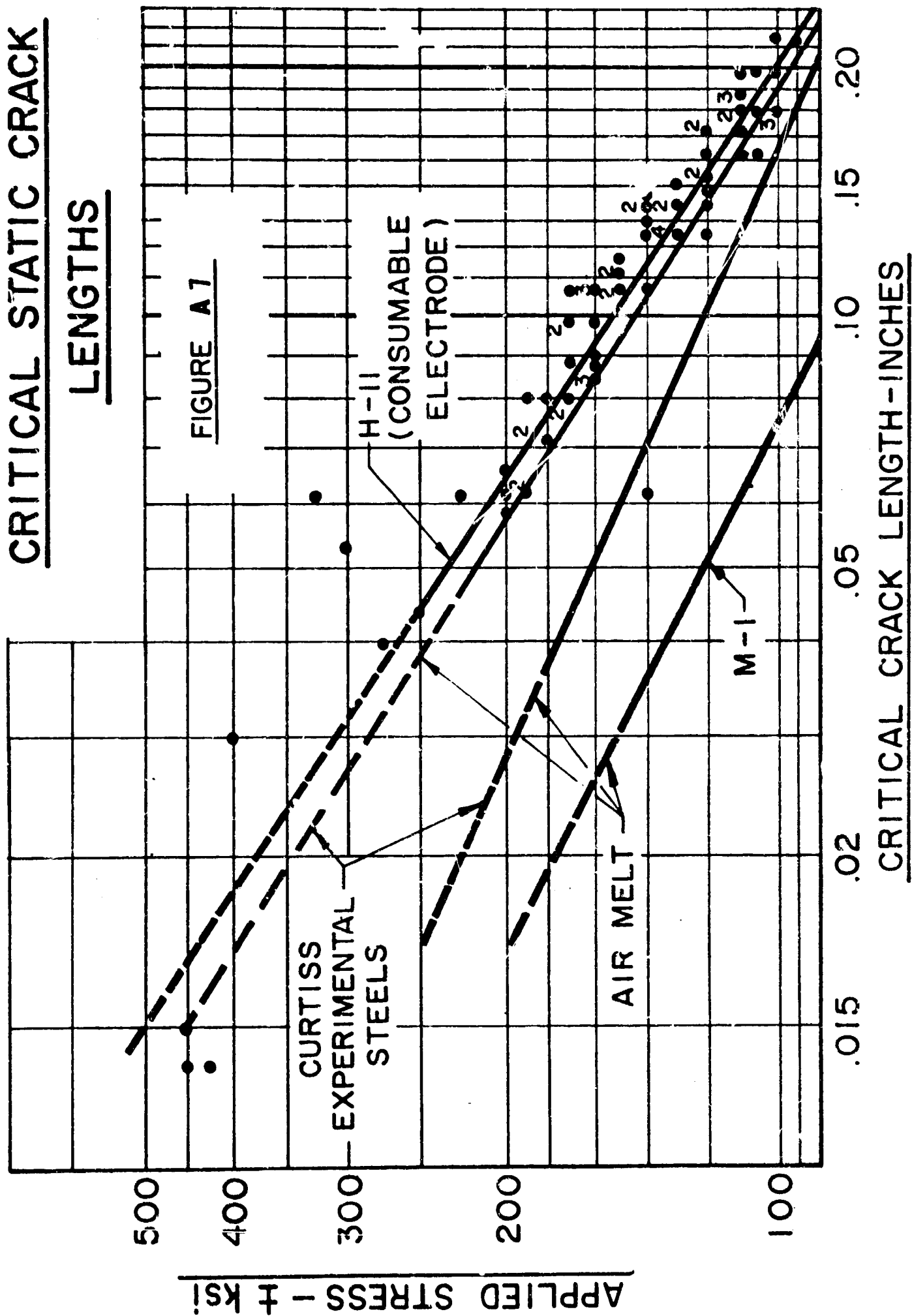
FATIGUE SPECIMEN OF CERTAIN

HIGH-STRENGTH STEELS

FATIGUE
FRACTURE

RAPID FAILURE,
APPEARING LIKE
A STATIC FAILURE

A-29

FIGURE A 6

CRITICAL STATIC CRACK
LENGTHS

FIGURE A 1

Low Cycle Fatigue

Up to this point in the development of this theory, it was tacitly assumed that the alternating stress imposed on the part was not excessively high, that is, the maximum alternating stress was somewhat below the conventional yield point. This section will discuss the S-N fracture curve at high cyclic stresses or strains.

It has been observed by Kommers (38) and Low (39) that a log-log plot of the cyclic total strain of a metal versus the cycles to failure is a straight line for the higher stresses, and that many alloys fall within one straight-sided band. This is shown in Fig. A8 On the other hand, Coffin (41, 42) finds that a straight line on a log-log plot is obtained provided the cyclic plastic strain is used rather than the cyclic total strain.

Tavernelli and Coffin (42) have compiled the available data on cyclic strain fatigue tests of metals, and have found that the following formula best fits all data regardless of the type of metal or the test temperature:-

$$\sqrt{N} \quad \Delta \epsilon \quad = \quad \frac{\epsilon_f}{2} \quad - - - - - - - - - - - - - (8)$$

The value of ϵ_f is readily computed by:

$$\log_e \left(\frac{100}{100 - R.A.} \right) = \epsilon_f$$

It is to be noted that the cyclic plastic strain range can be expressed in terms of cyclic stress by the well-known relation:

$$\frac{\Delta \epsilon}{2} = k \ s^{\lambda} - - - - - - - - - - - - - - - - (9)$$

Equation (8) becomes in terms of stress:

$$N \ s^{2\lambda} = \left(\frac{\epsilon_f}{4 k} \right)^2 - - - - - - - - - - - - - (10)$$

This equation is the same form as equation (2) for lower stresses when the initiation period has been eliminated. However, it is not certain at present whether or not equation (10) which is valid for relatively high cyclic stresses has the same exponent and constant as equation (2) which was developed for the low or moderate cyclic stresses.

FIGURE A 8
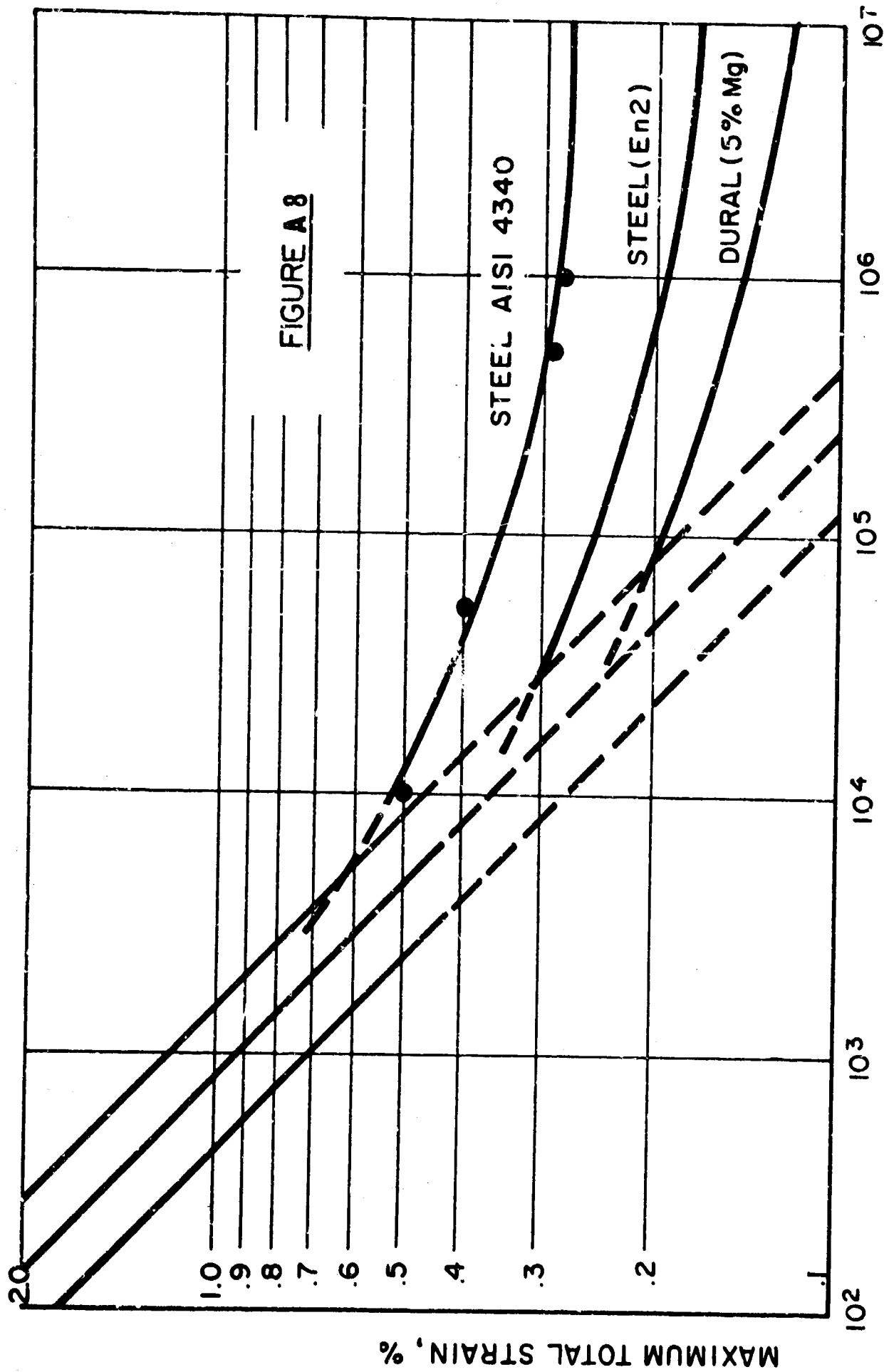
LOG STRAIN AS A FUNCTION OF LOG N FOR LARGE
STRAINS IN VARIOUS METALS

Modification of the Propagation Relation for Superimposed Steady Stresses

Possibly the only investigation on the effect of combined steady and alternating stresses on fatigue crack propagation has been reported by Liu (26). In this work, he investigated crack propagation in 2024 S-T3 under combined uniaxial stresses, and proposed a relation for the observed rates of propagation.

However, it was found that his data will fit the following relation with good accuracy:-

$$\log \frac{\ell}{\ell_o} = k (1 + b \; s_m) \; s^{\alpha} \; N_p \quad - - - - - - - - -(11)$$

This formula is the same as equation (3) except for the modifying factor, $(1 + b \; s_m)$, to account for the mean or steady stress. It was found that this formula (11) fits all of Liu's values of C_{ave} within an average of $\pm 2.8\%$ except for two points. Including these two points, the highest error was 6.5%. For this material, the following equation was obtained:-

$$\log \frac{\ell}{\ell_o} = 1.66 \times 10^{-8} \; (1 + 0.50 \; s_m) \; s^{2.42} \; N_p$$

It is to be noted that equations (4) and (4a) for acceleration relations were developed for the case where the mean stress is equal to zero. The more general case of cumulative damage will not be developed.

Using the same reasoning for crack propagation developed in conjunction with equation (3), equation (11) is substituted for equation (3). This leads to a more general relationship:-

$$\frac{1}{(1 + b \; s_m) N_r} \sum_{i=1}^{i=z} (1 + b \; s_{m_i}) \left(\frac{s_i}{s_r} \right)^{\alpha} n_i = \frac{\log \frac{\ell}{\ell_o}}{\log \frac{\ell_{fr}}{\ell_c}} = D \quad - -(12)$$

As before, the quantities, s_r (the highest stress in the spectrum) and N_r, correspond to a reference point on the crack propagation S-N curve (without the initiation period) for the case of zero mean stress. The corresponding relation for the type A notch is obtained by substituting ℓ'_o for ℓ_o.

The value of b may be determined by testing specimens with a localized notch under combined steady and alternating stresses.

FATIGUE REFERENCES

1. Grover, H.J., _Cumulative Damage Theories._ Proc. Fatigue of Aircraft Structures, WADC Symposium, WADC TR 59-507, August, 1959.

2. Demer, L.J., _Review of Experimental Data on Initiation and Propagation of Fatigue Cracks._ WADC TR 55-86, Part 2, June, 1955.

3. Henry, D.L., _A Theory of Fatigue Damage in Steel._ Trans. ASME, Vol. 77, 1955.

4. Schijve, J., _Fatigue Crack Propagation in Light Alloys._ Report M.2010, National Luchtvaartlaboratorium, July, 1956.

5. Cummings, H.N., Stulen, F.B., and Schulte, W.C., _Investigation of Materials Fatigue Problems._ WADC TR 56-611, March, 1957.

6. Cummings, H.N., Stulen, F.B., and Schulte, W.C., _Research on Ferrous Materials Fatigue._ WADC TR 58-43, August, 1958.

7. Hunter, M.S., and Fricke, W.G., Jr., _Metallographic Aspects of Fatigue Behavior of Aluminum._ Proc. ASTM, Vol. 54, 1954.

8. Hunter, M.S., and Fricke, W.G., Jr., _Fatigue Crack Propagation in Aluminum Alloys._ Proc. ASTM, Vol. 56, 1956.

9. Hunter, M.S., and Fricke, W.G., Jr., _Cracking of Notch Fatigue Specimens._ Proc. ASTM, Vol. 57, 1957.

10. Forsythe, P.J.E., _The Basic Mechanism of Fatigue and Its Dependance on the Initial State of the Material._ Proc. International Conference on Fatigue of Metals, London, 1956.

11. Orowan, E., _Theory of the Fatigue of Metals._ Proc. London Royal Society, Vol. 171A, 1939.

12. Hempel, M., _Metallographic Observations on the Fatigue of Steels._ Proc. International Conference on Fatigue of Metals, London, 1956.

13. Thompson, N., _Experiments Relating to the Basic Mechanism of Fatigue._ Proc. International Conference on Fatigue of Metals, London, 1956.

14. Langer, B.F., _Fatigue Failure from Stress Cycles of Varying Amplitude._ Trans. ASME, Vol. 59, 1937.

15. Lipsitt, H.A., Forbes, F.W., and Baird, R.B., Anisotropy of Crack Initiation and Propagation in Cold Rolled Aluminum Sheet, Paper Presented to ASTM Annual Meeting, June, 1959.

16. Cummings, H.N., Stulen, F.B., and Schulte, W.C., Tentative Fatigue Strength Reduction Factors for Silicate-Type Inclusions in High-Strength Steels. Proc. ASTM, Vol. 58, 1958.

17. Mann, J.Y., The Effect of Stress Concentrations on the Fatigue Resistance of 24S-T Aluminum Alloy. Report ARL/SM217, Melbourne, 1953.

18. Peterson, R.W., Interpretation of Service Failures, Handbook of Experimental Stress Analysis, M. Hetenyi, Editor-in-Chief. John Wiley & Sons, 1950.

19. Marco, S.M., and Starkey, W.L., A Concept of Fatigue Damage, Trans. ASME, Vol. 76, 1954.

20. Shanley, F.R., Discussion of Methods of Fatigue Analysis, Proc. Fatigue of Aircraft Structures, WADC Symposium, WADC TR 59-507, August, 1959.

21. Head, A.K., The Growth of Fatigue Cracks, Report ARL/Met. 5, Melbourne, 1954.

22. Bennett, J.A., A Study of the Damaging Effect of Fatigue Stressing on X4130 Steel, Proc. ASTM, Vol. 46, 1946.

23. Weibull, W., The Propagation of Fatigue Cracks in Light-Alloy Plates, SAAB TN 25, 1954.

24. Frost, N.E., and Dugdale, D.S., The Propagation of Fatigue Cracks in Sheet Specimens, J. Mech. Phys. Solids, 6, No. 2, 1958.

25. McEvily, A.J., Jr., and Illg, W., The Rate of Fatigue-Crack Propagation in Two Aluminum Alloys. NACA TN 4394, September, 1958.

26. Liu, H.W., Crack Propagation in Thin Metal Sheet Under Repeated Loading, Trans. ASME, Journal of Basic Engineering, March, 1961, Vol. 83, Series D. No. 1, p. 23.

27. Corten, H.T., and Dolan, T.J., Cumulative Fatigue Damage, International Fatigue of Metals, London, Sept. 1956.

28. Cummings, H.N., Qualitative Aspects of Fatigue of Materials. WADC TR 59-230, September, 1959.

29. Frost, N.E., and Phillips, C.E., Studies in the Formation and Propagation of Cracks in Fatigue Specimens, Proc. International Conference on Fatigue of Metals, London, 1956.

30. Coffin, L.F., Jr., A Mechanism for Non-Propagating Fatigue Cracks. Proc. ASTM, Vol. 58, 1958.

31. Stulen, F.B., Effect of Material Property Variations in Fatigue. Proc. Fatigue of Aircraft Structures, WADC Symposium, WADC TR 59-507, August, 1959.

32. Lessells, J.M., and Jacques, H.E., Effect of Fatigue on the Transition Temperature of Steel, Welding Journal, Research Supplement, Vol. 29, 1950.

33. Stulen, F.B., Cummings, H.N., and Schulte, W.C., Relation of Inclusions to the Fatigue Properties of High Strength Steel, Proc. International Conference on Fatigue of Metals, London, 1956.

34. Minamoizi, K., and Okubo, H., Note on Notch Effect of Metals. Journal, Franklin Institute, Vol. 249, No. 1, 1950.

35. McClintock, F.A., A Theory of Catastrophic Shear Fracture in Ductile Materials, Solid State Sciences Division, Air Force Office of Scientific Research, ARDC, Contract No. AF 18(600)-957, Division File No. 10-12, July, 1957.

36. McClintock, F.A., Prediction of Tear Resistance of Foil, Sheet and Plate. AF Office of Scientific Research, Contract No. AF 18(600)-957, Research Memo. No. 13, April, 1959. A discussion of paper by Irwin, G.R., entitled "Fracture Mode Transition for a Crack Traversing a Plate". ASME Metals Engineering Conference, 1959.

37. Irwin, G.R., Kies, J.A., and Smith, A.L., Fracture Strengths Relative to Onset and Arrest of Crack Propagation. Naval Research Laboratory, Report 5222, November, 1958.

38. Kommers, J.B., International Association for Testing Materials VIth Congress, New York, 1912.

39. Low, A.C., Short Endurance Fatigue, Proc. International Conference on Fatigue of Metals, London, 1956.

40. Pian, T.H.H., and D'Amato, R., Low Cyclic Fatigue of Notched and Unnotched Specimens of 2024 Aluminum Alloy Under Axial Loading, WADC TN 58-27, February, 1958.

41. Coffin, L.F., Jr., A Study of the Effects of Cyclic Thermal Stresses on a Ductile Metal, Trans. ASME, Vol. 76, 1954.

42. Tavernelli, J.F., and Coffin, L.F., Jr., A Compilation and Interpretation of Cyclic Strain Fatigue Tests on Metals, Trans. ASM, Vol. 51, 1959.

43. Hall and Thomas, R.E., Batelle Memorial Inst., Accelerated Testing as a Problem of Modelling, Proceeding of 6th Nat'l. Symposium on Reliability and Quality Control, Jan., 1960.

44. Hall, Arthur D., A Methodology for Systems Engineering, D. VanNostrand & Co., Princeton, N.J., 1962.

45. Von Neumann, J., and Morgenstern, O., Theory of Games and Economic Behavior, Princeton University Press, 1953.

APPENDIX B

BIBLIOGRAPHY

(B1)   "ON UTILITY. I. THE VALIDITY OF THE EXPECTED UTILITY HYPOTHESIS, II.
ON BERNUULIAN UTILITY FOR GOODS AND MONEY", by S. N. Afriat, AD-269 682,
ASTIA 62-1-6, DIV 15.   A model of behavior in circumstances of uncertainty
is presented by a preference order between certain distributions which
determines a best distribution among any that are attainable.   Choice is
determined by the maximum of possible expected utility.

(B2)   "ACCELERATED LIFE TESTS OF ITEMS WITH MANY MODES OF FAILURE", by W. R. Allen,
AD-276 743, ASTIA 62-3-6, DIV.15.   Paper is concerned with definitions,
examples, and some ideas that may be useful in considering accelerated
processes with more than one mode of failure.   An example is given which
illustrates a major pitfall of accelerated testing, when more than a single
mode of failure is present.

(B3)   "GUIDE TO DESIGN OF MECHANICAL EQUIPMENT FOR MAINTAINABILITY", J. W. Altman
and A. C. Marchese, AD-269 332, ASTIA 62-1-6, DIV. 28.   A guide for design-
ing mechanical equipment for increased ease, speed and accuracy of maintenance.
Written for engineers responsible for design.   Treats design features common
to all mechanical equipment as well as features unique to certain classes of
equipment.

(B4)   "MINIMIZING RELIABILITY DEMONSTRATION FOR A GIVEN EXPENDITURE", by
B. L. Amstadter, from the Proceedings of the 1963 AIAA-SAE-ASME Aerospace
Reliability and Maintainability Conference.   A method is presented for
achieving maximum reliability demonstration for a given expenditure; or,
its equivalent, attainment of a given level of reliability at a minimum
expenditure.   Only two parameters are used, the degree of reliability
demonstration and the direct testing cost.

(B5)   "SAFETY ANALYSIS OF THE VARIABLE EXHAUST NOZZLE CONTROL FOR THE J85
GAS TURBINE ENGINE", by J. N. Anderson, document C-2733, Curtiss-Wright
Corporation, Curtiss Division.   Original dated March 21, 1958; revision
A dated December 28, 1960.   It presents the results of a safety analysis
of the variable exhaust nozzle area changing mechanism for the J-85 engine.

(B6)   "LOADING SPECTRA FOR FATIGUE DESIGN CRITERIA", by I. Bouton, from Aerospace
Engineering, Vol. 19, No. 3, March 1960.   The author states that there is
no such thing as a fatigue failure.   Generalized aircraft spectra are not
sufficient to determine fatigue failure rate, so structural component and
element spectra must be derived.   These spectra must define two conditions
the past history of the element and the present probability of exceeding
a given load.

(B7) "SYMBOLIC REPRESENTATION OF COMPLEX SYSTEM", by J. S. Brady and S. Goff, a Jet Propulsion Laboratory Technical Report No. 32-390, January 1963. A number of logical and Mathematical concepts relevant to the development of an overall representation of the performance of complex man-machine systems are derived and related to the JPL/NASA space flight operations complex. The requirements for a rigorous program of model development are defined.

(B8) "PREDICT RELIABILITY FIRST - BUILD IT LATER", by R. E. Bussiere, from S.A.E. Journal, Vol. 69, July 1961. Before hardware is available the reliability can be predicted. Two statistical distributions must be available -1, probability density function of the maximum strength -2, probability density function of the maximum stress, that the component will experience.

(B9) "METHODS FOR PREDICTING COMBINED ELECTRONIC AND MECHANICAL SYSTEM RELIABILITY", by T. L. Bush and C. E. Gebhart, AD-291 919, ASTIA 63-2-1, DIV 8A. The feasibility of a number of approaches to the mechanical reliability prediction problem are considered. A survey was made of information available in area of mechanical failure mechanisms, including fracture, creep, wear, instabilities, corrosion. A suggested prediction technique is called the functional module level. This title refers to an array of elements or components performing a specific function.

(B10) "ACCELERATED TESTING AS A PROBLEM OF MODELING", by Hall Cary and Ralph E. Thomas, from the Proceedings of the Sixth National Symposium on Reliability and Quality Control, 1960. The theory of models furnishes criteria and methods suitable for rapid generation of experimental data applicable to prediction of reliability of reliable systems. Developed mathematical criteria indicate conditions under which reliability data obtained from accelerated tests can be used to predict reliability under normal use.

(B11) "RELIABILITY - NEW ENGINEERING DIMENSION", by R. S. Catlin and W. E. Cox, from Machinery, August 1960, Ref. Section. Presents quality and reliability program at Norair Division of Northrup Corporation.

(B12) "SAMPLING PROCEDURES AND TABLES FOR LIFE AND RELIABILITY TESTING (BASED ON EXPONENTIAL DISTRIBUTION), a Department of Defense Quality Control and Reliability Handbook (Interum) H108, April 1960. A handbook prepared to meet a growing need for the use of standard sampling plans for life and reliability testing. Such plans may be used to demonstrate the conformance of equipments, subassemblies and component parts to established reliability requirements.

(B13)   "FAILURE STRESSES", by D. R. Earles and M. F. Eddens, from the Proceedings
of the 1963 AIAA-SAE-ASME Aerospace Reliability and Maintainability Conference.
The definitions and tabulations give a first look into the failure stressor,
failure stress, failure mechanism, failure mode relationship. Failure stressor
and failure stresses are the basis for some tools of reliability engineering,
such as derating, safety factors, fail-safe design analyses, environmental
damping, environmental profiles, and failure-effect analyses.

(B14)   "RELIABILITY TESTING OF THE MERCURY CAPSULE REACTION CONTROL SYSTEM",
by A. J. Friona, from Proceedings of the 1961 IAS Aerospace Support
and Operations Meeting. An evaluation, performed in system configuration,
of procedures and servicing techniques, and their related handling and
human factors problems. Wear characteristics of various components, and
characteristic performance variation of functional parts are determined.
By scheduled replacement of parts, it is possible to obtain a large test
sample faster than by testing at the component level.

(B15)   "THE EFFECTS OF UNCERTAINTY AND MONETARY INCENTIVES ON ESTIMATION", by
E. I. Golding, AD-285 263, ASTIA 63-1-1, DIV 28. A discussion of the
correlation between estimates and actual outcomes with emphasis on the
monetary and bonus incentive effects.

(B16)   "AN INTRODUCTION TO SET THEORY", by C. K. Gordon, Jr., AD-285 310, ASTIA
63-1-1, DIV 15. The terminology, symbology, axioms, and some principle
theorems of set theory are presented. The organization and style are intended
to guide inexperienced readers towards a sound comprehension of the principles.
Application of set theory to probability is demonstrated.

(B17)   "MISSILE MODIFICATIONS AND THEIR EFFECT ON RELIABILITY", by J. W. Gurr,
from Proceedings of the 1961 IAS Aerospace Support and Operations Meeting.
Changes to the older sequentially progressive testing method of R and D
programs in the form of concurring plans and accelerated schedules have
altered many basic concepts. It is necessary to place restrictions on the
acceleration to prevent premature incorporation of changes which defeat
the purpose. The outcome of a decision to sacrifice change testing for
schedule is a gamble.

(B18)   "BAYESIAN PROCEDURES AND RELIABILITY INFORMATION", by C. W. Hamilton,
from the Proceedings of the 1963 AIAA-SAE-ASME Aerospace Reliability
and Maintainability Conference. Basic properties of Bayesian reference
procedures are described and compared with classical inference procedures
in a reliability context. The application of Bayesian methods to inference
problems involving limited experimental data is described. An example is
shown concerning the estimation of reliability and the determination of
confidence statements from life test data assuming exponentially distributed
failure times.

(B19)   "GEAR DRIVE RELIABILITY", by N. S. Hodska, from Space/Aeronautics,
        Vol. 33, No. 3, April 1960. Reliability studies show that 50 percent
        or more of all spur gear failures can be traced to misapplication of
        gears and improper material specification. Design experience by itself
        will not prevent failures in power transmission systems. Each critical
        gear mesh should be rated in terms of operating speed, power dissipation,
        gear accuracy, finish and backlash.

(B20)   "STATISTICAL TECHNIQUES FOR ENVIRONMENTAL TESTING", by Richard M. Jaeger,
        from the proceedings of the 1963 annual meeting of the Institute of
        Environmental Sciences. A discussion of the available statistical tools
        of which the environmental engineer could be aware.

(B21)   "EVALUATION OF MECHANICAL SYSTEMS SERVICE EXPERIENCE AND ITS APPLICATION
        TO RELIABILITY IN PRELIMINARY DESIGN", by W. F. Johnson, Jr., from the
        Proceedings of the 1963 AIAA-SAE-ASME Aerospace Reliability and Maintain-
        ability Conference. Simplified methods of analyzing reliability potential
        and growth are described. The data and methods of analyses presented cover
        the range of mechanical energy conversion, control, transmission and actuation
        equipment of the type and quality now used in safety-of-flight applications
        in manned aircraft systems.

(B22)   "PREDICTING RELIABILITY", by M. I. Kaufmann and R. A. Kaufmann, from
        Machine Design, August 18, 1960. The article describes the state of
        the art of predicting reliability via outlines of two current techniques.
        It presents a new method that is still speculative but supported by results
        of studies in complex projects. Current techniques reviewed are use of a
        standard, and rating factors. The new concept is called relative-utility
        evaluation. It does not explain interaction between systems. It is
        statistical.

(B23)   "SYSTEMS RELIABILITY OVER AN OPERATIONAL SPECTRUM", by H. I. Leve, from
        the Proceedings of the 1963 AIAA-SAE-ASME Aerospace Reliability and
        Maintainability Conference. Formulas are developed for obtaining the
        reliability of a system or vehicle over a set of possible life histories.
        By considering the operational spectrum to be a weighed set of deterministic
        time-wise histories, it has been found for a simple time independent failure
        mode case that the life history of an element is characterized by conditions
        existing at the instant of minimum element reliability. The result is ex-
        tended to include the cases of time dependent failure modes, multiple fail-
        ure modes per element considering strength dependcy, and time-variable
        strength distributions.

(B24) "STATISTICAL DESIGN OF COMPLEX EXPERIMENTAL PROGRAMS. II. THE DECISION THEORY APPROACH TO COMPLEX EXPERIMENTATION", by M. O. Locks, AD-289 256, ASTIA 63-1-4, DIV 15. Application of decision theory to analysis of results of multifactorial experiments. A tentative utility function is presented including gain of information from testing and losses due to fluctuations from a planned reliability schedule.

(B25) "PARALLEL STEP STRESSING - A METHOD OF ACCELERATED LIFE TESTING", by Richard E. Loomis and Donald C. Snyder, from the transactions of the 17th annual convention of the ASQC, May 1963. The parallel step method is a modification of the technique of step stressing for demonstrating device reliability in a relatively short time. It is faster and more economical.

(B26) "PREDICTING RELIABILITY", by Robert Lusser, a publication of the Redstone Arsenal, Huntsville, Alabama, dated October 1957. The author raises the question - is it true that reliability of complex equipment can be predicted by life testing, and by employment of the exponential function? The paper presents reasons why reliability cannot be predicted, and that the exponential formula is not applicable.

(B27) "RELIABILITY THROUGH SAFETY MARGINS", by Robert Lusser, a publication of the U.S. Army Ordnance Command, Redstone Arsenal, Alabama, dated October 1958. This study is an expanded version of a earlier paper, "Reliability Specifications for Guided Missiles" by the same author. A reliability code consisting of 21 paragraphs is formulated to supplement and override specifications of the 1958 era.

(B28) "ON THE VALIDITY OF SCALES DERIVED BY RATIO-AND-MAGNITUDE ESTIMATION METHODS", by Madjid Mashour, AD-276 385, ASTIA 62-3-5, DIV 29. The procedure for scale construction by ratio estimation is analyzed. A brief summary for procedures for scale construction is given. It is shown that under special experimental conditions scales derived by magnitude estimation can be tested.

(B29) "FINAL REPORT - OFFICIAL COMPONENTS TEST - MECHANICAL EXHAUST NOZZLE ACTUATION SYSTEM FOR GENERAL ELECTRIC J85-GE-5", by E. G. Milne, document C-2841, Curtiss-Wright Corporation, Curtiss Division. In two volumes dated November 21, 1960. It covers the qualification testing of the J85-GE-5 Mechanical Exhaust Nozzle Actuation System performed in accordance with paragraph 4.3 of Specification MIL-E-5009A and per EPS 1052C.

(B30) "HOW TO ESTIMATE SYSTEM RELIABILITY", by H. Niewood, from Aerospace Management, Vol. 4, No. 11, November 1961. Reliability goals are set early in a system development, hopefully, that all will be attained. This article outlines a way to estimate reliability before the overall system is available for testing in its natural environment.

(B31) "U.S. AIR FORCE RADC RELIABILITY NOTEBOOK - ELECTRONIC EQUIPMENT", RADC-TR-59-111, revision of December 31, 1961. ASTIA document No. AD-148868. Presents the general mathematics of reliability and reliability prediction, and failure rate information for those interested in evaluating the reliability of complex electronic equipment.

(B32) "NEW CONCEPTS IN THE PREDICTION OF MECHANICAL AND STRUCTURAL RELIABILITY", by A. A. Rothstein, from the proceedings of the 1963 AIAA-SAE-ASME Aerospace Reliability and Maintainability Conference. Three reliability prediction techniques are presented. These are described under the general grouping of a function concept, an equational concept and a properties concept. For each grouping the concept, methodology and limitations are described.

(B33) "RELIABILITY CONTROL IN AEROSPACE EQUIPMENT DEVELOPMENT", by S.A.E Sub-Committee for Reliability, from S.A.E. Technical Progress Series, Volume 4. With the individuals in mind who directly influence the reliability designed into the product, the document was prepared for engineers to assist them in their work as designers; or as project, test and specification engineers. Its limited discussions provide general background for better understanding of all facts of the reliability problem and their relationships with development functions.

(B34) "DEMONSTRATING SYSTEM RELIABILITY BY SEQUENTIAL PROBABILITY RATIO TEST", by B. Tiger and W. H. Brewington, from Jet Propulsion, Volume 27, August 1957, No. 8, Part 1. The sequential probability ratio test is presented as a practical statistical approach to demonstrating the reliability requirements of rocket systems and sub-systems. It is shown that the required calculation can be reduced to determining the equations of two straight lines, which, when plotted on graph paper serve as decision lines for rejection or acceptance after sequential testing of systems.

(B35) "POINT ESTIMATE OF RELIABILITY FROM RESULT OF A SMALL NUMBER OF TRIALS", by Z. A. Typaldos and D. E. Brimley, AD-276 150, ASTIA 62-3-5, DIV 15. An approach to estimation of reliability on the basis of a few trials. In this method, based on information theory concepts, when the probability of success is not known, the proposed way to assign probabilities is to maximize the measure of uncertainty.

(B36) "HAZARD ANALYSIS", by G. S. Watson, AD-265 349, ASTIA 62-1-2, DIV 15. The hazard function of a life distribution which has the same role in reliability studies as the spectral density function has in stationary time series is studied.